CONTRACT REPORT BY

DENISON MINES LIMITED

THE USE OF CONSOLIDATED FILLS FOR CONTROLLING VIOLENT PILLAR FAILURE IN ONTARIO MINES

CONTRACT NO. 23440-6-9010/01-SQ

MICROMEDIA

TABLE OF CONTENTS

ABSTRACT		2
1.0	INTRODUCTION	3
2.0	BACKGROUND	6
	2.1 Previous Studies - Considerations of Backfill for Pillar Support	6
	2.2 Previous Backfilling Experience for Ground Stabilization-Denison Mine	8
	2.3 Selection of 26 Panel as the Backfill Research Site	10
	2.4 Summary - Reasons for Selection of Test Area	15
3.0	PROJECT OBJECTIVES	17
4.0	FILLING HISTORY	20
5.0	HIGH FREQUENCY ACOUSTIC MONITORING RESEARCH	24
6.0	RESULTS AND ANALYSIS	27
7.0	CONCLUSIONS	31

ABSTRACT

This study demonstrates that a cemented backfill can significantly reduce the frequency and severity of rockbursting in failure-prone pillars. Over a six year period of records, no rockburst of over 1.0 Mn has occurred in a pillar surrounded by backfill.

There is indication that water associated with the hydraulic filling period may have accelerated local seismic activity. After filling, seismic activity appears limited to pillars on the immediate edge of filled areas. Similar results have been observed in uncontrolled backfilled panels in other areas of the mine.

Experimental high-frequency acoustic monitoring equipment was tested concurrent with the fill trial.

1.0 INTRODUCTION

A Contract was awarded by Department of Supply and Services, Federal Government of Canada, in mid-1986 to Denison Mines Limited, Elliot Lake, Ontario for the purpose of evaluating and demonstrating, with a large scale field trial, the effects of consolidated tailings backfill in controlling violent pillar failure. The site selected for the backfill trial was the 26 Panel at the Denison Mine. This panel was mined by room and pillar methods in 1976. Subsequently pillar failures, manifested by pillar spalling, seismic activity and minor rockbursting occurred prior to it being backfilled. These failure conditions and the size of the affected area were considered appropriate for a field assessment of this role of cemented backfill.

This backfill research project was funded under the Ontario/Canada Mineral Development agreement and was valued at $610,000, with an additional direct and indirect contribution by Denison Mines Limited totalling about $1,445,000. A cost summary of main expenditures incurred are provided in the report.

This project involved pouring approximately 109,000 tonnes of a 1:30 mix by weight of cement and classified mill tailings into a selected section of the 26 Panel. In conjunction with the fill placement, the behaviour of pillars and hanging wall in the immediate area were monitored with rock mechanics instrumentation. The equipment included a 32 channel microseismic system with a close array of geophones dedicated to the test panel area, convergence meters installed for monitoring of hanging wall/footwall closure and instruments for monitoring relative magnitude and direction of ride action of hanging wall/footwall of the adjacent panels. Additionally, experimental high frequency based microseismic equipment developed recently at Queen's University at Kingston Ontario was tested for the purpose of yielding possible new information on pillar seismicity and pillar stress states. In-situ testing of the fill to determine fill stiffness was conducted at two sites. Numerical modelling using both elastic and non-linear type programs was carried out to simulate effects of fill on stresses and displacements in the pillars.

Concerning background for carrying out this project, there had been very limited experience with use of backfill as a stabilizing medium in rockburst prone ground both in Ontario Mines and elsewhere. The only significant area where experience that had been gained at the Denison Mine in backfilling with cemented tailing for ground stabilization around rockburst prone pillars in the boundary pillar area adjacent to the Quirke Mine of Rio Algom Limited (Figure 1). The results of filling were considered to be successful in the significant reduction of recorded seismic events and ground conditions in that area (Figure 12, 13 & 14).
In the absence of systematic stabilizing pillars, backfill is the only support technique with the capability of controlling the spread and violence of these type of failures.

Regarding rockburst incidence, in the period 1984-86 just prior to the awarding of the Contract, approximately 200 rockbursts were recorded in Ontario hardrock mines. About 80% of these occurred in pillars and 75% of these were in the gently-dipping room and pillar Elliot Lake mines.

In steeply-dipping deposits, which are usually mined with cut-and-fill or open stoping with delayed fill methods, the energy absorbing capability of "stiff" fill can serve to reduce the release of seismic energy associated with wall closure. Research in this area has been on-going in Ontario mines and elsewhere for a number of years and the mechanism appears to be fairly well understood.

In gently dipping deposits, which are usually mined by a room and pillar method, pillar failures controlled by fill involve a completely different function of backfill. This has only recently been recognized and it is probably achieved through modification of the post - failure behaviour of pillars surrounded by fill. Laboratory studies have demonstrated that samples surrounded or confined by cemented fill fail non-violently whereas those with no confinement or surrounded with uncemented fill fail violently.

The reasons for this behaviour are only vaguely understood. It was recognized that both fundamental research and a large-scale in situ placement of cement consolidated fill was required to further develop these concepts. The backfill research project involving filling 26 panel and monitoring the behaviour of the filled area was directed to fulfilling the requirement to assess the results of fill, in a large scale trial.

All tasks relating to the Contract have been completed and related documentation submitted. This report concludes the requirements of the Contract. Refer to Appendix A for a summary of the individual tasks or milestones involved in the Contract, and a schedule of work listed as a Management Control Chart. Work was largely performed by Denison engineering and operating personnel. Work involving the experimental high frequency acoustic emission sensing system was sub-contracted to Queen's University at Kingston, Ontario and in situ fill stiffness determination using pressuremeter equipment was sub-contracted to Trow Limited. Technical advice and assistance was provided by CANMET through Dr. D. Hedley, who was the project scientific authority.

The purpose of this report is to: provide a background of the experience gained at Denison mine in backfilling for ground stabilization and reasons for selection of the 26 panel for the trial area, detail the project objectives, summarize fill pour history and in-situ fill property testing results, summarize rock mechanics monitoring instrumentation and results relating to the project, analysis of results and to provide conclusions to the project work.

2.0 BACKGROUND

2.1 Previous Studies - Considerations of Backfill for Pillar Support

Backfill has been recognized as a passive support system, in that, because of its characteristically high porosity it has to be compressed before exerting a support pressure other than that occasioned by its self-weight. Figure 18 shows a typical in-situ stress closure curve for an uncemented and a cemented backfill (1:10 cement/tailing ratio). It shows that a considerable amount of closure is required before a significant support pressure is induced. Studies by Nicholson and Busch in 1968 have shown backfill to require 15-20% strain depending on initial porosity prior to development of significant load-bearing capacity in confined compression, regardless of cement content. See Figure 19. This has indicated against the use of backfill as a support medium in flat-lying room and pillar mines because:

(a) Stope closure is very small and is limited largely to elastic movement since it is controlled by rigid pillars.
(b) Backfill can only be introduced at the end of the mining cycle after most of the closure has occurred.

In the case of cut and fill or high blast hole stopes with fill, however; the role of fill, particularly stiff fills, in stabilizing ground by providing lateral support thus enhancing load-bearing capacity and reducing seismicity associated with excavation closure has been recognized for some time. In regard to the reduction of seismicity of rock bursting, the role of backfill can be explained by the absorption of strain energy using an energy balance concept (Blight 1984). It is indicated that if an excavation is filled with a compressible material, part of the released energy due to excavation is absorbed in compressing the fill. This would reduce the remaining energy available for fracture or potential damaging seismic (Kinetic) energy components. It was also indicated, in this work, that for less compressible fills less excavation convergence occurs and that more of the released energy will be converted into fracture energy.

In the case of backfill for pillar support in flat-lying room and pillar mines a number of laboratory studies on rock samples were conducted in the early 1980's. The purpose was to determine on a laboratory scale the effect of cemented and uncemented tailing surrounding specimens tested in compression and effects on test specimens with varying cement binder contents.
It was found with testing that the lateral constraint of the backfill affected

the post failure characteristics of a pillar and in the case of cemented fill resulted in non-violent type failure (Swan 1985, Blight 1984). Uncemented tailing fill did not mitigate the occurrence of violent failure.

Following are summaries of some of the work done:

1. Blight and Clarke (1983) first conducted laboratory tests on rock samples confined with different types of backfill. A soft backfill, (i.e. cemented tailings) had no effect on the peak strength of the rock sample but resulted in a high residual strength after failure. A stiff backfill, (i.e. cemented rockfill), on the other hand, increased the strength of the rock sample as well as producing a higher residual strength.

2. It was decided to duplicate these tests at CANMET's Elliot Lake Laboratory using quartzite samples and the types of cemented tailings available at Denison Mine. The testing set-up is shown in Fig. 19 and the stress-strain curves in Fig. 20. Two types of tests were conducted; tight fill where both the rock and fill were loaded, and the rock protruding above the fill so that only the rock was loaded.

   The graphs in Fig. 20 show that the rock by itself failed violently with an instantaneous reduction in stress from peak strength to zero. When the rock was surrounded by uncemented tailings the same violent failure was observed. Rock samples surrounded by 15:1 and 10:1 cemented tailings, with the rock protruding above the fill, showed a different post failure behaviour. There was still an instantaneous reduction in stress from peak strength, but the stress stabilized at a residual strength of 6% and 50% of peak strength for the 15:1 and 10:1 fills respectively. The stress then slightly increased with increasing closure. Rock samples surrounded with 15:1 and 10:1 tight cemented backfill showed a different type of post-failure behaviour. This time there was no instantaneous reduction in stress from peak strength but a gradual reduction which stabilized at 60% and 75% respectively of peak strength and again slightly increasing with additional closure. In these two cases failure occurred non-violently.

A number of deductions can be drawn from these tests:

a) Cemented tailings backfill has no effect on the peak strength of the rock, which is the same conclusion as Blight and Clarke.
b) Uncemented tailings has no effect on the post-failure behaviour of the rock.
c) Cemented tailings not poured tight, still allow partial unstable failure of the rock, but the rock has a residual strength.
d) Cemented tailings poured tight, exhibit a stable post-failure behaviour in the rock with a substantial residual strength.
e) The post-failure behaviour of the rock improves with increasing cement contents.
f) It is difficult to extrapolate these laboratory results to underground pillars, surrounded by backfill, but it is suspected that backfills with a cement content will produce similar results to the laboratory tests.
g) Probably the best conditions will be achieved underground by pouring the backfill tight to the roof and before pillars have begun to fail.

2.2 Previous Backfilling Experience for Ground Stabilization-Denison Mine

Experience in backfilling and observations on the performance of cemented tailings fill for the purpose of ground stabilization had been gained at the Denison Mine between 1982 and the start of the backfill research project in 1987. This background experience was useful for operations concerns including; establishment of parameters for pour rates, pulp density for the delivery system, experience with fill retaining fence and cemented plug installations, performance of the backfill drainage system and experience with setting times and in-stope behaviour of the fill. This background also provided the mine with confidence in the in-situ performance of cemented fill for reduction of rockbursting and seismicity in the filled areas.

Backfilling for ground stabilization was carried out in 29-37 Panels in the No. 1 Shaft area of the mine. This area is immediately down dip from the Quirke Mine of Rio Algom Ltd. and is adjacent to the boundary pillar of the two mines. The backfilled area is about 550m below surface.
The area backfilled for ground stabilization showed signs of progressive deterioration of pillars from the period 1982 onward. It was manifested by generally moderate to locally severe pillar sidewall spalling and by extensive seismic activity including rockbursting. In addition, a local microseismic network dedicated to the area and shared with the Quirke mine showed the

area was very active with rockburst events. The cause of the seismic activity and bursting, based on underground observations, appeared to be pillar failures. The cause of the sudden on-set of pillar instability in this area was coincident with and appeared to be related to an adjacent up dip major ground failure. This major failure is described in the literature in some detail by Hedley, 1984.

The decision to backfill with cemented tailing was based on various laboratory studies, on rock specimens confined by fills, including those conducted by Blight and Clarke (1983) and Swan (1985). Numerical modelling using NFOLD code, assigning pillars residual strengths to account for the effects of fill was also conducted, to confirm the decision to backfill. It was decided to fill with 1:30 cemented tailings although testing had only been conducted on 1:10 and 1:15 samples in the laboratory.

The results of backfilling the Western Boundary showed the following:

(a) A significant reduction in the amount of seismic energy liberated from seismic activity in this area, after backfilling. Figures 12 & 13 show events during the seismically active pre-filling period of 1985-86, and post-filling. Seismic energy and magnitude are related by Hedley (1989) in the form: log ES(MJ)=1.3 Mn - 1.75.

(b) A reduction in the rate and total number of seismic events after filling. Figure 12 shows the locations and number of events for a 9 month period in 1985 during filling of 37 Panel. Figure 14 shows the same type of data (for both small and larger energy events) for the 3 year period 1987-88-89. It shows a major reduction in the number of events when compared with the previous period.

(c) Figures 12 and 13 show that most of the seismic events occurred in pillars outside the backfilled stopes.

In summary, backfilling with 1:30 cemented tailings in the boundary pillar area appears to have significantly reduced both the severity and frequency of seismic activity in the filled area.

2.3 Selection of 26 Panel as the Backfill Research Site

The mine had two locations that were considered applicable to study the effect of backfilling on the control of violent pillar bursting phenomena. They were:

1. The area in the western exhaust corridor of the mine near the Denison/Rio Algom east-west boundary. This area described earlier has been seismically active and pillar deterioration has been visually apparent for the last few years. About 500,000 tonnes of both cement consolidated and unconsolidated hydraulic tailing fiil had been placed for ground stabilization in this area. The severity and frequency of rockbursting and seismic activity has significantly decreased since the area has been backfilled. A number of stopes remained open which could have been used for the research trial area.

2. A section of the 26 Panel located immediately up dip from and adjacent to the 26 mobile equipment repair facility. This area is located in the eastern end of the mine about 1500 m from No. 1 shaft and 1700 m from No. 2 shaft. The depth below surface is approximately 500 m. The panel had a recent history of working ground including relatively large magnitude seismic events and rockbursting. The pillars in the proposed test panel and in the adjacent up-dip 24 Panel showed signs of crushing and locally severe spalling was also evident.

   This panel was selected for the cemented backfill trial because it was considered more appropriate with respect to the larger volume available for filling the area. The area was more seismically active and it was isolated from other regional interferences.

2.3.1 Mining Background and Rock Mechanics Considerations

The 26 panel test area was mined between 1975 and 1978. Mining was conducted by the on-strike jumbo method followed by benching with a hydrofore blasthole drill and slotting of the long strike pillars by a long-hole method. The overall extraction was approximately 75%. The final mining height varied from about 7.5 m to 11 m. The dimensions of the test area are approximately 310 m length by 37 m width. It is wedge shaped. The effect of slotting and benching of these strike or longitudinal pillars resulted in a series of high post pillars with dimensional aspect ratios generally less than unity. Factors

of safety were calculated using a criterion for pillar stability based on the empirical expression developed for pillar strength determination by Salamon and Munro (1967) and Hedley (1972) and assumed field stresses. This method of determining factors of safety is part of the pillar design method used routinely in the Elliot Lake camp. Values ranging from 0.8 to about 1.5 were indicated. The empirical expression used to determine pillar strength is expressed as:

$$Q = K (W^a/H^b)$$

where, Q = Pillar strength, MPa
K = Rock mass strength, 133 MPa
W = Pillar width, m
H = Pillar height, m
a,b = Statistically determined constants with values of 0.5 and 0.75, respectively.

The expression used for pillar stress determination is based on the tributary area loading theory and a rigid pillar concept. It includes the following parameters: mining depth, dip of the reef, field stress to account for superincumbent and horizontal stresses and the areal extraction. The expression is:

$$Op = \frac{(3.609(D)\cos^2(a) + 3000\sin^2(a))\ 0.00689}{1\text{-}R}$$

Where, Op = Pillar stress, MPa
D = Depth below surface, m
a = Dip of reef, degrees
R = % Extraction, decimal form

Factors of safety are determined in a conventional manner by expressing the pillar strength as a ratio of field stress.

In this panel there was a fair correlation between pillar seismicity and observed indications of pillar deterioration such as crushing and spalling with pillars having factors of safety less than 1. This observation applied to the pre-filling period. Conversely, the larger pillars such as the Negri dyke, and those with factors of safety determined to be substantially greater than 1, i.e. $\geq$ 1.5 appeared to be visually stable with only occasional microseismic activity.

The ground conditions in the pillars of the test area started to deteriorate shortly after mining was completed, and they were further aggravated by benching and pillar slotting in the adjacent 24 panel during the period 1980-82. This appears from the records and discussions with mine personnel to be particularly apparent after 24951 roadway was benched. It is likely that the benching of this roadway would have significantly weakened the strike pillar separating it from 26302 heading. Stresses probably would have shifted down-dip onto the post pillars in the test panel. Ground instabilities, which appeared from visual assessment to be confined almost exclusively to the pillars, consisted of:

- Severe spalling and obvious complete failure of some of the smaller pillars mainly in the east end of the panel. Pillar fracturing was stress related resulting in various stages of hour-glassing profiles and in some cases axial splitting of the pillar was apparent.
- Numerous instances of shear failure along infilled bedding planes in the pillars. It was not possible to determine if this shearing-type failure was a reaction to pillar overloading or the pillar reacting passively due to the normal stress reduction across the bedding planes due to pillar unloading; subsequently permitting shear failure.
- Rockbursting and ground movements audible to personnel in near-by active mining areas and maintenance facilities.
- Local roof falls primarily restricted to a wide span section in 26305 in the east end of the test area. These appeared to be related to wedge type failures caused by intersecting low angled faults and bedding plane slips.
- Broken mechanical-type rockbolts from the back area indicating roof movement.

See Figure 10 for Photographic records and Appendix 4 for photographs.

The panels immediately up-dip from the test panel, i.e. sections of 24 and 22 panels in particular had experienced local large roof-falls, pillar spalling and some low magnitude of energy seismic activity. The mining layout was similar to 26 panel with respect to extraction, pillar dimensions and pillar orientation and pillar failures were attributed to excessive stress.

It was recognized that the 26 panel was not an isolated area and the results of backfilling would likely be affected by the deterioration of the adjacent panels.

2.3.2 Geology

1. General Geology

As shown on Figure 4, Geological Section Through Shafts No. 1 and No. 2 there are two ore zones separated by about 43 m of quartzite in the south dipping Matinenda formation underlain by an igneous Archean basement complex and overlain by a series of Huronian sedimentary formations dated at 2.2 billion years.

The Huronian formations were subjected to north-south compression and intrusion of Nipissing diabase dykes at 1.7 to 2.1 billion years ago, forming the Quirke Lake syncline. Strata dips undulate from 0-60 degrees averaging 15 to 20 degrees. The folding caused high angled joints and faults, bedding plane slip joints and faults, and low to medium angled joints and thrust faults. Displacements range from 0 to 100 meters.

Thermal metamorphism of the sedimentary formations was only to a low chlorite grade. Except for features such as the Quirke Lake overthrust, dynamic metamorphism is limited to a layer of sericitic or chloritic mud or gouge a few millimeteres thick, on the surfaces of a small percentage of the joints and faults. Some of these joint and fault surfaces are also slickensided. Most joints and faults can be described as being very tight. Water seepage is very rare.

The 26 backfill research panel is located in the lower ore zone. The upper ore zone has not yet been mined in this area. Figure 5, 26 Shop Area Geology, shows the principal joints and faults and the vertical 13 meter wide Negri dyke. The reefs have an average strike of 096 degrees and a dip of 23 to 35 degrees South.

The lower ore zone consists of two, 3 to 5 meter thick pyritic, quartz pebble conglomerate reefs (upper or A reef and lower or B reef) separated by 0.8 to 2 meters of interbedded quartzite (IQ). The total lower zone thickness in the test area is 3 to 5 meters thicker than most of the adjacent areas.

Each reef is made up of a varying number of individual beds, cross beds and lenses with a composition ranging from densely packed quartz pebble conglomerate to pebble quartzite to fine and coarse grained quartzites. Each of these individual beds can range in thickness from one centimetre to one meter.

The hanging wall and footwall (Matinenda) quartzites are also a series of individual beds, with similar thicknesses, usually composed of fine to coarse grained quartzite with occasional pebbly bands and occasional silt layers a few millimetres thick.

When bedding plane slip joints or faults are present, they frequently are at the contact between these individual beds. Individual slips can be traced over more than 100,000 square meters (northeast area of Figure 5) or they may be only visible over 1 to 2 square meters.

The regional north-south compression stresses forming the syncline were transferred along these bedding slips and across the beds on low to medium angled joints, slips and thrust faults. A major scale example of the latter is the Quirke Lake overthrust, shown on Figure 4.

2. Summary - Prominent Geological Features

There are a number of prominent geological features which are considered to have an influence on the stability of the pillars in the research panel. They include:

- The Negri diabase dyke which is located on the south boundary of the test area. It likely acts as an abutment pillar on the down-dip side of the panel. A large area on that side, immediately adjacent to the dyke, is used for a mobile equipment repair shop (26 shop). Ground conditions have remained largely unchanged in this area until recently, suggesting that the dyke has acted as a barrier pillar.

- Steeper than average dips of 23-35 degrees occur in this panel. This would have had the effect of weakening the pillars.

- Prominent sericitic, chloritic lined bedding slips occur at the contact at the hanging wall of the ore zone, and others can be observed within the reef horizons. They would be expected to have the effect of reducing the shear strength of the pillars.

3. Rock Mechanical Properties

Hanging Wall and Footwall:

Rock Type	Uniaxial Compressive Strength (intact)MPa	Youngs (intact) Modulus-GPa
Quartzite	175-200	70-85
Pyritic Quartz Pebble Conglomerate	175-200	70-85

2.4 Summary - Reasons for Selection of Test Area

1. The 26 Panel selected had been identified as an unstable area, this was manifested by seismic activity and pillar deterioration.

   Background data on the ground conditions in this panel were available and included comprehensive visual records and convergence measurements on hanging wall/footwall closure. It was felt that this background information would provide a good baseline for comparison with post filling conditions.

2. Previous laboratory testing indicated the benefits of cemented fill for control of violent pillar failure. This area would provide an in-situ trial.

3. The proposed test area was immediately up-dip and adjacent to the 26 shop, a large mobile equipment repair facility. The stability of this garage would in time be affected by ground problems in the 26 panel which had resulted in an operational decision to backfill for this purpose.

4. The layout and size of the panel was favourable as a test area. A

diabase dyke (Negri dyke) had been left in place along the south boundary which acted as a natural fill bulkhead, so as a result only three fill retaining fences were required. The layout of the pillars in the test area was favourable in that it resulted in them being "buried" by fill which would not necessarily be the case in other test areas considered.

The size of the fill test area required approximately 100,000 tonnes of backfill to fill it (see Figure 2). At proposed fill pour rates of 2000-2500 tonnes/pour shift it would have been possible to backfill and conduct any in-situ testing and monitoring programs planned within the approximate 3-year project life.

5. The area around the periphery of the test area was largely accessible for installation of monitoring instrumentation, such as microseismic geophones, closure and ride instruments (see Figure 6).

6. A minimal amount of ground rehabilitation (scaling, securing ground with Swellex and rockbolts) was required to permit access of personnel to install drainage mousetraps and fill fences.

3.0 PROJECT OBJECTIVES

The primary objective of this backfill research project was to evaluate and to demonstrate by a large scale in-situ trial the effect of controlling violent or catastrophic type pillar failure by surrounding the pillars with cement consolidated tailings fill. The specific goals were:

i) To evaluate and to demonstrate the potential of cemented tailings backfill in reducing the incidence and severity of violent pillar failures.

ii) To show that fill contributes significantly to stabilizing local ground conditions and can be used to contain an area of pillar failure.

The Contract for this project stipulated a number of procedures, requirements and project milestones. These are provided in Appendix 1.

1. Place consolidated tailings fill in a multiple stope (ore room-and-pillar) area of a large extent (10,000-15,000 square metres). The area chosen should have a modest but proven (or anticipated) history of failure activity.

2. Install a 32 channel microseismic monitoring system, owned by CANMET and to be made available for the study, and operate the system on day-to-day basis. The sensor array was installed in a tight cluster in and around the trial backfilled area.

3. Install and operate a sufficient quantity of simple failure indicator devices and pressure cells around all intact pillars within the filled area prior to placement. Convergence meters, in situ stress measurements and ride - check instruments were installed.

4. Provide CANMET with two 11.4-12.7cm diameter holes, 10m long, in the fill for pressuremeter tests and monitoring. The holes were drilled with as much undisturbed sidewalls as was technically possible.

5. Evaluate the long-term performance of areas adjacent to the trial area filled by observing frequency of ground control problems - spalling falls, burst, etc.

6. Based on measurements of seismic activity, closure, fill pressure and computer modelling, compare the performance of fills with varying cement/binding agent contents and make recommendations on the minimum cement/binding agent contents required to control violent pillar failures.

7. Test novel microseismic equipment and/or stress measuring instrumentation

which can be found to yield new information on pillar seismicity and pillar stress states. Suggest further work of significance to this task.

In order to accomplish the objectives, the project was broken down into project milestones or tasks.

Project Milestones

The project was divided on the basis of the contract, into 43 milestones or tasks. The duration of the project was July 1986 to March 1989. For internal project control it was divided into two phases.

Phase I (Milestones 1-22 inclusive)

This phase involved the following main items of work:

1. Site selection. The main criteria being a room and pillar area of large areal extent and with a history or likelihood of ground problems.

2. Preparation and rehabilitation of the test area. This involved upgrading of the ventilation and significant rock work.

3. Installation of fill lines, drainage facility and construction of two fill fences.

4. Installation of instruments to monitor the behaviour of the fill and pillars prior to, during and after filling.

5. Installation of separate "research type" microseismic systems to attempt to correlate pillar seismicity and stress level changes that are anticipated to occur after filling. This was sub-contracted to Queen's University.

6. Assessment of the pre-fill status of ground conditions.

Phase II (Milestones 23-43 inclusive)

This phase included the following main items.

1. Placing approximately 100,000 tonnes of fill in about 20,000 tonne stages.

2. Ground condition assessments and reporting.
3. Monitoring of existing instrumentation, installation of additional equipment and conducting of special tests to check fill and pillar behaviour.

4.0 FILLING HISTORY

Backfilling of the 26 Panel was started in April 1987 and was completed in October 1988. Approximately 109,000 tonnes of 1:30 hydraulic tailing fill was placed in the test area. Prior to the initial pour a substantial amount of preparatory work had to be done. Preparatory work included ground rehabilitation to provide access to the area as it had been inactive since 1978, ventilation upgrading, fill drain water handling system, construction and installation of the underground fill line from No. 1 Shaft to the fill discharge point located in 24951 roadway. A plan of the fill area (Figure 6) shows the location of the discharge and Figure 11 shows a schematic of the backfill lines from the surface fill plant to the pour discharge location.

The following is a summary of the preparation work carried out prior to filling.

1. Rehabilitation of ground in the 24951 and 26305 headings for fill line and fill fence and mousetrap installations respectively. Pumping accumulated water out of low areas, scaling and installation of 4.2 m Swellex bolts, 4.2 m lengths in blocky areas and 1.8 m length mechanical bolts.

2. The establishment of a fill water drainage system down-dip to the Stanrock mine sump for subsequent pumping to surface.

3. The installing of fans and ducting for ventilation for personnel engaged in rehab work, fence and mousetrap drain construction.

4. Installing a fill pipe line from no. 1 shaft via the main connecting ramp from 1 shaft to 26 shop to the discharge point located in 24951 roadway.

The underground fill line placed for this project was 20 cm diameter high density polyethylene pipe (Sclair) rated bursting pressure of 3.3 MPa. A section of this line was later replaced with same diameter schedule 80 steel pipe due to excessive hydraulic fill pressure resulting in plastic pipe failures. Length of the underground pipe line was approximately 1700m with the inlet end connected directly to a surface borehole (20cm diameter 510m length) and the outlet end discharging over a bench above the test panel.

5) Diamond drill holes were drilled at selected locations in the pillars in the test panel area for installation of microseismic geophones for ground monitoring purposes.

The three fill fences required to retain the hydraulic fill in the test area until it drained and consolidated were constructed of timber and were considered to be free-draining structures. They were of similar design to fill fences of comparable dimensions and identical application used elsewhere in the mine. A plug of cement consolidated tailings fill was poured in small lifts to an elevation of about 2.4-3m above the tops of the fence and allowed to set prior to bulk pouring. A ratio of 1:30 cement/tailings by weight was used for the plugs.

The drainage system which was installed prior to filling, consisted of three mousetraps installed parallel to the back through the two fences in 26305 and extended to the top of the panel by attachment to the back. The mousetraps consisted of fine fabrene mesh material (or filter medium) wrapped onto 15cm diameter perforated flexible plastic pipes, and were of typical design used at the Denison Mine.

Backfilling started in June 1987 and was completed in October 1988. Original estimated tonnage of hydraulic fill required to fill the panel was about 90,000 tonnes. The actual amount poured was about 122,500 tonnes. This included 26302, 26303, 26304 and 26305 as well as the east end of 24951 roadway. The variance in fill requirement was due to the variability in stope heights in the test area. The following is a summary of fill placement by year:

Year	Tonnes Placed	Cement/Tailing
1987	35,500	1:30
1988	78,000	1:30
1988	9,000	Straight Tailing

Fill was scheduled at a rate averaging 1500-2000 tonnes/day. Backfilling on the project until mid 1988 (total fill placed at that time about 77,500 tonnes) was restricted to one 8-hr. shift. After that date pouring was advanced to 2-shifts/day, due to a change in overall priority on backfilling at the mine and in an effort to get the contract back on schedule.

The pulp density varied from about 0.49-0.60 with overall average of about 0.55 (solids fraction by weight). The purpose of the relatively low density was to assist in maintaining a critical flow velocity of 2.1m/sec. to prevent sanding out of coarse fractions throughout the long horizontal run of the underground fill pipe line.

Cementitious ground ferrous blast furnace slag was used to bind the tailings.

Laboratory testing had been conducted for strength determinations and operating experience had been documented at the mine on use of the specific slag and tailing material.

Operating Performance

Overall fill placement was considered satisfactory. The following operating parameters were considered to have been satisfied:

1. Drainage. Mousetraps remained open for the duration of pour. Drainage of the decanted water from the top of the fill was achieved rapidly and local pools of water that accumulated in low spots drained as they were displaced by subsequent pours. Drainage was monitored visually by operators throughout the project.

2. Fill consolidation. Fill was checked routinely to assess whether the cement used as a binder for consolidation was reacting as expected. Except for some problems with the blast furnace slag near the end of the project, the bulk of the fill appeared to set up well.

3. Tight Filling. This criteria was achieved because of favourable geometry of the orebody. Visual inspections showed the fill was placed "tight" against the hanging wall.

In-Situ Fill Testing

In-situ backfill testing for the purpose of determining fill stiffness was carried out during February 1989. The work was contracted to Trow Limited, who have experience using pressuremeters in soft fills. (Appendix 2 contains data for this testing program).

The field testing was carried out in 22960 and 24070. Fill tested was consolidated 1:30, it had the same draining arrangement and had a similar geometry to the test panel. It was not possible, because of operating problems, to carry out the in-situ testing in the test panel itself.

The testing was done by drilling through the timber fill fences and into consolidated fill with conventional diamond drill equipment. The holes were drilled at controlled feed rates (<5cm/minute), with minimal water, and employed a drilling mud (polymer) to minimize hole caving. Hole sizes were BX and casing shoes were used for drilling. It was not found necessary to install casing and recovery of core and condition of holes were considered good.

The drilling program involved drilling four (4) holes to final depths of about 9.0m each. Pressuremeter tests were carried out at 0.9-1.5m intervals. Total number of pressuremeter tests was 28.

Following are a summary of results:

1. The cemented backfill has a stiffness of 60-80 MPa, or about 0.1% that of the quartzite rock. A log of core recovered at these test locations showed high visual cement content.

2. The softer material indicated stiffness values between 0.4 - 4 MPa. These corresponded to visually weakly cemented and sandy pockets encountered during testing.

3. It is likely that segregation of the coarse tailing fraction and fines caused the alternating layers of strongly and weakly cemented tailings fill. This condition has been observed in other fill exposures and is not considered unusual with hydraulic fill placement.

4. A satisfactory method for drilling in cemented hydraulic tailings fill was used. Relatively intact core samples were recovered, holes remained open for subsequent testing and the surrounding fill mass appeared to be undisturbed by the testing.

5.0 HIGH FREQUENCY ACOUSTIC MONITORING RESEARCH

A part of the research work in this project involved testing and evaluating an experimental high frequency acoustic emission monitoring system. The aim was to assess the system and analysis techniques at this site for the purpose of the long term development of an in-situ rockburst precursor system. This involved in-situ monitoring of microseismic waveforms in the frequency range of 50-300 kHz. This was followed by a computer based analysis. It included Fast Fourier Transformation for analysis of the frequency domains and establishment of waveform pattern recognition techniques for the purpose of differentiating between low and high stress conditions. It involved attempts to correlate parameters derived from the analysis of the waveforms such as microseismic event rate, energy sum and wave form duration with shifts or changes in ground stress levels. The instrumentation used differed in the frequency response range from a conventional microseismic system network used widely in Ontario mines such as the Electro-Lab MP250. That system has a microseismic frequency detection range considerably less than 20 kHz. The higher frequency range system was limited to detection of acoustic events that occurred within several meters of the geophone site, Archibald (1989). In contrast, the lower frequency system network, depending on spatial distribution of the transducers, has the advantage of being able to detect for source location determination of microseismic events over a large mine area. The high frequency system is limited to monitoring localized conditions.

This in-situ monitoring program was conducted at 6 underground sites at Denison Mine. Five of the test sites were located immediately adjacent to the 26 backfill research panel. They were located in the Negri Dyke and in a large post pillar at the east end of the test panel. One site was located in the 35 Panel rib pillar recovery area. The test work was initiated prior to backfilling and was continued during the filling phase and post-filling of the 26 Panel. The test site in 35 Panel (#1 Shaft) involved monitoring the sill of the 35024 rib pillar as it was being mined between filled stopes. The criteria for selection of the monitoring sites were:

1. Potential for microseismic activity based on previous MP-250-System monitoring.

2. Probability of change in stress condition of the pillars monitored based on effect on backfilling, observed changes in local pillar support and on numerical modelling results.

3. In the case of 35024 rib pillar, an expected rapid increase in pillar stress and onset of microseismic activity as pillar support was reduced and mining approached the monitored site.

The work in summary involved the following main operations:

1. Site selection.

2. Determination of rock mechanical elastic properties - Youngs Modulus (E), and Poissons ratio (U). It was required for derivation of stress parameters from strain data acquired from in-situ measurements.

3. In-situ biaxial stress determination using a doorstopper gauge.

4. Installation of a single-axis geophone transducer in a borehole used for stress determination and connection for data acquisition.

5. Analysis of data using specific computer software developed for the project.

6. Numerical modelling of stresses and displacements using MINTAB code in the case of the 35024 rib pillar monitoring site.

Results and Conclusions

The details of specific results obtained at each of the six monitoring sites are discussed in the final report on this research in Appendix 3.

The following is a summary of the main results of this part of the work.

1. A general conclusion can not presently be drawn concerning the applicability of the high frequency system evaluated for rockburst prediction.

2. It was demonstrated that stress variation in the rock mass can be detected. This is based on microseismic waveform observation of trends and characterization.

3. A significant shortcoming experienced with the system was the limited monitoring distance of the transducers. It was indicated by the researchers that it may be less than 6m-7m. This is associated with attenuation of high frequency components of the waveform by the rockmass.

   This may limit this type of system to very localized research work.

6.0 RESULTS AND ANALYSIS

1. The results of backfilling in this trial were determined by visual assessment of changes in conditions and by rock mechanics instrumentation which consisted primarily of a conventional multi-channel microseismic monitoring system and some convergence meters and hangingwall/footwall ride movement instruments. Evaluation of the results of filling in the 26 test panel have been complicated somewhat by quite severe pillar deterioration in the immediately adjacent up-dip area from 24-18 panels. This deterioration was manifested by periodic occurrences of microseismic activity, related groundfalls and numerous occurrences of pillar failure. The test area was subsequently expanded up-dip in an attempt to stabilize the affected area and to arrest potential enlargement of that area. The decision to further backfill was made on the basis of results indicated in the test panel as well as those obtained elsewhere in the mine.

   The results in this research trial are reported on the basis of observations and measurements of seismic activity in the total backfilled area to date. This includes 26 test panel and the filled section of 24 panel. The total area and number of pillars surrounded by backfill is about double that of the test panel. The pillar conditions and fill type were the same in the expanded section as in the test panel area.

   Emphasis was placed on microseismic monitoring results to assess the effects of fill in reduction of violent-type ground failure and rockbursting. This monitoring method was also used to evaluate the growth of the failure area.

2. Instrumentation

   The rock mechanics instruments installations were focused on monitoring ground movements locally in the fill test panel and more regionally on the adjacent up-dip area of unstable pillars. The instrumentation in summary consisted of the following:

   - A 32-channel Electrolab MP250 model microseismic system. The system installed used accelerometers as pick-up transducers and was hardwired to surface via a 75-pair cable in the No. 2 shaft. The installation was unique in that it was dedicated to the test panel which was a relatively small area compared to areas monitored by most of these type of installations in other Ontario mines at the time. The

spacing of the initial geophone array was about 150 ft. - 250 ft. They were installed in pillars in the plane of the orebody. Source locations were determined by a direct solution method using least squares, programmed in the MP250, and by a manual graphical technique. A number of larger magnitude events that resulted in observed substantial rock displacement were used to check the reliability and the accuracy of the source location methods.

The geophone array has now been modified to provide a more regional coverage of the panels when it became obvious that the failure area was growing. This was done to provide a more accurate source location of seismic events.

- Convergence meters - Convergence meters were installed in the test panel at the beginning of the project. They were intended for monitoring hanging wall/footwall closure during prefilling and post filling periods for expected correlation between closure and seismic activity and for confirmation of numerical modelling results. These instruments became non-serviceable due to suspected moisture intrusion in the electronics shortly after installation.

  As a follow-up, closure stations were installed around the periphery of the filled area.

  Figure 6 shows locations of these installations.

- Ride Monitoring Instruments: Monitoring of hangingwall/footwall ride was initiated after it became apparent that it comprised a significant component of ground movement. The area affected includes a number of panels up-dip and down-dip of the backfilled test area and appears to be related to a localized subsidence - basin caused by collapse and failure of a number of pillars in the 20-22 panels. Figure 6 shows the direction and magnitude of movements at the stations established. The approximate outline of the assumed hanging wall subsidence basin is shown. Movement monitored is relative lateral displacement of hanging wall and footwall. The movement appears to be associated with active shearing of the back and floor. Passive shearing within pillars is also indicated.

All the methods of monitoring described are continuing and in the case of closure and ride stations are being currently expanded (Dec. 1989).

3. Results

A number of measureable results of backfilling regarding ground behaviour are summarized. The significance of these results, although subjective, is that backfill had a dramatic effect on the frequency and severity of microseismic activity in the area where pillars where surrounded by fill. The results are summarized as follows:

(1) Seismic activity frequency of occurrence, in the test area, during the period October-December 1987 was 30 events/day. This corresponds to initial stages of backfilling which started in October of that year. This period was selected because the microseismic system had just been installed.

Subsequent microseismic activity during the period 1988 and 1989 was 8-10/day and 2/day respectively. The 1988 time frame was during pouring and 1989 was post-filling.

Figures 7, 8, and 9 show locations of plotted activity during the period and Figure 17 shows a graphical presentation of the reduction in seismicity during this time.

(2) The seismic activity in the post-filling period shows most of the events plotted on the edge of the area where pillars were surrounded by fill. Figure 8 for period 1988 and Figure 9 for 1989 show this trend.

This apparent effect of fill had been observed previously at the Denison Mine in the boundary pillar area in a similiar filling application.

(3) Figure 17 shows a plot of seismic energy during the period 1989. Figure 17 shows a decrease after 1987 and an increase in 1989 over the 1988 period. Energy released during 1985-86 shows a periodic flucation in the cumulative energy during the time it was analyzed. This apparent phenomenon may be partially explained by:

- During the period 1985-86 events with energy <2.0 Mn could not be detected.

- During period 1987 and 1989, the occurrence of large magnitude (>1,0 Mn) events were coincident with hydraulic fill placement. It has been suggested that extra water associated with the fill may have caused a reduction in the shear strength of the pillars by affecting the cohesion and angle of friction of the soft infilling material of the bedding planes and slips.

The effect on energy reduction expected was that exhibited with filling in the boundary pillar area of the mine. Figure 15 shows the reduction in seismic energy released during period 1985-1989

(4) Based on a qualitative assessment, there was an obvious reduction in audible rock noise in the test panel area after filling. This was noted by personnel working in the adjacent 26 maintenance shop and by backfill personnel.

7.0 CONCLUSIONS

Based on observations and recorded seismic activity, in both the boundary pillar and 26 Panel areas, the following conclusions can be made on the use of backfill to control violent pillar failure and stabilize deteriorating areas;

(1) Over a 6 year period no rockburst of magnitude over 1.0 Mn has occurred in any pillar surrounded by backfill.

(2) Microseismic activity is predominantly located in pillars at the edge of the backfilled areas, with very few events in pillars surrounded by backfill.

(3) The introduction of backfill in 26 Panel coincided with an increase in seismic activity in the area. Backfill is poured with about 45% water contents. It is known that when water is sprayed on highly-stressed rock it becomes seismically active and small fragments of rock are violently ejected from the rock face. Consequently, the introduction of backfill into 26 Panel could have caused the increase in seismic activity. However, once the pillars are encased with backfill, seismic activity in them essentially ceased. This behaviour was not observed when pouring backfill in the boundary pillar and pillar recovery areas. However, these pillars had higher factors of safety than those in the 26 Panel area.

(4) In the boundary pillar area both the number of seismic events and the amount of seismic energy liberated has shown a continuous decline since the backfill program in that area was completed in 1987. The rate of pillar deterioration along the boundary pillar has slowed considerably. Naturally backfill has not improved conditions, but has prevented them from getting deteriorating further.

(5) In the 26 Panel area the ability of backfill to control and confine the seismically active area is at present unproven. The southern boundary of the area next to the Negri Dyke has been stabilized by the backfill poured so far. At a cost of approximately $4 million, Denison Mines is pouring a 120 m wide backfill corridor along the north-west boundary of the affected area. Pouring of backfill into the centre of the affected area, where it would have the most benefit, is practically impossible due to access and drainage problems. The next few years will indicate whether these remedial actions are sufficient to contain this area of pillar deterioration.

(6) The use of cement in a 30:1 ratio appears to be sufficient to control the

violent failure of pillars, rather than the 10:1 or 15:1 ratios found in the laboratory studies.

(7) When a chain-reaction of pillar failures occur in a room-and-pillar mining layout, large areas of a mine can be affected. In the absence of systematic large stabilizing pillars, Denison Mines Limited believes that the only practical solution is to backfill the surrounding areas to isolate and contain the affected areas.

REFERENCES

Blight, G.E. "Soil Mechanics Principles in Underground Mining", J. Goetech. Eng. of ASCE, 110, 567-581 (1984).

Hedley, D.G.F. and F. Grant. "Stope and Pillar Design for the Elliot lake Uranium Mines", CIM Trans., LXXV, 121-128 (1972).

Hedley et al. "A Case History of Rockbursts at Elliot Lake", in Stability in Underground Mining II (A.B. Szwilski and C.O. Brawner, Eds.), pp. 210-234. Lexington, Kentucky: AIME, 1984.

Nicholson, D.E., and R.A. Busch. "Earth Pressure at Rest and One-Dimensional Compression in Mine Hydraulic Backfills", USBM RI-7198, 1968.

Rodie, S. "Numerical Modelling of the 26 Garage Area at Denison Mine", Denison Mines Limited Report, 1986.

Brady, H., Board, M.P., Mack, M.G., "Analyses of Pillar Performance in the 20-26 Panel Area", Itasca Consulting Group, Inc., Internal Report to Denison Mines Limited, March 1988.

Hedley et al., Personal Communication and Notes, November-December 1989.

Steffen, Robertson and Kirsten (SRK) (BC), Inc. "Numerical Modelling and Stability Evaluation for the Denison/Quirke Boundary Pillars and No. 1 Shaft Area", Report No. 55801/2 to Denison Mines Limited, June 1985.

Wagner, H., "Pillar Design in Coal Mines", J.S. Afr. Inst. Min. Mtall., 80, 37-45 (1980).

LIST OF FIGURES

Figure 1	Key Plan - Boundary Pillar and 26 Shop Area
Figure 2	Plan showing outline of Backfill Project and Section Line "A-A"
Figure 3	Section through 26 Panel
Figure 4	Geological Sections through Shafts No. 1 and No. 2
Figure 5	26 Shop Area Geology
Figure 6	26 Shop Area Instrumentation Location Plan
Figure 7	Microseismic Activity - Sept 1-Dec. 31, 1987 - 26 Panel Area
Figure 8	Microseismic Activity - January 1-December 31, 1988 -26 Panel Area
Figure 9	Microseismic Activity - January 1-October 1, 1989 - 26 Panel Area
Figure 10	26 Shop Backfill Area Photograph Location Plan
Figure 11	Schematic, Backfill line to 26 Test Panel Area
Figure 12	1 Shaft area Microseismic Activity and Backfill Progression 1985
Figure 13	1 Shaft area Microseismic Activity and Backfill Progression 1986
Figure 14	1 Shaft area Microseismic Activity and Backfill Progression 1987-88-89

Figure 15	Seismic Events Prefilling
Figure 16	Seismic Energy Measured - Boundary Pillar Area Denison Mine side.
Figure 17	Seismic Energy Measured - 26 Panel Area
Figure 18	In-situ pressure - closure characteristics of Backfill
Figure 19	Laboratory Set-up of Rock/Backfill Tests
Figure 20	Stress Closure Characteristics of Rock Surrounded by Different Types of Fill

APPENDICES

#1	Contract Milestones
#2	Trow Report on Pressuremeter Testing
#3	Queen's Report on Pressuremeter Testing
#4	Photographic Records

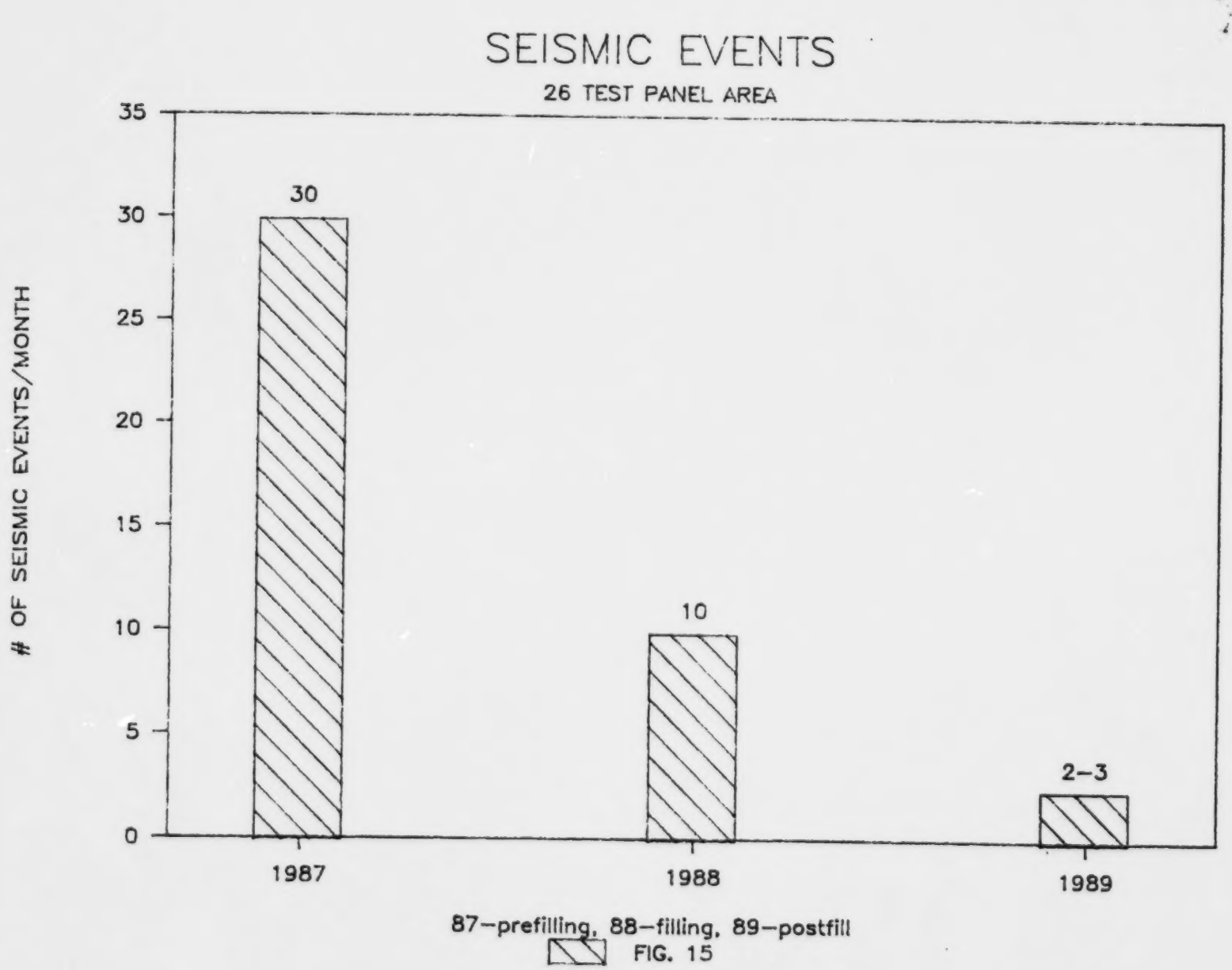
SEISMIC EVENTS
26 TEST PANEL AREA
OF SEISMIC EVENTS/MONTH
35
30
25
20
15
10
5
0
30
10
2–3
1987
1988
1989
87–prefilling, 88–filling, 89–postfill

FIG. 15

SEISMIC ENERGY MEASURED

BOUNDARY PILLAR AREA DENISON MINE SIDE

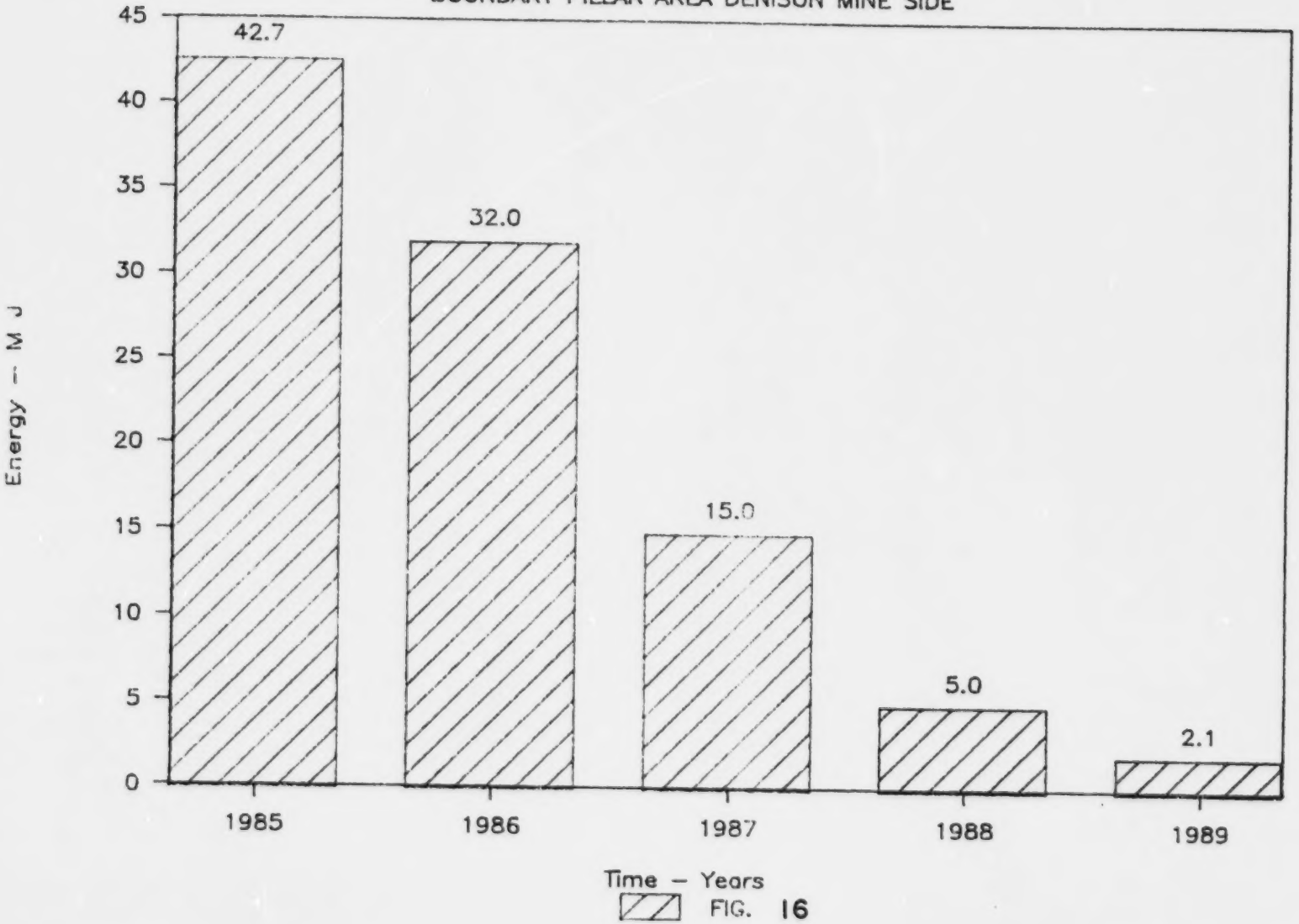

FIG. 16

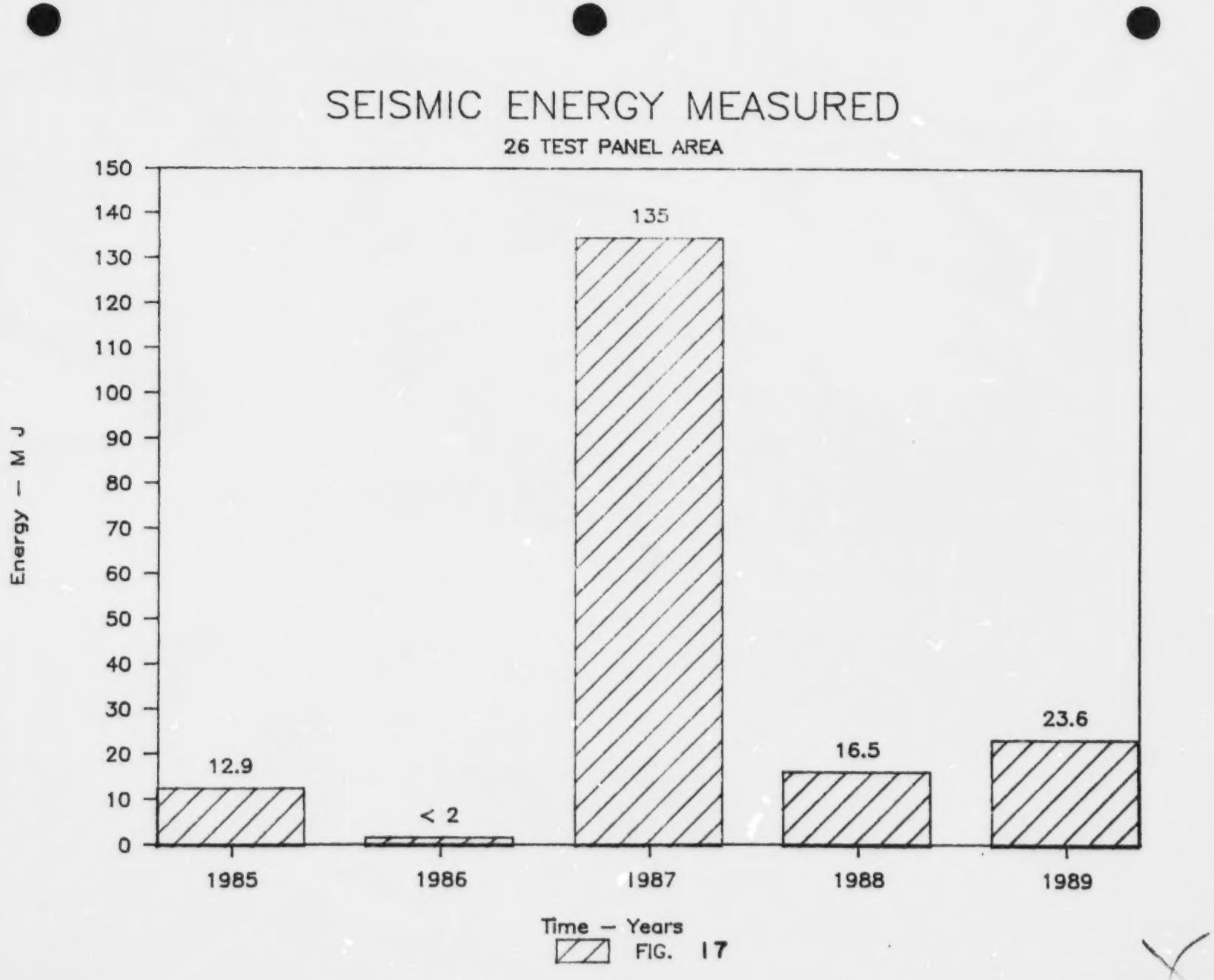
SEISMIC ENERGY MEASURED
26 TEST PANEL AREA
Energy – M J
150
140
130
120
110
100
90
80
70
60
50
40
30
20
10
0
12.9
< 2
135
16.5
23.6
1985
1986
1987
1988
1989
Time – Years

FIG. 17

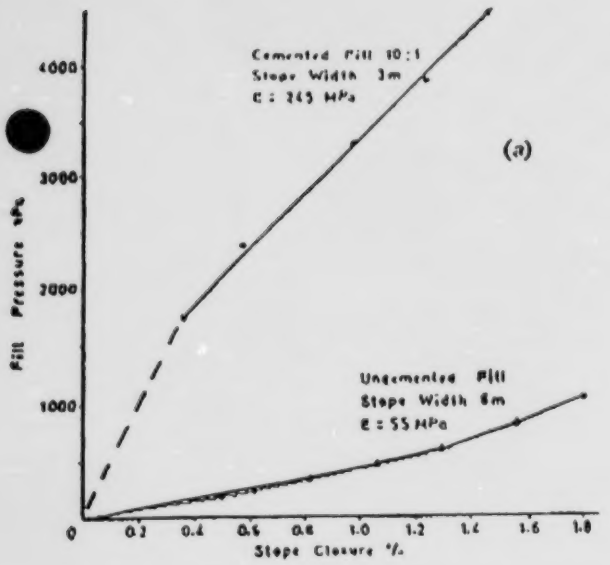

FIG. 18 In-situ pressure-closure characteristics of backfill

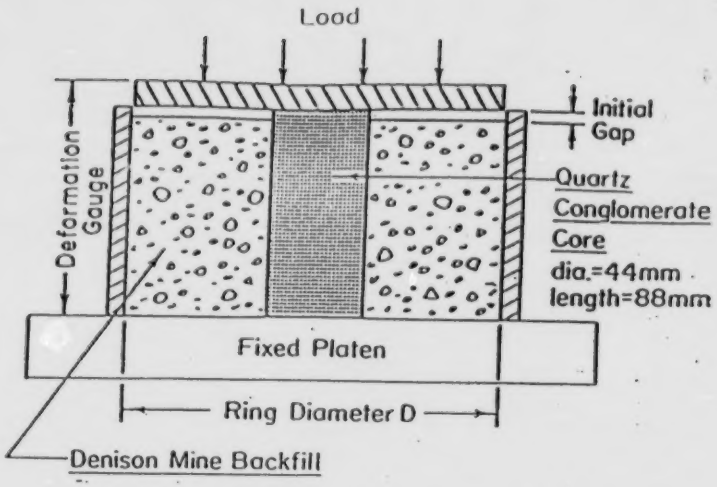

FIG. 19 Laboratory Set-Up of Rock / Backfill Tests

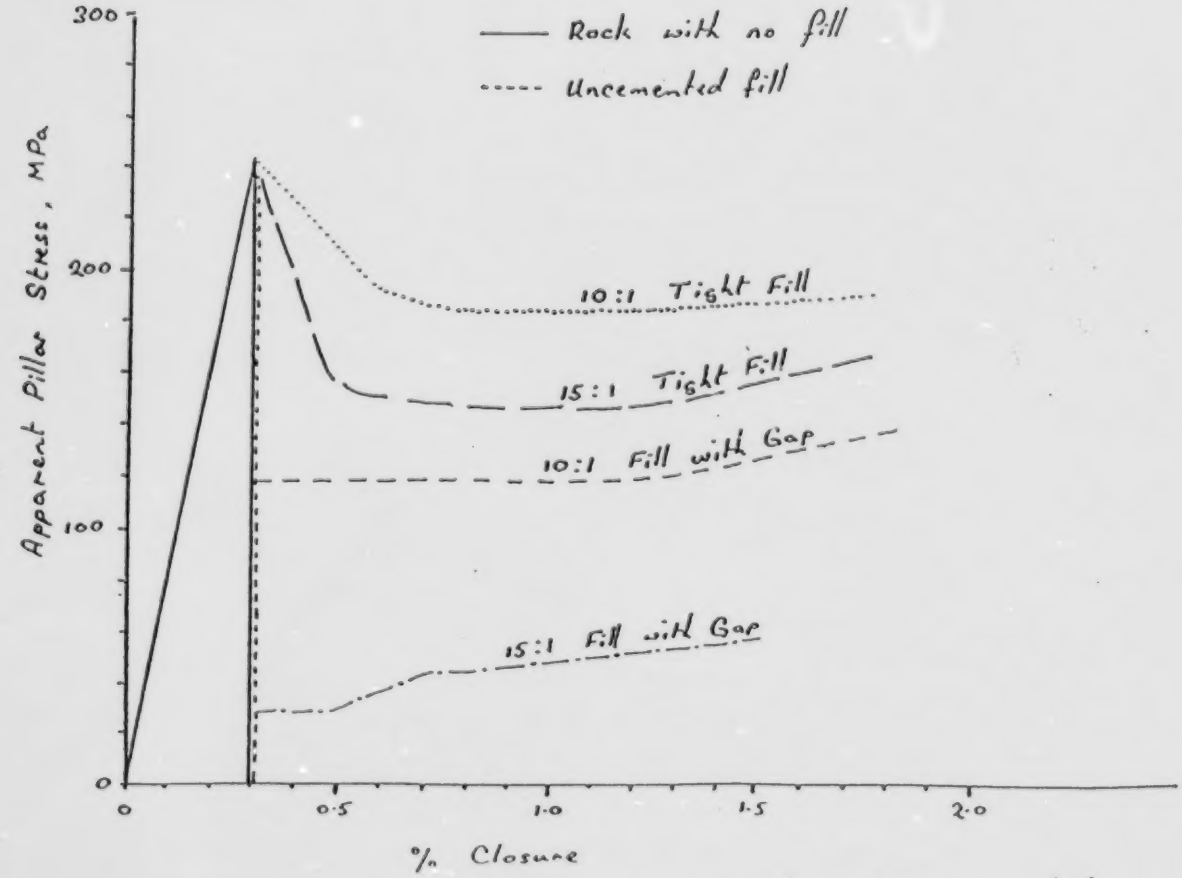

FIG. 20 Stress-Closure characteristics of rock surrounded by different types of backfill.

APPENDIX 1

CONTRACT SERIAL NUMBER / NUMÉRO DE SÉRIE DU CONTRAT
23440-6-9010/01-SQ.

CONTINUATION

DSS FILE NUMBER - NUMÉRO DU DOSSIER MAS
15SQ.23440-6-9010

BASIS OF PAYMENT

The Contractor will be paid in accordance with the following:

Task No.	Description		Amount	Completion
1	Pump and rehab 26305	Firm	$20,200.00	July 86
2	Muck out slimes, drill accelerometer holes	Firm	$ 7,100.00	July 86
3	Secure opening at raise	Firm	$ 4,500.00	July 86
4	Prepare auxiliary ventilation	Firm	$ 2,600.00	July 86
5	Permanent ventilation to 26 garage	Firm	$27,500.00	August 86
6	Run accelerometer cables	Firm	$31,800.00	August 86
7	Drill holes completed for equipment	Firm	$ 6,000.00	August 86
8	Run shaft cables	Firm	$22,500.00	September 86
9	Set up monitoring station and meters	Firm	$ 4,000.00	September 86
10	Run fill line to Panel 18	Firm	$ 2,000.00	September 86
11	Run fill line to Panel 20	Firm	$ 2,000.00	September 86
12	Run fill line to Panel 24	Firm	$ 2,000.00	September 86
13	Run fill line to Panel 26	Firm	$ 2,000.00	September 86
14	Construct first fill fence 26305	Firm	$ 9,000.00	October 86
15	Construct second fill fence 26305	Firm	$20,400.00	October 86
16	Hook up seismic system/Queen's work	Firm	$35,800.00	November 86
17	Run mousetraps in stopes (added ones)	Firm	$ 7,500.00	December 86
18	Run drainage to raise (cable)	Firm	$10,000.00	December 86
19	Run drainage to Stanrock	Firm	$14,500.00	January 87
20	Rehab 24 Panel	Firm	$12,000.00	March 87
21	Run fill line to discharge points	Firm	$18,500.00	March 87
22	Assess prefill status of area and report	Firm	$22,000.00	April 87
23	Place 15,000 tons of fill	Firm	$17,000.00	May 87
24	Assess ground conditions and report	Firm	$16,000.00	May 87
25	Place another 20,000 tons of fill	Firm	$21,500.00	July 87
26	Assess ground conditions and report	Firm	$16,000.00	July 87
27	Build third fill fence	Firm	$ 7,000.00	September 87
28	Pour another 20,000 tons of fill	Firm	$21,500.00	September 87
29	Assess ground conditions and report	Firm	$16,000.00	September 87
30	Pour another 20,000 tons of fill	Firm	$21,500.00	November 87
31	Assess ground conditions and report	Firm	$16,000.00	November 87
32	Pour remaining fill	Firm	$12,000.00	December 87
33	Assess ground conditions and report	Firm	$16,000.00	January 88
34	Adjust ventilation requirements	Firm	$15,000.00	March 88
35	Adjust microseismic equipment	Firm	$28,600.00	March 88
36	Install remaining convergence stations	Firm	$ 8,000.00	April 88
37	Rehab 24951 E	Firm	$14,000.00	April 88
38	Monitor pillar deterioration, test	Firm	$12,000.00	May 88
39	Conduct dilitometer tests	Firm	$22,000.00	June 88
40	Queen's preliminary research report	Firm	$20,000.00	August 88
41	Denison preliminary research report	Firm	$16,000.00	September 88
42	Acceptance of final report	Firm	$ 5,000.00	March 89
43	Conduct final research seminar	Firm	$ 5,000.00	March 89
		TOTAL	$610,000.00 est.	

LIMITATION OF EXPENDITURE

No increase in the total liability of Her Majesty resulting from any design changes, modifications or interpretations of specifications, made by the Contractor, will be authorized or paid to the Contractor unless such design changes, modifications or interpretations, have been approved by this Department prior to their incorporation in the work.

Supply and Services Canada | Approvisionnements et Services Canada

DSS-MAS 9143-2 (4/81)

CONTRACT PLAN AND REPORT FORM – FORMULE DE PROJET DE CONTRAT ET DE RAPPORT

CONTRACT TITLE – TITRE DU CONTRAT: GISMO DEVELOPMENT, ENGINEERING MODEL

CONTRACTOR – ENTREPRENEUR: ACME INDUSTRIES LTD.

FILE NO. – N° DU DOSSIER	SERIAL NO. – N° DE SÉRIE

TASK DESCRIPTION DESCRIPTION DE LA TÂCHE	TASK DURATION IN MONTHS – DURÉE DE LA TÂCHE EN MOIS												TASK COST – COÛT DE LA TÂCHE		
	1 MAY MAI	2 JUNE JUIN	3 JULY JUILLET	4 AUG. AOÛT	5 SEPT. SEPT.	6 OCT. OCT.	7 NOV. NOV.	8 DEC. DÉC.	9 JAN. JANV.	10 FEB. FÉV.	11 MAR. MARS	12 APR. APRIL	PLANNED PRÉVU À L'ORIGINE	ACTUAL PRÉSENTEMENT	E.T.C. À VENIR
MECHANICAL SUBSYSTEM SOUS-SYSTÈME MÉCANIQUE													ALL NUMBERS IN MILLIONS TOUS LES CHIFFRES REPRÉSENTENT DES MILLIONS		
MATERIAL PROCUREMENT ACHAT DE MATÉRIEL													5M	4M	1M
FABRICATION													3M	1,2M	1,8M
ASSEMBLY ASSEMBLAGE													2M	–	2M
ELECTRICAL SUBSYSTEM SOUS-SYSTÈME ÉLECTRIQUE															
MATERIAL PROCUREMENT ACHAT DE MATÉRIEL													2,5M	2,5M	–
FABRICATION													2,5M	2,5M	–
ASSEMBLY ASSEMBLAGE													1M	.5M	.5M
DISPLAY, CONTROL SUBSYSTEM SOUS-SYSTÈ. DE CONTRÔLE DE L'AFFICHA.															
MATERIAL PROCUREMENT ACHAT DE MATÉRIEL													2M	1M	1M
FABRICATION													2M	1M	1M
ASSEMBLY ASSEMBLAGE													1M	–	1M
SYSTEM INTEGRATION INTÉGRATION DU SYSTÈME													3M	–	3M
SYSTEM TEST VÉRIFICATION DU SYSTÈME													2M	–	2M
PLANNED COST BY MONTH COÛT PRÉVU POUR CHAQUE MOIS	1,5M	3,1M	3,6M	5,1M	5,1M	2,1M	1,5M	1M	1M	1M	1M		PLAN 26M		
ACT. PRÉSEN. / E.T.C. BY MONTH PRÉVISION POUR CH. MOIS	.5M	3M	4,1M	5,1M	4,6M		1,1M	1,5M	1M	1M	1M	1M		ACTUAL COÛTS RÉELS 12,7M	E.T.C. À VENIR 13,3M

APPENDIX 2

IN-SITU BACKFILL TESTING

PREPARED FOR:

DENISON MINES LTD.

TROW ONTARIO LTD.

Toronto, Hamilton, London
Sudbury, North Bay, Ottawa

Project: S00029R
April 13, 1989

1074 Webbwood Drive
Sudbury, Ontario. P3C 3B7
TEL: (705) 674-9681
FAX: (705) 674-8271

Trow

Rock Mechanics and Mining Division

Trow Ontario Ltd.
Consulting Engineers
1074 Webbwood Drive
Sudbury, Ontario. P3C 3B7
Telephone: (705) 674-9681

S00029R

April 13, 1989

Denison Mines Ltd.
P. O. Box B2600
Elliot Lake, Ontario
P5A 2K2

ATTENTION: Mr. Cy Monahan, P. Eng.

Dear Sirs:

IN-SITU BACKFILL TESTING
P.O. # S-1963

Subsequent to our proposal dated February 7, 1989, and your authorization, Trow Ontario Ltd. undertook the work outlined in the aforementioned proposal. The testing program was to start on March 1, 1989, however once on site, we were informed that Denison personnel were not ready to start testing. Subsequently, the Trow Ontario Ltd.'s team returned to Sudbury and a new date of March 6th, was set as a starting date. The field work was completed on March 15, 1989.

1.0 INTRODUCTION

Testing of mine backfill was carried out at the two locations selected by Denison Mine personnel. These included the 22960 and 24070 bulkheads. A total of four boreholes were advanced by Denison, two at each bulkhead, to a nominal depth of 9.14 m (30'). The location of the boreholes at the 22960 and 24070 bulkheads are outlined on Dwgs. 1 and 2, respectively.

Pressuremeter tests were conducted at between .91 m (3') and 1.5 m (5') intervals along the length of each borehole with occasional tests being conducted at closer spacings. Nominally, between 6 and 10 tests were carried out at each borehole. In total 28 pressuremeter tests were conducted in four borehole locations.

2.0 PRESSUREMETER TESTING

Testing at site 1, backfill fence 22960, was conducted in two diamond drill holes. Borehole 1 was drilled at an angle of -5° from the horizontal. The total length of this hole was 9.14 m (30'). Drilling conditions were for the most part excellent with good core recovery. The core was subsequently saved for testing by Denison Mines. The gauge of this hole remained consistent. A probable sand zone was encountered at about .61 m (12') to 4.57 m (15') from the collapse.

Hole number 2 at the 22960 fill fence site was drilled at an angle of +25° from the horizontal with a total length of 7.93 m (26'). Again core recovery from this hole was good. The gauge of this hole remained consistent along its entire length.

Due to the nature of the fill material hole #1 at this location contained water, this however did not present any difficulties during the testing procedure.

The data related to boreholes 1 and 2 located at bulkhead 22960 is presented in Dwgs. 7 to 22 and is summarized in Dwgs. 3 and 4. The various zones encountered have been described as Grey Sand Fill, Grey Cemented Tailings and Grey/Green Cemented Tailings. It is our understanding that these classifications are based on the color of the return water and the difficulty of penetration. It is interesting to note that the pressuremeter tests conducted at various borehole depths were consistent with observed changes in the color of the drill water. Typically the data can be divided into two groups comprising cemented and uncemented materials. The first group indicated stiffnesses in the range of 60 to 80 MPa with occasional layering of stiffnesses greater than 90 MPa. The "uncemented" material indicates a stiffness range between .4 and .9 MPa with occasional slightly cemented areas with stiffnesses between 2 and 4 MPa.

At site 2, backfill fence 24070, two diamond drill holes were completed. Borehole number 3 was drilled at +38°. Drilling conditions on this hole were less ideal with only minor amounts of core being recovered. The gauge of the hole was expanded beyond 70 mm by the drilling process. Two probes were ruptured, possibly due to close proximity with the stope back (i.e., probe encounters sharp projections from the back). The total length of this hole was 9.14 m (30'). This hole was subsequently lost beyond 4.88 m to a sudden inflow of water at a rate of approximately 100 gpm. Borehole number 4 at this site also encountered soft material. Although the drilling was completed with little difficulty, very minor amounts of core was recovered. Testing with the pressuremeter indicated the hole was over-gauge resulting from the drilling procedure. Total length of the hole was 9.14 m (30 feet).

The data for boreholes 3 and 4 is reported in Dwgs. 23 to 34 and summarized on Dwgs. 5 and 6. The data was consistent with that observed in boreholes 1 and 2, with cemented materials showing stiffnesses in the order of 70 MPa and uncemented materials with stiffnesses below 1 MPa. In fact the data for borehole 2 is consistent with the observations made during drilling. It was observed that the drilling was "very soft" throughout the drill run, the pressuremeter data supports these observations.

3.0 CONCLUSIONS

The pressuremeter tests proved to be successful and reliable in defined subtle changes in material properties. The pressuremeter was also useful in detecting weak segregation zones. It is noted here that the data reported in this report is consistent with that reported by Piciacchia[1] using the Pencel Pressuremeter, see Appendix 1.

Typically, the cemented material indicates stiffnesses in the range between 60 and 80 MPa and uncemented and/or saturated materials with stiffnesses below 1 MPa.

Should you have any questions, please do not hesitate to contact our office.

Yours very truly,
TROW ONTARIO LTD.

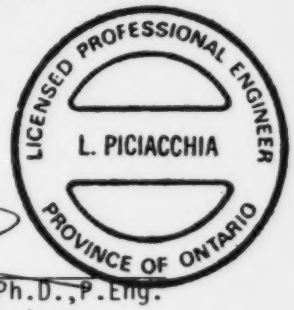

Luciano Piciacchia, Ph.D., P.Eng.
Sr. Rock Mechanics Engineer

LP:lstp
Encl.
Dist: Denison Mines Ltd. (3)
Mr. C. Monahan, P. Eng.

BACKFILL — BOREHOLE LOG

Trow

Drawing No. 3

Project: Denison Backfill Testing	Orientation: -5°	Collar Elevation:	Datum:	Borehole No.: 1
Location: 22960 Bulkhead	Date Started: Mar. 6/89	Completed: Mar. 6/89	Logged By: C.P.	Sheet 1 of 1
Client: Denison Mines Ltd.	Drilling Agency: Denison	Drill Type: JV/ Truck Mount	Core Barrel & Bit Design: Shoe Bit/BQ	Project No.: S00029R

DEPTH m / ft	GENERAL DESCRIPTION	PRESSUROMETER TEST DEPTH ■	MODULUS MPa	LIMIT PRESSURE	COMMENTS
1	2	3	4	5	6
	Grey Cemented Tailings Fill	.91 2.44	75.9 84.4		Grey Sand Fill
2.44	Grey/green Cemented Tailings Fill	3.96	53.3		Grey Cemented Tailings
3.96	Grey Sand Fill	4.57	.83		
4.57	Grey/green Cemented Tailings	5.18 5.79 6.40 7.01 7.93 8.84	66.5 70.2 69.4 75.3 71.7 67.1		Grey/ Green Cemented Tailings
9.14	E.O.H.				

REMARKS Material descriptions provided by Denison Mines Ltd.

BACKFILL — BOREHOLE LOG

Trow

Drawing No. 4

Project	Orientation	Collar Elevation	Datum	Borehole No.
Denison Backfill Testing	+25°			2
Location	**Date Started**	**Completed**	**Logged By**	**Sheet** 1 of 1
22960 Bulkhead	Mar. 7/89	Mar. 9/89	C.P.	
Client	**Drilling Agency**	**Drill Type** JV/	**Core Barrel & Bit Design**	**Project No.** S00029R
Denison Mines Ltd.	Denison	Truck Mount	Shoe Bit/BQ	

DEPTH m / ft	GENERAL DESCRIPTION	PRESSUREMETER TEST DEPTH m	MODULUS MPa	LIMIT PRESSURE	COMMENTS
1	2	3	4	5	6
	Grey Sandfill (grey cemented tailings)	.91	67.5		
.91 1	Probable Grey Sand fill (grey cemented tailings)	2.29	70.7		
5					
2		3.66	97.8		
3 10					
3.66	Grey Sand fill (grey cemented tailings)	4.88	88.7		
4 15					
4.88 5	Grey/Green Sand Fill (grey/green cement tailings)	6.10	81.1		
6.10 6 20					
	Grey/Green Cemented Tailings Fill -solid core recovered	7.62	116.4		
7					
25					
7.9 8	E.O.H.				
9 30					

Grey Sand Fill

Grey Cemented Tailings

Grey/ Green Cemented Tailings

REMARKS Most probable material descriptions have been redefined by Trow Ontario Ltd.

BACKFILL — BOREHOLE LOG

Trow

Drawing No. 5

Project	Orientation	Collar Elevation	Datum	Borehole No.
Denison Backfill Testing	+38°			3
Location	**Date Started**	**Completed**	**Logged By**	**Sheet**
24070 Bulkhead	Mar. 10/89	Mar. 13/89	C.P.	1 of 1
Client	**Drilling Agency**	**Drill Type**	**Core Barrel & Bit Design**	**Project No.**
Denison Mines Ltd.	Denison	JV/ Truck Mount	Shoe Bit/BQ	S00029R

DEPTH m / ft	GENERAL DESCRIPTION	PRESSUROMETER TEST DEPTH m	MODULUS MPa	LIMIT PRESSURE	COMMENTS
1	2	3	4	5	6
	Grey Sand Fill	.91	4.2		
		1.52	1.86		Grey Sand Fill
1.52 5					
	Green Cemented Tailing Fill	1.83	96.0		
2	(possibly some other backfill category below 3m)	2.74	22.0		
		3.05	72.3		Grey Cemented Tailings
3 10					
4					
4.20					
15	Grey Sand Fill	4.57	.63		Grey/ Green Cemented Tailings
4.88					
5	Could not be recorded				
6 20					
7					
25					
8					
9 30					
9.14					
	E.O.H.				

REMARKS Hole lost below 4.86 m, water inflow at ±100 Gpm noted.

BACKFILL — BOREHOLE LOG

Trow

Drawing No. 6

Project: Denison Backfill Testing	Orientation: +12°	Collar Elevation:	Datum:	Borhole No.: 4
Location: 24070 Bulkhead	Date Started: Mar. 14/89	Completed: Mar. 15/89	Logged By: C.P.	Sheet: 1 of 1
Client: Denison Mines Ltd.	Drilling Agency: Denison	Drill Type: JV/ Truck Mount	Core Barrel & Bit Design: Shoe Bit/BQ	Project No.: S00029R

DEPTH m / ft	GENERAL DESCRIPTION	PRESSUREMETER TEST DEPTH m	MODULUS MPa	LIMIT PRESSURE	COMMENTS
1	2	3	4	5	6
0	Grey Sand Fill				
1	(very soft drilling)	1.52	1.86		Grey Sand Fill
2					
3		3.05	.87		Grey Cemented Tailings
4					
5		4.57	.50		Grey/ Green Cemented Tailings
6		6.10	.50		
7					
8		7.32	.40		
9		8.84	.44		
9.14					

REMARKS

TROW
DILATOMETER/PRESSUREMETER TESTS

BOREHOLE Nº :	1
TEST Nº :	3
DEPTH :	3'
HOLE SIZE :	BQ

PROJECT Nº :	S00029R
SITE :	Backfill Fence 22960

SURFACE ELEVATION :

TEST ELEVATION :

PRESSURE	READINGS			INJECTED VOLUME (cc)	CORRECTED VOLUME (cc)
	1 min.	2 min.	3 min.		
12				350	
25				400	
30				450	
50				500	
70				550	
112				600	
175				650	
350				700	
750				750	
1000				770	
1375				800	
1900				850	

VOLUMETRIC CALIBRATION :

OBSERVATIONS : $\mu = .33$ $\Delta V = 800 - 750 = 50$ cc $\Delta p = 625$ Kpa

$V_m = 775$ cc

$E_\phi = 2.66\ (1270 + 775)\left(\frac{1}{50/625 - .84\times10^{-2}}\right) = 75975.46$ Kpa

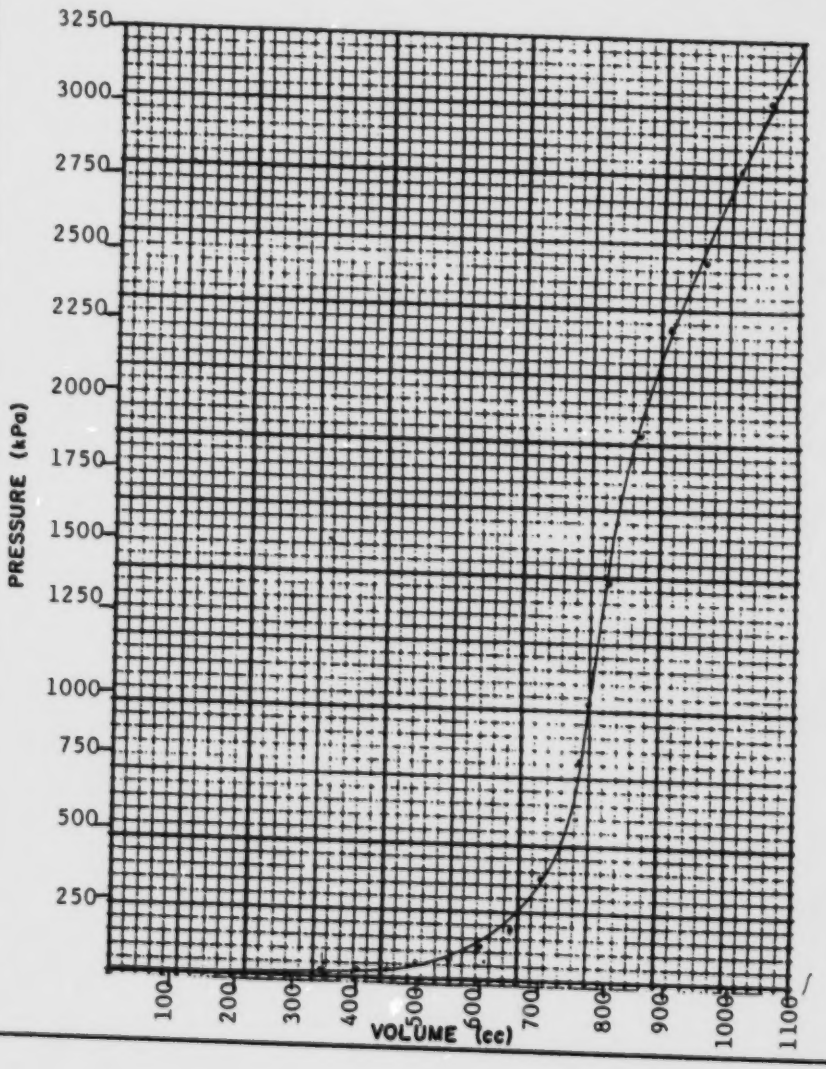

Drawing No. 7

TROW
DILATOMETER/PRESSUREMETER TESTS

BOREHOLE Nº	1
TEST Nº	cont'd
DEPTH	3'
HOLE SIZE	BQ

PROJECT Nº	S00029R
SITE	Backfill Fence 22960

SURFACE ELEVATION :

TEST ELEVATION :

PRESSURE	READINGS			INJECTED VOLUME (cc)	CORRECTED VOLUME (cc)
	1 min.	2 min.	3 min.		
900				900	
950				950	
1000				1000	
1050				1050	
3250				1100	

VOLUMETRIC CALIBRATION :

OBSERVATIONS :

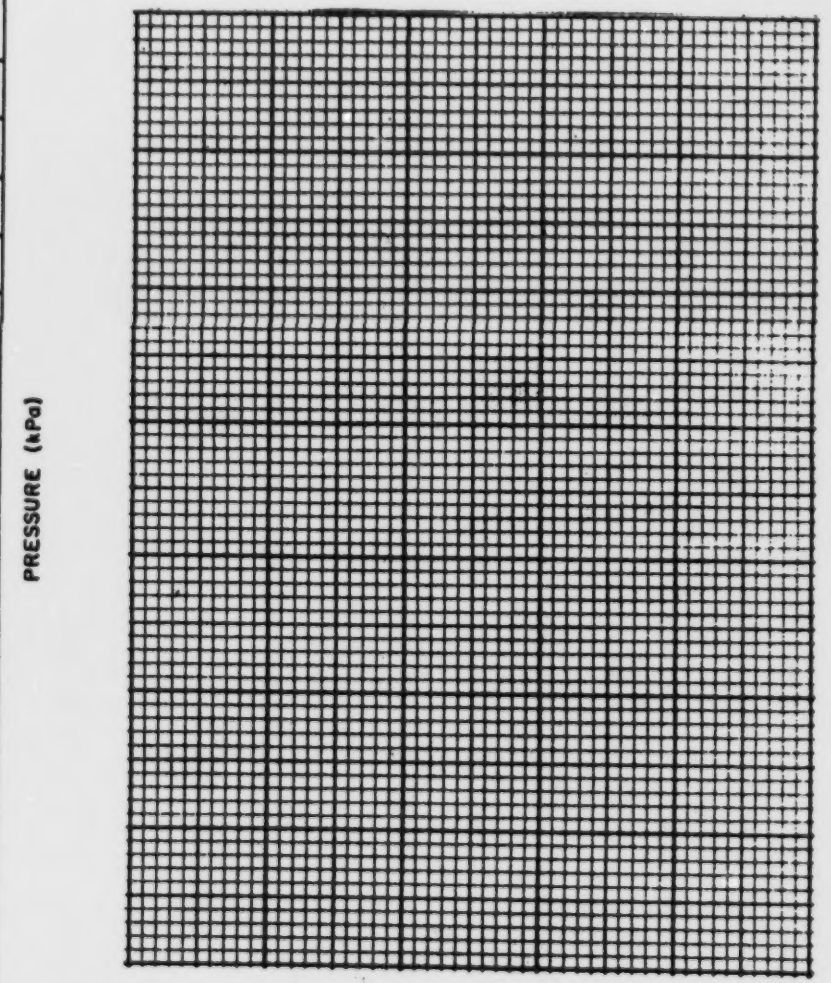

Drawing No. 7 (cont'd)

TROW
DILATOMETER/PRESSUREMETER TESTS

BOREHOLE Nº :	1
TEST Nº :	2
DEPTH :	8
HOLE SIZE :	BQ

PROJECT Nº :	S00029R
SITE :	Backfill Fence 22960

SURFACE ELEVATION :

TEST ELEVATION :

PRESSURE	READINGS			INJECTED VOLUME (cc)	CORRECTED VOLUME (cc)
	1 min.	2 min.	3 min.		
12				300	
20				350	
25				400	
28				450	
30				500	
50				550	
75				600	
100				650	
140				700	
212				750	
359				800	
712				850	

VOLUMETRIC CALIBRATION :

OBSERVATIONS : $\mu = .33$ ΔV 910 − 850 = 60cc ΔP = 788 Kpa

V_m = 880 cc

$E_\phi = 2.66 \quad (1270 + 880) \dfrac{1}{60/788 - .84 \times 10^{-2}} = 84423.09$ Kpa

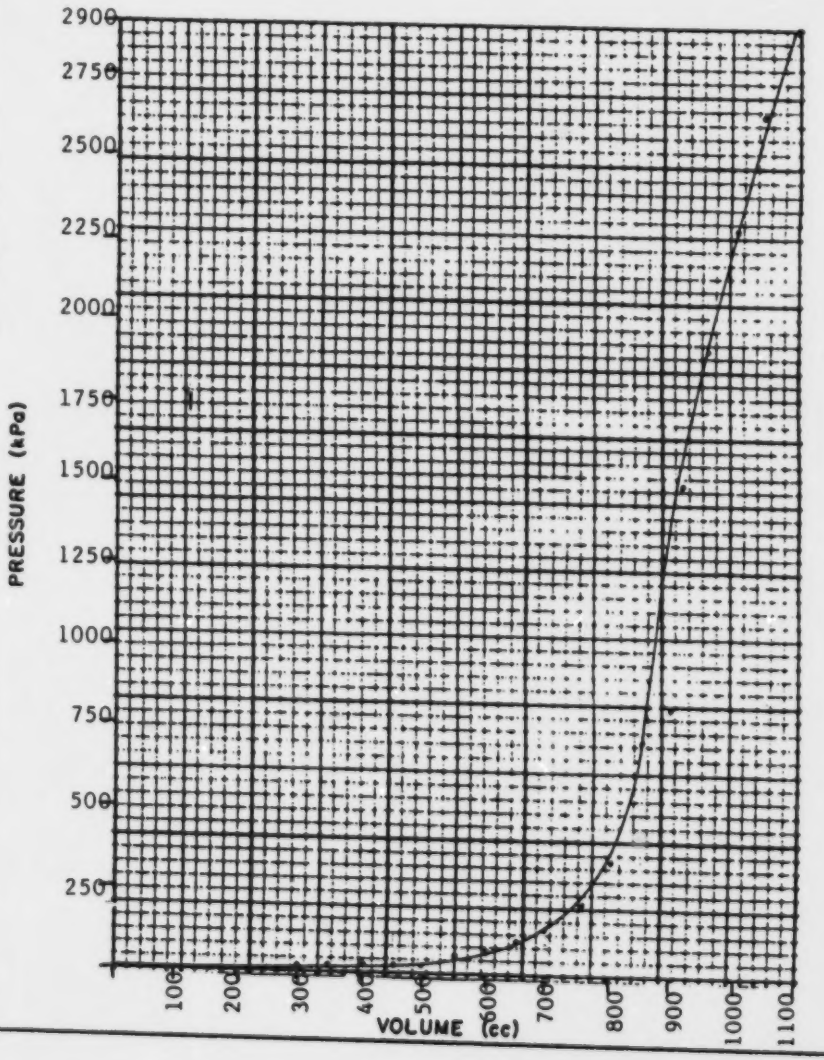

Drawing No. 8

TROW
DILATOMETER/PRESSUREMETER TESTS

BOREHOLE Nº : 1
TEST Nº : cont'd
DEPTH : 8
HOLE SIZE : BQ

PROJECT Nº : S00029R
SITE : Backfill Fence 22960

SURFACE ELEVATION :

TEST ELEVATION :

PRESSURE	READINGS			INJECTED VOLUME (cc)	CORRECTED VOLUME (cc)
	1 min.	2 min.	3 min.		
825				900	
1500				910	
1925				950	
2300				1000	
2650				1050	
2900				1100	

VOLUMETRIC CALIBRATION :

OBSERVATIONS :

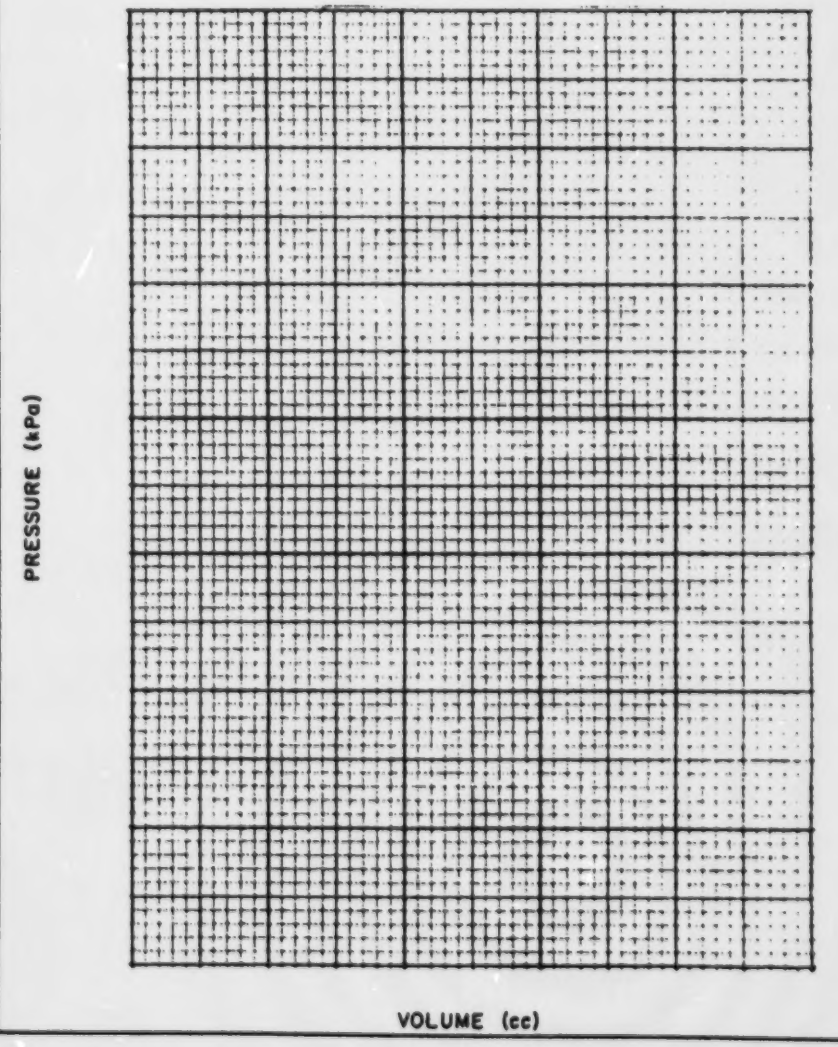

TROW
DILATOMETER/PRESSUREMETER TESTS

BOREHOLE Nº :	1
TEST Nº :	1
DEPTH :	13
HOLE SIZE :	BQ

PROJECT Nº : S00029R
SITE : Backfill Fence 22960

SURFACE ELEVATION :

TEST ELEVATION :

PRESSURE	READINGS			INJECTED VOLUME (cc)	CORRECTED VOLUME (cc)
	1 min.	2 min.	3 min.		
12				250	
25				300	
28				350	
30				400	
50				450	
75				500	
100				550	
125				600	
175				650	
250				700	
375				750	
625				800	

VOLUMETRIC CALIBRATION :

OBSERVATIONS : $\mu = .33$ $\Delta V = 900 - 800 = 100$ cc $\Delta p = 875$ KPa

$V_m = 850$ cc

$$E_p = 2.66\,(1270 + 850)\left(\frac{1}{100/875 - .84\times10^{-2}}\right) = 53257.42 \text{ KPa}$$

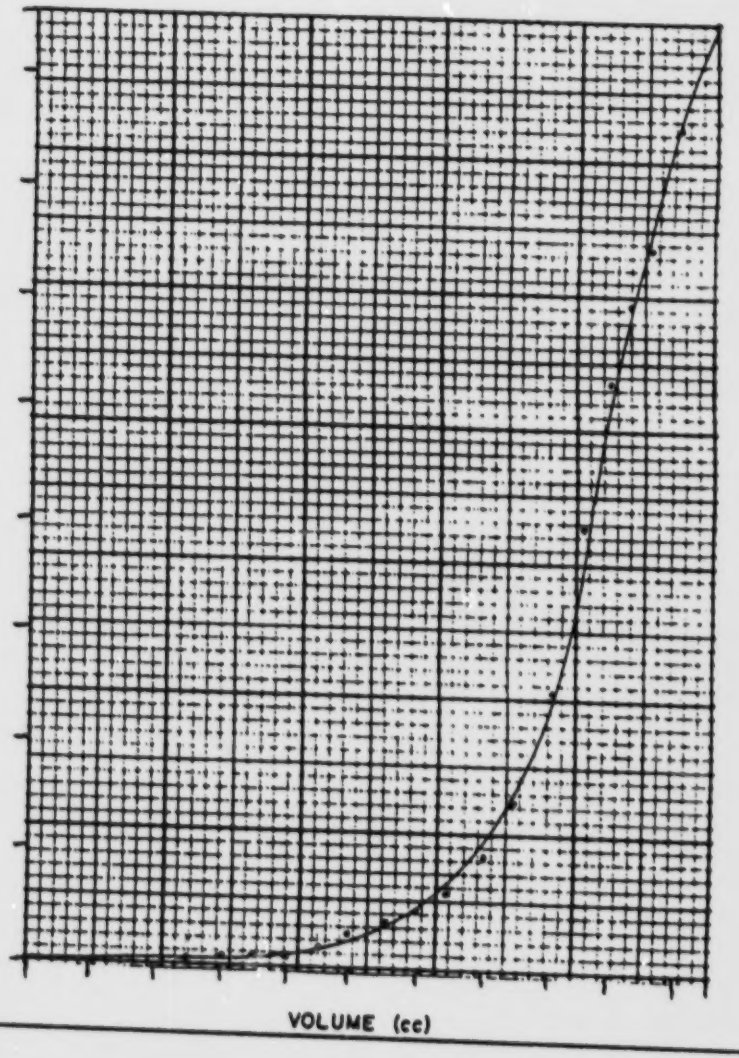

Drawing No. 9

TROW
DILATOMETER/PRESSUREMETER TESTS

SURFACE ELEVATION :	TEST ELEVATION :

BOREHOLE Nº : 1
TEST Nº : cont'd
DEPTH : 13
HOLE SIZE : BQ

PROJECT Nº : S00029R
SITE : Backfill Fence 22960

PRESSURE	READINGS			INJECTED VOLUME (cc)	CORRECTED VOLUME (cc)
	1 min.	2 min.	3 min.		
1325				850	
1500				900	
1625				950	
1900				1000	
2130				1050	

VOLUMETRIC CALIBRATION :

OBSERVATIONS :

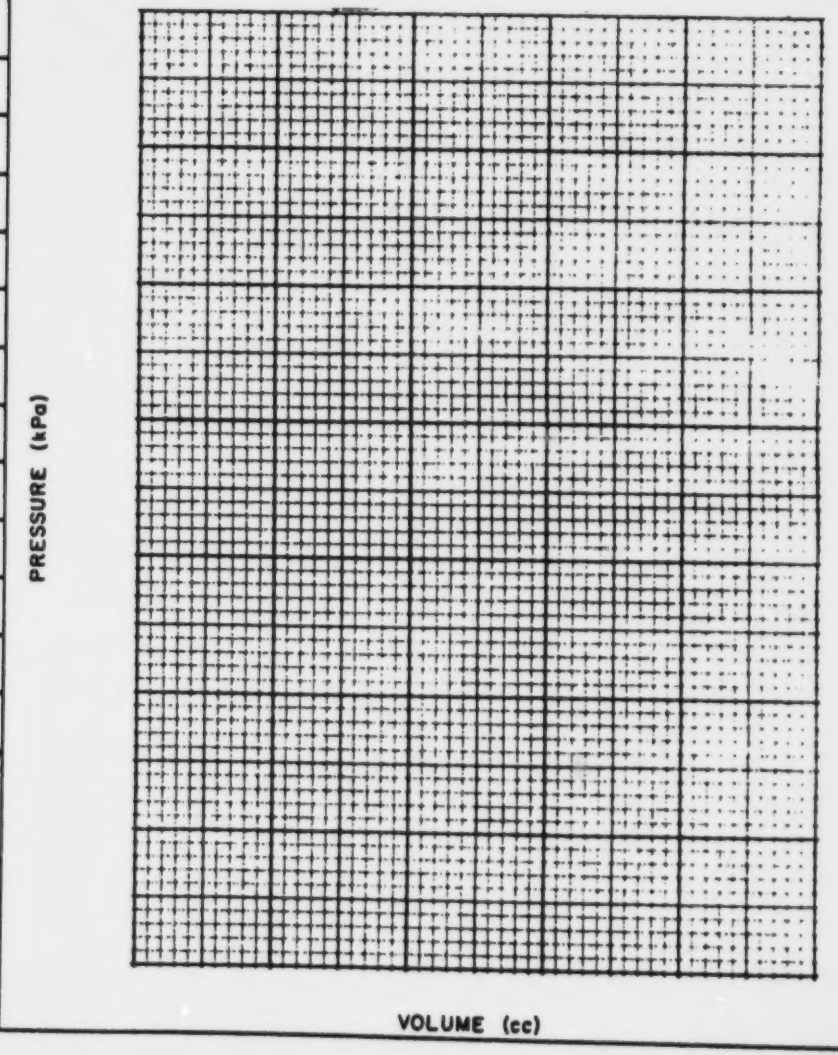

TROW
DILATOMETER/PRESSUREMETER TESTS

BOREHOLE Nº :	1
TEST Nº :	7
DEPTH :	15
HOLE SIZE :	BQ

PROJECT Nº :	S00029R
SITE :	Backfill Fence 22960

SURFACE ELEVATION :

TEST ELEVATION :

PRESSURE	READINGS			INJECTED VOLUME (cc)	CORRECTED VOLUME (cc)
	1 min.	2 min.	3 min.		
20				300	
25				350	
30				450	
50				550	
60				600	
70				650	
80				750	
90				800	
100				850	
100				900	
112				950	
120				1000	

VOLUMETRIC CALIBRATION :

OBSERVATIONS : $\alpha = .83$ $\Delta V = 750 - 450 = 300$ cc $\Delta p = 50$ Kpa

$V_m = 600$ cc

$E_p = 2.66 \ (1270 + 600) \left(\frac{1}{300/50 - .84 \times 10^{-2}} \right) = 830.20$ Kpa

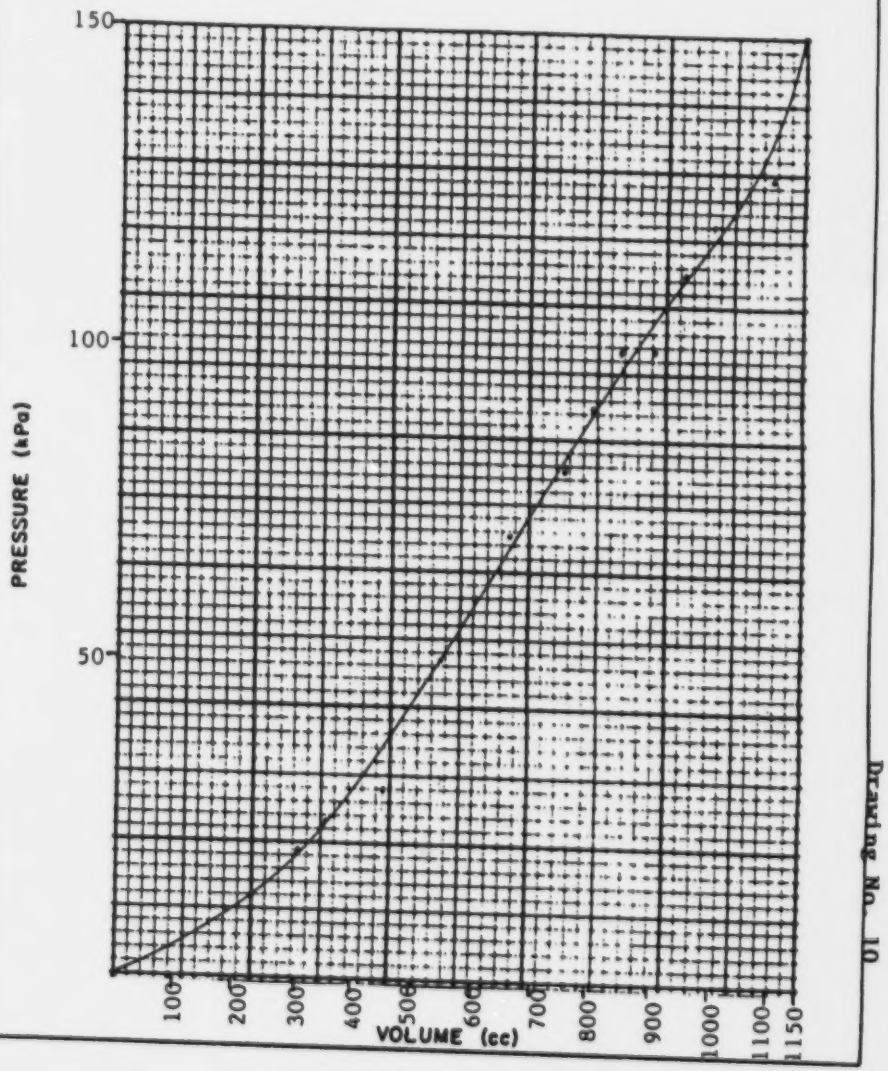

Drawing No. 10

TROW
DILATOMETER/PRESSUREMETER TESTS

BOREHOLE-Nº	1
TEST Nº	cont'd
DEPTH	15
HOLE SIZE	BQ

PROJECT Nº : S00029R
SITE : Backfill Fence 22960

SURFACE ELEVATION :

TEST ELEVATION :

PRESSURE	READINGS			INJECTED VOLUME (cc)	CORRECTED VOLUME (cc)
	1 min.	2 min.	3 min.		
127				1050	
150				1128	

VOLUMETRIC CALIBRATION :

OBSERVATIONS :

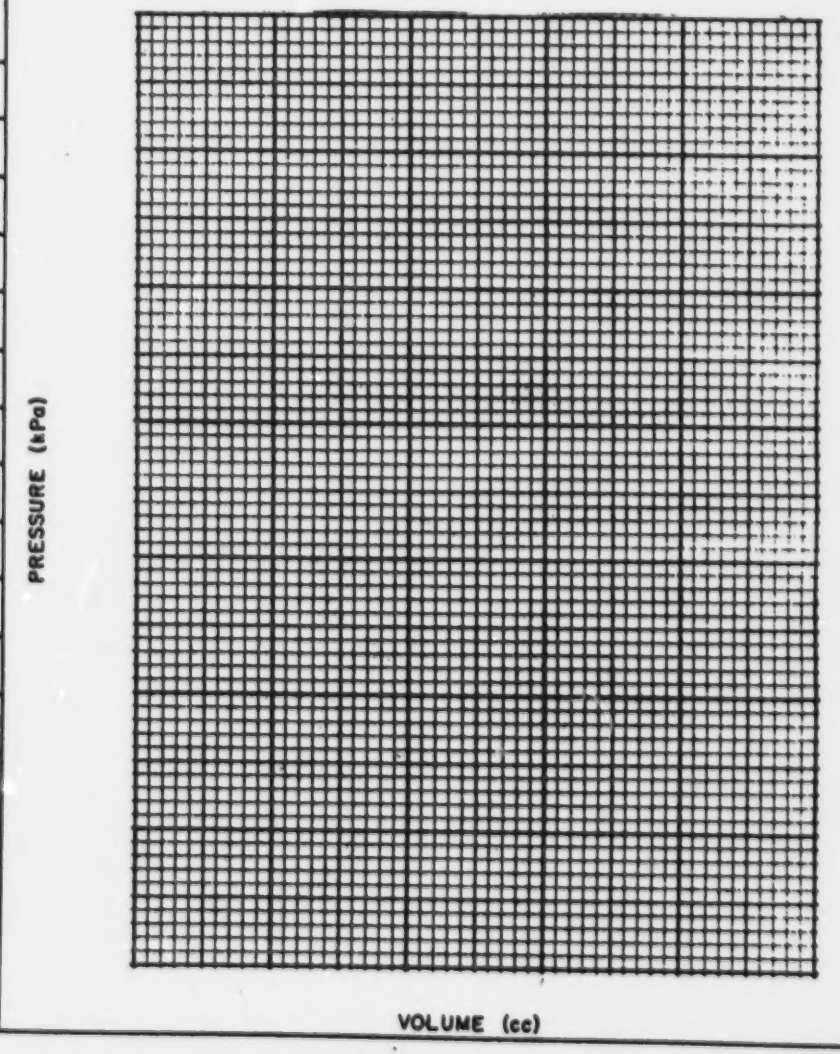

Drawing No. 10 (cont'd)

TROW
DILATOMETER/PRESSUREMETER TESTS

BOREHOLE Nº :	1
TEST Nº :	6
DEPTH :	17
HOLE SIZE :	BQ

PROJECT Nº : S00029R
SITE : Backfill Fence 22960

SURFACE ELEVATION :

TEST ELEVATION :

PRESSURE	READINGS			INJECTED VOLUME (cc)	CORRECTED VOLUME (cc)
	1 min.	2 min.	3 min.		
25				250	
70				350	
130				400	
412				450	
1025				500	
1675				550	
2100				600	
2500				650	
2700				700	
3000				750	
3200				800	
3350				850	

VOLUMETRIC CALIBRATION :

OBSERVATIONS : $u = .33$ $\Delta V = 550 - 450 = 100$ cc $\Delta p = 1263$ Kpa.

$V_m = 500$ cc

$$E_p = 2.66\,(1270 + 500)\left(\frac{1}{\frac{100}{1263} - .84\times10^{-2}}\right) = 66522 \text{ Kpa.}$$

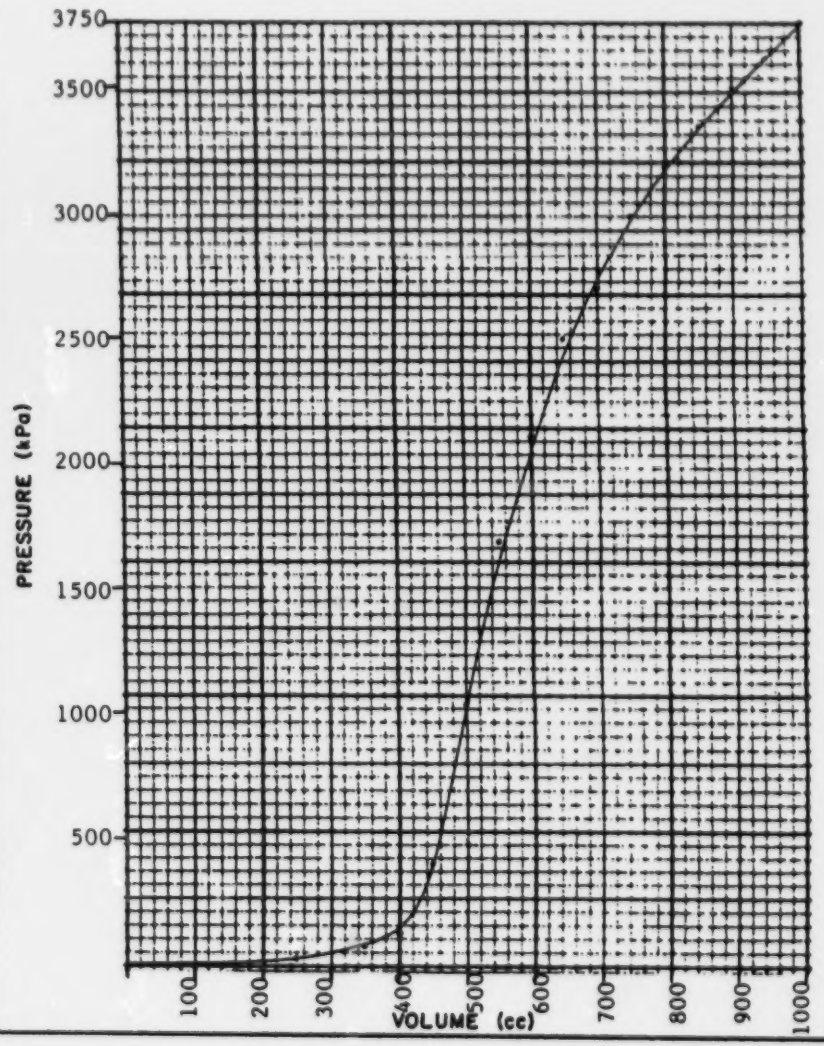

Drawing No. 11

TROW
DILATOMETER/PRESSUREMETER TESTS

BOREHOLE Nº : 1
TEST Nº : cont'd
DEPTH : 17
HOLE SIZE : BQ

PROJECT Nº : S00029R
SITE : Backfill Fence 22960

SURFACE ELEVATION :

TEST ELEVATION :

PRESSURE	READINGS			INJECTED VOLUME (cc)	CORRECTED VOLUME (cc)
	1 min.	2 min.	3 min.		
3500				900	
3600				950	
3750				1000	

VOLUMETRIC CALIBRATION :

OBSERVATIONS :

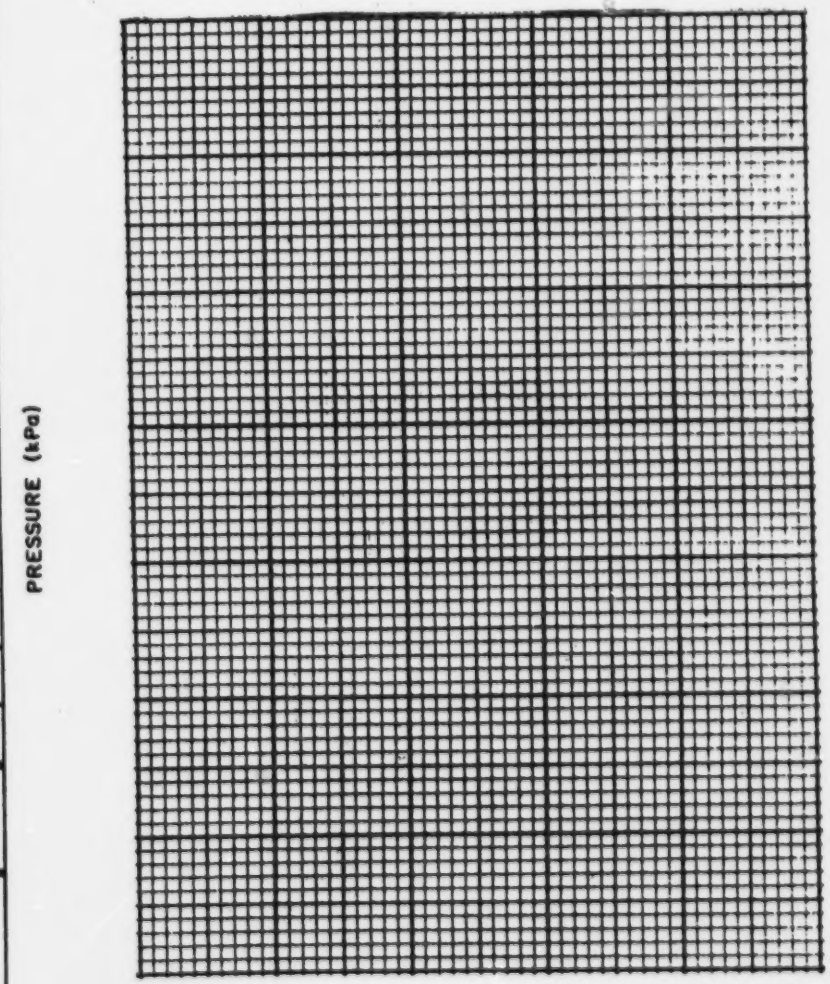

Drawing No. 11 (cont'd)

TROW
DILATOMETER/PRESSUREMETER TESTS

BOREHOLE Nº :	1
TEST Nº :	5
DEPTH :	19'
HOLE SIZE :	BQ

PROJECT Nº :	S00029R
SITE :	Backfill Fence 22960

SURFACE ELEVATION :

TEST ELEVATION :

PRESSURE	READINGS			INJECTED VOLUME (cc)	CORRECTED VOLUME (cc)
	1 min.	2 min.	3 min.		
12				250	
30				300	
75				350	
180				400	
575				450	
1000				480	
1300				500	
1900				550	
2250				600	
2500				650	
2800				700	
3000				750	

VOLUMETRIC CALIBRATION :

OBSERVATIONS : $\mu = .33$ $\Delta V = 550 - 450 = 100$ cc $\Delta P = 1325$ Kpa $V_m = 500$ cc

$E_p = 2.66 \ (1270 + 500) \left(\frac{1}{\frac{110}{1325} - .84 \times 10^{-2}} \right) = 70196.52$ Kpa

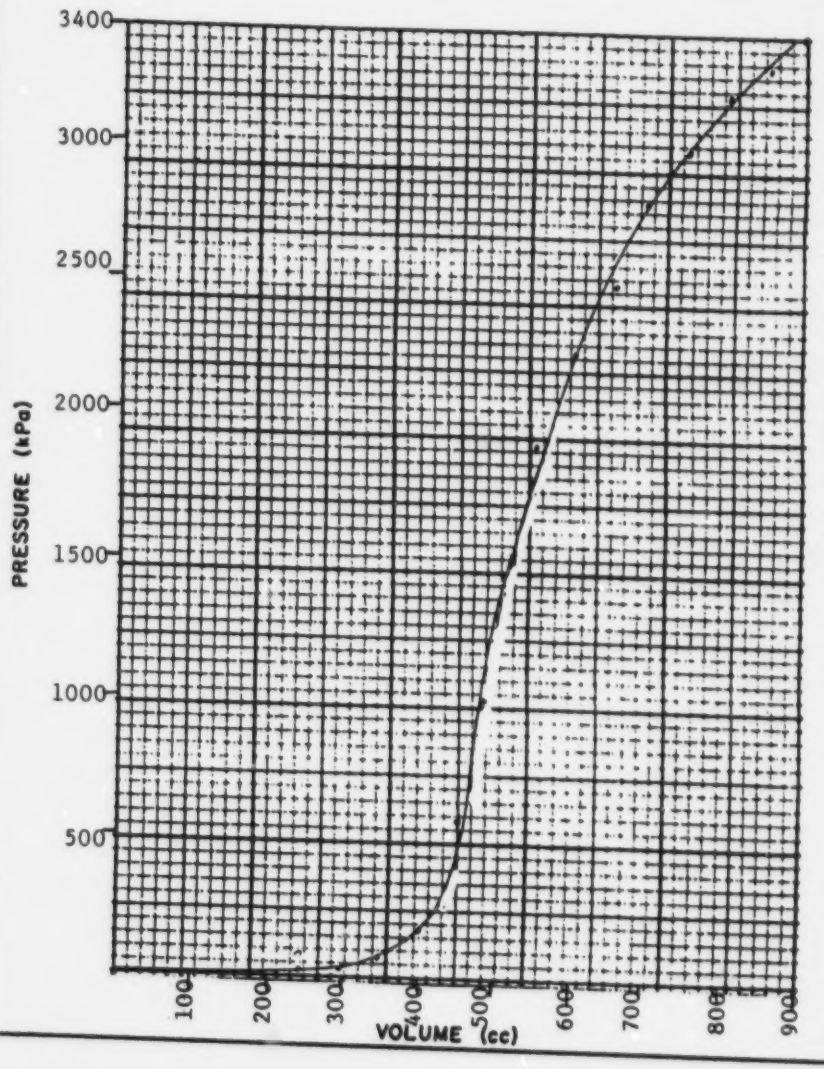

Drawing No. 12

TROW
DILATOMETER/PRESSUREMETER TESTS

BOREHOLE-Nº	1
TEST Nº	cont'd
DEPTH	19
HOLE SIZE	BQ

PROJECT Nº : S00029R
SITE : Backfill Fence 22960

SURFACE ELEVATION :

TEST ELEVATION :

PRESSURE	READINGS			INJECTED VOLUME (cc)	CORRECTED VOLUME (cc)
	1 min.	2 min.	3 min.		
3200				800	
3300				850	
3400				900	

VOLUMETRIC CALIBRATION :

OBSERVATIONS :

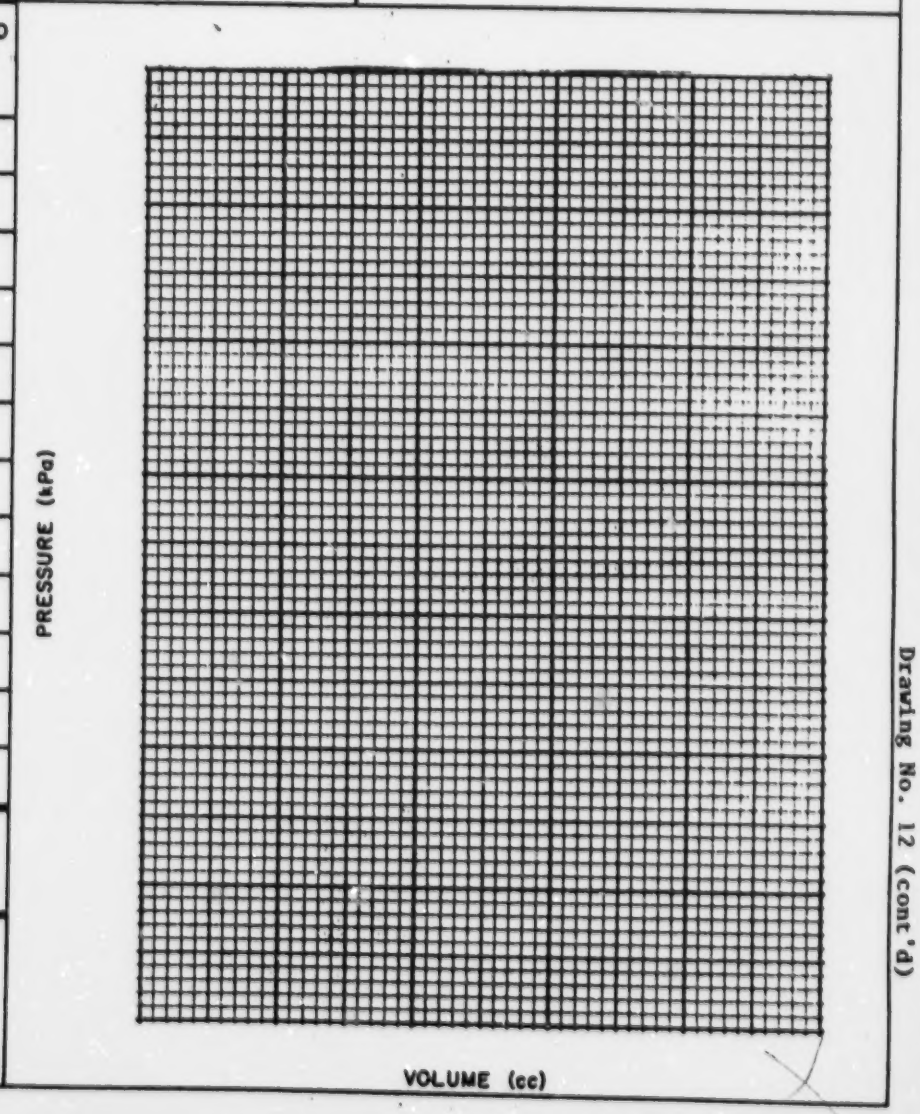

Drawing No. 12 (cont'd)

TROW
DILATOMETER/PRESSUREMETER TESTS

BOREHOLE Nº :-	1
TEST Nº :	4
DEPTH :	21
HOLE SIZE :	BQ

PROJECT Nº :	S00029R
SITE :	Backfill Fence 22960

SURFACE ELEVATION :

TEST ELEVATION :

PRESSURE	READINGS			INJECTED VOLUME (cc)	CORRECTED VOLUME (cc)
	1 min.	2 min.	3 min.		
25				200	
81				250	
275				300	
800				350	
1000				360	
1500				400	
2000				450	
2325				500	
2600				550	
2900				600	
3000				650	
3300				700	

VOLUMETRIC CALIBRATION :

OBSERVATIONS : $\mu = .33$ $\Delta V = 400 - 350 = 50$ cc $\Delta P = 700$ Kpa.

$V_m = 375$ cc

$$E_\phi = 2.66 \quad (12.70 + 375) \left(\frac{1}{50/700 - .84 \times 10^{-2}} \right) = 69424.07 \text{ Kpa.}$$

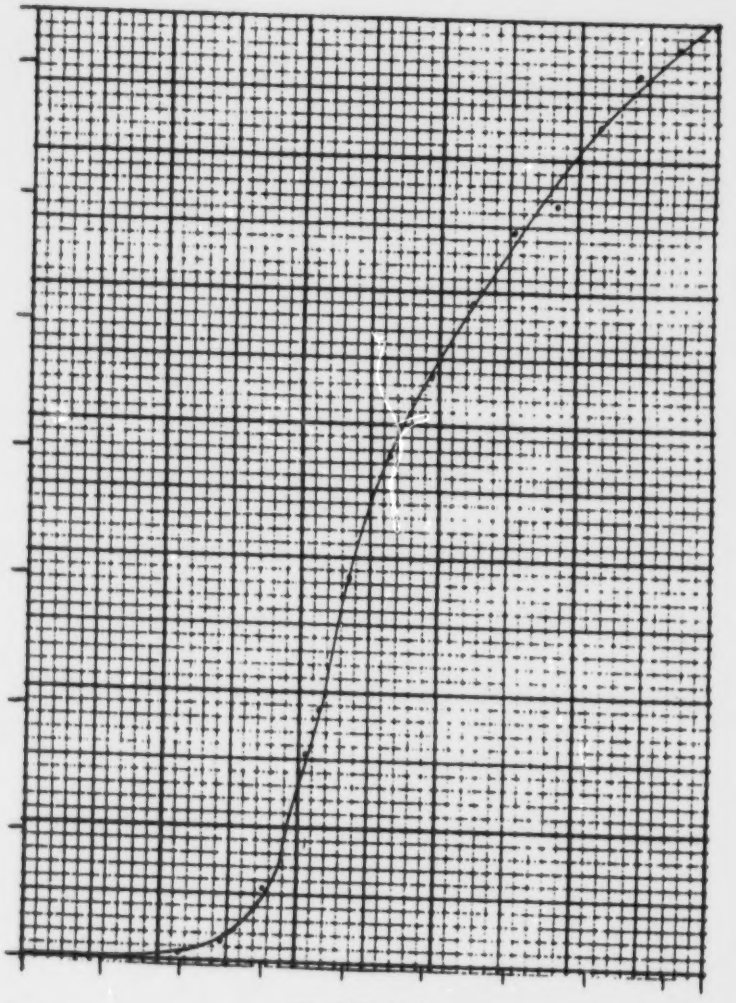

Drawing No. 13

TROW
DILATOMETER/PRESSUREMETER TESTS

BOREHOLE Nº : 1
TEST Nº : cont'd
DEPTH : 21
HOLE SIZE : BQ

PROJECT Nº : S00029R
SITE : Backfill Fence 22960

SURFACE ELEVATION :

TEST ELEVATION :

PRESSURE	READINGS			INJECTED VOLUME (cc)	CORRECTED VOLUME (cc)
	1 min.	2 min.	3 min.		
3500				750	
3600				800	
3700				850	

VOLUMETRIC CALIBRATION :

OBSERVATIONS :

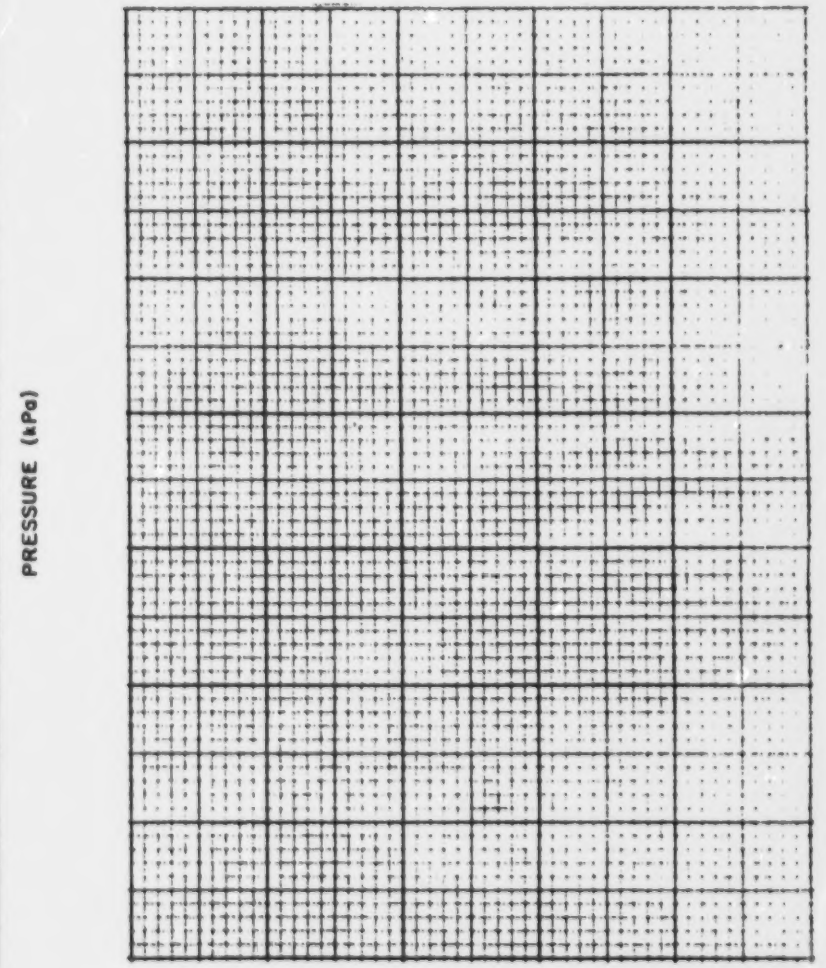

TROW
DILATOMETER/PRESSUREMETER TESTS

BOREHOLE Nº :	1
TEST Nº :	10
DEPTH :	23
HOLE SIZE :	BQ

PROJECT Nº : S00029R
SITE : Backfill Fence 22960

SURFACE ELEVATION :

TEST ELEVATION :

PRESSURE	READINGS			INJECTED VOLUME (cc)	CORRECTED VOLUME (cc)
	1 min.	2 min.	3 min.		
25				200	
40				250	
55				300	
75				350	
160				400	
500				450	
1230				500	
1910				550	
2325				600	
2676				650	
2850				700	
3190				750	

VOLUMETRIC CALIBRATION :

OBSERVATIONS : $u = .33$ $\Delta V = 550 - 450 = 100\,cc$ $\Delta p = 1410\ Kpa$

$V_m = 500\ cc$

$$E_p = 2.66\ (1270 + 500)\left(\frac{1}{100/1410 - .84 \times 10^{-2}}\right) = 75304.71\ Kpa$$

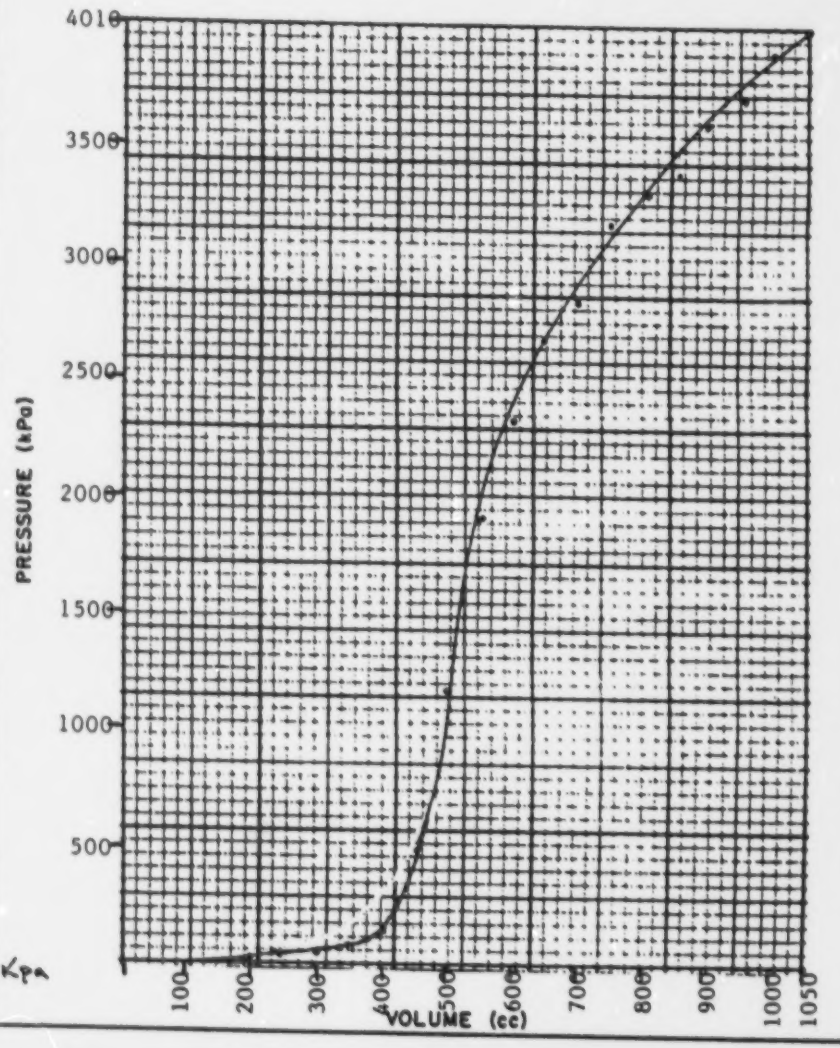

Drawing No. 14

TROW
DILATOMETER/PRESSUREMETER TESTS

BOREHOLE Nº : 1
TEST Nº : cont'd
DEPTH : 23
HOLE SIZE : BQ

PROJECT Nº : S00029R
SITE : Backfill Fence 22960

SURFACE ELEVATION :

TEST ELEVATION :

PRESSURE	READINGS			INJECTED VOLUME (cc)	CORRECTED VOLUME (cc)
	1 min.	2 min.	3 min.		
3320				800	
3386				850	
3610				900	
3720				950	
3900				1000	
4010				1050	

VOLUMETRIC CALIBRATION :

OBSERVATIONS :

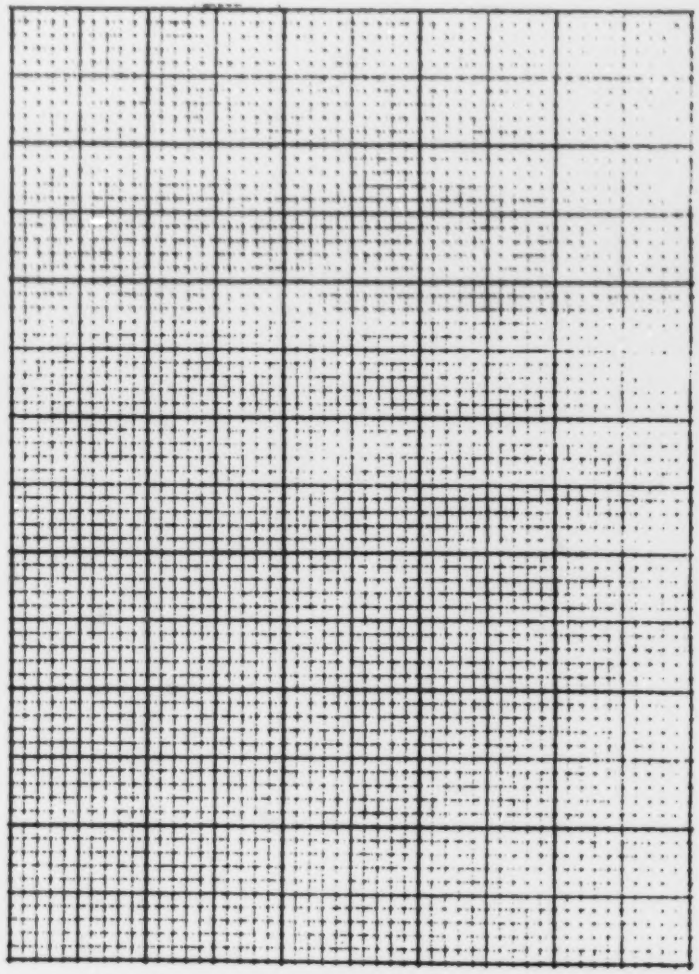

TROW
DILATOMETER/PRESSUREMETER TESTS

BOREHOLE Nº :	1
TEST Nº :	9
DEPTH :	26
HOLE SIZE :	BQ

PROJECT Nº :	S00029R
SITE :	Backfill Fence 22960

SURFACE ELEVATION :

TEST ELEVATION :

PRESSURE	READINGS			INJECTED VOLUME (cc)	CORRECTED VOLUME (cc)
	1 min.	2 min.	3 min.		
25				250	
35				300	
80				350	
260				400	
875				450	
1725				500	
2225				550	
2670				600	
3020				650	
3230				700	
3420				750	
3550				800	

VOLUMETRIC CALIBRATION :

OBSERVATIONS : $\mu = 0.33$ $\Delta V = 650 - 450 = 100$ cc $\Delta p = 1350$ Kpa

$V_m = 500$

$E_\phi = 2.66 \left(1270 + 500\right) \left(\frac{1}{100/1350 - 0.84 \times 10^{-2}} \right) = 71690.39$ Kpa

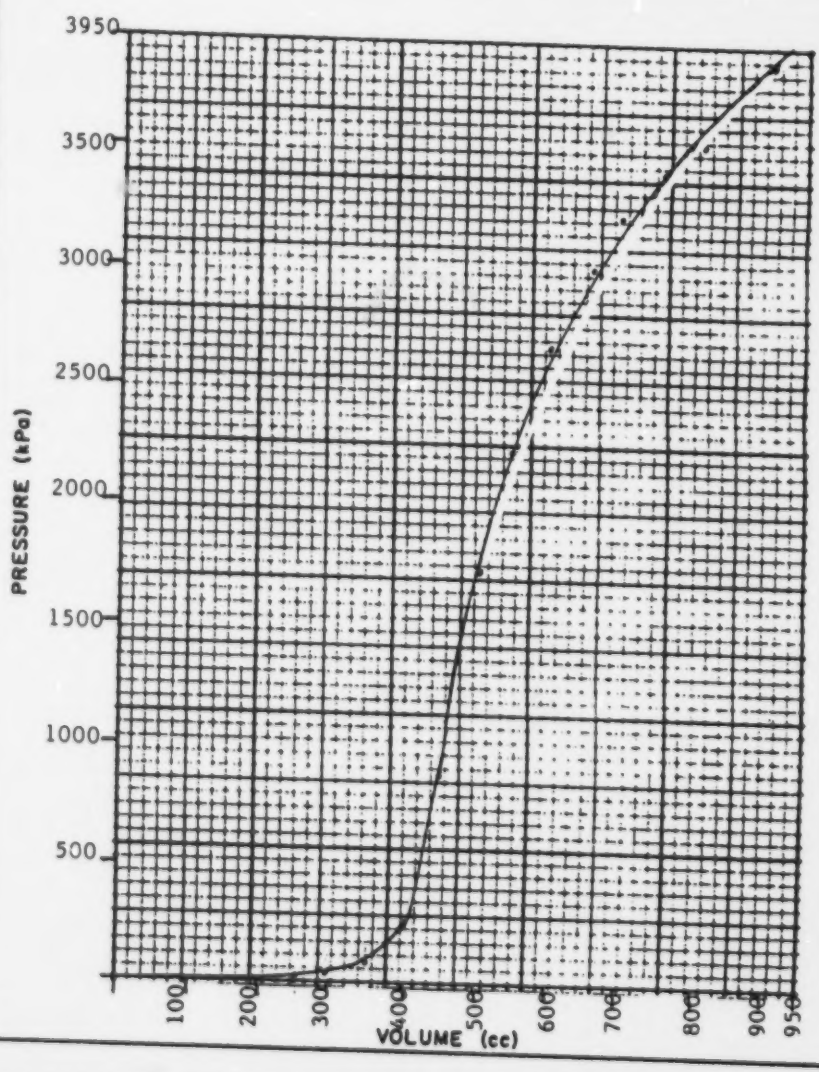

Drawing No. 15

TROW
DILATOMETER/PRESSUREMETER TESTS

BOREHOLE Nº	1
TEST Nº	cont'd
DEPTH	26
HOLE SIZE	BQ

PROJECT Nº	S00029R
SITE	Backfill Fence 22960

SURFACE ELEVATION :

TEST ELEVATION :

PRESSURE	READINGS			INJECTED VOLUME (cc)	CORRECTED VOLUME (cc)
	1 min.	2 min.	3 min.		
3730				850	
3890				900	
3950				950	

VOLUMETRIC CALIBRATION :

OBSERVATIONS :

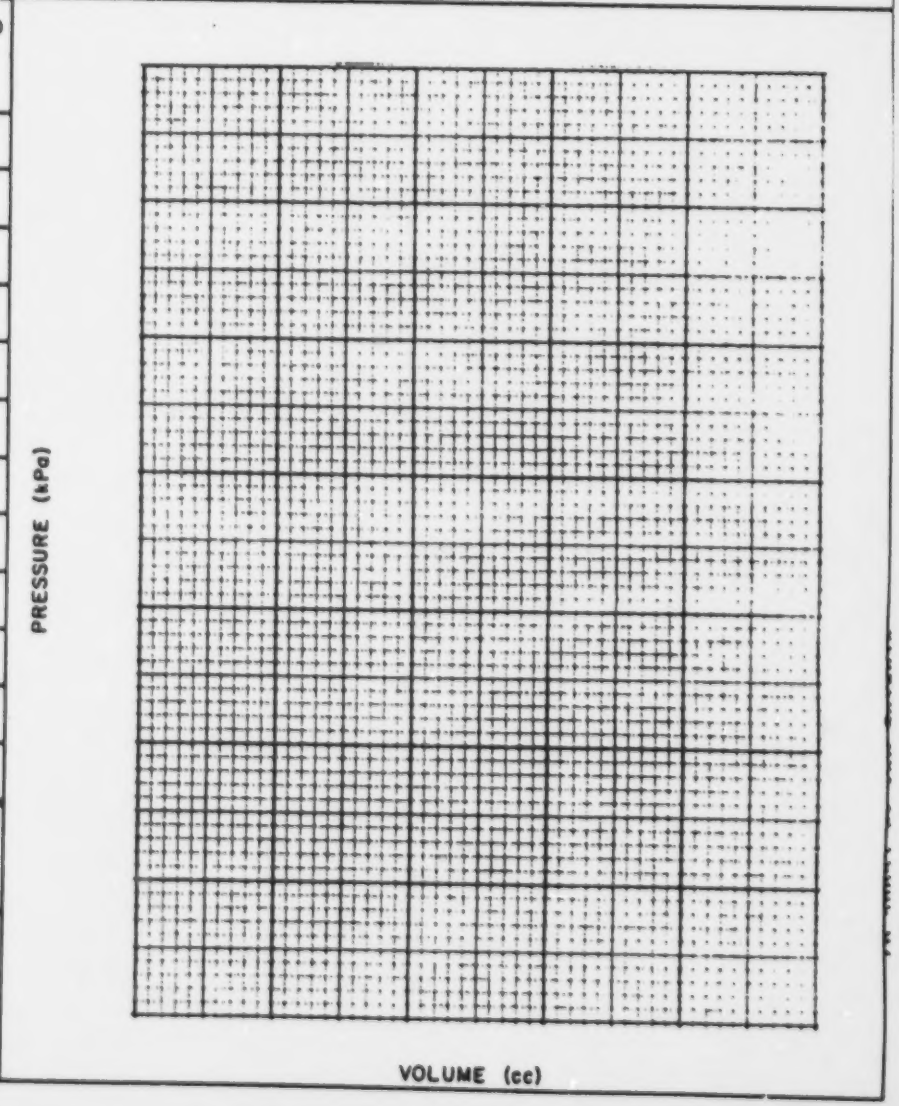

TROW
DILATOMETER/PRESSUREMETER TESTS

BOREHOLE Nº :-	1
TEST Nº :	8
DEPTH :	29
HOLE SIZE :	BQ

PROJECT Nº : S00029R
SITE : Backfill Fence 22960

SURFACE ELEVATION :

TEST ELEVATION :

PRESSURE	READINGS			INJECTED VOLUME (cc)	CORRECTED VOLUME (cc)
	1 min.	2 min.	3 min.		
40				250	
165				300	
550				350	
1300				400	
1890				450	
2420				500	
2750				550	
3000				600	
3300				650	
3500				700	

VOLUMETRIC CALIBRATION :

OBSERVATIONS : $\mu = .33$ $\Delta V = 450 - 350 = 100$ cc $\Delta p = 1340$ Kpa.

$V_m = 400$ cc

$$E_p = 2(1+.33)(1340+400)\left(\frac{1}{100/1340 - .84\times10^{-2}}\right) = 67075.50 \text{ Kpa.}$$

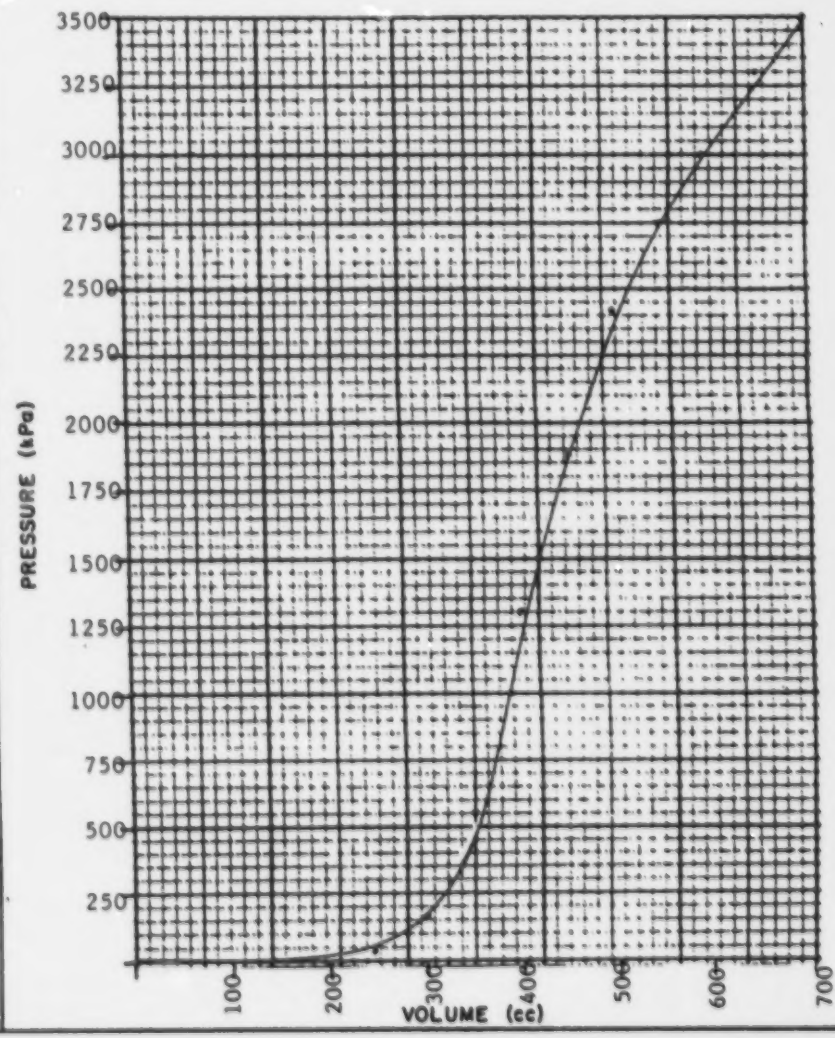

Drawing No. 16

TROW
DILATOMETER/PRESSUREMETER TESTS

BOREHOLE Nº	: 2
TEST Nº	: 2
DEPTH	: 3
HOLE SIZE	: BQ

PROJECT Nº	: S00029R
SITE	: Backfill Fence 22960

SURFACE ELEVATION :

TEST ELEVATION :

PRESSURE	READINGS			INJECTED VOLUME (cc)	CORRECTED VOLUME (cc)
	1 min.	2 min.	3 min.		
40				50	
50				100	
70				150	
70				200	
70				250	
80				300	
90				350	
110				400	
130				450	
210				500	
390				550	
890				600	

VOLUMETRIC CALIBRATION :

OBSERVATIONS : $u = .33$ $\Delta V = 700 - 600 = 100$ cc $\Delta p = 1190$ Kpa

$V_m = 650$ cc

$$E_p = 2.66\,(1270 + 650)\left(\frac{1}{100/1190 - .84\times10^{-2}}\right) = 67525.53 \text{ Kpa}$$

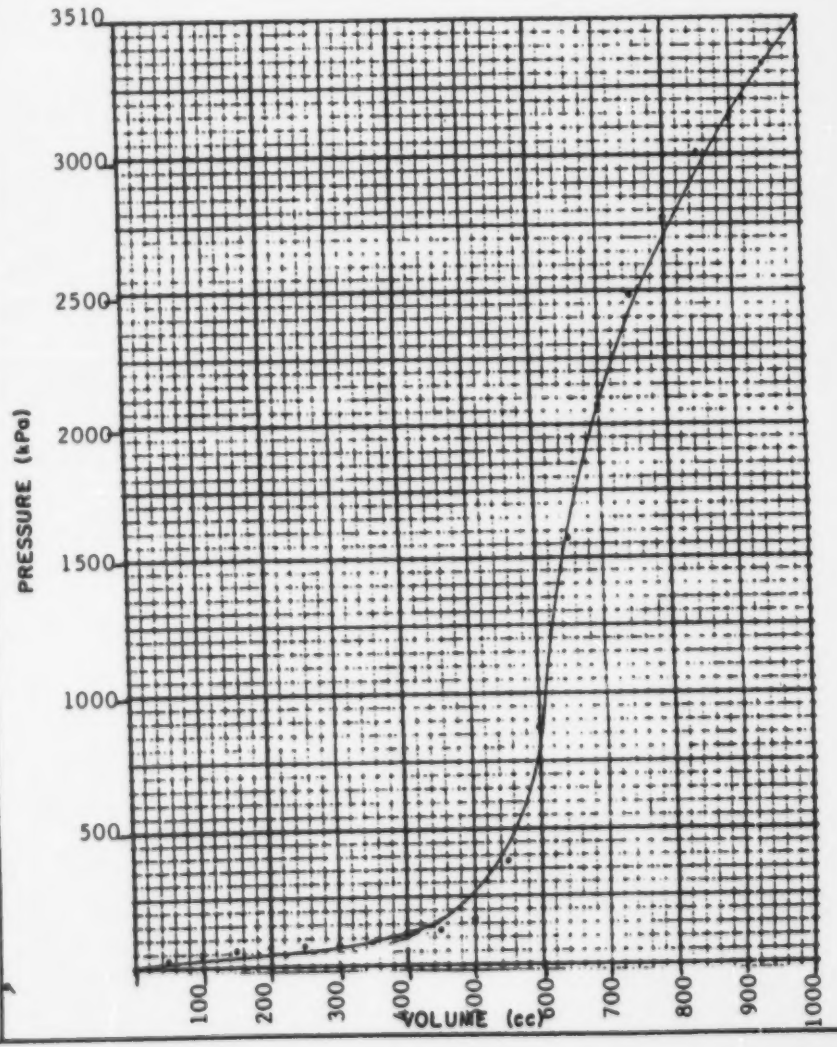

Drawing No. 17

TROW
DILATOMETER/PRESSUREMETER TESTS

BOREHOLE Nº : 2
TEST Nº : cont'd
DEPTH : 3
HOLE SIZE : BQ

PROJECT Nº : S00029R
SITE : Backfill Fence 22960

SURFACE ELEVATION :

TEST ELEVATION :

PRESSURE	READINGS			INJECTED VOLUME (cc)	CORRECTED VOLUME (cc)
	1 min.	2 min.	3 min.		
1575				650	
2080				700	
2490				750	
2780				800	
3010				850	
3150				900	
3350				950	
3510				1000	

VOLUMETRIC CALIBRATION :

OBSERVATIONS :

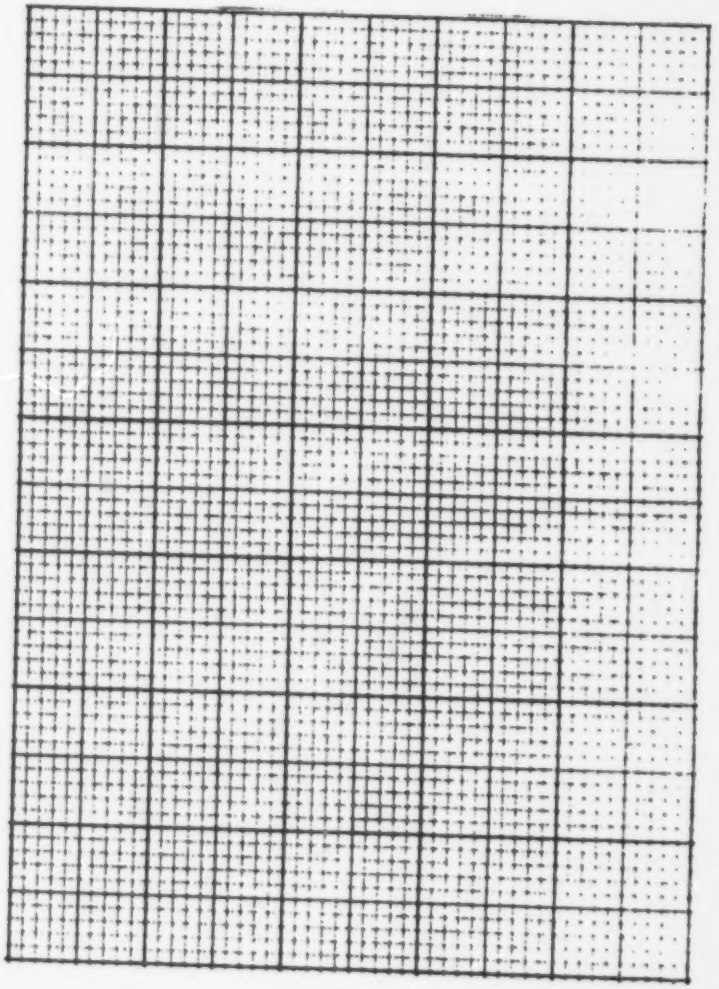

TROW
DILATOMETER/PRESSUREMETER TESTS

BOREHOLE Nº : 2
TEST Nº : 1
DEPTH : 7½
HOLE SIZE : BQ

PROJECT Nº : S00029R
SITE : Backfill Fence 22960

SURFACE ELEVATION :

TEST ELEVATION :

PRESSURE	READINGS			INJECTED VOLUME (cc)	CORRECTED VOLUME (cc)
	1 min.	2 min.	3 min.		
25				50	
40				100	
55				150	
70				200	
90				250	
125				300	
210				350	
480				400	
1220				450	
2380				500	
3150				550	
3680				600	

VOLUMETRIC CALIBRATION :

OBSERVATIONS : u_o = 55 $\quad \Delta V$ = 600 − 500 = 100 cc $\quad \Delta p$ = 1300 Kpa

V_m = 550 cc

$$E_\phi = 2.66\,(1270 + 550)\left(\frac{1}{100/1300 - .84\times10^{-2}}\right) = 70650.45 \text{ Kpa}$$

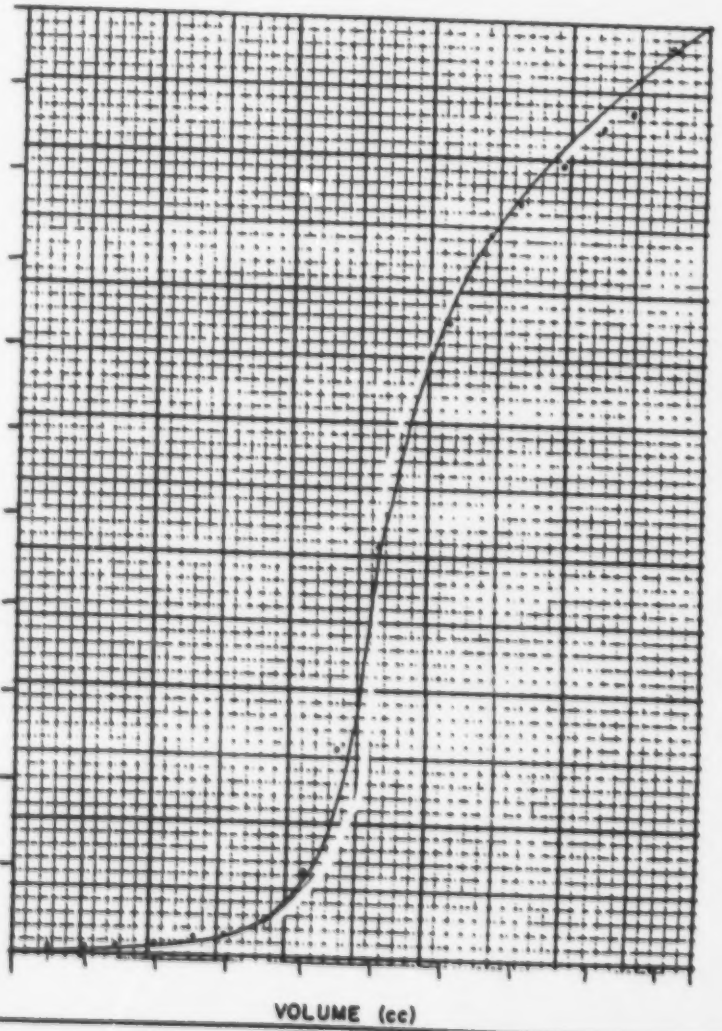

Drawing No. 18

TROW
DILATOMETER/PRESSUREMETER TESTS

BOREHOLE-Nº	2
TEST Nº	cont'd
DEPTH	7½
HOLE SIZE	BQ

PROJECT Nº : S00029R
SITE : Backfill Fence 22960

SURFACE ELEVATION :

TEST ELEVATION :

PRESSURE	READINGS			INJECTED VOLUME (cc)	CORRECTED VOLUME (cc)
	1 min.	2 min.	3 min.		
4180				650	
4380				700	
4610				750	
4790				800	
4910				850	
5280				900	
5400				950	

VOLUMETRIC CALIBRATION :

OBSERVATIONS :

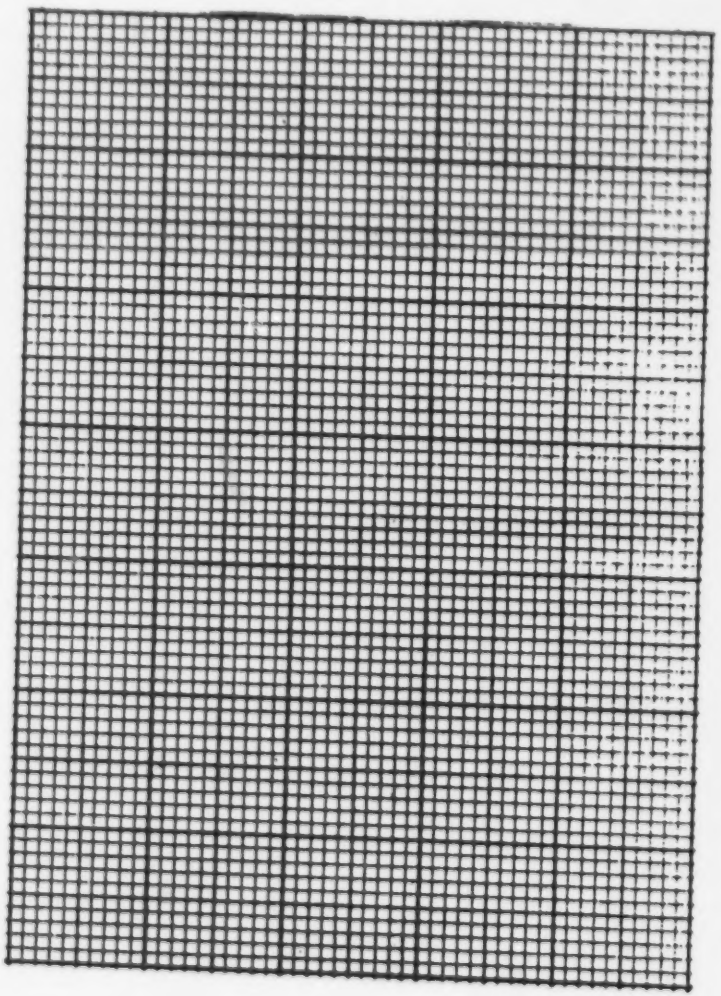

Drawing No. 10 (cont'd)

TROW
DILATOMETER/PRESSUREMETER TESTS

BOREHOLE Nº :-	2	PROJECT Nº :	S00029R
TEST Nº :	6	SITE :	Backfill Fence 22960
DEPTH :	12		
HOLE SIZE :	BQ		

SURFACE ELEVATION :

TEST ELEVATION :

PRESSURE	READINGS			INJECTED VOLUME (cc)	CORRECTED VOLUME (cc)
	1 min.	2 min.	3 min.		
50				50	
60				100	
70				150	
70				200	
80				250	
80				300	
90				350	
---				400	
100				450	
110				500	
120				550	
130				600	

VOLUMETRIC CALIBRATION :

OBSERVATIONS : $\mu = .33$ $\Delta V = 1050 - 900 = 150$ cc $\Delta p = 2160$ Kpa

$V_m = 975$ cc

$$E_p = 2.66\ (1270 + 975)\left(\frac{1}{150/2160 - .84 \times 10^{-2}}\right) = 97825.45 \text{ Kpa}$$

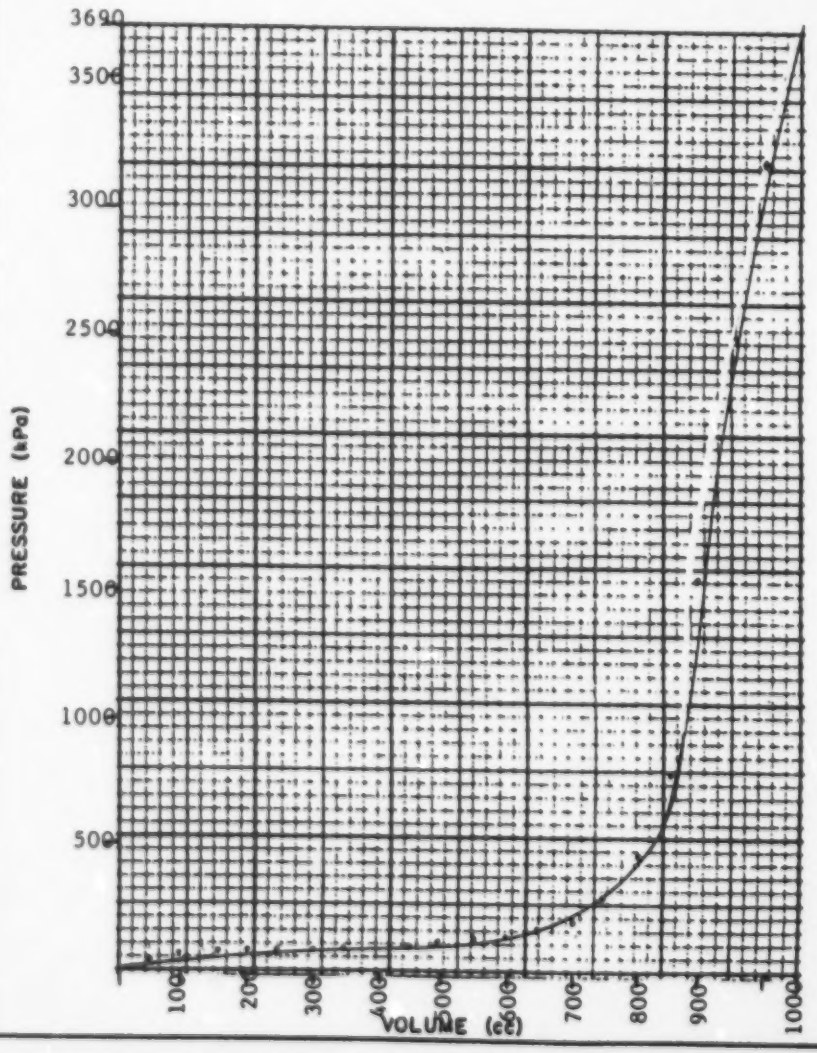

Drawing No. 19

TROW
DILATOMETER/PRESSUREMETER TESTS

BOREHOLE Nº : 2
TEST Nº : cont'd
DEPTH : 12
HOLE SIZE : BQ

PROJECT Nº : S00029R
SITE : Backfill Fence 22960

SURFACE ELEVATION :

TEST ELEVATION :

PRESSURE	READINGS			INJECTED VOLUME (cc)	CORRECTED VOLUME (cc)
	1 min.	2 min.	3 min.		
160				650	
205				700	
280				750	
460				800	
790				850	
1530				900	
2500				950	
3180				1000	
3690				1050	

VOLUMETRIC CALIBRATION :

OBSERVATIONS :

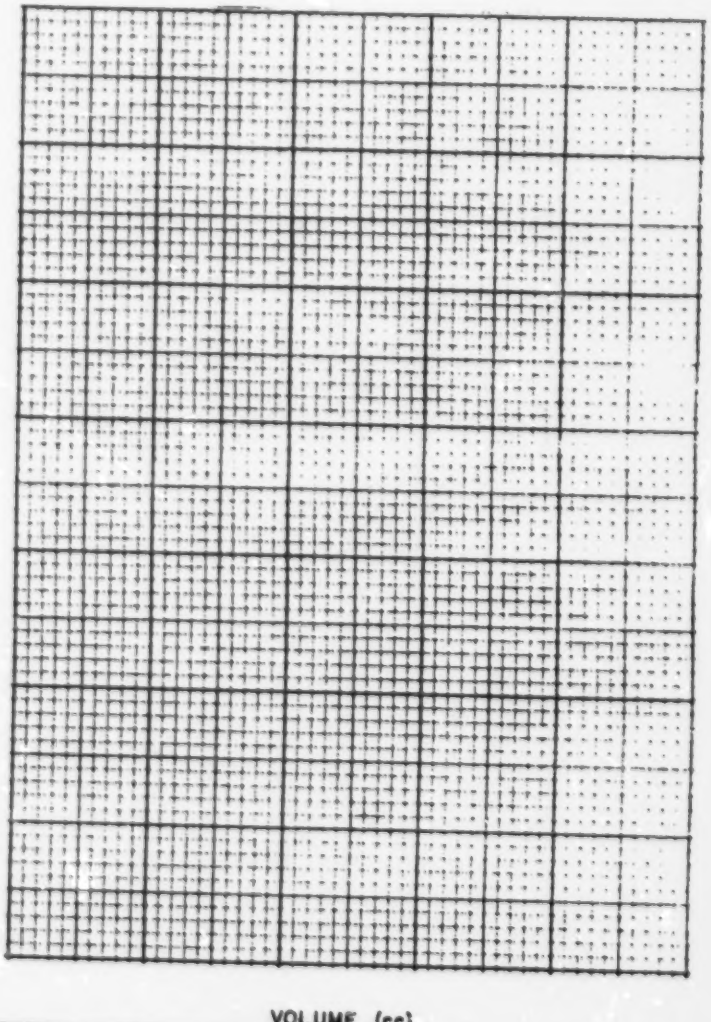

TROW
DILATOMETER/PRESSUREMETER TESTS

BOREHOLE Nº : 2
TEST Nº : 5
DEPTH : 16
HOLE SIZE : BQ

PROJECT Nº : S00029R
SITE : Backfill Fence 22960

SURFACE ELEVATION :

TEST ELEVATION :

PRESSURE	READINGS			INJECTED VOLUME (cc)	CORRECTED VOLUME (cc)
	1 min.	2 min.	3 min.		
60				50	
75				100	
100				150	
100				200	
100				250	
100				300	
105				350	
100				400	
120				450	
130				500	
180				550	
270				600	

VOLUMETRIC CALIBRATION :

OBSERVATIONS : $u_0 = 55$ $\Delta V = 800 - 700 = 100$ cc $\Delta p = 1450$ Kpa

$V_m = 750$ cc

$E_p = 2.66 \left(1270 + 750\right)\left(\frac{1}{100/1450 - 0.84 \times 10^{-2}}\right) = 88717.15$ Kpa.

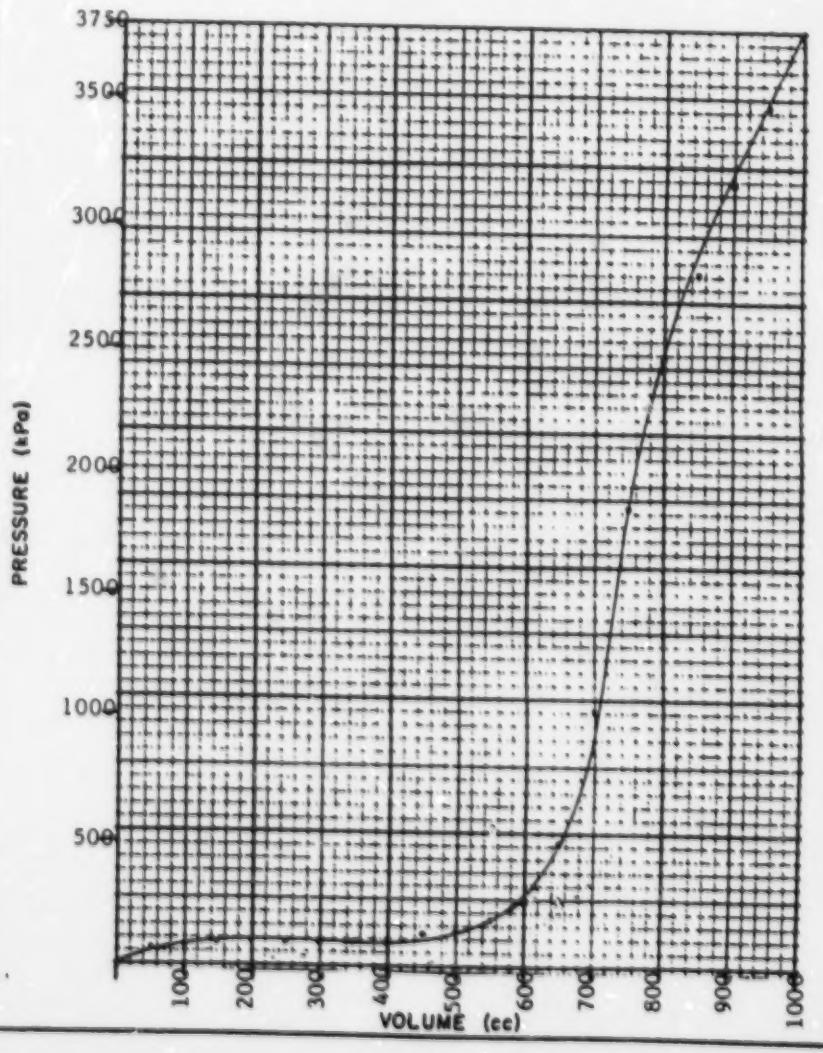

Drawing No. 20

TROW
DILATOMETER/PRESSUREMETER TESTS

BOREHOLE Nº : 2
TEST Nº : cont'd
DEPTH : 16
HOLE SIZE : BQ

PROJECT Nº : S00029R
SITE : Backfill Fence 22960

SURFACE ELEVATION :

TEST ELEVATION :

PRESSURE	READINGS			INJECTED VOLUME (cc)	CORRECTED VOLUME (cc)
	1 min.	2 min.	3 min.		
490				650	
1030				700	
1860				750	
2480				800	
2820				850	
3190				900	
3480				950	
3780				1000	

VOLUMETRIC CALIBRATION :

OBSERVATIONS :

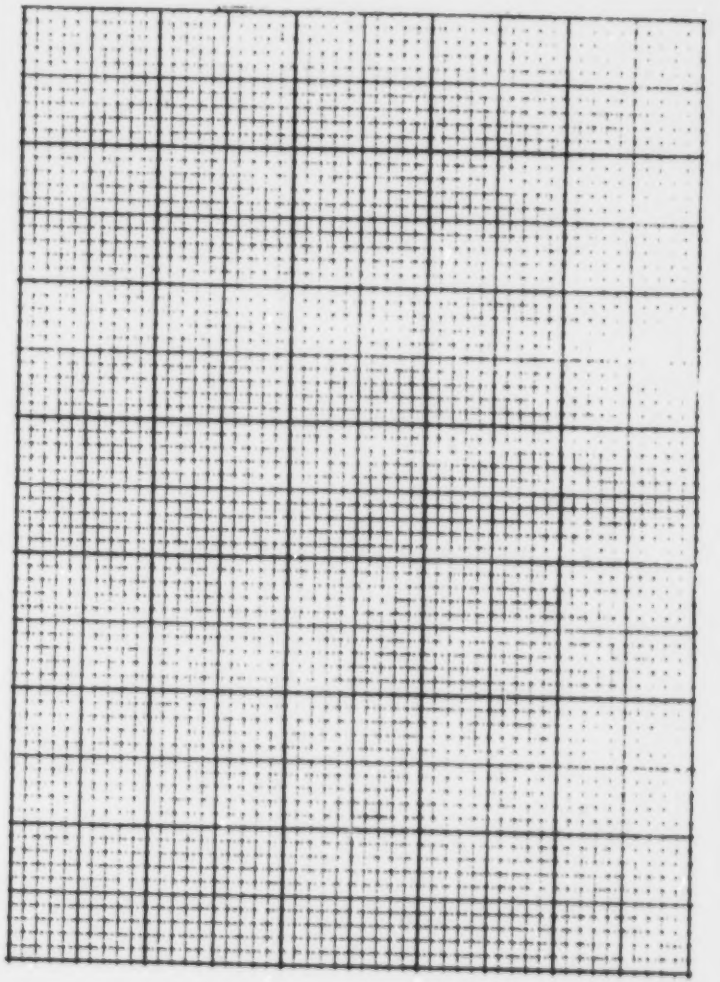

TROW
DILATOMETER/PRESSUREMETER TESTS

BOREHOLE Nº :	2
TEST Nº :	4
DEPTH :	20
HOLE SIZE :	BQ

PROJECT Nº :	S00029R
SITE :	Backfill Fence 22960

SURFACE ELEVATION :

TEST ELEVATION :

PRESSURE	READINGS			INJECTED VOLUME (cc)	CORRECTED VOLUME (cc)
	1 min.	2 min.	3 min.		
50				50	
60				100	
70				150	
75				200	
80				250	
85				300	
90				350	
100				400	
120				450	
150				500	
210				550	
370				600	

VOLUMETRIC CALIBRATION :

OBSERVATIONS : $\mu = .33$ $\Delta V = 750 - 650 = 100$ cc $\Delta p = 1370$ Kpa

$E_p = 2.66 \left(1270 + 700\right) \left(\frac{V_m = 700 \text{ cc}}{\frac{1}{100/1370} - .84 \times 10^{-2}} \right) = 81126.81$ Kpa.

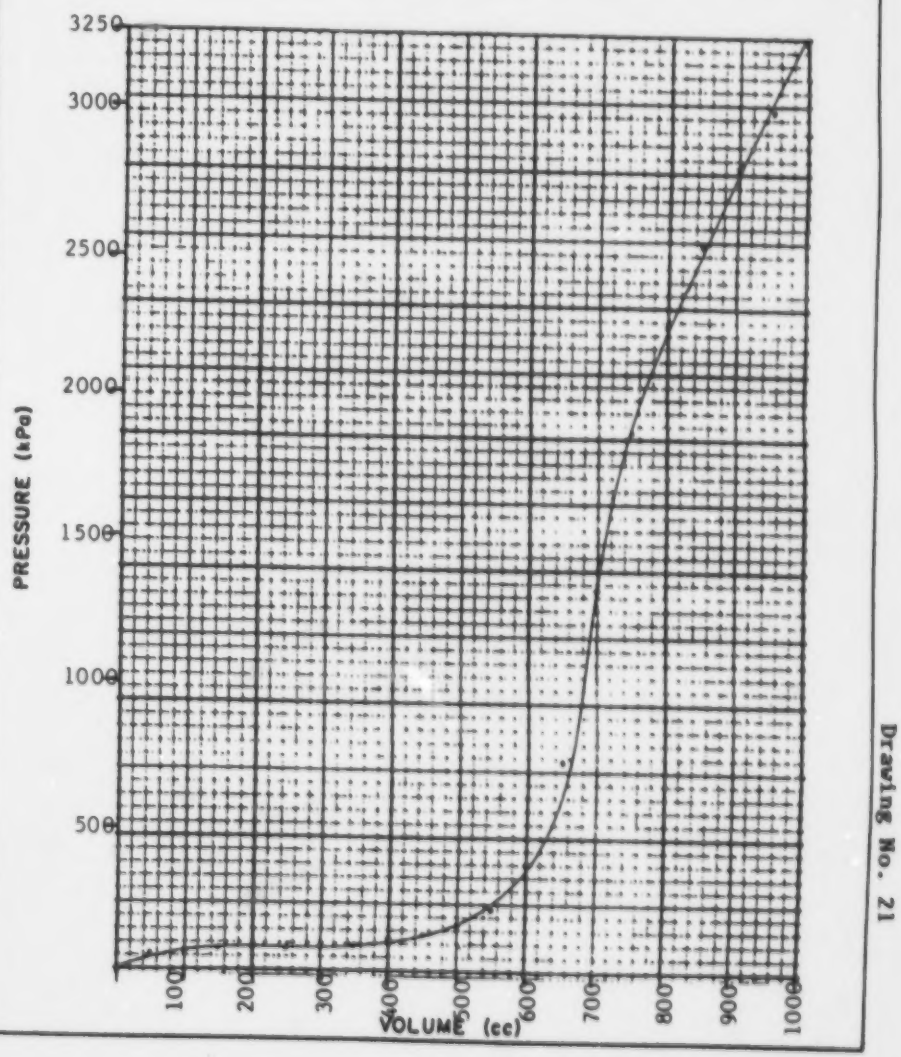

Drawing No. 21

TROW
DILATOMETER/PRESSUREMETER TESTS

BOREHOLE Nº : 2
TEST Nº : cont'd
DEPTH : 20
HOLE SIZE : BQ

PROJECT Nº : S00029R
SITE : Backfill Fence 22960

SURFACE ELEVATION :

TEST ELEVATION :

PRESSURE	READINGS			INJECTED VOLUME (cc)	CORRECTED VOLUME (cc)
	1 min.	2 min.	3 min.		
490				650	
1030				700	
1860				750	
2480				800	
2820				850	
3190				900	
3480				950	
3790				1000	

VOLUMETRIC CALIBRATION :

OBSERVATIONS :

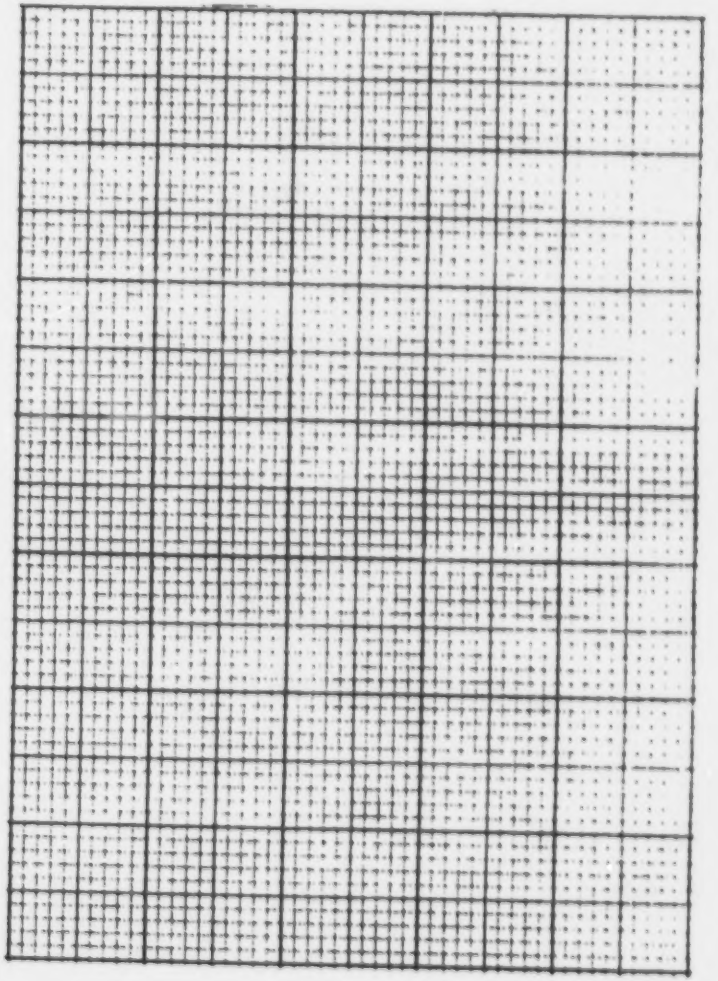

TROW
DILATOMETER/PRESSUREMETER TESTS

BOREHOLE Nº :	2
TEST Nº :	3
DEPTH :	25
HOLE SIZE :	BQ

PROJECT Nº :	S00029R
SITE :	Backfill Fence 22960

SURFACE ELEVATION :

TEST ELEVATION :

PRESSURE	READINGS			INJECTED VOLUME (cc)	CORRECTED VOLUME (cc)
	1 min.	2 min.	3 min.		
30				50	
50				100	
60				154	
70				200	
80				250	
100				300	
130				350	
220				400	
475				450	
1290				500	
2500				550	
3290				600	

VOLUMETRIC CALIBRATION :

OBSERVATIONS : $\mu = 0.33$ $\Delta V = 600 - 500 = 100cc$ $\Delta p = 2000$ Kpa

$V_m = 550$ cc

$$E_{pf} = 2.66\ (1270 + 550)\left(\frac{1}{100/2000 - 0.84\times10^{-2}}\right) = 116\,375 \text{ Kpa}$$

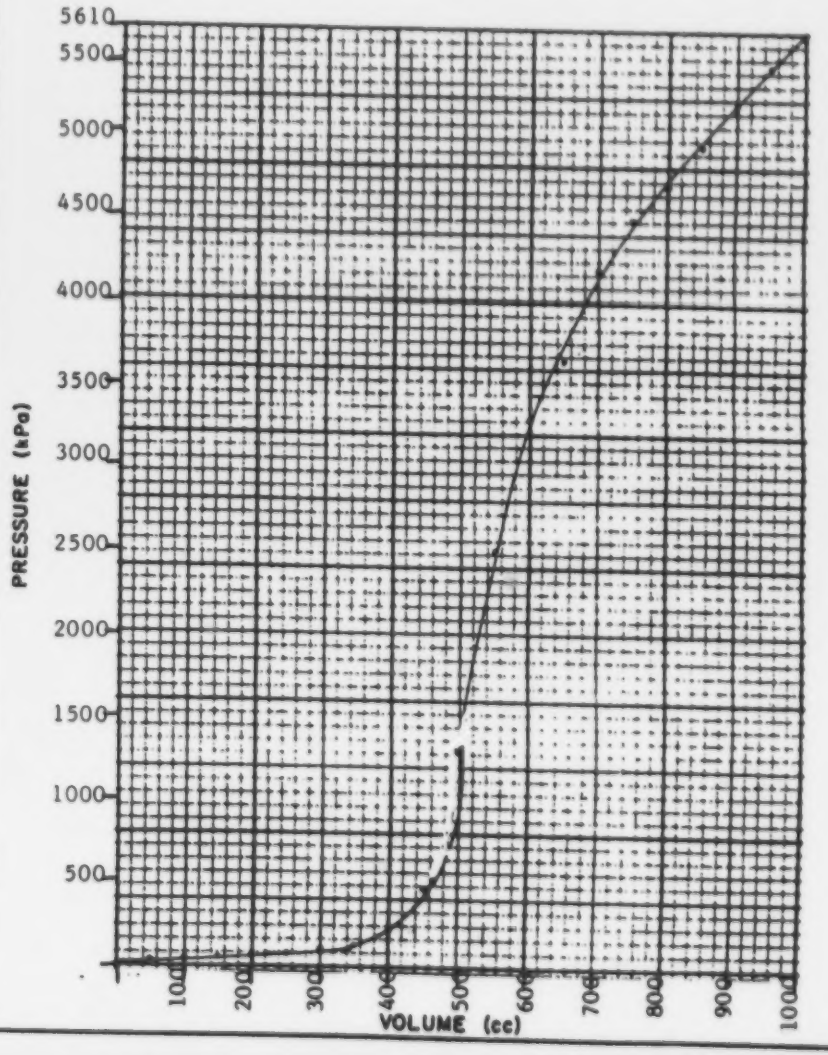

Drawing No. 22

TROW
DILATOMETER/PRESSUREMETER TESTS

BOREHOLE Nº : 2
TEST Nº : cont'd
DEPTH : 25
HOLE SIZE : BQ

PROJECT Nº : S00029R
SITE : Backfill Fence 22960

SURFACE ELEVATION :

TEST ELEVATION :

PRESSURE	READINGS			INJECTED VOLUME (cc)	CORRECTED VOLUME (cc)
	1 min.	2 min.	3 min.		
3680				650	
4200				700	
4490				750	
4690				800	
4930				850	
5200				900	
5400				950	
5610				1000	

VOLUMETRIC CALIBRATION :

OBSERVATIONS :

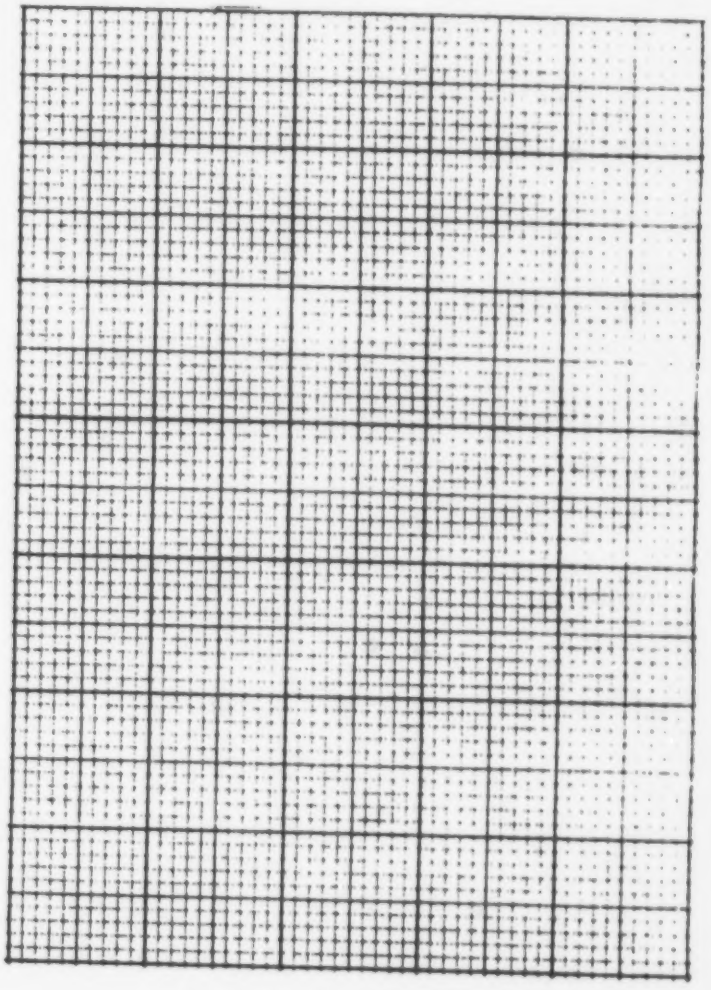

TROW
DILATOMETER/PRESSUREMETER TESTS

BOREHOLE Nº :	3
TEST Nº :	6
DEPTH :	3
HOLE SIZE :	BQ

PROJECT Nº :	S00029R
SITE :	Backfill Fence 24070

SURFACE ELEVATION :

TEST ELEVATION :

PRESSURE	READINGS			INJECTED VOLUME (cc)	CORRECTED VOLUME (cc)
	1 min.	2 min.	3 min.		
20				50	
30				100	
45				150	
50				200	
60				250	
70				300	
70				350	
70				400	
75				450	
80				500	
80				550	
90				600	

VOLUMETRIC CALIBRATION :

OBSERVATIONS : $\mu = .33$ $\Delta V = 1000 - 900 = 100$ cc $\Delta p = 70$ Kpa.

$V_m = 950$ cc

$$E_\phi = 2.66 \quad (1270 + 950) \left(\frac{1}{100/70 - .84 \times 10^{-2}} \right) = 4158.09 \text{ Kpa.}$$

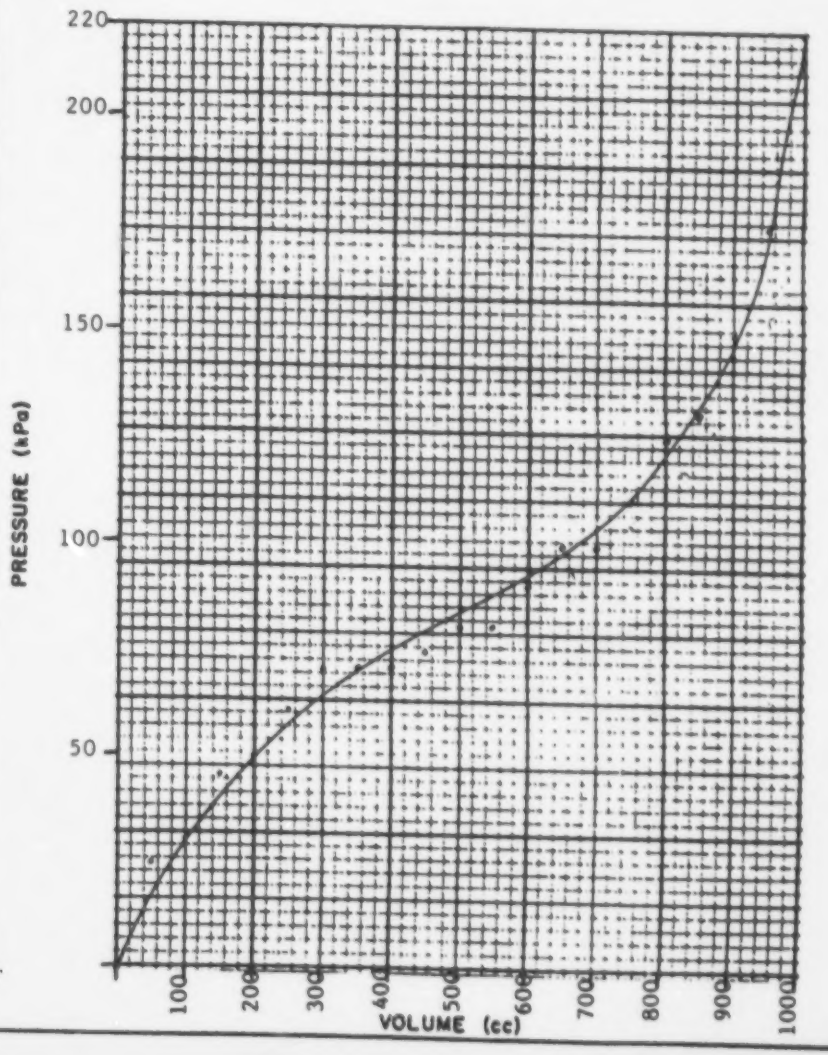

Drawing No. 23

TROW
DILATOMETER/PRESSUREMETER TESTS

BOREHOLE Nº : -
TEST Nº : cont'd
DEPTH : 3
HOLE SIZE : BQ

PROJECT Nº : S00029R
SITE : Backfill Fence 24070

SURFACE ELEVATION :

TEST ELEVATION :

PRESSURE	READINGS			INJECTED VOLUME (cc)	CORRECTED VOLUME (cc)
	1 min.	2 min.	3 min.		
100				650	
100				700	
110				750	
125				800	
130				850	
150				900	
175				950	
220				1000	

VOLUMETRIC CALIBRATION :

OBSERVATIONS :

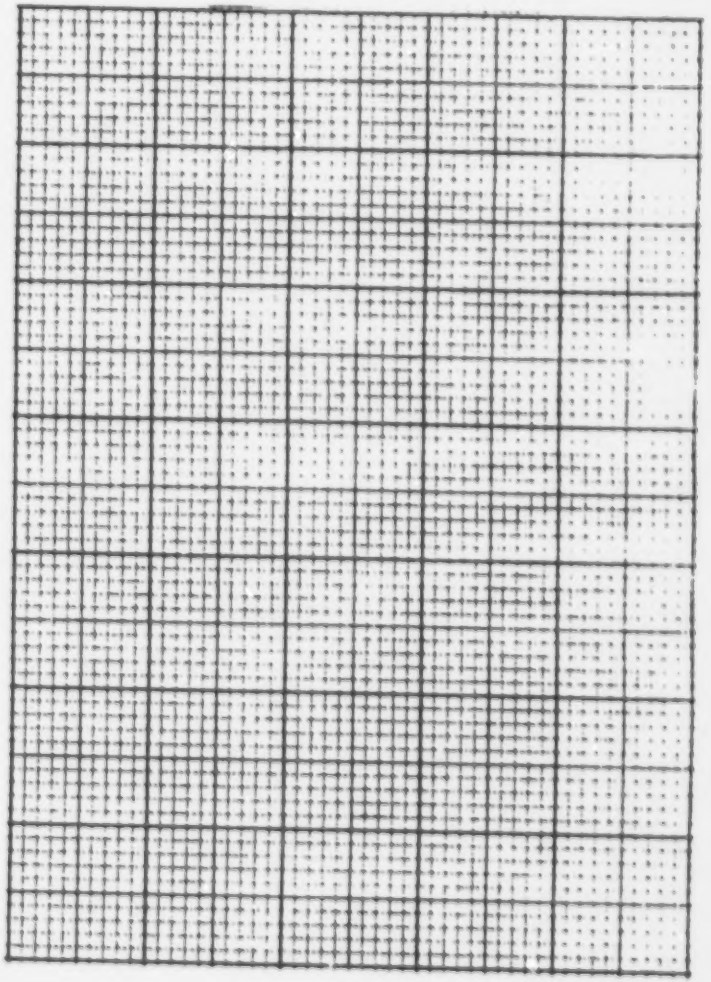

TROW
DILATOMETER/PRESSUREMETER TESTS

BOREHOLE Nº :	3
TEST Nº :	5
DEPTH :	5
HOLE SIZE :	BQ

PROJECT Nº :	S00029R
SITE :	Backfill Fence 24070

SURFACE ELEVATION :

TEST ELEVATION :

PRESSURE	READINGS			INJECTED VOLUME (cc)	CORRECTED VOLUME (cc)
	1 min.	2 min.	3 min.		
12				200	
20				250	
25				300	
25				350	
30				400	
40				450	
40				500	
50				550	
50				600	
60				650	
75				700	
100				750	

VOLUMETRIC CALIBRATION :

OBSERVATIONS : $u = .33$ $\Delta V = 900 - 750 = 150$ cc $\Delta P = 50$ Kpa

$V_m = 825$ cc

$$E_p = 2.66\,(1270 + 825)\left(\frac{1}{150/50 - .84 \times 10^{-2}}\right) = 1862.78 \text{ Kpa}$$

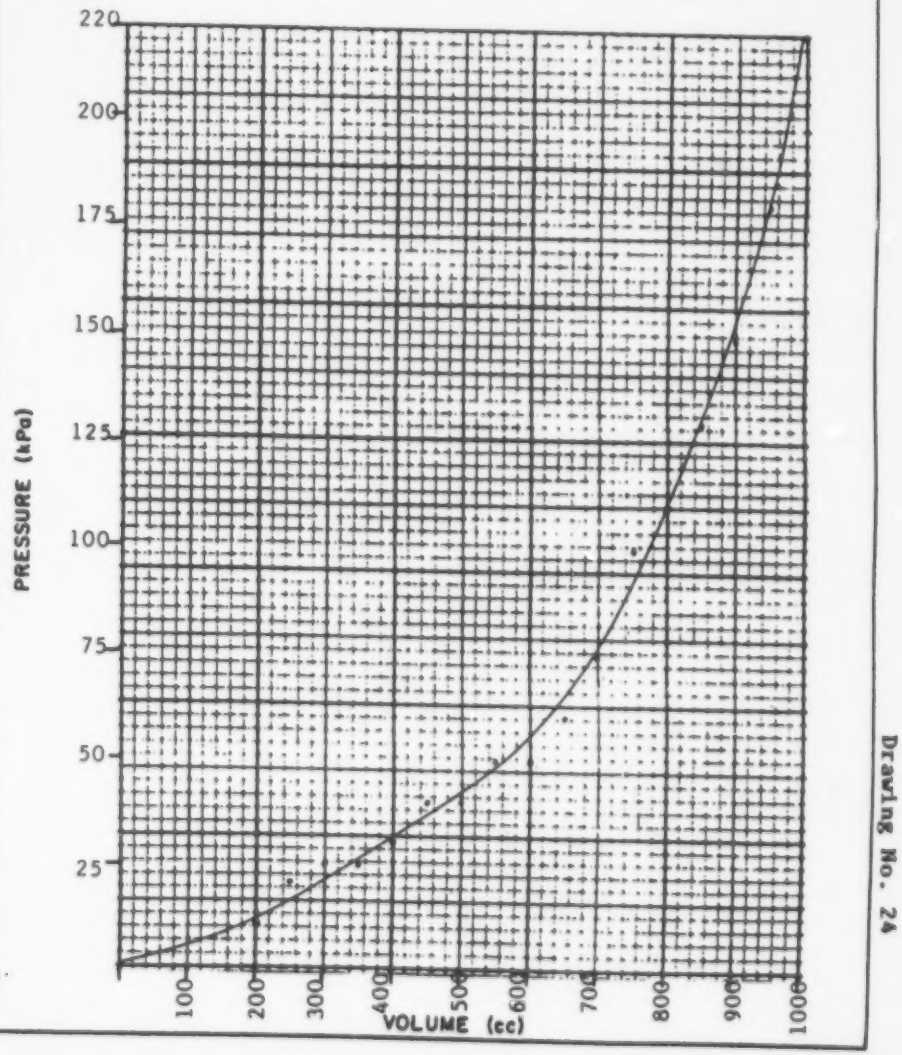

Drawing No. 24

TROW
DILATOMETER/PRESSUREMETER TESTS

BOREHOLE Nº : 3
TEST Nº : cont'd
DEPTH : 5
HOLE SIZE : BQ

PROJECT Nº : S00029R
SITE : Backfill Fence 24070

SURFACE ELEVATION :

TEST ELEVATION :

PRESSURE	READINGS			INJECTED VOLUME (cc)	CORRECTED VOLUME (cc)
	1 min.	2 min.	3 min.		
110				800	
130				850	
150				900	
180				950	
220				1000	

VOLUMETRIC CALIBRATION :

OBSERVATIONS :

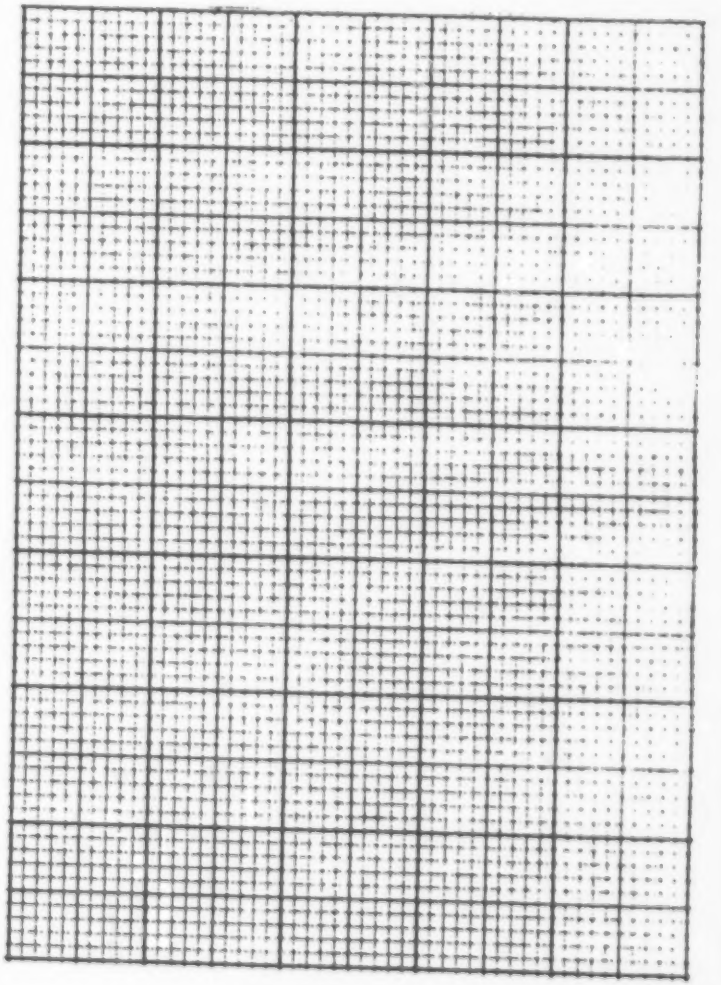

TROW
DILATOMETER/PRESSUREMETER TESTS

BOREHOLE Nº :	3
TEST Nº :	4
DEPTH :	6
HOLE SIZE :	BQ

PROJECT Nº : S00029R
SITE : Backfill Fence 24070

SURFACE ELEVATION :

TEST ELEVATION :

PRESSURE	READINGS			INJECTED VOLUME (cc)	CORRECTED VOLUME (cc)
	1 min.	2 min.	3 min.		
20				100	
25				150	
30				200	
40				250	
60				300	
70				350	
100				400	
160				450	
380				500	
1430				550	
3400				600	
3580				650	

VOLUMETRIC CALIBRATION :

OBSERVATIONS : $\mu = .33$ $\Delta V = 600 - 550 = 50$ cc $V_m = 575$ cc $\Delta p = 1970$

$$E_d = 2.66 \,(1230 + 515)\left(\frac{1}{50/1970 - .84 \times 10^{-2}}\right) = 28901617 \text{ kPa}$$

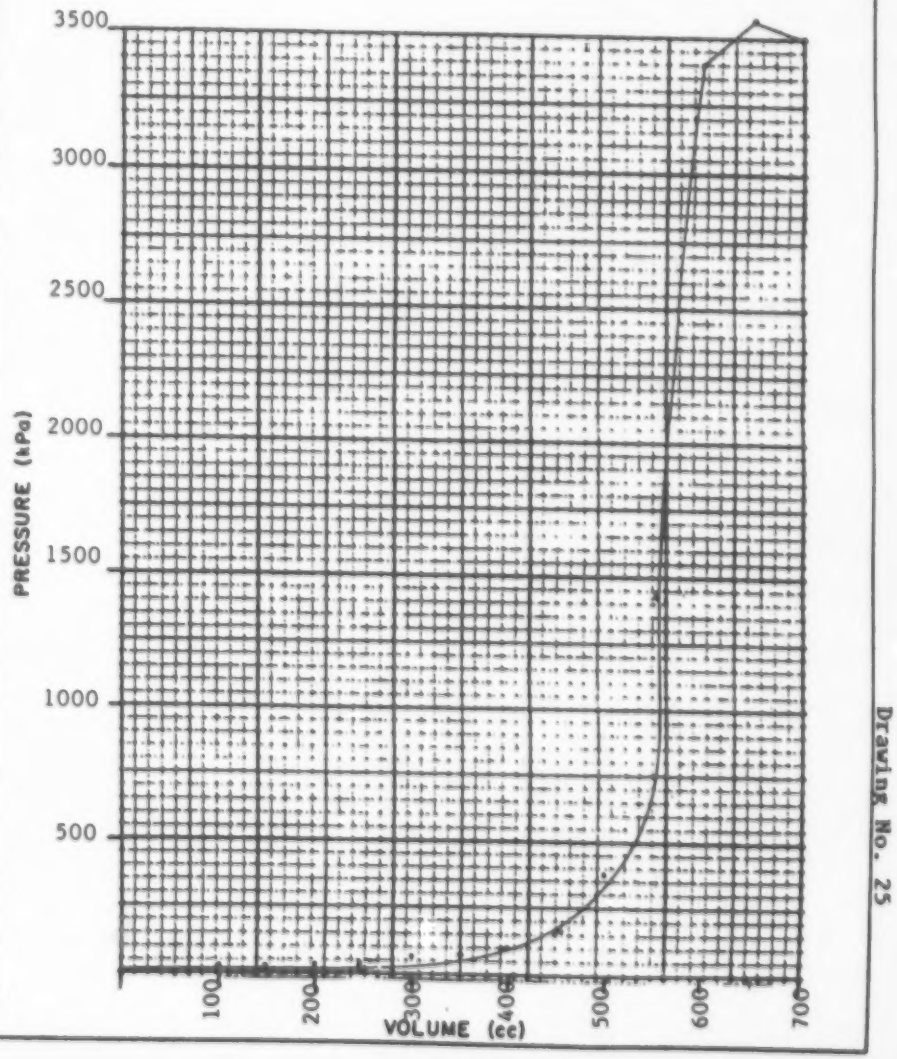

Drawing No. 25

TROW
DILATOMETER/PRESSUREMETER TESTS

BOREHOLE Nº : 3
TEST Nº : cont'd
DEPTH : 6
HOLE SIZE : BQ

PROJECT Nº : S00029R
SITE : Backfill Fence 24070

SURFACE ELEVATION :

TEST ELEVATION :

PRESSURE	READINGS			INJECTED VOLUME (cc)	CORRECTED VOLUME (cc)
	1 min.	2 min.	3 min.		
3500				700	

VOLUMETRIC CALIBRATION :

OBSERVATIONS :

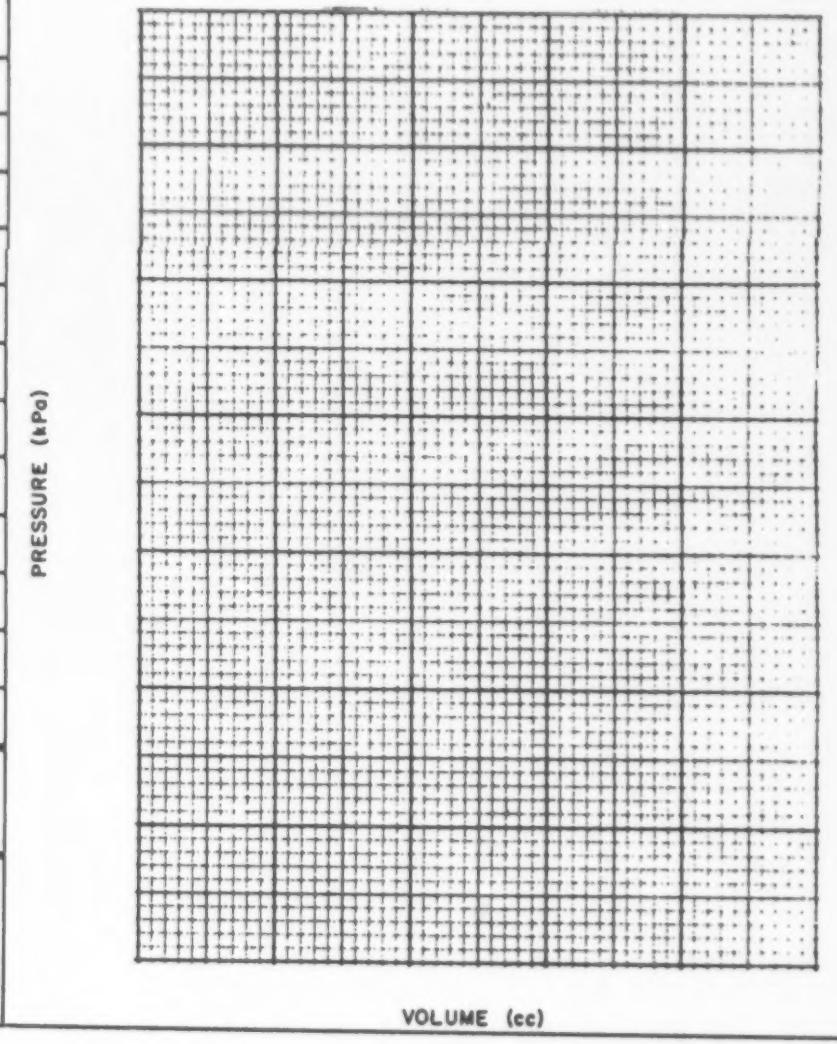

TROW
DILATOMETER/PRESSUREMETER TESTS

BOREHOLE Nº :	3
TEST Nº :	3
DEPTH :	9
HOLE SIZE :	BQ

PROJECT Nº : S00029R
SITE : Backfill Fence 24070

SURFACE ELEVATION :

TEST ELEVATION :

PRESSURE	READINGS			INJECTED VOLUME (cc)	CORRECTED VOLUME (cc)
	1 min.	2 min.	3 min.		
25				50	
30				100	
40				150	
50				200	
60				250	
75				300	
80				350	
110				400	
170				450	
290				500	
475				550	
675				600	

VOLUMETRIC CALIBRATION :

OBSERVATIONS : $\mu = .33$ $\Delta V = 700 - 500 = 200$ cc $\Delta p = 860$ Kpa
$V_m = 600$ cc

$$E_d = 2.66\ (1270 + 600)\left(\frac{1}{200/860 - .84 \times 10^{-2}}\right) = 22190.58 \text{ Kpa}$$

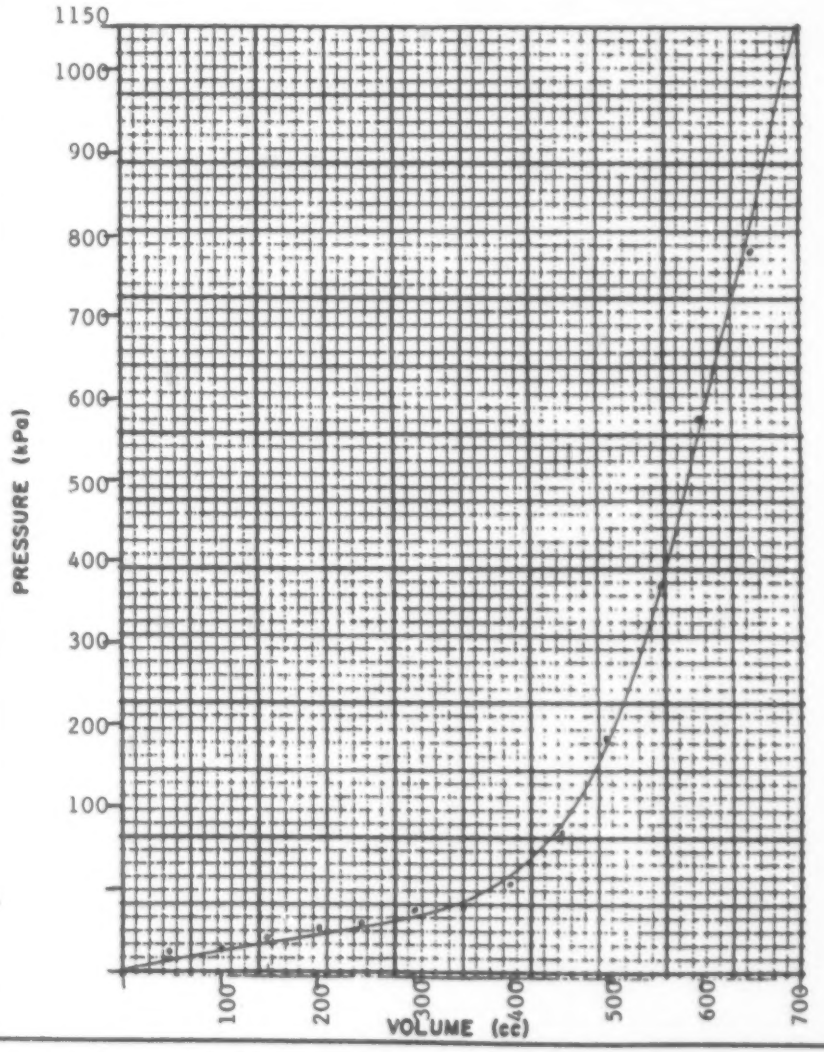

Drawing No. 26

TROW
DILATOMETER/PRESSUREMETER TESTS

BOREHOLE-Nº	3
TEST Nº	cont'd
DEPTH	9
HOLE SIZE	BQ

PROJECT Nº	S00029R
SITE	Backfill Fence 24070

SURFACE ELEVATION :

TEST ELEVATION :

PRESSURE	READINGS			INJECTED VOLUME (cc)	CORRECTED VOLUME (cc)
	1 min.	2 min.	3 min.		
880				650	
1150				700	

VOLUMETRIC CALIBRATION :

OBSERVATIONS :

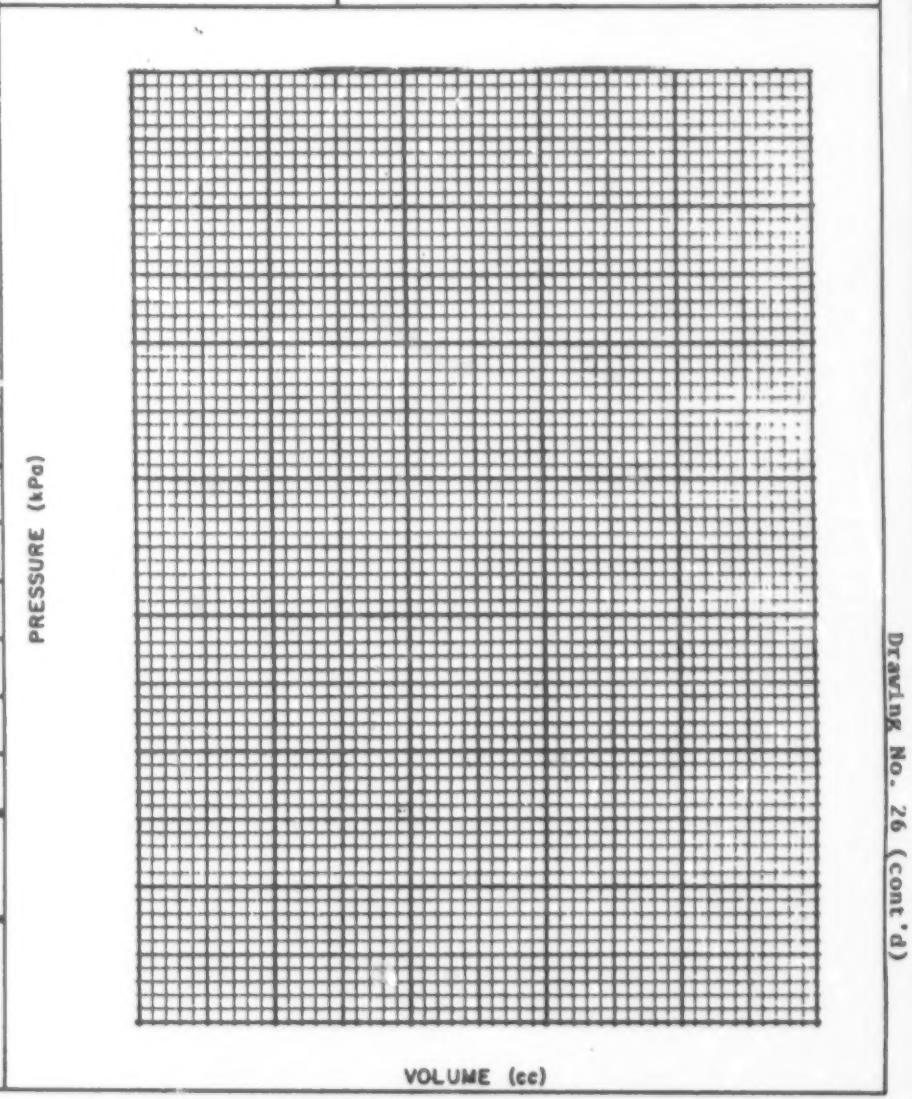

Drawing No. 26 (cont'd)

TROW
DILATOMETER/PRESSUREMETER TESTS

BOREHOLE Nº	3
TEST Nº	2
DEPTH	10
HOLE SIZE	BQ

PROJECT Nº : S00029R
SITE : Backfill Fence 24070

SURFACE ELEVATION :

TEST ELEVATION :

PRESSURE	READINGS			INJECTED VOLUME (cc)	CORRECTED VOLUME (cc)
	1 min.	2 min.	3 min.		
25				50	
30				100	
40				150	
60				200	
75				250	
100				300	
155				350	
300				400	
720				450	
1138				500	
2080				550	
2490				600	

VOLUMETRIC CALIBRATION :

OBSERVATIONS : $\mu = .33$ $\Delta V = 550 - 450 = 100cc$ $\Delta P = 1340$ Kpa

$V_m = 500cc$

$E_\phi = 2.66\ (1270 + 500)\left(\frac{1}{100/1340 - .84\times10^{-6}}\right) = 72\,289.92$ Kpa

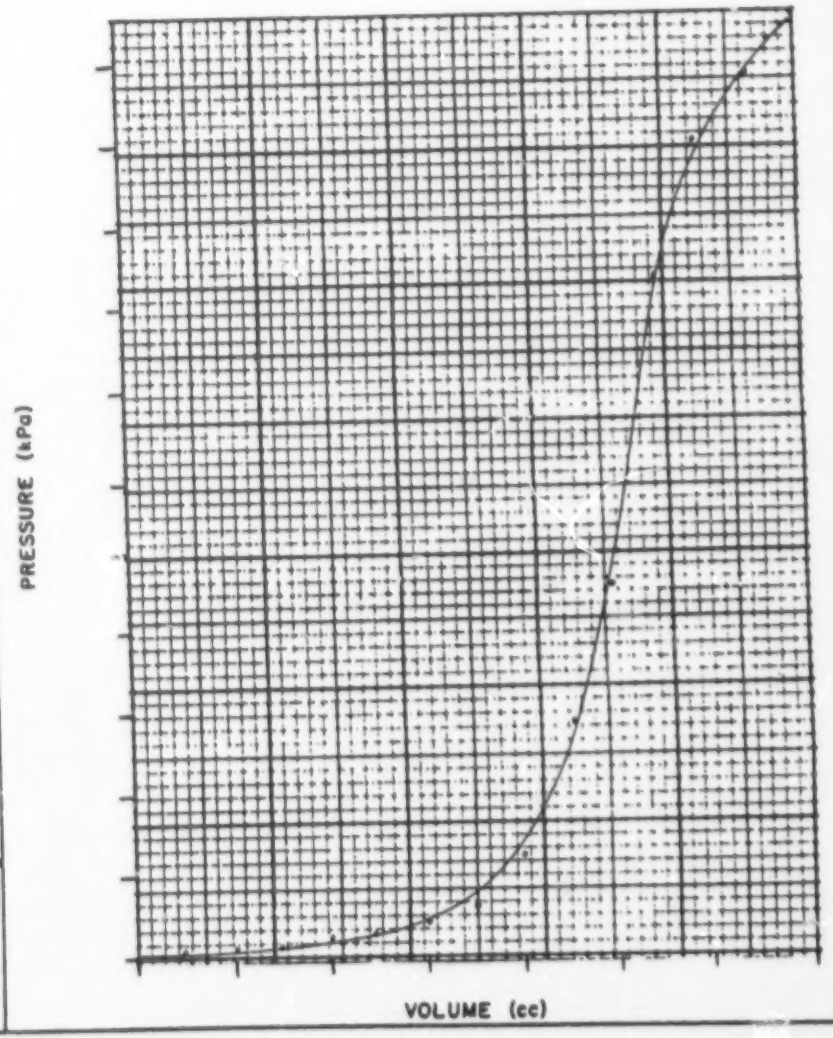

Drawing No. 21

TROW
DILATOMETER/PRESSUREMETER TESTS

BOREHOLE Nº : 3
TEST Nº : cont'd
DEPTH : 10
HOLE SIZE : BQ

PROJECT Nº : S00029R
SITE : Backfill Fence 24070

SURFACE ELEVATION :

TEST ELEVATION :

PRESSURE	READINGS			INJECTED VOLUME (cc)	CORRECTED VOLUME (cc)
	1 min.	2 min.	3 min.		
2700				650	
2890				700	

VOLUMETRIC CALIBRATION :

OBSERVATIONS :

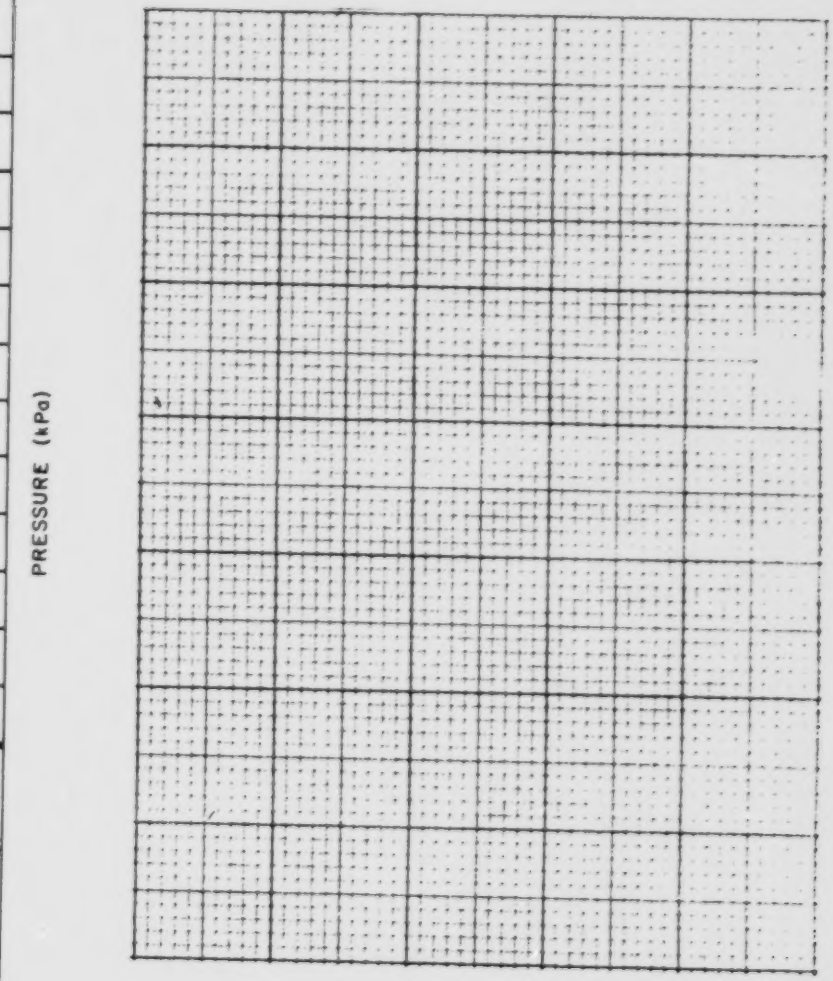

TROW
DILATOMETER/PRESSUREMETER TESTS

BOREHOLE Nº :	3
TEST Nº :	1
DEPTH :	15
HOLE SIZE :	BQ

PROJECT Nº :	S00029R
SITE :	Backfill Fence 24070

SURFACE ELEVATION :

TEST ELEVATION :

PRESSURE	READINGS			INJECTED VOLUME (cc)	CORRECTED VOLUME (cc)
	1 min.	2 min.	3 min.		
30				50	
50				100	
60				150	
70				200	
75				250	
80				300	
90				350	
100				400	
105				450	
110				500	
120				550	
125				600	

VOLUMETRIC CALIBRATION :

OBSERVATIONS :

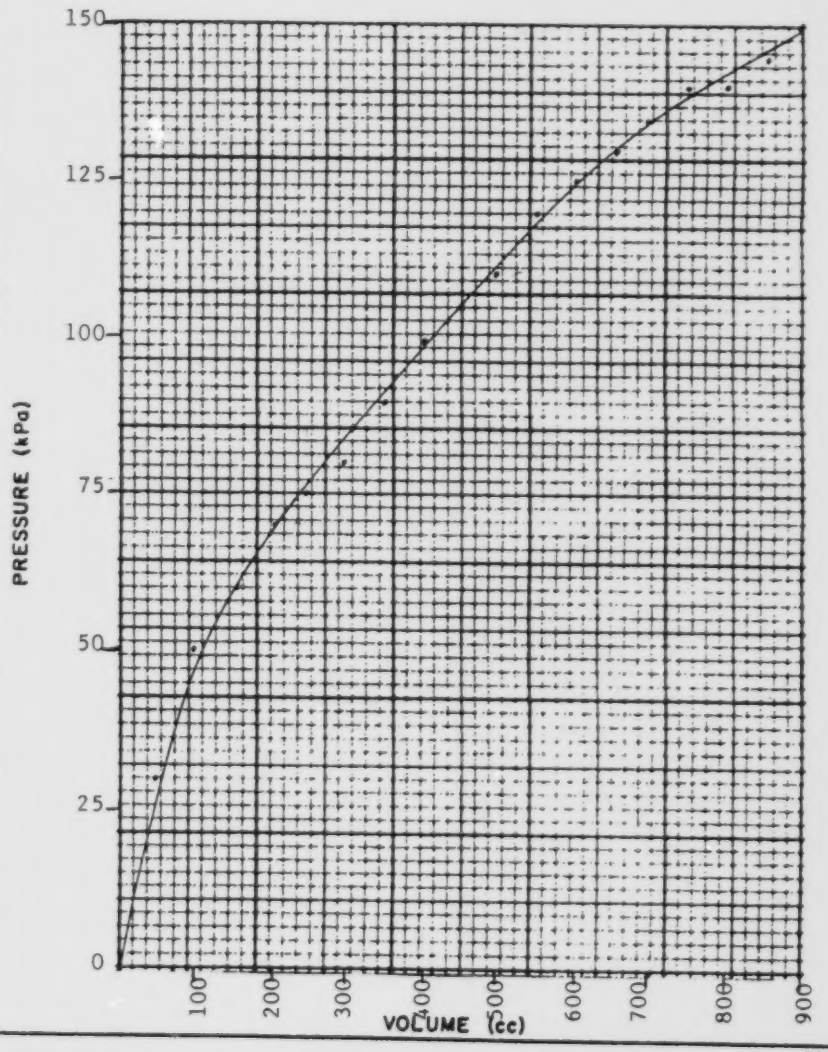

Drawing No. 28

TROW
DILATOMETER/PRESSUREMETER TESTS

BOREHOLE Nº : 3
TEST Nº : cont'd
DEPTH : 15
HOLE SIZE :

PROJECT Nº : S00029R
SITE : Backfill Fence 24070

SURFACE ELEVATION :

TEST ELEVATION :

PRESSURE	READINGS			INJECTED VOLUME (cc)	CORRECTED VOLUME (cc)
	1 min.	2 min.	3 min.		
130				650	
135				700	
140				750	
140				800	
145				850	
150				900	

VOLUMETRIC CALIBRATION :

OBSERVATIONS :

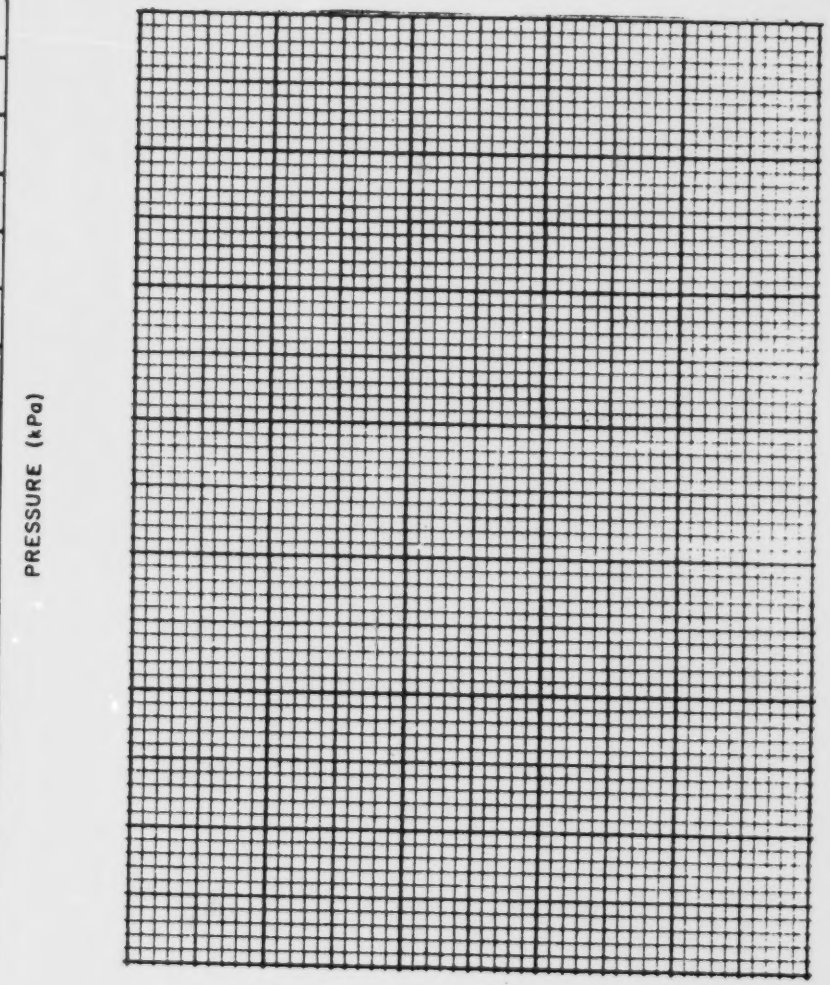

Drawing No. 28 (cont'd)

TROW
DILATOMETER/PRESSUREMETER TESTS

BOREHOLE Nº	4
TEST Nº	3
DEPTH	5'
HOLE SIZE	BQ

PROJECT Nº	S00029R
SITE	Backfill Fence 24070

SURFACE ELEVATION :

TEST ELEVATION :

PRESSURE	READINGS			INJECTED VOLUME (cc)	CORRECTED VOLUME (cc)
	1 min.	2 min.	3 min.		
12				200	
20				250	
25				300	
25				350	
30				400	
40				450	
40				500	
50				550	
50				600	
60				650	
75				700	
100				750	

VOLUMETRIC CALIBRATION :

OBSERVATIONS : $\mu = 0.33$ $\Delta V = 900 - 750 = 150$ cc $\Delta P = 50$ kPa

$V_m = 825$ cc

$E_\phi = 2.66\ (1270 + 825)\left(\frac{1}{150/50 - .84\times10^{-2}}\right) = 1862.78$ kPa

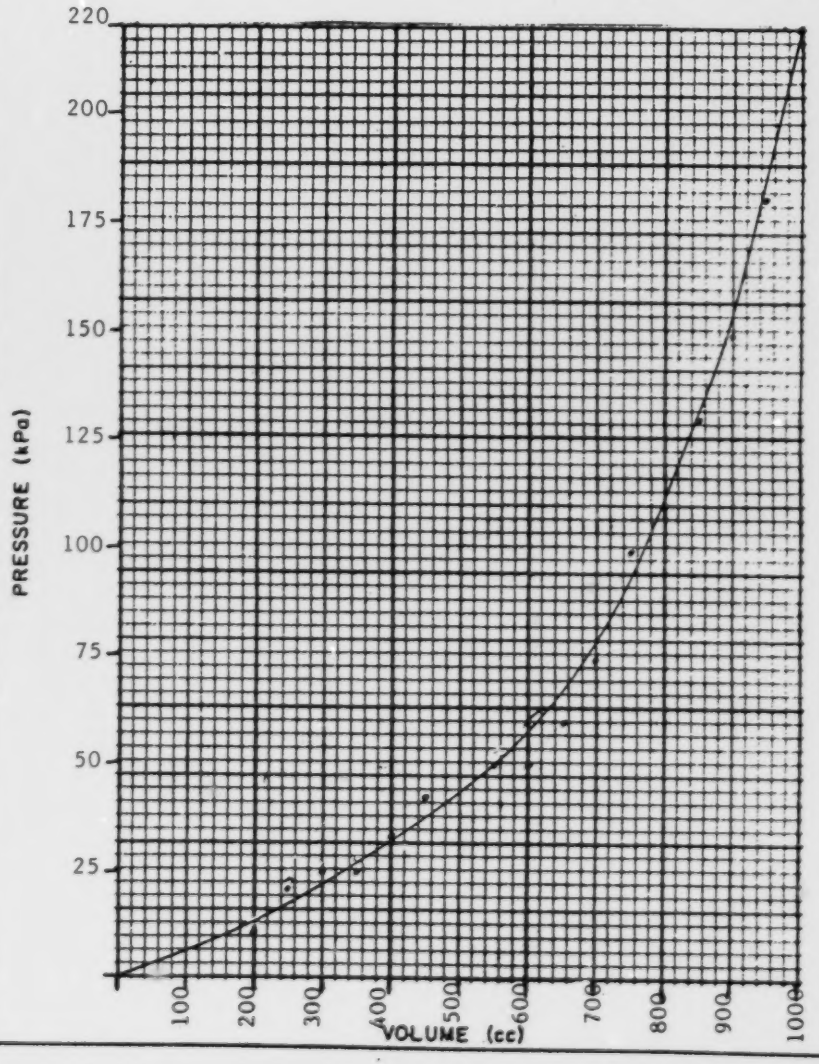

Drawing No. 29

TROW
DILATOMETER/PRESSUREMETER TESTS

BOREHOLE-Nº : 4
TEST Nº : cont'd
DEPTH : 5'
HOLE SIZE : BQ

PROJECT Nº : S00029R
SITE : Backfill Fence 24070

SURFACE ELEVATION :

TEST ELEVATION :

PRESSURE	READINGS			INJECTED VOLUME (cc)	CORRECTED VOLUME (cc)
	1 min.	2 min.	3 min.		
110				800	
130				850	
150				900	
180				950	
220				1000	

VOLUMETRIC CALIBRATION :

OBSERVATIONS :

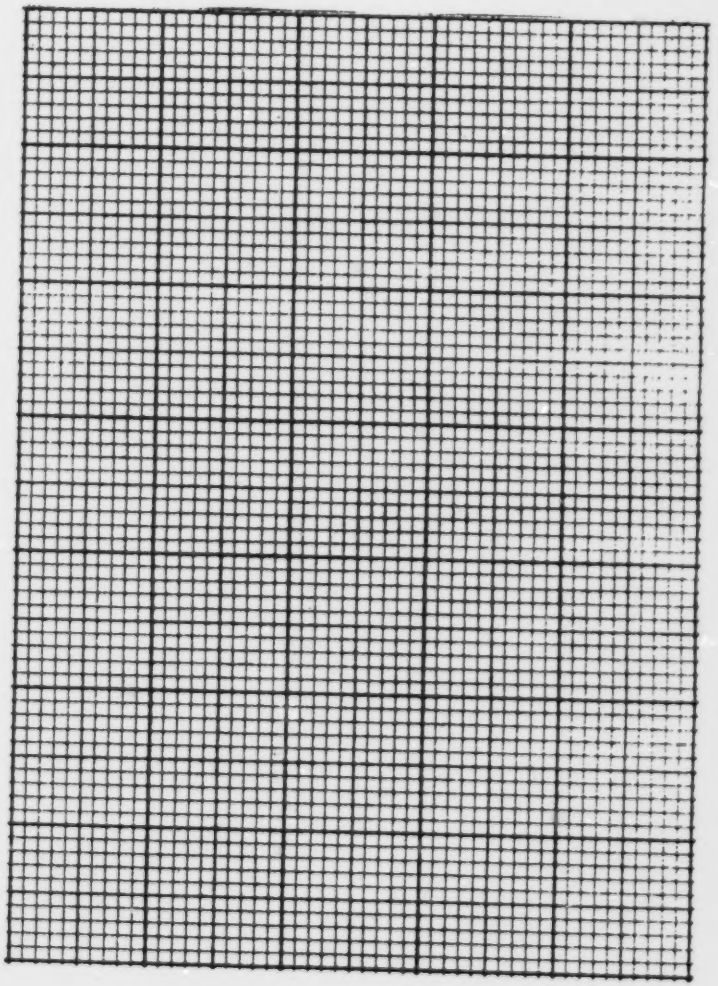

Drawing No. 29 (cont'd)

TROW
DILATOMETER/PRESSUREMETER TESTS

BOREHOLE Nº :- 4
TEST Nº : 2
DEPTH : 10
HOLE SIZE : BQ

PROJECT Nº : S00029R
SITE : Backfill Fence 24070

SURFACE ELEVATION :

TEST ELEVATION :

PRESSURE	READINGS			INJECTED VOLUME (cc)	CORRECTED VOLUME (cc)
	1 min.	2 min.	3 min.		
20				250	
25				300	
30				350	
35				400	
40				450	
45				500	
50				550	
60				600	
70				650	
80				700	
90				750	
90				800	

VOLUMETRIC CALIBRATION :

OBSERVATIONS :

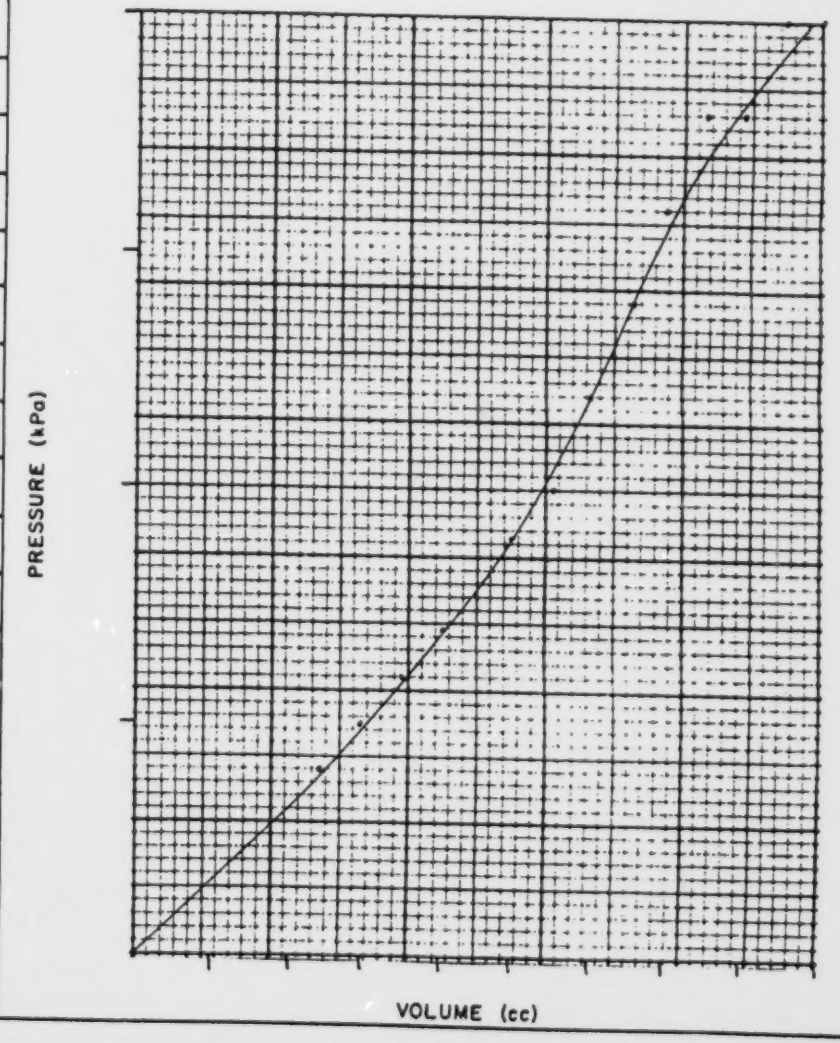

Drawing No. 30

TROW
DILATOMETER/PRESSUREMETER TESTS

BOREHOLE Nº : 4
TEST Nº : cont'd
DEPTH : 10
HOLE SIZE : BQ

PROJECT Nº : S00029R
SITE : Backfill Fence 24070

SURFACE ELEVATION :

TEST ELEVATION :

PRESSURE	READINGS			INJECTED VOLUME (cc)	CORRECTED VOLUME (cc)
	1 min.	2 min.	3 min.		
100				850	
100				900	

VOLUMETRIC CALIBRATION :

OBSERVATIONS :

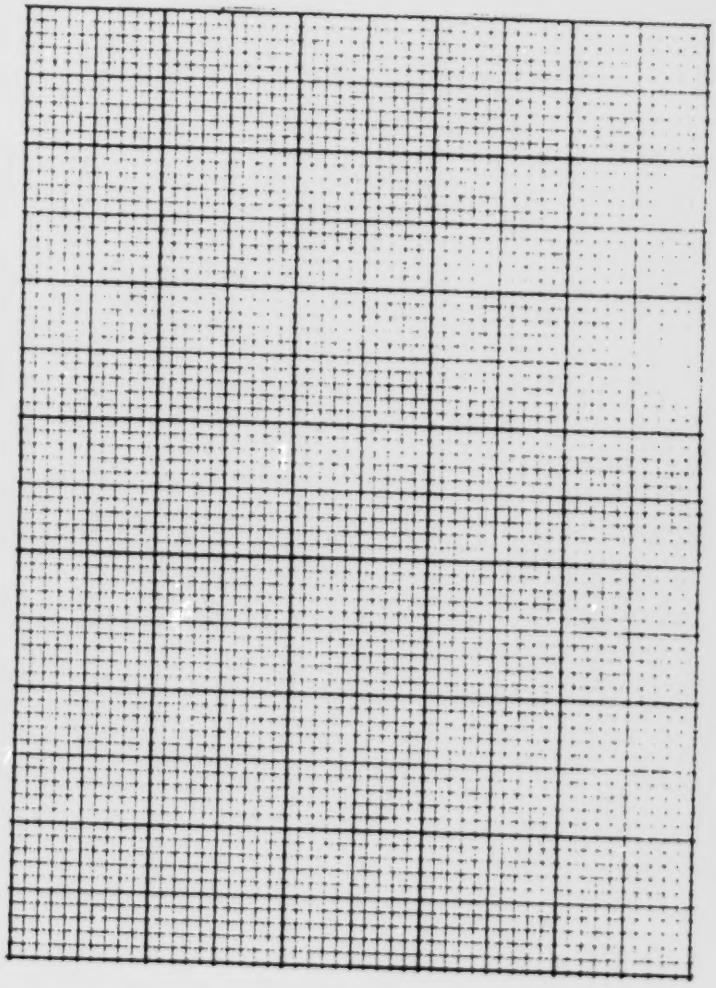

TROW
DILATOMETER/PRESSUREMETER TESTS

BOREHOLE Nº :	4
TEST Nº :	1
DEPTH :	15
HOLE SIZE :	BQ

PROJECT Nº : S00029R
SITE : Backfill Fence 24070

SURFACE ELEVATION :

TEST ELEVATION :

PRESSURE	READINGS			INJECTED VOLUME (cc)	CORRECTED VOLUME (cc)
	1 min.	2 min.	3 min.		
25				150	
25				200	
30				250	
40				300	
40				350	
50				400	
55				450	
60				500	
70				550	
75				600	
75				650	
80				700	

VOLUMETRIC CALIBRATION :

OBSERVATIONS : $u_o = 53$ $\Delta V = 500 - 200 = 300$ cc $\Delta p = 35$ Kpa

$E_\phi = 2.66 \quad (1270 + 350) \left(\frac{1}{\frac{300}{35} - .84 \times 10^{-2}} \right) = 503.23$ Kpa.

$V_m = 350$ cc

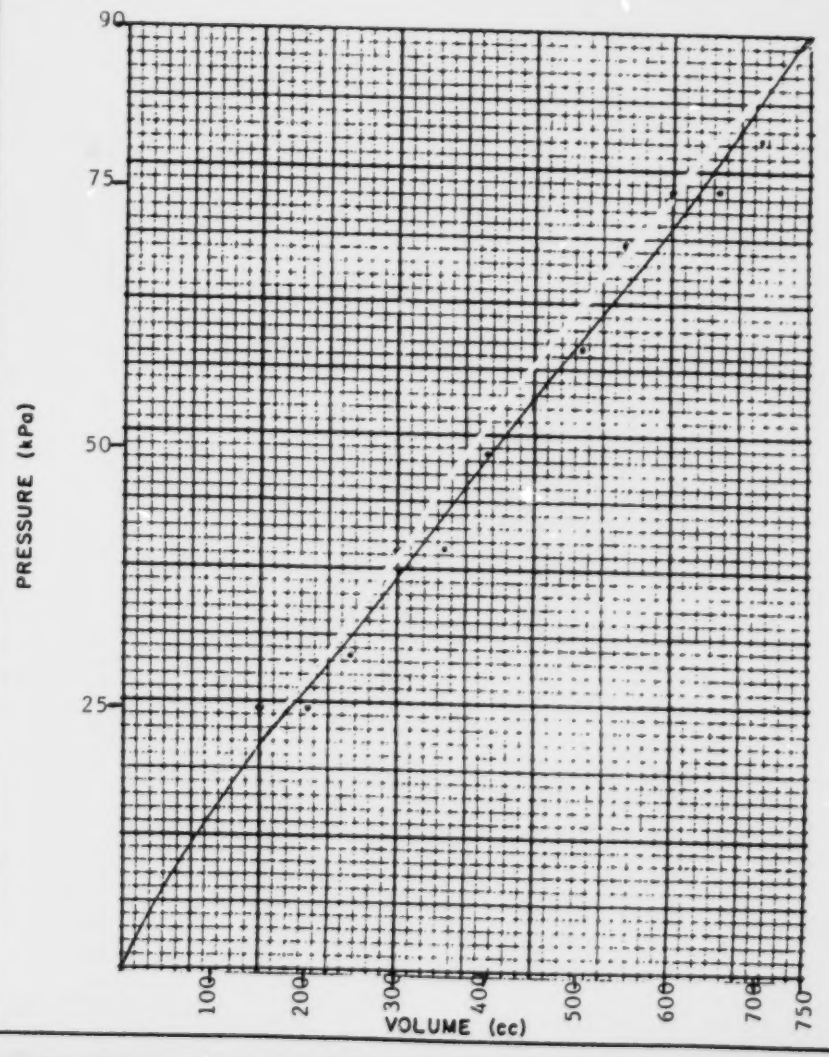

Drawing No. 31

TROW
DILATOMETER/PRESSUREMETER TESTS

BOREHOLE Nº	4
TEST Nº	cont'd
DEPTH	15
HOLE SIZE	BQ
PROJECT Nº	S00029R
SITE	Backfill Fence 24070

SURFACE ELEVATION :

TEST ELEVATION :

PRESSURE	READINGS			INJECTED VOLUME (cc)	CORRECTED VOLUME (cc)
	1 min.	2 min.	3 min.		
90				750	

VOLUMETRIC CALIBRATION :

OBSERVATIONS :

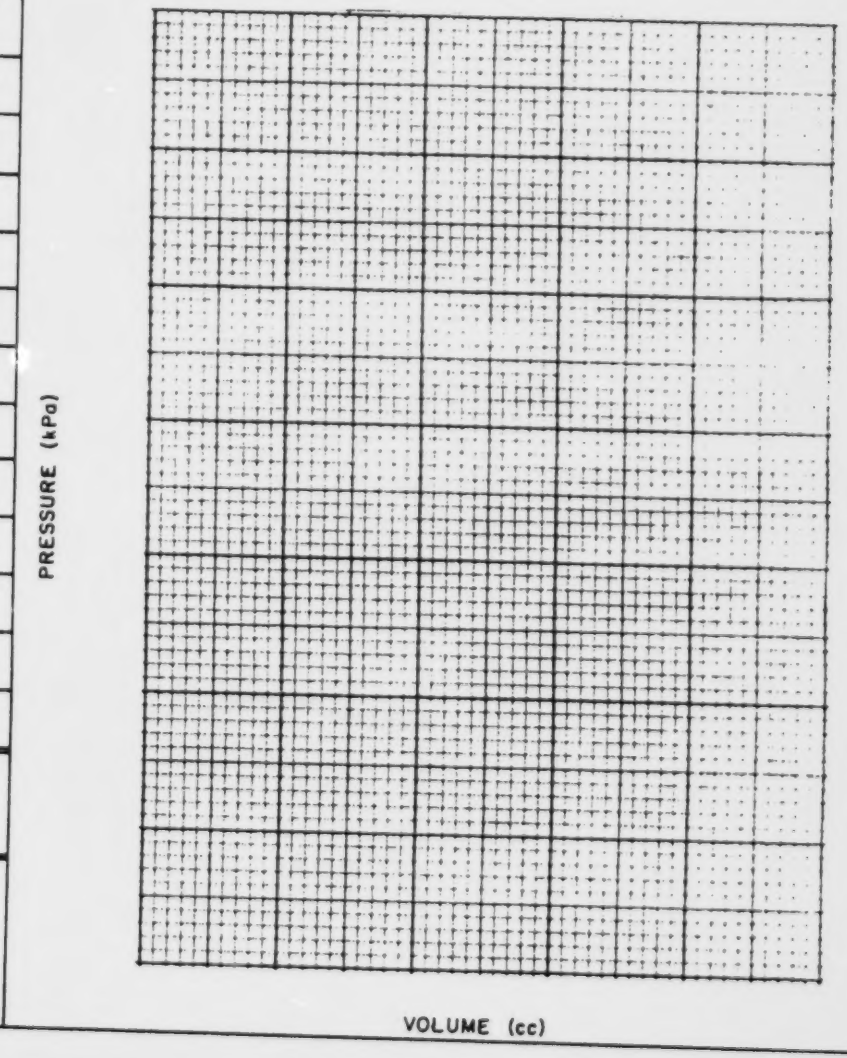

TROW
DILATOMETER/PRESSUREMETER TESTS

BOREHOLE Nº : 4
TEST Nº : 6
DEPTH : 20'
HOLE SIZE : BQ

PROJECT Nº : S00029R
SITE : Backfill Fence 24070

SURFACE ELEVATION :

TEST ELEVATION :

PRESSURE kPa	READINGS 1 min.	2 min.	3 min.	INJECTED VOLUME (cc)	CORRECTED VOLUME (cc)
--				250	
12				300	
20				350	
20				400	
25				450	
30				500	
35				550	
40				600	
45				650	
50				700	
55				750	
70				800	

VOLUMETRIC CALIBRATION :

OBSERVATIONS : $\mu = .33$ $\Delta V = 700 - 500 = 200$ cc $\Delta P = 20$ Kpa

$V_m = 600$ cc

$$E_\phi = 2.66\ (1270 + 600)\left(\frac{1}{200/20 - .84 \times 10^{-2}}\right) = 497.84 \text{ Kpa.}$$

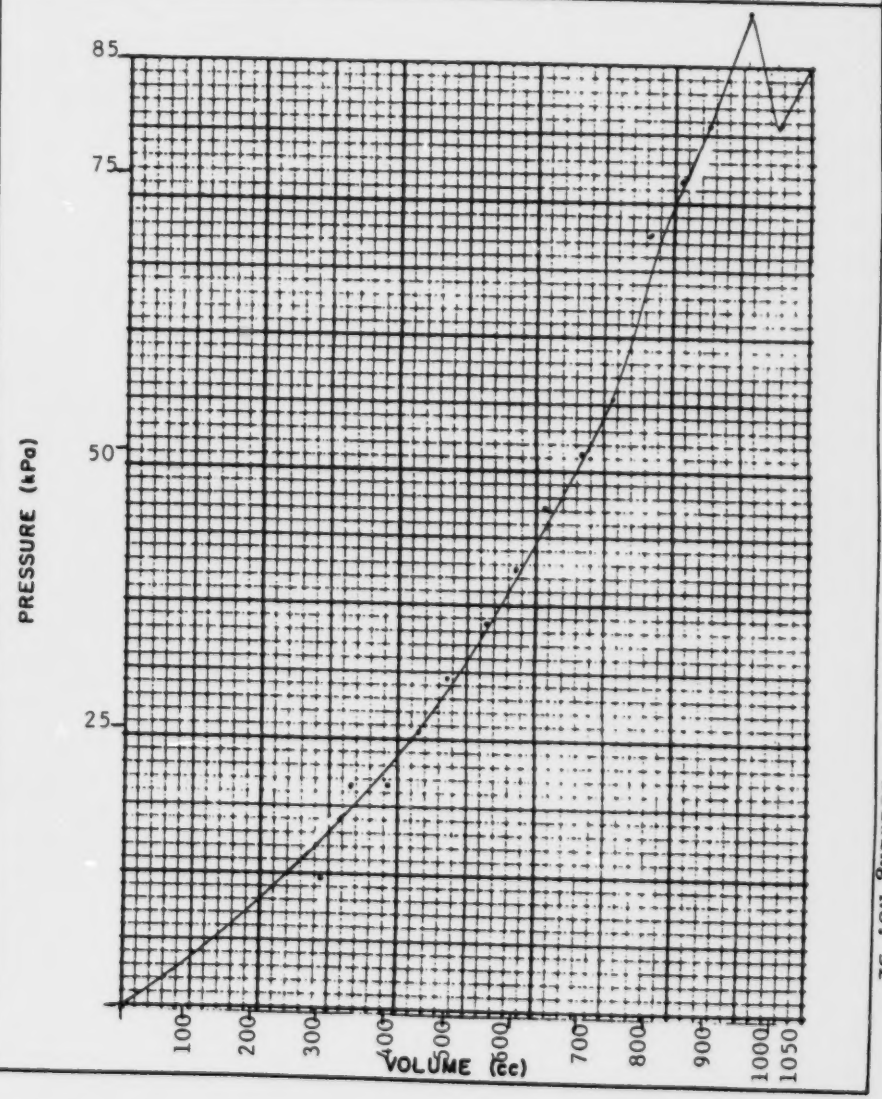

Drawing No. 32

TROW
DILATOMETER/PRESSUREMETER TESTS

BOREHOLE-Nº : 4
TEST Nº : cont'd
DEPTH : 20'
HOLE SIZE : BQ

PROJECT Nº : S00029R
SITE : Backfill Fence 24070

SURFACE ELEVATION :

TEST ELEVATION :

PRESSURE	READINGS			INJECTED VOLUME (cc)	CORRECTED VOLUME (cc)
	1 min.	2 min.	3 min.		
75				850	
80				900	
90				950	
80				1000	
85				1050	

VOLUMETRIC CALIBRATION :

OBSERVATIONS :

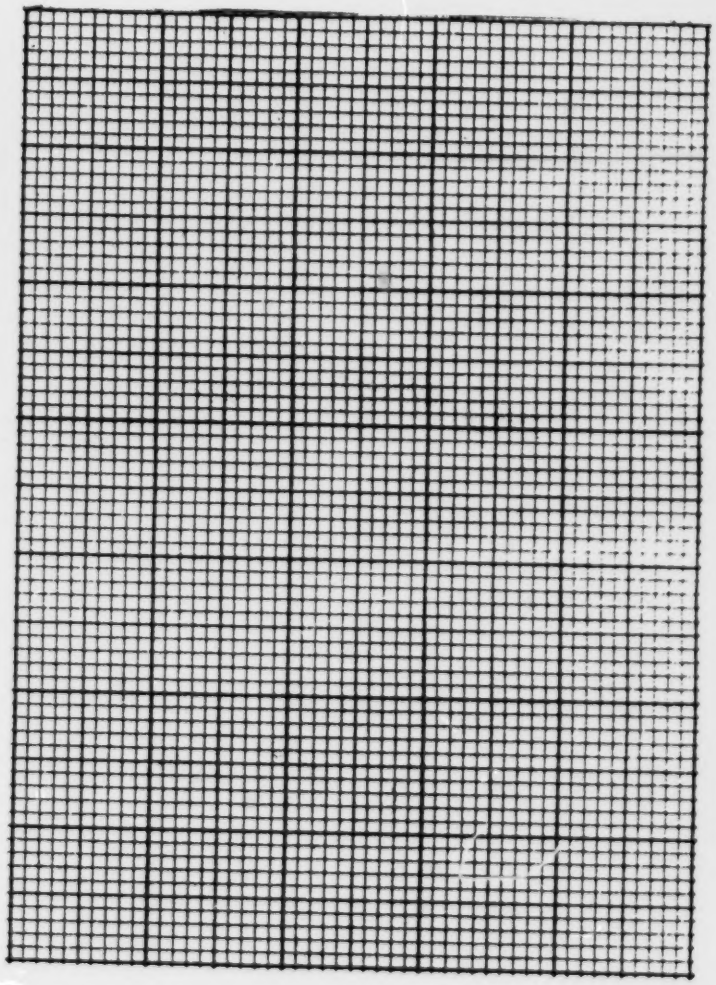

Drawing No. 32 (cont'd)

TROW
DILATOMETER/PRESSUREMETER TESTS

BOREHOLE Nº :-	4
TEST Nº :	5
DEPTH :	24
HOLE SIZE :	BQ

PROJECT Nº : S00029R
SITE : Backfill Fence 24070

SURFACE ELEVATION :

TEST ELEVATION :

PRESSURE	READINGS			INJECTED VOLUME (cc)	CORRECTED VOLUME (cc)
	1 min.	2 min.	3 min.		
				250	
				300	
20				350	
25				400	
30				450	
35				500	
40				550	
45				600	
50				650	
60				700	
60				750	
65				800	

VOLUMETRIC CALIBRATION :

OBSERVATIONS : 42.33 $\Delta V = 650 - 300 = 350$ cc $\Delta P = 30$ Kpa

$V_m = 475$ cc

$E_\phi = 2.66\ (1290 + 475)\left(\frac{1}{\frac{350}{30} - 84 \times 10^{-2}}\right) = 398.15$ Kpa.

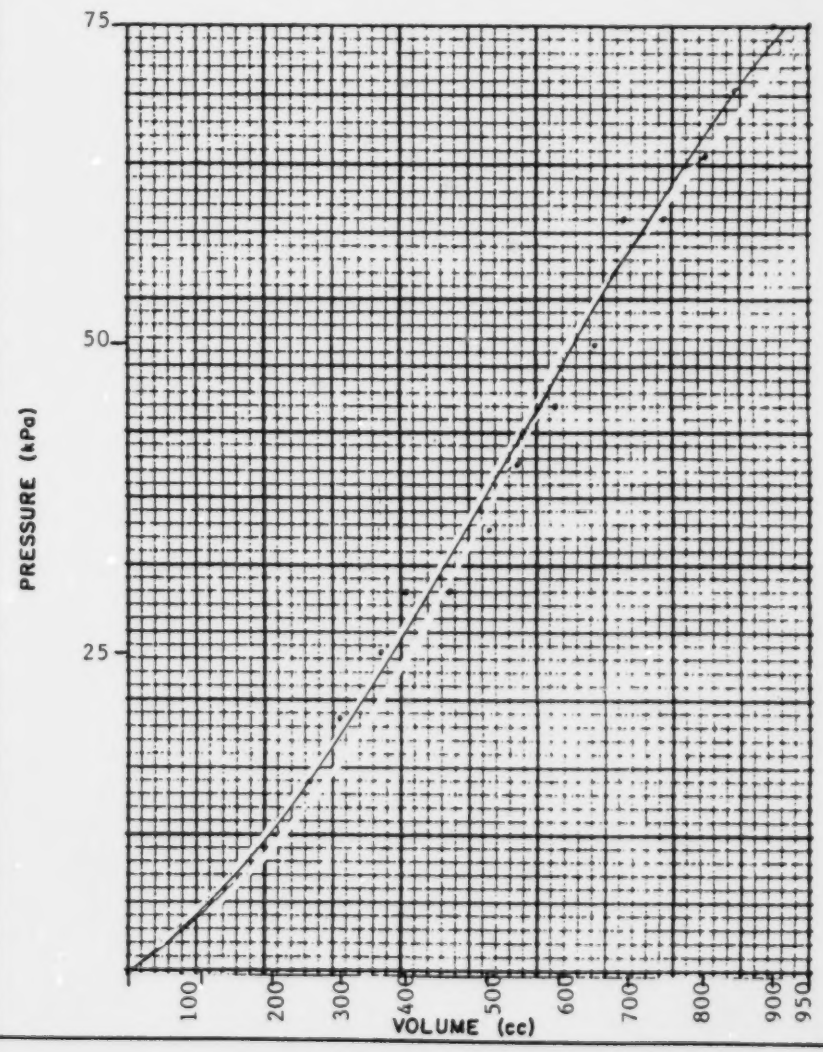

Drawing No. 33

TROW
DILATOMETER/PRESSUREMETER TESTS

BOREHOLE Nº : 4
TEST Nº : cont'd
DEPTH : 24
HOLE SIZE : BQ

PROJECT Nº : S00029R
SITE : Backfill Fence 24070

SURFACE ELEVATION :

TEST ELEVATION :

PRESSURE	READINGS			INJECTED VOLUME (cc)	CORRECTED VOLUME (cc)
	1 min.	2 min.	3 min.		
70				850	
75				900	
75				950	

VOLUMETRIC CALIBRATION :

OBSERVATIONS :

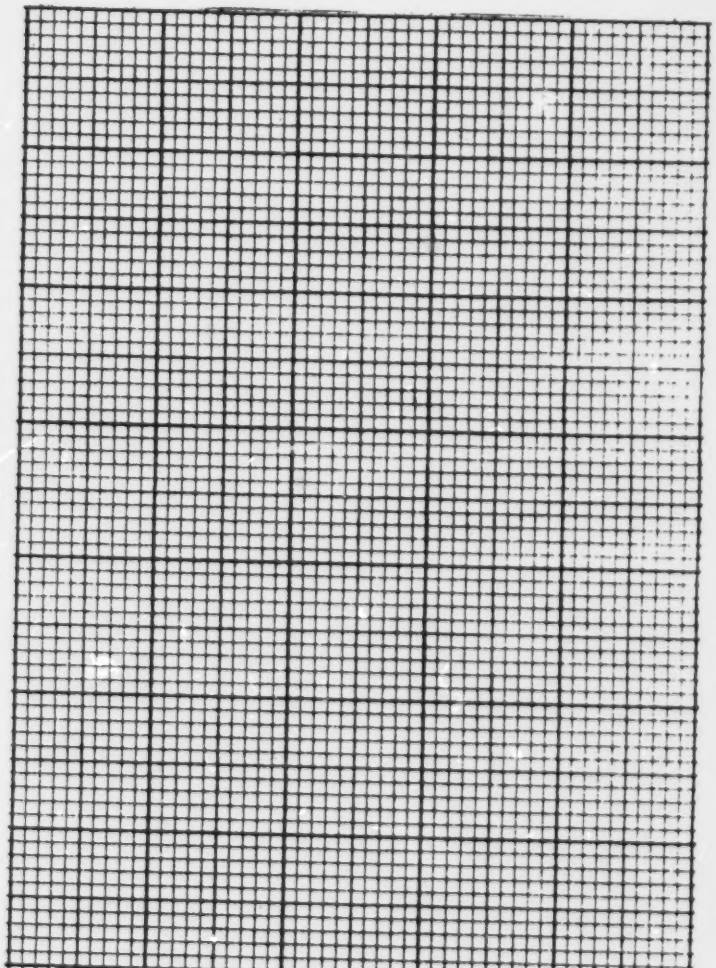

Drawing No. 33 (cont'd)

TROW
DILATOMETER/PRESSUREMETER TESTS

BOREHOLE Nº :	4
TEST Nº :	4
DEPTH :	29
HOLE SIZE :	BQ

PROJECT Nº : S00029R
SITE : Backfill Fence 24070

SURFACE ELEVATION :

TEST ELEVATION :

PRESSURE	READINGS			INJECTED VOLUME (cc)	CORRECTED VOLUME (cc)
	1 min.	2 min.	3 min.		
25				150	
25				200	
30				250	
35				300	
40				350	
50				400	
75				450	
100				500	
150				550	
190				600	
140				650	
140				700	

VOLUMETRIC CALIBRATION :

OBSERVATIONS : $\mu = .33$ $\Delta V = 600 - 500 = 100$ cc $\Delta p = 90$ Kpa

$V_m = 550$ cc

$$E_\phi = 2.66 \ (1270 + 550) \left\langle \frac{1}{\frac{100}{90} - .84 \times 10^{-2}} \right\rangle = 4390.27 \text{ Kpa}$$

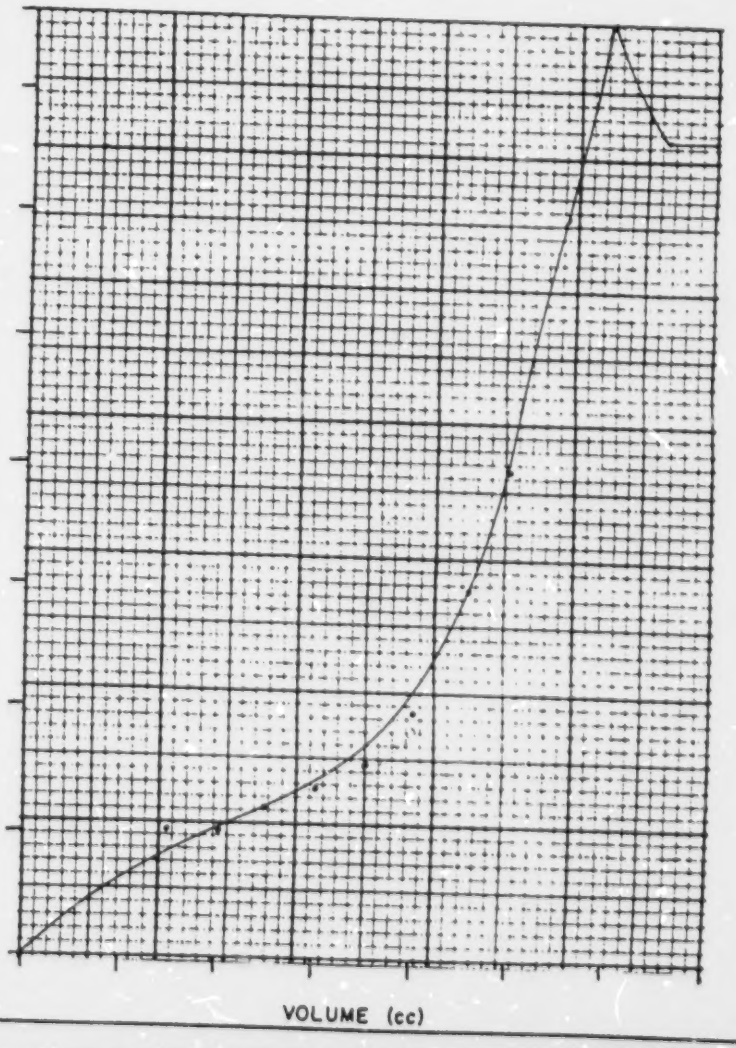

Drawing No. 34

Trow

APPENDIX 1

McGill University

Department of Mining & Metallurgical Engineering
McConnell Engineering Building Telephone: (514) 392-5427 Telex: 05-268-510

August 19, 1986

Mr. Greg Hunt
Denison Mines
Elliot Lake, Ontario
P5A 2K2

Dear Greg,

This letter is intended to update you on the status of our backfill study which was initiated at Denison Mines on June 23rd. We are now in a position to report on our findings.

The data as observed in the field has now been processed, corrections for instrument characteristics have been made and points of interest has been extracted from the individual curves. The major characteristics of interest include Shear Modulus (G_m), Deformation Modulus (E_m) and the Limit Pressure (P_L).

The Shear Modulus (G_m) is calculated from the straight line portion of the curve and can be determined by the formula:

$$G_m = V_m \times \frac{\Delta P}{\Delta V} \qquad (1)$$

where V_m = the volume of the cavity at mid-expansion

$= V_0 + 1/2\ V_L$

where V_0 = initial volume of the Pencel (230 cc)

V_L = Volume range of linear portion of curve

and $\frac{\Delta P}{\Delta V}$ = slope of straight line portion of curve

Furthermore the Deformation Modulus (E_m) is related to the Shear Modulus (G_m) by the formula:

$$E_m = 2(1 + \nu)\ G_m \qquad (2)$$

.....2/

Postal address: 3480 University Street, Montreal, PQ, Canada H3A 2A7

If we assume a Poissions Ratio of .33 we can calculate E_m from G_m. We further note that an actual variation of Poissions ratio from .2 to .5 causes only a $\pm$ 12% variation in E_m. Lastly, we determine the limit pressure (P_L) by extending the plastic range of the curve to twice the original diameter of the instrument.

It is hoped that this lengthly explanation will provide you with a basis for understanding the data and its limitations.

Attached to this letter is a data package consisting of the corrected raw data curves for each location tested, data summaries of parameters of interest for the Denison tests and lastly these parameters are tabulated against tests done at other locations.

You will notice that the data from 33047 is missing. This has been deliberately done because as you recall the tests kept breaking through to old CANMET holes. As such I have no confidence in this data.

A limitation of the data obtained at the bulkhead of 37046 stope should also be pointed out. You will notice that each of the curves never reaches the plastic range. This gives rise to two limitations. Firstly, it inhibits us from determining the limit pressure, P_L. Secondly, the deformation modulus is slightly underestimated as V_m can not be determined with precision. This comes about as a result of not being able to account for the entire volume range of the linear portion of the curve, V_L. If we start by analyzing this data we find shear and deformation moduli of 24.6 and 65.6 MPa respectively. Although we can not precisely determine the limit pressure P_L, past experience has shown us that the E_m/P_L ratio for this type of material varies between 10 and 20. This would translate in a P_L value between 3.5 and 6.5 MPa. This would undoubtedly make this material the strongest and stiffest tested to date. I believe this to have been caused by the Portland cement being carried by the slurry water down to the bulkhead area thus giving a much stiffer material.

Three sets of tests were carried out in the pillar extraction area between 37036 and 37038 stopes. Each of these tests gave very similar results. As an example the tests done in both the light grey and dark grey fills on the 37036 side gave limit pressures of .9 and 1.2 MPa, shear modulus of 7.1 and 4.6 MPa and Young's modulus of 18.8 and 1.21 MPa for the light and dark grey fills respectively. The third test done on the 37038 side of the pillar in straight fill yielded P_L, G_m and E_m values of 1.08, 4.5 and 1.2 MPa respectively. This data is almost identical to the dark grey fill on the opposite side of the pillar extraction area, 37036. This data is consistant with the tests performed in the uncemented mill tailings at Lac Matagami with a limit pressure of 1 MPa, shear modulus of 4.5 MPa dn deformation modulus of 11.97 MPa.

The last location of interest is the 37046 filling raise. P_L, G_m, and E_m values of 1.97, 16.9 and 44.9 MPa respectively were obtained at this location. These values are very similar to those obtained in a 20:1 cemented material with .03 lb/tonne of flocculants added. This yield P_L, G_m and E_m values averaging 2, 15.4 and 41.2 MPa at Kiena Mine.

...3/

I hope you will find this data both informative and useful. If you should have any questions regarding the data, please feel free to contact me at anytime.

Yours sincerely,

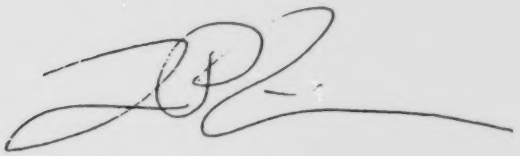

Luciano Piciacchia

Encl.

Denison – Corrected Data

37046 Stope – Uppercut

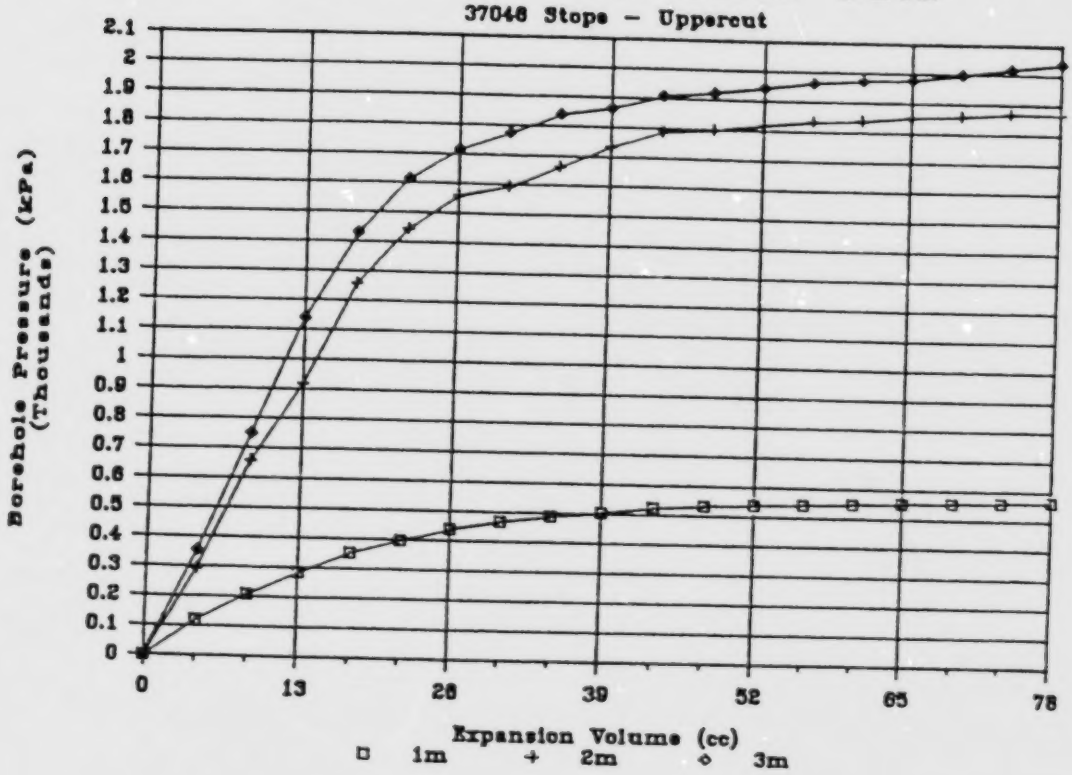

Denison – Corrected Data

37038 Stope – Dry Light Grey Fill

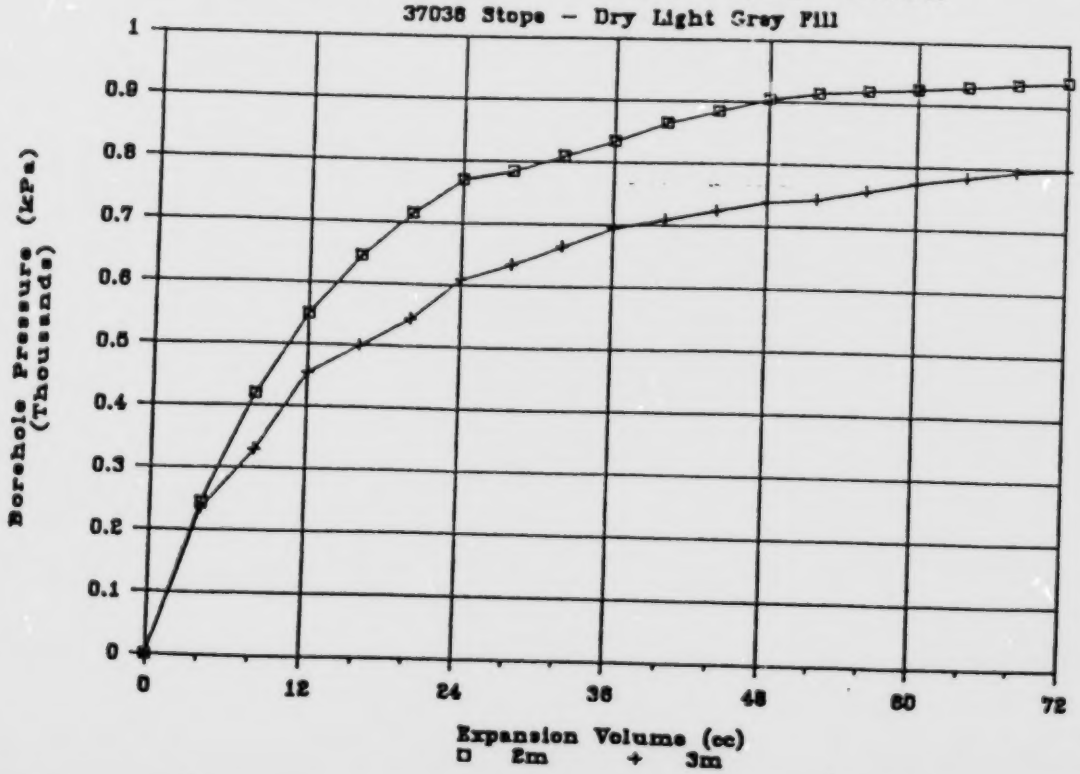

Denison – Corrected Data

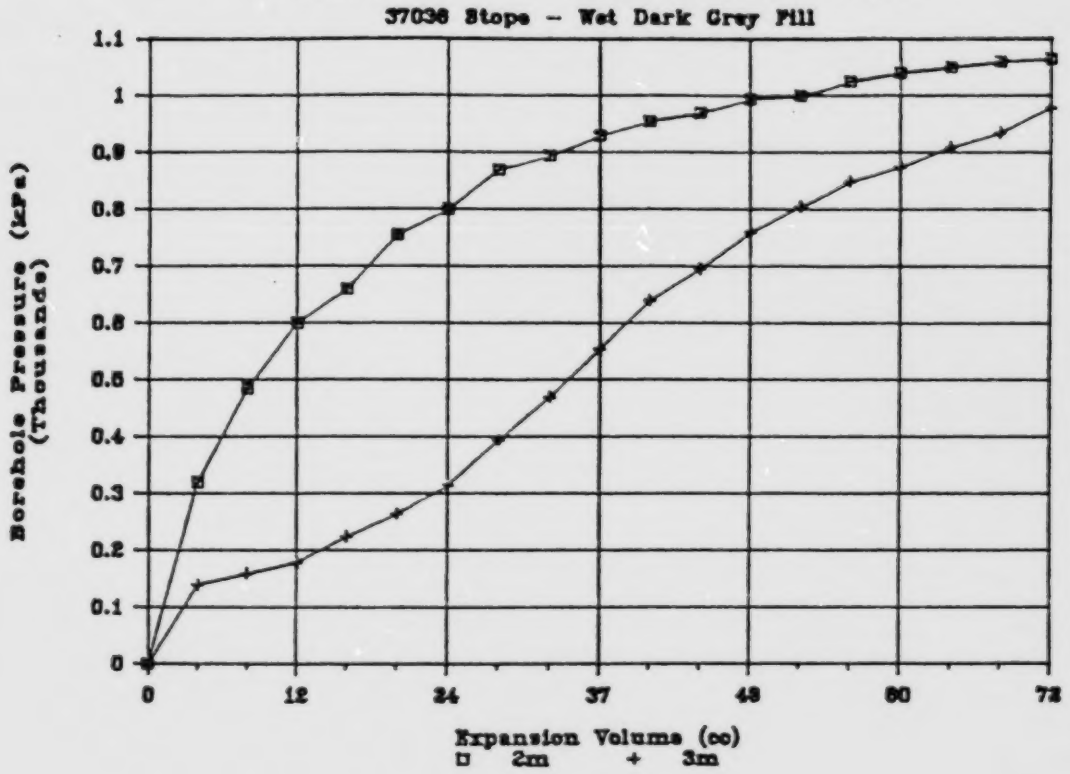

Denision – Corrected Data

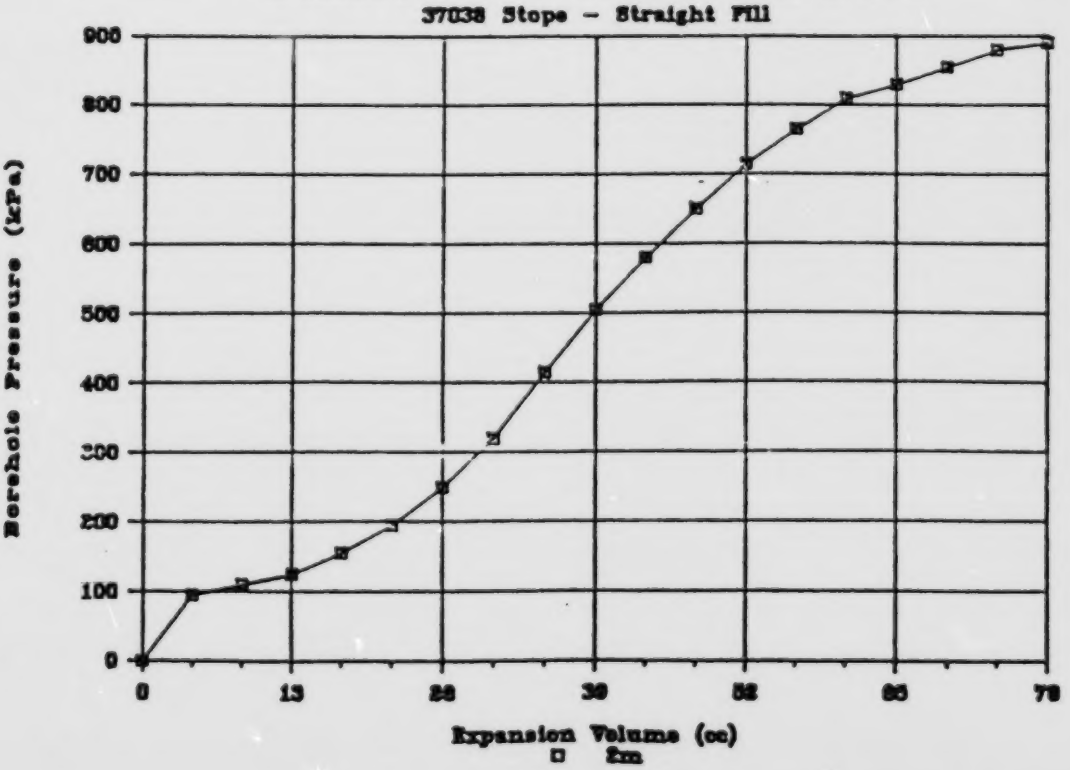

Denison Mines

Data Summary - Shear Modulus

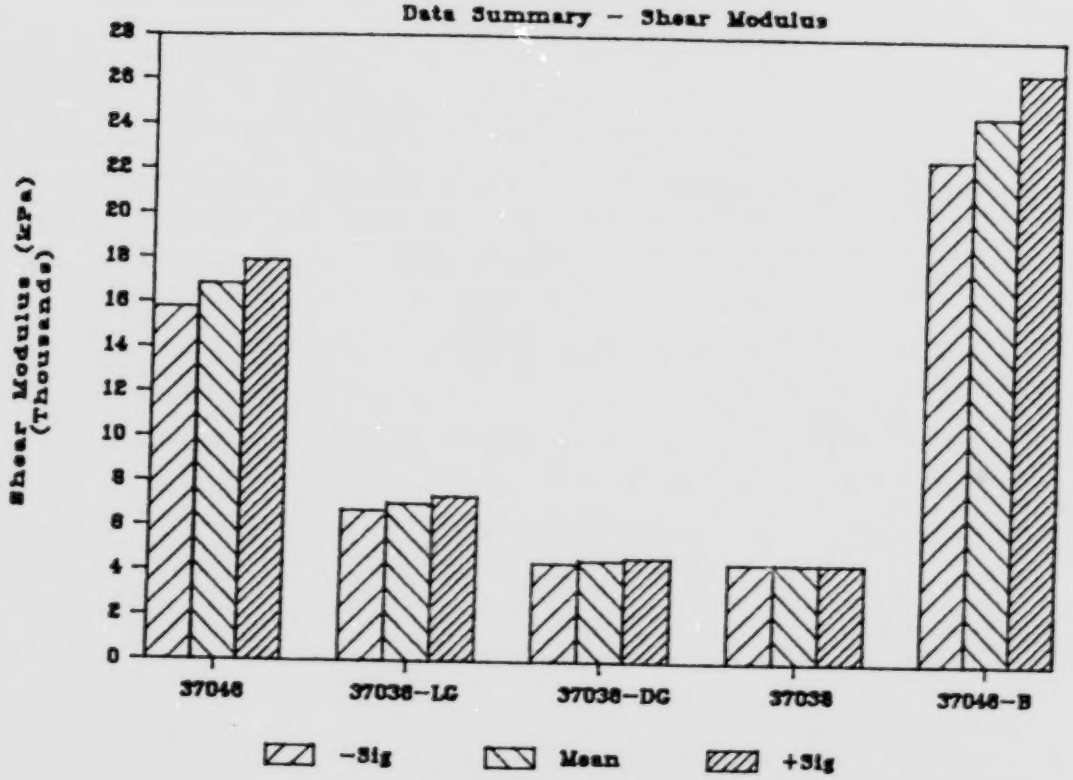

Denison Mines

Data Summary - Limit Pressure

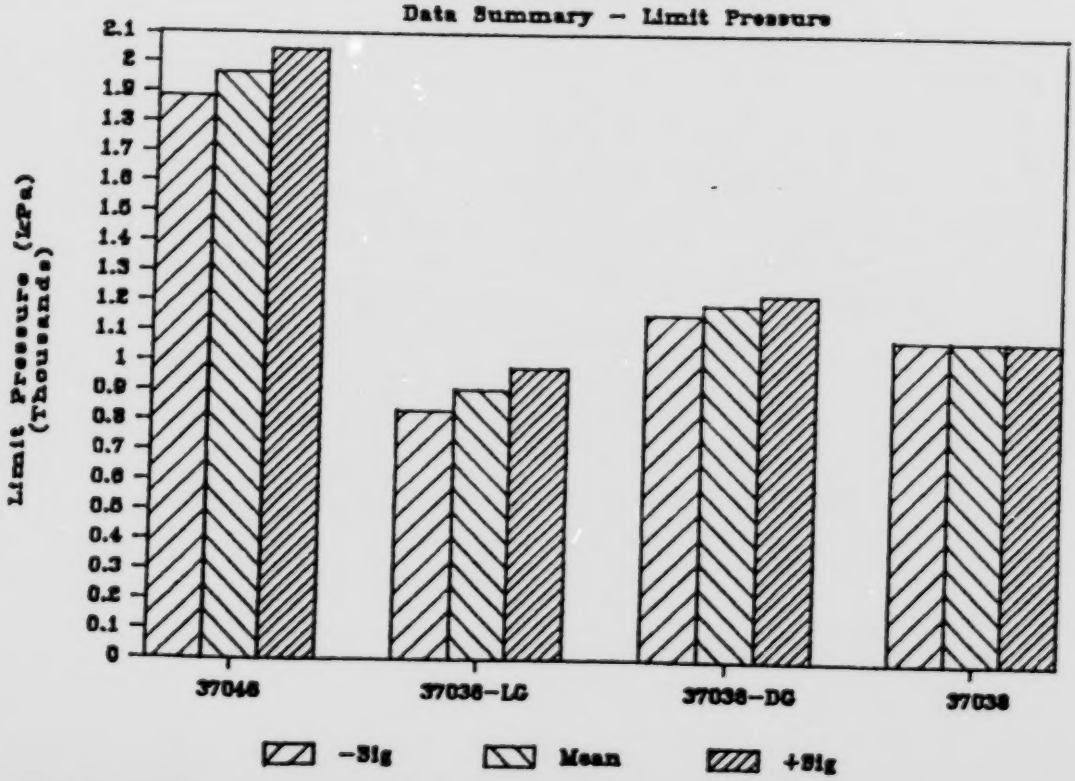

Denison – Corrected Data

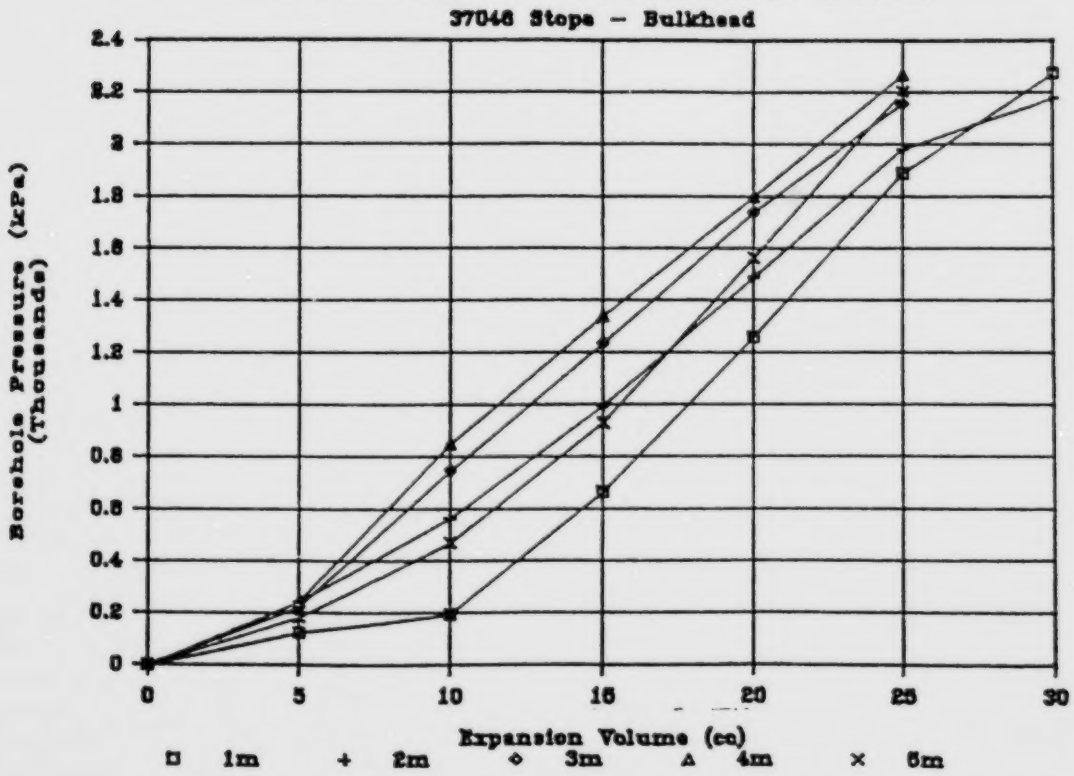

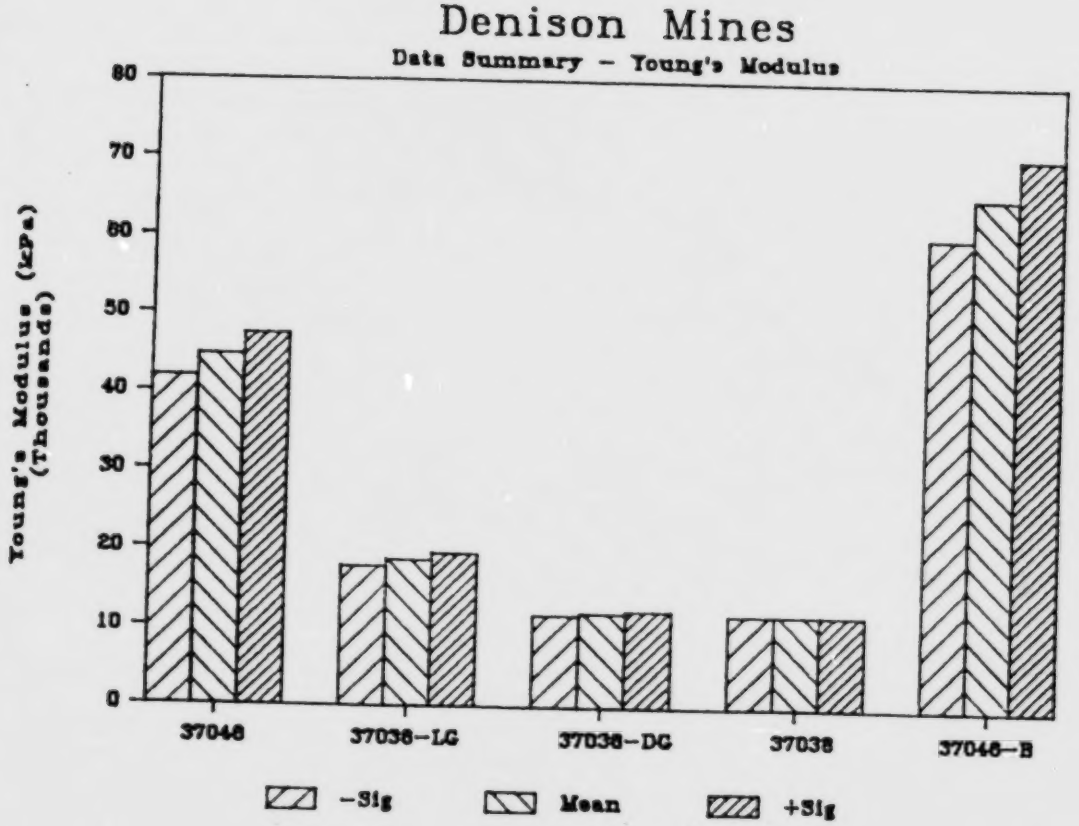
Denison Mines
Data Summary - Young's Modulus
Young's Modulus (kPa)
(Thousands)
80
70
60
50
40
30
20
10
0
37046
37038-LG
37038-DG
37038
37046-B
-Sig
Mean
+Sig

Data Summary

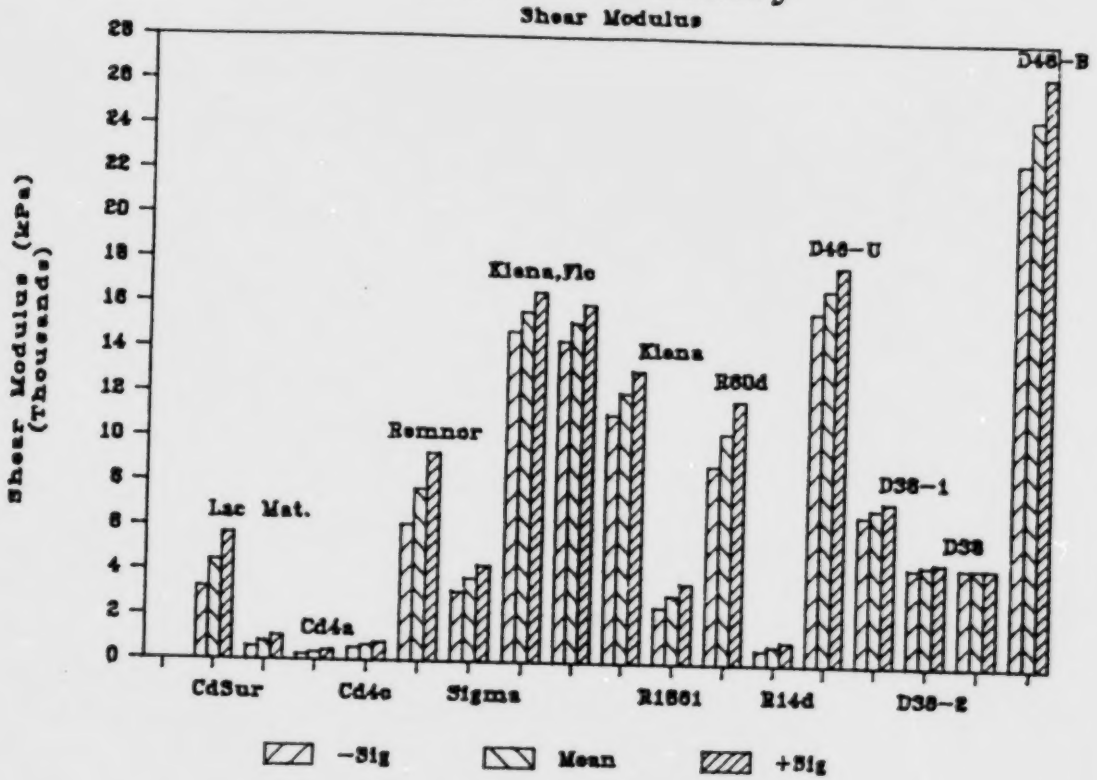

Data Summary

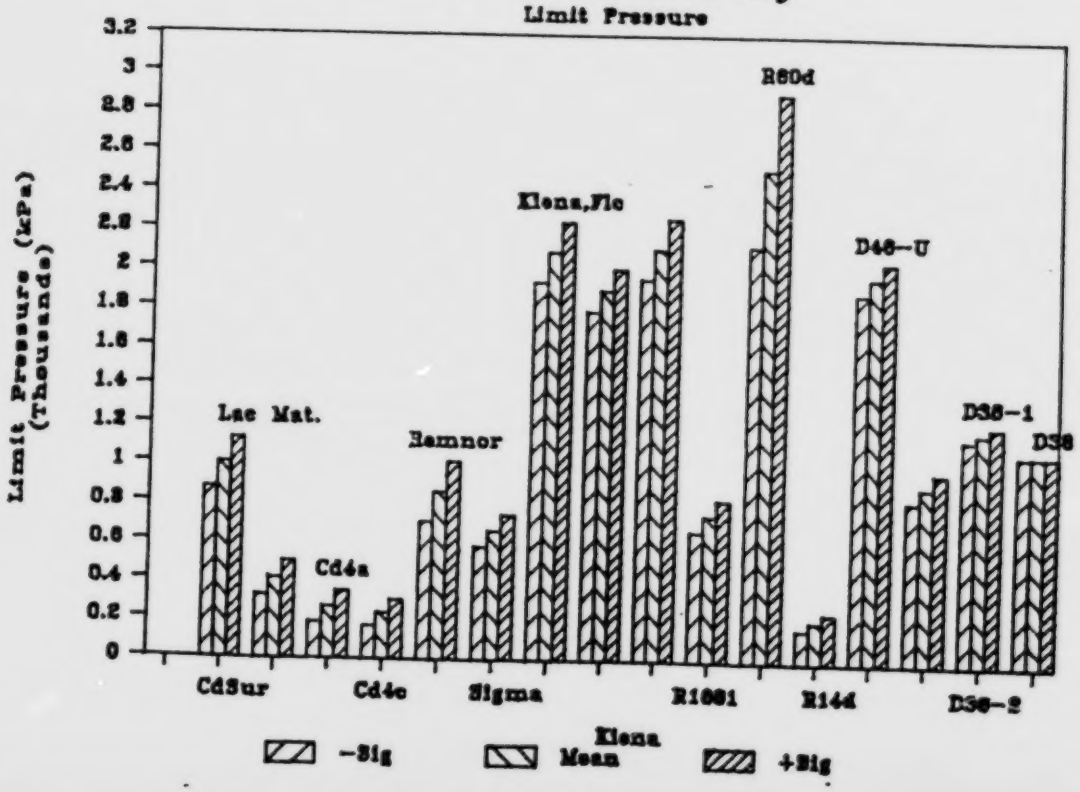

Data Summary

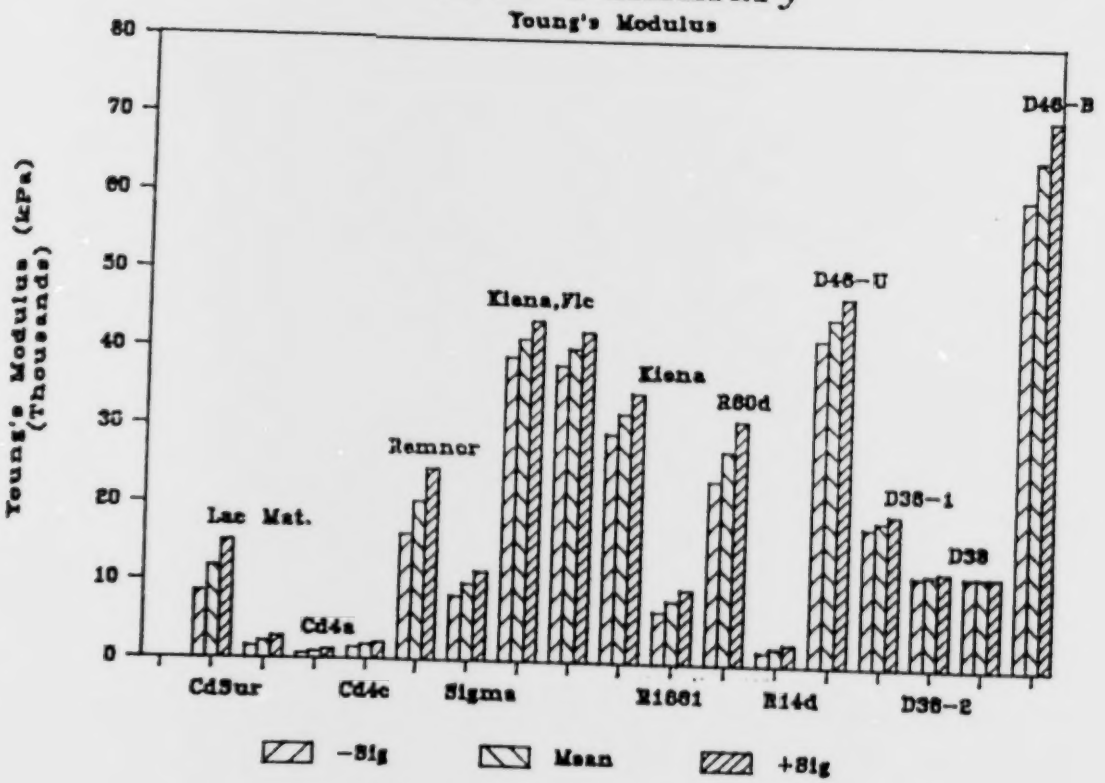

APPENDIX 3

D R A F T F I N A L R E P O R T

PROJECT TITLE:	Development of In-Situ Rockburst Precursor Warning Systems
CONTRACT DURATION:	January, 1987 - March, 1989
FUNDING AGENCY:	Denison Mines Limited
CONTRACTORS:	Dr. J.F. Archibald and Dr. P.N. Calder Department of Mining Engineering Queen's University at Kingston
SUBMISSION DATE:	March 30, 1989

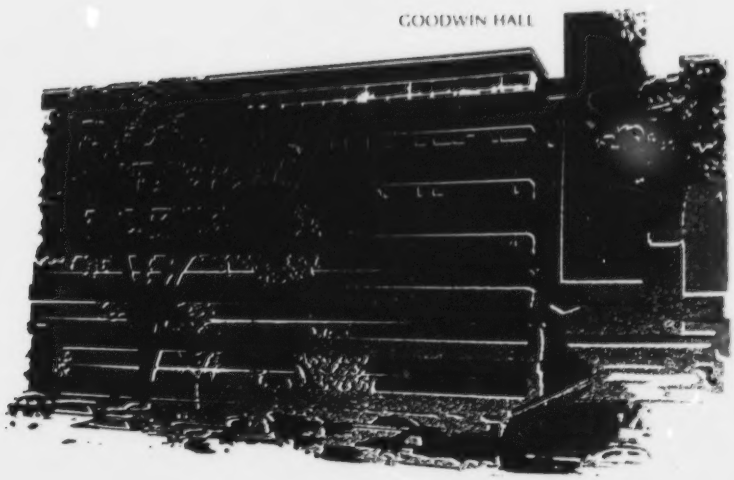

MINING ENGINEERING

QUEEN'S UNIVERSITY at kingston, ontario, canada

DRAFT FINAL REPORT

PROJECT TITLE:	Development of In-Situ Rockburst Precursor Warning Systems
CONTRACT DURATION:	January, 1987 - March, 1989
FUNDING AGENCY:	Denison Mines Limited
CONTRACTORS:	Dr. J. F. Archibald and Dr. P. N. Calder, Department of Mining Engineering, Queen's University at Kingston
SUBMISSION DATE:	March 30, 1989

Project Summary

Contract research was commissioned by Denison Mines Limited in January, 1987, to investigate methods whereby the phenomenon of in-situ rockbursting could be effectively monitored and predicted using innovative acoustic sensing/recognition technology. This technology has been developed by the Queen's University Department of Mining Engineering to complement existing rockburst monitoring systems currently being used by mines to identify rockburst event source locations in post-event cases.

A long term program involving both laboratory and in-situ monitoring was proposed and carried out. As a result of this research, both equipment and software technology necessary to permit successful monitoring of high frequency acoustic emissions and the limited capability to assess variation in ground stress states leading to possible rockburst instability in pillar-associated ground was successfully developed.

During initial research stages, standard microcomputing hardware and software was developed for the purpose of enabling in-situ installation studies. During consequent field trials, individual microseismic monitoring units were observed to perform with outstanding success for periods in excess of two years with minimum maintenance and without provision of ruggedizing capabilities. A series of six different pillar sites, each subjected to dissimilar stress influence, were initially identified for monitoring purposes; of the six, three were selected for long term microseismic evaluation.

On the basis of in-situ stress analysis, stress modelling review and acoustic emission data obtained, significant differences in site behaviour were observed. Specific software, derived from pattern recognition technology, has permitted the rapid and efficient evaluation of site stress conditions and has been shown successful in identifying differences in site stress conditions solely on the basis of acoustic emission examination. In one instance, successful mapping of gradual stress build-up within a rib pillar, tributary to pillar extraction operations, resulted in the capture of a localized rockburst event and the subsequent characterization of acoustic data associated with the rockburst event.

TABLE OF CONTENTS

		Page
	Project Summary	i
1.0	Introduction	1
2.0	Acquisition Hardware and Software	2
3.0	Denison Research Program	8
	3.1 Preliminary Site Investigation Work	8
	3.2 Monitoring Site Stress Assessment	11
	3.2.1 Laboratory Rock Mechanical Property Evaluation	14
	3.2.2 In-Situ Stress (Doorstopper Gage) Evaluation	28
	3.2.2.1 Site #1 Stress Component Determination	29
	3.2.2.2 Site #2 Stress Component Determination	30
	3.2.2.3 Site #3 Stress Component Determination	32
	3.2.2.4 Site #4 Stress Component Determination	33
	3.2.2.5 Site #5 Stress Component Determination	35
	3.2.2.6 Site #6 Stress Component Determination	36
	3.2.3 Summary of Doorstopper Gage Stress Determination Trials	37
	3.2.4 Additional Stress Evaluation Analysis	39
4.0	Microseismic Precursor Evaluation Program	53
	4.1 Site #1/ Site #2 (Low Stress Zone)	54
	4.2 Site #4/ Site #5 (High Stress Zone)	58
	4.3 Site #6 (Medium Stress Zone)	62

TABLE OF CONTENTS

		Page
5.0	Pattern Recognition Assessment	86
6.0	Conclusions and Recommendations	89
	List of References	92
	Appendices	
	Appendix A - Summary of In-Situ MIcroseismic Monitoring Instrumentation Used	94
	Appendix B - Summary of MINTAB Modelled Pillar Stress Conditions Existing About the Site #6 Microseismic Installation	96

LIST OF FIGURES

		Page
1	Schematic View of In-Situ Microseismic Monitoring Station and Photograph of Microcomputer Hardware Assembly	4
2	Help Menu of the QSTRESS Software Program	5
3	Typical Amplitude (Time Domain) and Fourier Transformed (Frequency Domain) Plots of Seismic Waveform Information	5
4	Components of High Frequency Microseismic Precursor Detection System	7
5	Queen's Microseismic Monitoring Stations Adjacent to the 26 Garage Area (Sites #1, #2, #3, #4 and #5)	10
6	North-South Section Through 26 Garage Seismic Drilling Sites	12
7	Microseismic Monitoring at Sites #4 and #5 (26 Garage)	12
8	Microseismic Monitoring Station at Site #6 (35 Panel)	13
9	Variation in Unconfined Compressive Strength and Young's Modulus Behaviour versus Depth Within Stress Monitoring Boreholes at Site #1 (26 Garage Area)	22
10	Variation in Unconfined Compressive Strength and Young's Modulus Behaviour versus Depth Within Stress Monitoring Boreholes at Site #2 (26 Garage Area)	23
11	Variation in Unconfined Compressive Strength and Young's Modulus Behaviour versus Depth Within Stress Monitoring Boreholes at Site #3 (26 Garage Area)	24
12	Variation in Unconfined Compressive Strength and Young's Modulus Behaviour versus Depth Within Stress Monitoring Boreholes at Site #4 (26 Garage Area)	25
13	Variation in Unconfined Compressive Strength and Young's Modulus Behaviour versus Depth Within Stress Monitoring Boreholes at Site #5 (26 Garage Area)	26

LIST OF FIGURES

		Page
14	Variation in Unconfined Compressive Strength and Young's Modulus Behaviour versus Depth Within Stress Monitoring Boreholes at Site #6 (35 Panel Area)	27
15	Average Stress Components for Site #1 Doorstopper Tests	30
16	Average Stress Components for Site #2 Doorstopper Tests	31
17	Average Stress Components for Site #3 Doorstopper Tests	33
18	Vertical Section Through Site #4 Borehole	34
19	Average Stress Components for Site #4 Doorstopper Tests	35
20	Average Stress Components for Site #5 Doorstopper Tests	36
21	Average Stress Components for Site #6 Doorstopper Tests	38
22	Plan View of Site #6 Pillar Zone Modelled by MINTAB	41
23	Plan View Showing Close-up of Pillar Modelling Grid	42
24	MINTAB Modelled Stress Distribution About Site #6 During Initial Stage of Microseismic Monitoring (July, 1987)	44
25	Cross Section of Theoretical Stress Distribution in 35022 Rib Pillar	45
26	Plan View Showing MINTAB Modelled Vertical Displacements About Site #6 Monitoring Location during Initial Phase (July, 1987)	46
27	MINTAB Modelled Stress Conditions About Site #6 During Final Stage of Microseismic Monitoring (October 21, 1987)	48
28	Cross Section of Theoretical Major Principal Stress Distribution in 35024 Rib Pillar	50
29	Long Section of 35024 Pillar Showing Predicted Normal Pillar Stress Components at Various Stages of Mining	51

LIST OF FIGURES

		Page
30	MINTAB Modelled Vertical Displacements About the 35022 Pillar Site During Final Pillar Extraction (October, 1987)	52
31	Amplitude and Frequency Domain Plots of Typical Acoustic Waveforms Monitored at Site #1 (June, 1987)	56
32	Amplitude and Frequency Domain Plots of Typical Acoustic Waveforms Monitored at Site #2 (June - July, 1987)	57
33	Amplitude and Frequency Domain Plots of Typical Acoustic Waveforms Monitored at Site #4 (October - November, 1987)	60
34	Amplitude and Frequency Domain Plots of Typical Acoustic Waveforms Monitored at Site #5 (October - November, 1987)	61
35	Event Rate Activity versus Interval Time for Site #6 Monitoring Site (July 29 - November 3, 1987)	64
36	Peak Event Rate Activity (Site #6) versus Cumulative Stress Change and (Cumulative Stress Change)^3 Effects	65
37	Cumulative Event Rate versus Day for Site #6 Monitoring Site (July 29 - November 4, 1987)	67
38	Amplitude and Frequency Domain Plots of Typical Acoustic Waveforms Monitored at Site #6 (July 29 - November 3, 1987)	69
39	Peak Magnitude versus Time Summary and Frequency Distribution of Total Magnitude Data for Site #6 Monitoring Location	70
40	Cumulative Peak Magnitude versus Interval Time for Microseismic Waveforms at Site #6 (July 29 -November 3, 1987)	72
41	"b" Value Analysis for Site #6 Waveform Data	73
42	Average Centre Frequency versus Day (Site #6)	76
43	Normal Distribution Plot of Centre Frequencies for Site #6	77

LIST OF FIGURES

		Page
44	Centre Frequency Distribution for Low and High Stress Interval Monitoring Periods at Site #6	78
45	Centre Frequency Distribution for Low Stress Ranges at Site #6	79
46	Centre Frequency Distribution for Medium Stress Ranges at Site #6	80
47	Centre Frequency Distribution for High Stress Ranges at Site #6	81
48	Mean Centre Frequency versus Modelled Pillar Stress Condition for Site #6	82
49	Average and Cumulative Energy Sum versus Time for Site #6 Monitoring Site	83
50	Slope of Phase 2 Energy Release Rate Curve versus Ratio of (Pillar Stress / Pillar Strength)	85
B-1	MINTAB Modelled Stresses (Stage 1 - July, 1987)	97
B-2	MINTAB Modelled Stresses (Stage 2 - August 26, 1987)	98
B-3	MINTAB Modelled Stresses (Stage 3 - September 22, 1987)	99
B-4	MINTAB Modelled Stresses (Stage 4 - September 30, 1987)	100
B-5	MINTAB Modelled Stresses (Stage 5 - October 8, 1987)	101
B-6	MINTAB Modelled Stresses (Stage 6 - October 21, 1987)	102

LIST OF TABLES

		Page
1.0	Summary of In-Situ Doorstopper and Core Sample Physical Property Test Results (Site #1, 26 Garage Area)	16
2.0	Summary of In-Situ Doorstopper and Core Sample Physical Property Test Results (Site #2, 26 Garage Area)	17
3.0	Summary of In-Situ Doorstopper and Core Sample Physical Property Test Results (Site #3, 26 Garage Area)	18
4.0	Summary of In-Situ Doorstopper and Core Sample Physical Property Test Results (Site #4, 26 Garage Area)	19
5.0	Summary of In-Situ Doorstopper and Core Sample Physical Property Test Results (Site #5, 26 Garage Area)	20
6.0	Summary of In-Situ Doorstopper and Core Sample Physical Property Test Results (Site #6, 35 Panel)	21
7.0	Summary of Physical Parameter Results for Site Core Specimens	28
8.0	Site Summary of Drilling and Doorstopper Stress Measurement Data	38
9.0	Pattern Recognition Analysis Results for Site #6 Data	87
A-1	Components of Queen's High Frequency Monitoring System	95

1.0 Introduction

Acoustic monitoring techniques have been utilized for several decades within the mining industry for the purposes of rockburst analysis, though the reliability of such methods for both stress and rockburst prediction has been very poor. Successful applications have been made, though they are generally limited in use for post-event rockburst detection using low frequency monitoring networks in which source sites and energy magnitudes of rockburst emissions are evaluated. The majority of standard microseismic research has been restricted to low frequency acquisition, at frequencies considerably lower than 20 KHz, due to problems associated with attenuation of higher frequency signals in geologic materials.

Until recently, however, little pre-event information has been able to be gathered which would be of use in predicting rockburst activity related to such seismic information. The phenomenon of high frequency acoustic emission, often associated with changing in-situ stress conditions, and occasionally with the incidence of rockbursting, has been successfully monitored using innovative acoustic sensing techniques [1,2,3,4] which have been developed by the Queen's University Department of Mining Engineering. Since 1985, the Department of Mining Engineering has undertaken ongoing research to investigate the use of high frequency microseismic emissions in predicting in-situ stress levels and in providing advance warning of rockbursts. The thrust of this research has been to identify characteristics of the frequency spectra of microseismic emissions which may serve to act as precursors to rockbursting. The approach utilizes acoustic emission (AE) monitoring at much higher frequency ranges than is conducted by conventional locator-type systems, and provides the capability for capture and storage of complete waveform information, rather than only initial event arrival times recorded by conventional systems. Whereas conventional systems operate at low detection frequencies, the precursor system has been designed to sample waveform data at the frequency range between 50 - 300 KHz. Due to attenuation of high frequency components of acoustic emissions in geologic materials, the range of detection of acoustic sources is limited to the order of several metres from the geophone sites. It was therefore intended that such networks would be used to complement, rather than replace, conventional locator-type networks presently in use. Once seismically-active zones can be located within mines, portable, high frequency systems can then be installed to provide more intensive, localized stress and rockburst monitoring capability in areas of concern.

The initial research goal of the Queen's/Denison project was to identify characteristics of the frequency spectra of microseismic emissions which may serve to act as precursors to rockbursting. A proposal was submitted to Denison Mines Limited to permit the purchase of system components and to permit long term, in-

situ monitoring to be conducted in the their Elliot Lake mine. Research was to be directed toward development of a localized, acoustic emission monitoring system which could ultimately be used to determine, on the basis of acoustic emission characterization, stress magnitude conditions within pillars and pillar susceptibility to failure. In order to accomplish the goal of data acquisition, a significant amount of in-situ seismic monitoring activity was planned. Coincident with such activity, physical measurement of rock mechanical parametric data and in-situ stress conditions adjacent to monitoring sites was systematically evaluated. The proposed research program was designed to involve sensing and recording of acoustic emissions generated in pillars under a variable range of stress conditions, where both unsupported and backfill supported pillars were to be studied. Acoustic emission signals were to be analyzed using specialized signal conditioning processes. This information would then be correlated with known ground stress information, using pattern recognition technology, to provide a basis upon which stress prediction can be made when signals of unknown origin are monitored. The ultimate goal of the project will be to develop a practical, reliable and low cost tool which can be used by operators to provide reliable estimates of rock stress conditions and possibly to provide some advanced capability for rockburst prediction in real time.

2.0 Acquisition Hardware and Software

Prior to implementation of the Queens/Dension project, research activity sponsored by the Mining Industry Research Organization of Canada (MIROC) had resulted in the development of an effective and reliable laboratory tool for simultaneously recording, analyzing and saving microseismic emission data originating from highly stressed rock. The acquisition system, comprising standard microcomputing hardware and specially designed software (developed at Queen's), was shown, in limited use, to be capable of providing continuous operation with almost 100% availability in underground sites within mines in the Sudbury district of Ontario. The high frequency system which has been utilized during the Denison contract consists of a portable, ruggedized microcomputer capable of operating on a stand alone basis with almost 100% reliability in harsh underground mine environments. Originally consisting of a Zenith Model 151 microcomputer, monitoring application was switched to use of a COMPAQ Model 286 computer in order to insure field survivability. Each monitoring microcomputer unit was designed to have the capability for monitoring a total of sixteen data channels (geophone transducers). Due to the high frequency range of waveforms being addressed in this study (400 KHz), only single geophone transducers were monitored using single microcomputer units. It is possible, however, where waveform frequencies not exceeding 35000 KHz are to be monitored, that the present system could provide a capability to address sixteen channels simultaneously.

Sensors which are used for field monitoring consist of piezoelectric

transducers (Physical Acoustics Corporation, Type μ30D) mounted upon thin, metal plates which facilitate rapid installation and recovery within boreholes at testing sites. The bonded piezoelectric transducers are designed for installation either within jackleg-drilled or diamond-drilled holes at depths exceeding 5-6 metres, such depths being selected to avoid problems induced by high frequency waveform attenuation within localized zones of fractured rock normally present about most underground excavations. The plate-bonded transducers were designed for rapid installation and removal from such holes to minimize both the costs and effort of drilling and installation. From the onset of drilling at each test site, maximum installation time approximates two hours. Geophone recovery can be implemented within minutes.

Elastic ground waves, created by seismic activity at levels above a pre-set threshold level, induce voltage output at the transducers as they pass sampling sites. Seismically-induced voltage signals are then amplified using both in-hole and external amplifiers and are transmitted using 50 ohm coaxial cable as analog signals to the microcomputer. AE analog signals are thereupon converted to digital form using a digitizing board with 12 bit analog-to-digital conversion capability. Each component AE signal was digitized at the rate of one million data points per second (to provide the ability to sample waveform frequencies at the upper limit of 500 KHz). Typical waveform activity was recorded over total sampling interval times approximating 4 milliseconds, initiating at a time approximately 1 millisecond prior to the time at which a pre-set voltage trigger level was exceeded. Typical installation hardware for a single underground site is illustrated in the schematic and photograph of **Figure 1**. The microcomputer is utilized to digitize, store and analyze the incoming waveform signals using a priority-based multi-tasking program, called "QSTRESS", which was developed at Queen's. Priority of processing is based upon pre-set conditions, the prime condition being that waveform recognition, digitization and storage has precedence over all other operations. Additional program tasks include data processing (centre frequency determination, waveform energy content, waveform duration etc.) as well as data plotting and display operations so that acquired data may be viewed as it is received. Typical multi-tasking operations are user addressable to permit continuous monitoring of system operation and site seismic activity conditions. Operations which may be requested during data acquisition are illustrated by the screen menu which is illustrated in **Figure 2.**

Signal processing is currently limited to signal conditioning, to permit viewing in the time domain (amplitude versus time capability), and to frequency content transformation, to permit viewing of data in the frequency domain (frequency versus time capability). In order to accomplish the second conditioning task, Fast Fourier Transform (FFT) analysis is conducted. Typical waveform amplitude data (time domain) and Fourier transformed data (frequency domain) for a characteristic acoustic event are illustrated in **Figure 3** as they would appear on the microcomputer during different processing stages of single event arrival.

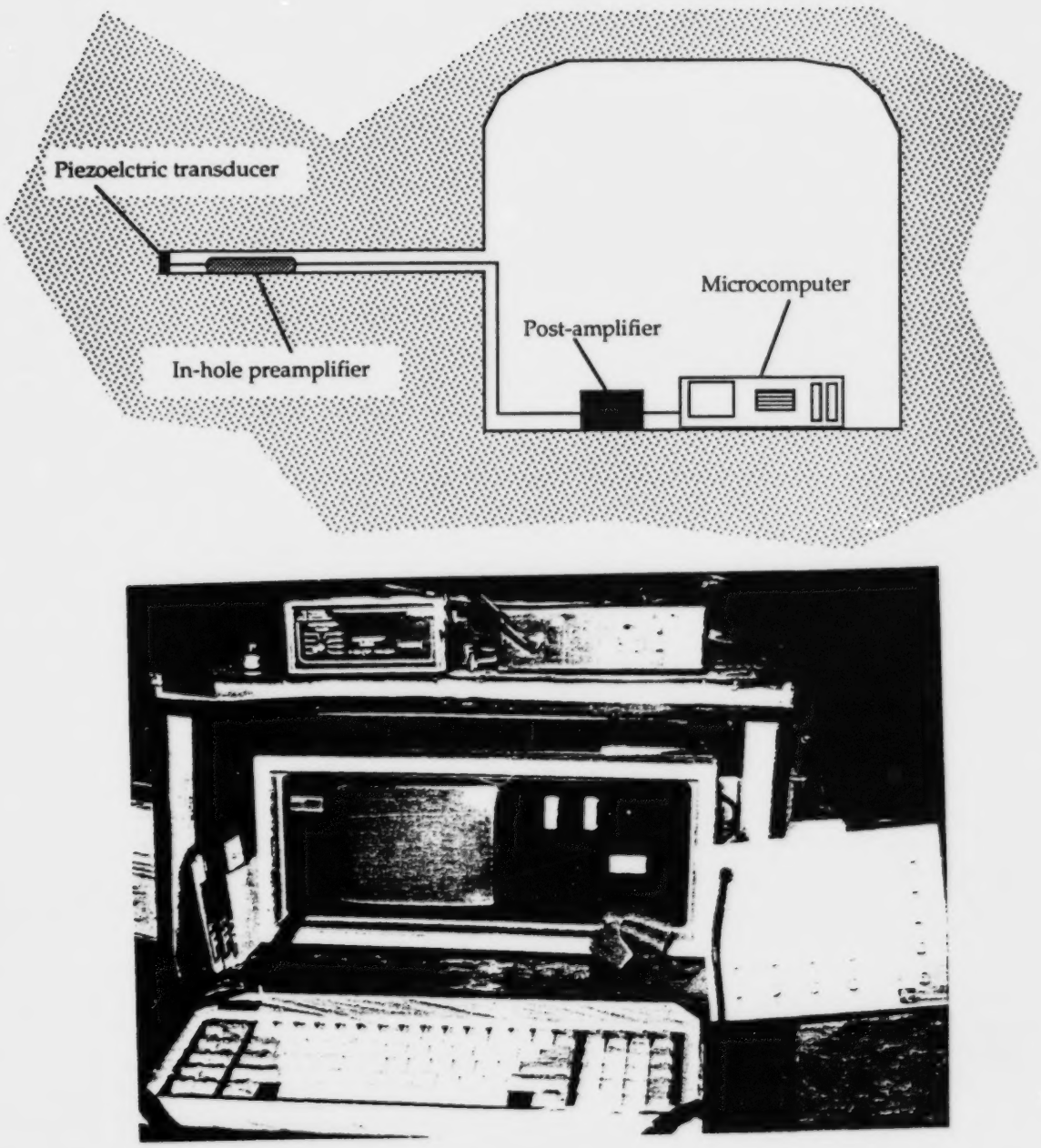

FIGURE 1 - Schematic View of In-Situ Microseismic Monitoring Station and Photograph of Microcomputer Hardware Assembly

---

HELP MENU

F_1 -	Help (this screen)
F_2 -	Plot incoming waveforms
F_3 -	Plot FFT outputs
F_4 -	Stress distribution display
F_5 -	Page previous waveforms
F_6 -	Page previous FFT outputs
F_7 -	Check operating status
1 -	Do signal conditioning
2 -	Do FFT's
3 -	Do feature extraction
4 -	Do waveform identification
ESC -	Terminate program

FIGURE 2 - Help Menu of the QSTRESS Software Program

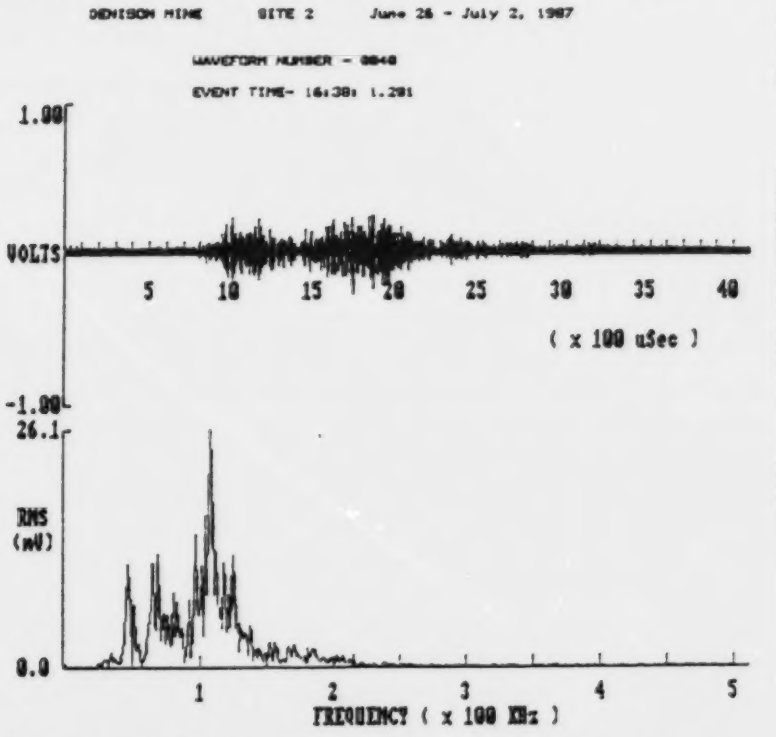

FIGURE 3 - Typical Amplitude (Time Domain) and Fourier Transformed (Frequency Domain) Plots of Seismic Waveform Information

On the basis of frequency and amplitude data which is extracted from acoustic emissions, features are extracted upon which rockburst and stress precursor analysis is performed to characterize the source site conditions. A flow chart of the system components and processing features incorporated in the seismic detection system utilized at the Denison Mine are illustrated in **Figure 4**. A summary of instrumentation is provided in **Appendix A**.

Feature extraction represents a series of data analysis functions performed by a specialized software program called FTFIELD to process data prior to pattern recognition application. The FTFIELD program derives FFT (frequency content) data of incoming waveforms as well as data concerning the event rate (rate at which microseismic waves are produced and captured), peak magnitude of the event, centre frequency of the waveform event, frequency distribution and other parameters which are characteristic of stress-related phenomena. Such data is analyzed for each (AE) event in order to determine precursor information which may be rockburst-related. Such precursors are defined to be any effects produced within the rock mass which may be indicative of processes leading to rock failure. Past research has documented the effects of several indicators as being significant, though not completely reliable, precursors to rockbursts. Typically, microseismic event rate increases have been shown to correspond to the possible onset of violent rock failure [5] and a frequency shift, towards higher frequency content of waveforms, has also been demonstrated to be associated with increasing ground stress in rock [6]. Both the QSTRESS and FTFIELD programs have been demonstrated to process arriving waveforms and to perform the feature extraction process in periods approximating 30 seconds after initial waveform capture. Where high rate acoustic activity may exist in-situ, operating precedence is given to waveform digitization and storage until sufficient free time between waveform arrivals exists to permit feature extraction conditioning. The extracted data is thereafter submitted for pattern recognition programming to programs called TRAIN and TEST, adapted from earlier research conducted by the Queen's group [7], [8] and written by T. K. Yeo [9] during the course of the Denison-Queen's research effort. At present, such recognition procedures are being developed to permit waveform classification or identification either according to site of origin or by absolute stress level, where in-situ stresses are previously known for various sites being studied. When feature extraction data can be obtained from waveforms obtained at sites having known or measured stress parameters, the TRAIN program is utilized to establish recognition function algorithms and system accuracy of identification based upon the orthogonal method of pattern classification. Once the training data has been inputted to the TRAIN system, unknown waveform data can then be inserted and processed by the TEST program for classification. Since the pattern recognition process utilizes mathematical reduction of extracted feature data, rather than time-consuming waveform matching techniques which have long been utilized, the entire classification process takes only 0.5 seconds once feature extraction conditioning of incoming waveforms has been completed by the detection system.

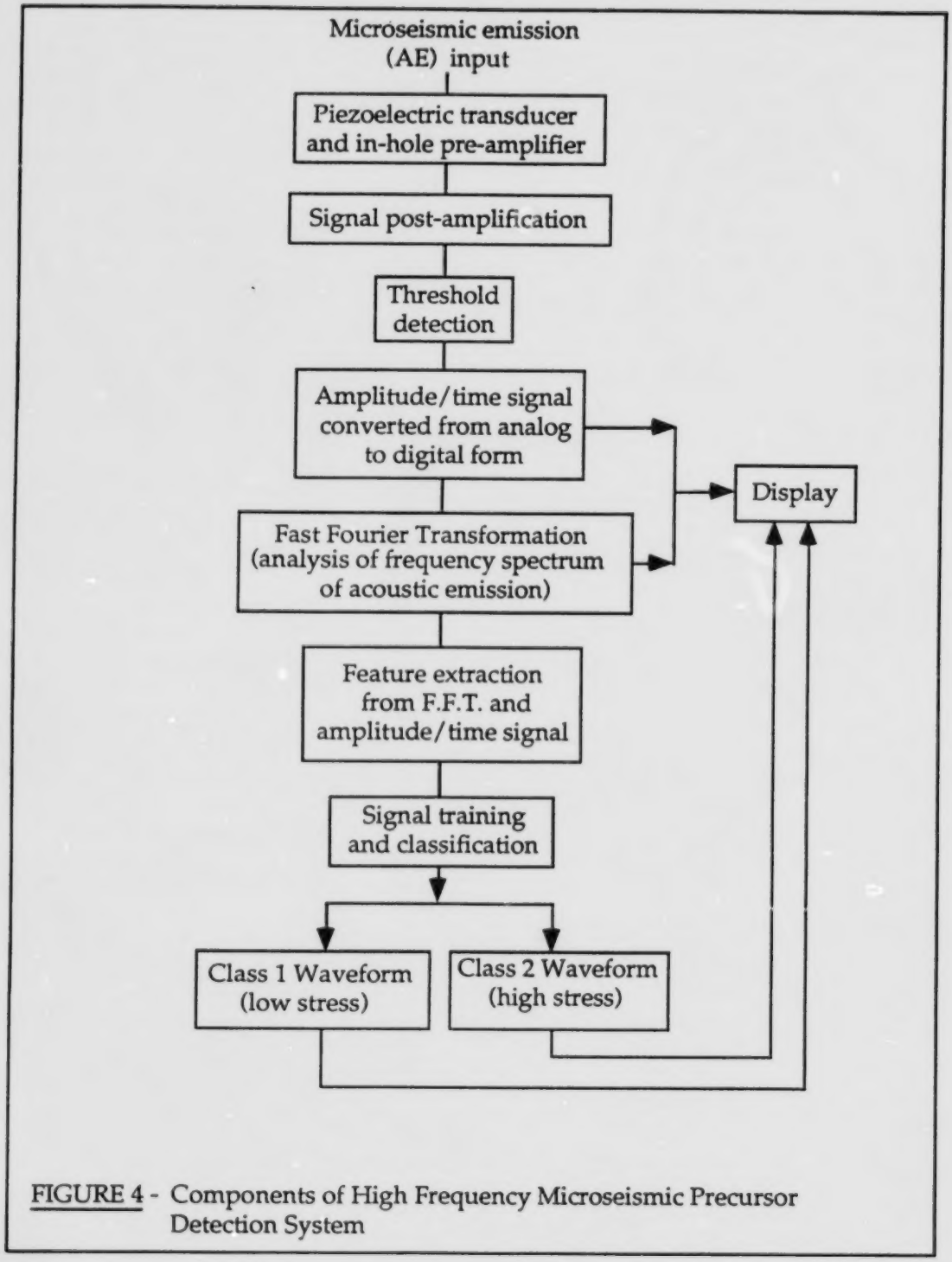

FIGURE 4 - Components of High Frequency Microseismic Precursor Detection System

A range of typical acoustic waveform data features, characteristic of site stress conditions, are reduced to mathematical parameters. When unknown waveform features are subsequently derived, they can be immediately sorted mathematically and the source stress state determined.

In conventional locator-type acoustic emission detection systems, only first arrival time data is recorded for multiple sites and is utilized for the sole purpose of determining source locations of seismic events. Engineering decisions concerning the removal of personnel and equipment prior to rockbursting cannot, therefore, be effectively made on the basis of such technology. The Queen's network, whether it utilizes single, high frequency sensors or multiple, lower frequency sensors at each site, provides the capability for acquiring complete waveform information which may then be analyzed to yield stress or rockburst characterization data. This complementary network design has been developed in order to test predictive capabilities of microseismic monitoring systems in advance of rockbursting. Where high density monitoring capabilities may be required, notably about unstable stoping or pillar recovery zones, the portable, multi-channel, complete waveform acquisition system presently being developed at Queen's shows promise as a practical, reliable and cost effective tool with which mining personnel may make informed decisions concerning rockburst potential in underground mining applications.

3.0 Denison Research Program

3.1 Preliminary Site Investigation Work

The Queen's/Denison Contract was initiated in December, 1986, and was established to run through March 31, 1989. During the initial three month contract interval, hardware and software items were purchased and tested prior to commencing field installation and monitoring trials. In April, 1987, and through the summer months of that year, initial site survey, drilling evaluation and transducer mounting tests were conducted by Queen's research staff (two graduate students and two undergraduate students) at a series of sites within the Denison Mine in Elliot Lake, Ontario.

In order that suitable site locations could be selected, rigorous evaluation of potential monitoring zones was conducted in close liaison with Denison staff. Certain minimum site conditions were mandated due both to necessary restrictions set by the equipment being used and by mine production requirements. Site preparation required that both local mine air and water be available to permit drill operation. Similarly, electric power availability was necessitated at sites which were selected for observation in order to provide continuous operating capability for the microcomputer units.

Both jackleg and diamond drilling methods were attempted in order to prepare holes into which sensing transducers were to be installed. The transducers, attached to thin steel plates, were designed to be installed within 5.0 cm diameter

holes upon end-of-hole faces which had to be ground flat in order to obtain good coupling with the rock mass. In order that complete characterization of the rock mass properties adjacent to each sampling site could be attempted, the use of jackleg drills was not implemented for the majority of Denison site tests. Jackleg drilling was found to produce adequate test holes for microseismic reconnaissance purposes but no rock samples could be provided for subsequent physical property evaluation tests. Rather, diamond drilling hole preparation was chosen in order to insure that similar hole dimensions could be maintained between sites and for the purpose of obtaining intact core sample materials for subsequent test analysis. All site drilling was completed during the interval period between May - October, 1987 by Denison staff.

A total of seven diamond drill sites, spaced between three distinct development zones within the mine, were selected and instrumented during the period between May and October, 1987. The sites were selected at the various locations on the basis of review of computer modelled stress conditions thought to exist within the mine, of field measured stress values and of visual observation information in order that a significant variety of in-situ stress conditions could be monitored. The seven stress measurement stations were established initially for stress determination purposes. Each was thereafter utilized to permit characterization of acoustic emission response of the locally adjacent rock mass within each of the observation zones. Of the total number of drill sites developed, six were selected as sites for microseismic monitoring. Following completion of stress determinations, acoustic transducers were installed at the bottom of each borehole. Monitoring trials were then conducted on a continuous basis by Queen's staff to acquire acoustic emission data and to both train and classify pattern recognition software.

Of the seven drill sites established, six were located in the general area of the 26 Level Garage, located at approximate mine co-ordinates (55,500 E, 20,500 N). Sites #1,#2 and #3 were located within the Negri Dyke which is illustrated in **Figure 5** (plan view) to strike in a generally East-West direction and to border the 26 Level Garage immediately to the North. Sites #4 and #5, similarly shown in **Figure 5**, were established within an unconfined pillar located in the 24962 Access Drift, at approximate co-ordinates (56,000 E, 20,500 N) and adjacent to the northeast boundary of the 26 Level Garage. The sum of sites were installed adjacent to the 26 Level Garage in order to monitor stress and acoustic activity which would exist in both stable pillar sites (Sites #1,#2,#3) and in yielding or unstable pillar sites (Sites #4,#5). During later stages of mining, backfilling of stopes immediately to the north of the Garage area was to be undertaken. Sites installed at the locations shown would therefore be useful for monitoring of changes in acoustic emission and stress activity in these pillars which would develop as the result of backfill installation. **Figure 6** illustrates a North-South section view of the Negri Dyke borehole installation holes. Of the three sites prepared, only Sites #1 and #2 were instrumented using microseismic equipment; Site #3 was established solely for the purpose of providing additional in-situ stress information during the initial

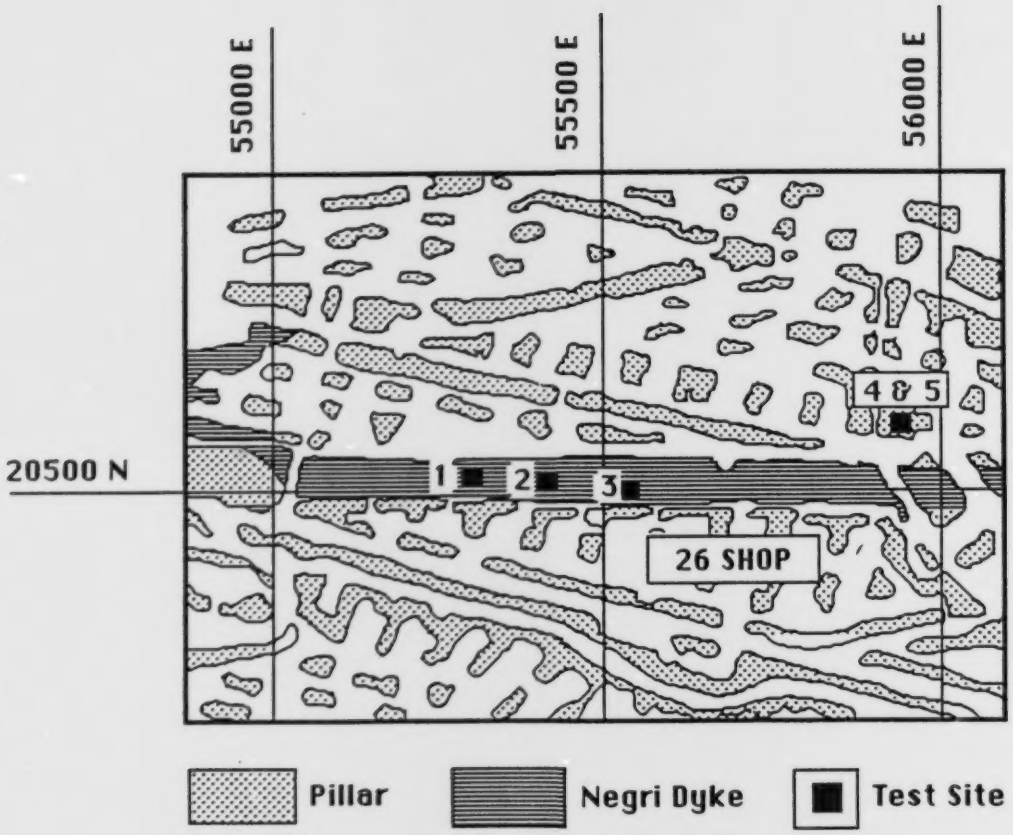

FIGURE 5 - QUEEN'S MICROSEISMIC MONITORING STATIONS ADJACENT TO THE 26 GARAGE AREA (SITES #1, #2, #3, #4 and #5)

research period. In order to provide representative stress and microseismic emission data, holes were drilled up dip (+ 10° North) toward the centre of Negri Dyke (an approximate distance of 9.15 metres) to avoid the influence of near excavation surface fracture effects. Holes for Sites #4 and #5 were drilled perpendicular to each other and within the 24962 Access Drift pillar such that installed transducers could be placed in a central pillar location, as shown in the section views of **Figure 7**. Depths of drilling for each of the site holes approximated 6.70 and 4.90 metres, respectively.

An additional two borehole monitoring sites were established in the 33950 Access Drive, located at approximate mine co-ordinates (49,500 E, 21,500 N) and closely adjacent to a backfill support zone. Drilling for Site #6 was completed by drilling down dip and parallel to the pillar axis within the 35024 stope pillar for a total distance approximating 6.40 metres. An adjacent borehole (Site #7, within the 35026 pillar) was terminated due to misalignment of the borehole collar. Monitoring at this site was established for the purpose of observing changes in local ground stress conditions which would develop as the result of pillar extraction taking place nearby. It was theorized by both Denison and Queen's staff that, as adjacent pillar structures were removed, incremental stress conditions would develop within the remaining pillar structures. Accordingly, Site #6 was established within the central pillar of a triple rib pillar layout. At the time of initial borehole drilling at Site #6 (June, 1987), the majority of the 33 Panel stopes had been fully backfilled and all stope pillars existed fully intact. Production sequencing in this panel required that pillars adjacent to the 35024 test pillar would be sequentially and gradually recovered during the interval period in which microseismic monitoring was being carried out. By September of 1987, the 35022 pillar, immediately East of the test site, had been substantially recovered, with the exception of sill drift remnants; subsequent to recovery of the 35022 pillar, the 35025 pillar, lying to the West of the test site, was also recovered. By the end of the third week of October, 1987, pillar extraction operations adjacent to Site #6 had been completed and seismic monitoring studies were suspended. A plan view of the Site #6 borehole monitoring station, illustrating the various site conditions which existed during the interval of installation and monitoring, is shown in **Figure 8**.

3.2 Monitoring Site Stress Assessment

Prior to implementing seismic monitoring tests at all Sites, diamond drill holes were instrumented for the purpose of determining the existing state of in-situ stress. Subsequent to seismic assessment, additional in-situ stress tests were planned to be implemented at regular intervals during the course of long term studies at each Site both to determine changing ground stress conditions or to verify earlier stress measurements. Information obtained was to be utilized to correlate stress and acoustic response parameters measured by the acoustic monitoring system.

Under the existing Queen's/Denison contract, however, no funding was allocated for the purpose of conducting such tests. Subsequently, both Queen's and

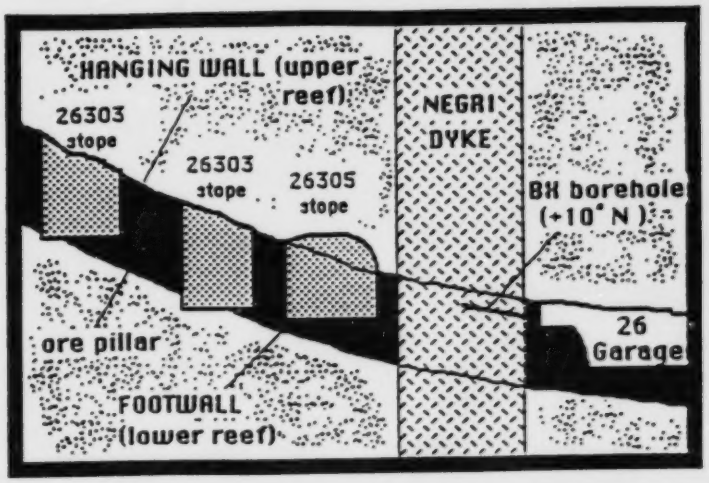

FIGURE 6 – NORTH-SOUTH SECTION THROUGH 26 GARAGE SEISMIC DRILLING SITES (LOOKING EAST)

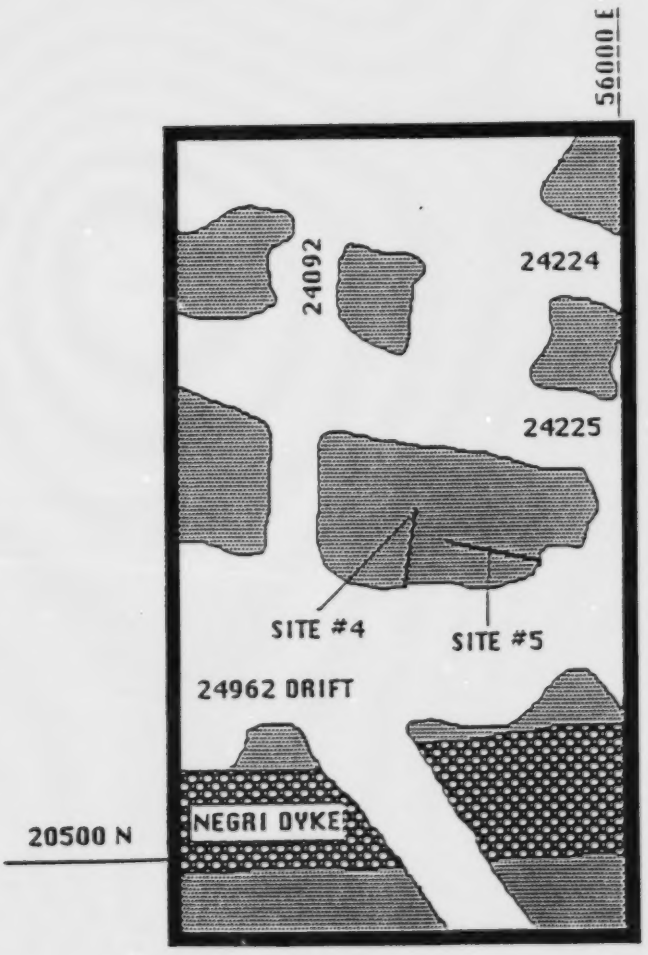

FIGURE 7 – MICROSEISMIC MONITORING AT SITES #4 and #5 (26 GARAGE)

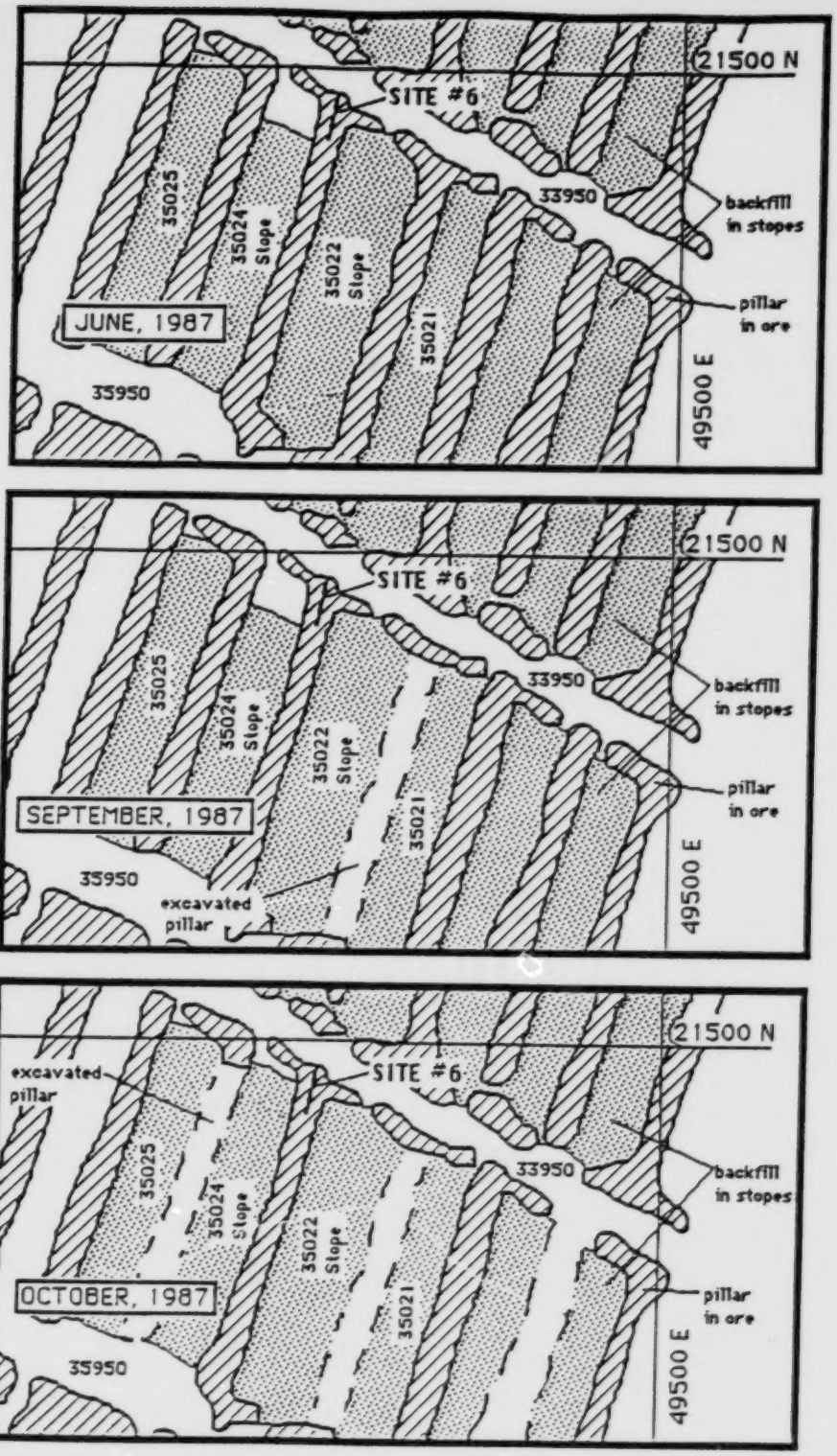

FIGURE 8 - MICROSEISMIC MONITORING STATION AT SITE #6 (35 PANEL)

Denison (through associated research agency funding and with internal financing) undertook to establish a preliminary stress measurement program in conjunction with the microseismic effort. All such efforts were financed external to the existing contact.

In view of the fact that all test sites were established within pillar structures, normally considered to exhibit plane stress behaviour, the Doorstopper Gage stress evaluation method was adopted to characterize site stress conditions. Within each site borehole, a minimum of three, and preferably four, stress tests were conducted at varying depths from the collar. In order to obtain representative stress data, both in-situ overcoring tests and laboratory rock compression failure tests upon recovered core specimens were necessitated.

3.2.1 Laboratory Rock Mechanical Property Evaluation

In order to be able to derive stress parameters from acquired in-situ strain data, the mechanical properties of the local rock mass must also be determined. In-situ stress data determination, in terms of principal planar stress magnitude and direction parameters, requires that knowledge of the rock Young's Modulus, (E), and Poisson's ratio, (μ), conditions be known. To accomplish such evaluation, a series of unconfined compression failure tests were conducted upon core materials recovered from each Site borehole.

Core specimens, at known depths within each borehole, were systematically retrieved and subjected to standard analytical processes. Samples were prepared in accordance with standards established by the International Society of Rock Mechanics (ISRM) to create cylindrical specimens exhibiting the following characteristics:

- all specimens were diamond sawed and lathed to present constant length-to-diameter aspect ratios approximating 2.5-to-1
- each sample was further lathed to prepare end loading faces parallel to within $\pm$ 0.025 mm

All specimens were then subjected to unconfined compression loading on a Material Test System (MTS) Model 810 electrohydraulic, servo-controlled, stiff testing frame. Axial loading was permitted to occur under conditions of uniform axial strain at rates approximating (10^{-5} s^{-1}). Continuous recording of sample axial load, axial deformation and circumferential deformation response was undertaken during failure. Based upon resolved axial stress and strain data, Young's Moduli values were determined for all specimens; similarly, Poisson's ratio parameters were determined on the basis of measured axial and circumferential strain data.

In all cases, corrections were made to measured deformation data to negate the effects of loading system reaction deflections. As well, the strain rate of loading was selected to be sufficiently low so as to induce static, rather than dynamic, failure conditions within specimens. Such loading conditions were instituted in order that more realistic estimates of the bulk modulus response of the rock (similar to that

exhibited by large rock volumes, in-situ) could be estimated. It is common that, where small volume samples and high strain rates of loading are utilized for laboratory testing purposes, excessively high estimates for deformation moduli and unconfined compressive strength often result. Laboratory analyses of rock strength and deformation parameters are invariably overestimated due to the nature of the specimens and test processes adopted. When such data is subsequently utilized for stress parameter calculation purposes, estimated stress parametric data is also invariably overestimated. In order to better simulate the bulk modulus response and provide more realistic estimates of ground stress conditions within the rock mass, within which stress measurement tests were performed, the preceding efforts were consistently followed.

At each test site selected, some, though not all, of the diamond drill core which was created was recovered and tested. In many cases, the localized presence of jointing was shown to induce low strength/low Young's Modulus response during failure testing; failure within such samples typically resulted by planar sliding along smooth, pre-existing fracture surfaces. Intact core samples characteristically failed at higher respective stress levels and along noticeably rougher, shear surfaces. Considerable variation in both strength and deformation modulus response versus hole depth (distance from the collar) was demonstrated for all sites tested. On this basis, it was demonstrated that averaged rock parametric data for both jointed and intact core material should not be utilized for stress data reduction purposes. Where possible, only that parametric data which had been derived for intact samples of core at depths within each test borehole where actual stress measurement tests had been performed was utilized in determination of stress parameter data. Typical strength, Young's Modulus and inferred biaxial stress data is demonstrated for all Sites in **Tables 1 through 6** respectively.

Summary physical property data versus hole depth is also illustrated in **Figures 9 through 14**, respectively. At most sites, core was not recovered until significant drilling depths, away from the hole collar sites, had been reached. Such steps were followed to preclude sampling within the 'fracture zone' which is known to exist about the surface of all underground excavations. Where significant core jointing effects were observed in samples, as indicated in **Figures 9 through 12**, measured reductions in strength and Young's Modulus behaviour were also realized on the basis of laboratory failure tests. **Figures 9 through 14** also demonstrate that significant changes in rock mechanical properties (largely due to geologic alteration) do exist between samples recovered in close spatial proximity within the same test borehole.

A summary of averaged hole physical property data, based upon laboratory failure test analysis, is listed in **Table 7**. Fair correlation between the average strength and Young's Modulus data was observed to occur between the adjacent holes at Sites #1 and #2, for similar depths of sampling into each borehole. Poor correlation, other than for rock strength data, was observed to occur between both of these Sites and Site #3. The primary reason for such a discrepancy is evident when it is observed that all samples taken from the Site #3 borehole were recovered at

TABLE 1- SUMMARY OF IN-SITU DOORSTOPPER AND CORE SAMPLE PHYSICAL PROPERTY TEST RESULTS (SITE #1, 26 GARAGE AREA)

Hole Depth meters (feet)	Test Number	Unconfined Compressive Strength MPa / (psi)	Young's Modulus GPa (psi x 10^6)	Poisson's Ratio
4.88 (16.0)	---	222.9 (32325)	75.0 (10.87)	.15
4.88 (16.0)	---	121.9 (17674)	42.8 (6.21)	-- (joint)
5.34 (17.5)	---	75.4 (10930)	22.1 (3.20)	-- (joint)
5.34 (17.5)	---	239.8 (34767)	70.0 (10.15)	.17
5.49 (18.0)	---	186.0 (26976)	73.9 (10.72)	.17
5.79 (19.0)	---	213.3 (30930)	81.8 (11.86)	.18
5.79 (19.0)	---	275.9 (40000)	78.5 (11.38)	.15
6.10 (20.0)	---	141.1 (20465)	40.0 (5.80)	.10
6.40 (21.0)	#1	179.6 (26046)	59.2 (8.58)	.14
6.55 (21.5)	---	70.6 (10232)	24.3 (3.52)	.15 (joint)
6.70 (22.0)	---	89.8 (13023)	39.0 (5.65)	.12 (joint)
7.47 (24.5)	---	80.2 (11628)	34.2 (4.96)	.12 (joint)
7.62 (25.0)	---	258.2 (37441)	69.8 (10.12)	.15
8.08 (26.5)	---	96.2 (13953)	39.3 (5.70)	.10 (joint)
8.23 (27.0)	#2 (fail)	72.8 (10558)	30.3 (4.39)	.10 (joint)
8.84 (29.0)	#3	126.7 (18372)	49.2 (7.13)	.15
9.15 (30.0)	#4	266.2 (38604)	84.4 (12.24)	.15

TABLE 2- SUMMARY OF IN-SITU DOORSTOPPER AND CORE SAMPLE PHYSICAL PROPERTY TEST RESULTS (SITE #2, 26 GARAGE AREA)

Hole Depth meters (feet)	Test Number	Unconfined Compressive Strength MPa / (psi)	Young's Modulus GPa (psi x 10^6)	Poisson's Ratio
5.33 (17.5)	---	158.5 (22985)	54.9 (7.96)	.19
5.49 (18.0)	---	88.9 (12890)	39.2 (5.68)	.16
5.79 (19.0)	---	142.2 (20616)	53.2 (7.72)	.19
6.10 (20.0)	---	78.4 (11370)	40.3 (5.84)	.11 (joint)
6.10 (20.0)	---	124.8 (18100)	43.4 (6.30)	.15
6.25 (20.5)	---	122.5 (17770)	57.0 (8.27)	.13
6.40 (21.0)	---	150.3 (21800)	50.5 (7.33)	.11
6.55 (21.5)	---	310.3 (45000)	72.1 (10.46)	.14
6.71 (22.0)	---	170.0 (24645)	58.5 (8.48)	.13
7.01 (23.0)	---	137.3 (19905)	40.2 (5.83)	.19 (joint)
7.16 (23.5)	---	117.7 (17060)	32.1 (4.65)	.16 (joint)
7.32 (24.0)	---	153.6 (22275)	60.1 (8.71)	.14
7.62 (25.0)	---	130.7 (18957)	63.2 (9.16)	.21
7.93 (26.0)	#1	85.0 (12322)	38.8 (5.63)	.10 (joint)
8.23 (27.0)	#2	119.3 (17298)	49.8 (7.22)	.11
8.54 (28.0)	---	60.5 (8767)	50.3 (7.30)	.12 (joint)
8.84 (29.0)	#3	109.5 (15876)	39.7 (5.75)	--- (joint)
9.15 (30.0)	#4	174.9 (25355)	71.7 (10.39)	.13

TABLE 3- SUMMARY OF IN-SITU DOORSTOPPER AND CORE SAMPLE PHYSICAL PROPERTY TEST RESULTS (SITE #3, 26 GARAGE AREA)

Hole Depth meters (feet)	Test Number	Unconfined Compressive Strength MPa / (psi)	Young's Modulus GPa (psi x 10^6)	Poisson's Ratio
0.76 (2.5)	---	52.3 (7582)	17.3 (2.51)	.21 (joint)
0.91 (3.0)	---	79.1 (11469)	15.6 (2.26)	.20 (joint)
1.68 (5.5)	---	111.1 (16110)	43.7 (6.34)	.11
1.83 (6.0)	#1	143.2 (20760)	57.8 (8.38)	.17
2.43 (8.0)	#2	231.0 (33500)	46.5 (6.75)	.12
3.35 (11.0)	#3	225.5 (32700)	38.7 (5.61)	.12
3.67 (12.0)	---	166.7 (24170)	40.7 (5.90)	.12
3.81 (12.5)	---	191.2 (27725)	53.6 (7.77)	.14
3.96 (13.0)	---	106.2 (15400)	19.0 (2.75)	--- (joint)
4.11 (13.5)	---	60.4 (8767)	18.6 (2.70)	.12 (joint)
4.27 (14.0)	#4	----- -------	---- -------	---

TABLE 4- SUMMARY OF IN-SITU DOORSTOPPER AND CORE SAMPLE PHYSICAL PROPERTY TEST RESULTS (SITE #4, 26 GARAGE AREA)

Hole Depth meters (feet)	Test Number	Unconfined Compressive Strength MPa / (psi)	Young's Modulus GPa (psi x 10^6)	Poisson's Ratio
3.20 (10.5)	----	66.0 (9579)	23.1 (3.35)	.10
3.20 (10.5)	----	127.3 (18457)	34.1 (4.93)	.09
3.51 (11.5)	----	122.5 (17757)	31.6 (4.58)	.12
3.51 (11.5)	----	103.1 (14953)	38.8 (5.63)	.13
3.81 (12.5)	----	91.8 (13317)	29.5 (4.28)	.12
3.81 (12.5)	----	125.7 (18224)	33.9 (4.92)	.13
3.96 (13.0)	----	76.9 (11542)	31.0 (4.49)	.11
3.96 (13.0)	----	80.6 (11682)	27.7 (4.02)	.13
4.27 (14.0)	----	126.3 (18317)	37.4 (5.42)	.12
4.27 (14.0)	----	111.8 (16214)	47.2 (6.85)	.16
4.42 (14.5)	----	143.4 (20794)	54.0 (7.83)	.13
4.57 (15.0)	----	54.8 (7943)	21.6 (3.13)	.12
4.57 (15.0)	----	101.5 (14719)	37.8 (5.48)	.13
5.03 (16.5)	----	83.1 (12056)	29.0 (4.21)	.13
5.18 (17.0)	----	161.1 (23364)	56.3 (8.17)	.11
5.18 (17.0)	----	76.7 (11121)	27.0 (3.92)	.11
5.18 (17.0)	----	64.4 (9345)	25.8 (3.74)	.13
5.49 (18.0)	Test #1	92.5 (13411)	31.0 (4.50)	.14
5.79 (19.0)	Test #2	103.1 (14953)	43.4 (6.29)	.12
6.10 (20.0)	----	112.1 (16261)	38.0 (5.51)	.12
6.71 (22.0)	----	74.1 (10747)	20.9 (3.03)	---

TABLE 5- SUMMARY OF IN-SITU DOORSTOPPER AND CORE SAMPLE PHYSICAL PROPERTY TEST RESULTS (SITE #5, 26 GARAGE AREA)

Hole Depth meters (feet)	Test Number	Unconfined Compressive Strength MPa / (psi)	Young's Modulus GPa (psi x 10^6)	Poisson's Ratio
1.68 (5.5)	----	172.4 (25000)	59.8 (8.67)	.16
1.68 (5.5)	----	170.8 (24766)	55.9 (8.11)	.12
1.98 (6.5)	----	106.3 (15420)	41.7 (6.04)	.22
1.98 (6.5)	----	53.2 (7710)	25.6 (3.71)	.13
2.13 (7.0)	----	67.7 (9813)	23.2 (3.36)	.12
2.29 (7.5)	----	151.5 (21962)	42.3 (6.13)	.20
2.43 (8.0)	----	114.4 (16588)	40.5 (5.87)	.15
2.74 (9.0)	----	134.0 (19439)	41.1 (5.96)	.14
2.74 (9.0)	----	120.8 (17523)	34.9 (5.06)	.15
2.90 (9.5)	----	191.7 (27803)	48.1 (6.97)	.13
2.90 (9.5)	----	99.9 (14485)	28.3 (4.11)	---
3.20 (10.5)	----	72.5 (10514)	23.2 (3.36)	.09
3.51 (11.5)	----	125.7 (18224)	44.7 (6.48)	.09
3.66 (12.0)	----	119.2 (17289)	40.9 (5.93)	.09
3.96 (13.0)	----	171.4 (24859)	60.7 (8.81)	.13
4.42 (14.5)	----	88.6 (12850)	26.9 (3.90)	.10
4.57 (15.0)	Test #1	190.1 (27570)	61.4 (8.90)	.10
4.72 (15.5)	----	87.0 (12616)	28.2 (4.09)	.11
4.88 (16.0)	Test #2	135.4 (19626)	38.7 (5.61)	.11

TABLE 6- SUMMARY OF IN-SITU DOORSTOPPER AND CORE SAMPLE PHYSICAL PROPERTY TEST RESULTS (SITE #6, 35 Panel)

Hole Depth meters (feet)	Test Number	Unconfined Compressive Strength MPa / (psi)	Young's Modulus GPa (psi x 10^6)	Poisson's Ratio
4.11 (13.5)	---	83.3 (12085)	25.9 (3.75)	--- joint?
4.27 (14.0)	---	55.6 (8056)	24.9 (3.61)	--- joint?
4.42 (14.5)	---	58.8 (8530)	21.2 (3.07)	.10 joint?
4.57 (15.0)	---	145.4 (21090)	57.1 (8.28)	.15
5.03 (16.5)	---	156.9 (22748)	61.7 (8.94)	.22
5.18 (17.0)	#1	124.2 (18010)	36.6 (5.30)	.13
5.33 (17.5)	---	150.3 (21800)	53.2 (7.72)	.14
5.49 (18.0)	#2	167.6 (24300)	43.9 (6.36)	.13
5.79 (19.0)	---	219.0 (31753)	64.0 (9.28)	.12

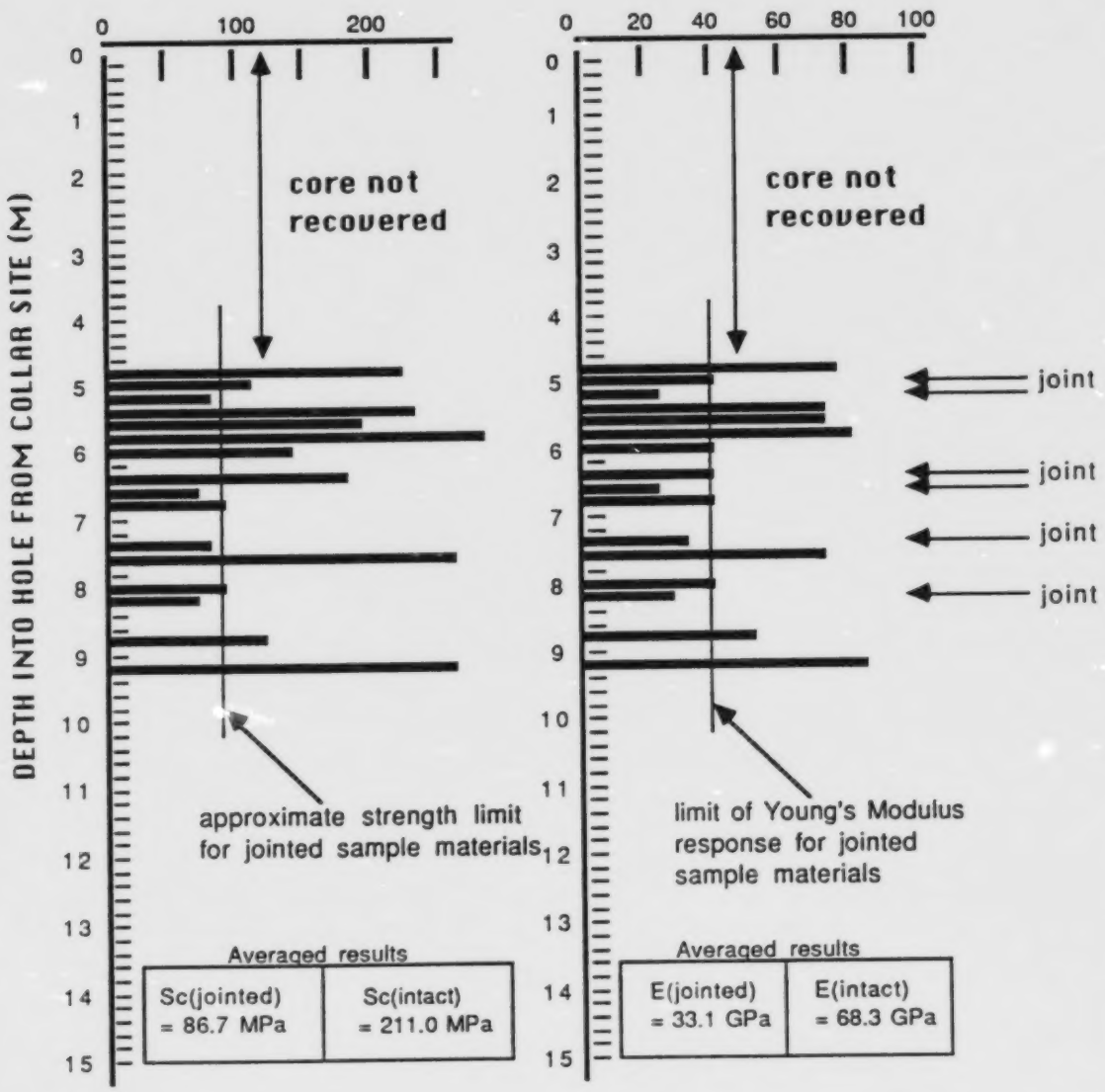

FIGURE 9 - **VARIATION IN UNCONFINED COMPRESSIVE STRENGTH AND YOUNG'S MODULUS BEHAVIOUR VERSUS DEPTH WITHIN STRESS MONITORING BOREHOLES AT Site #1 (26 Garage Area)**

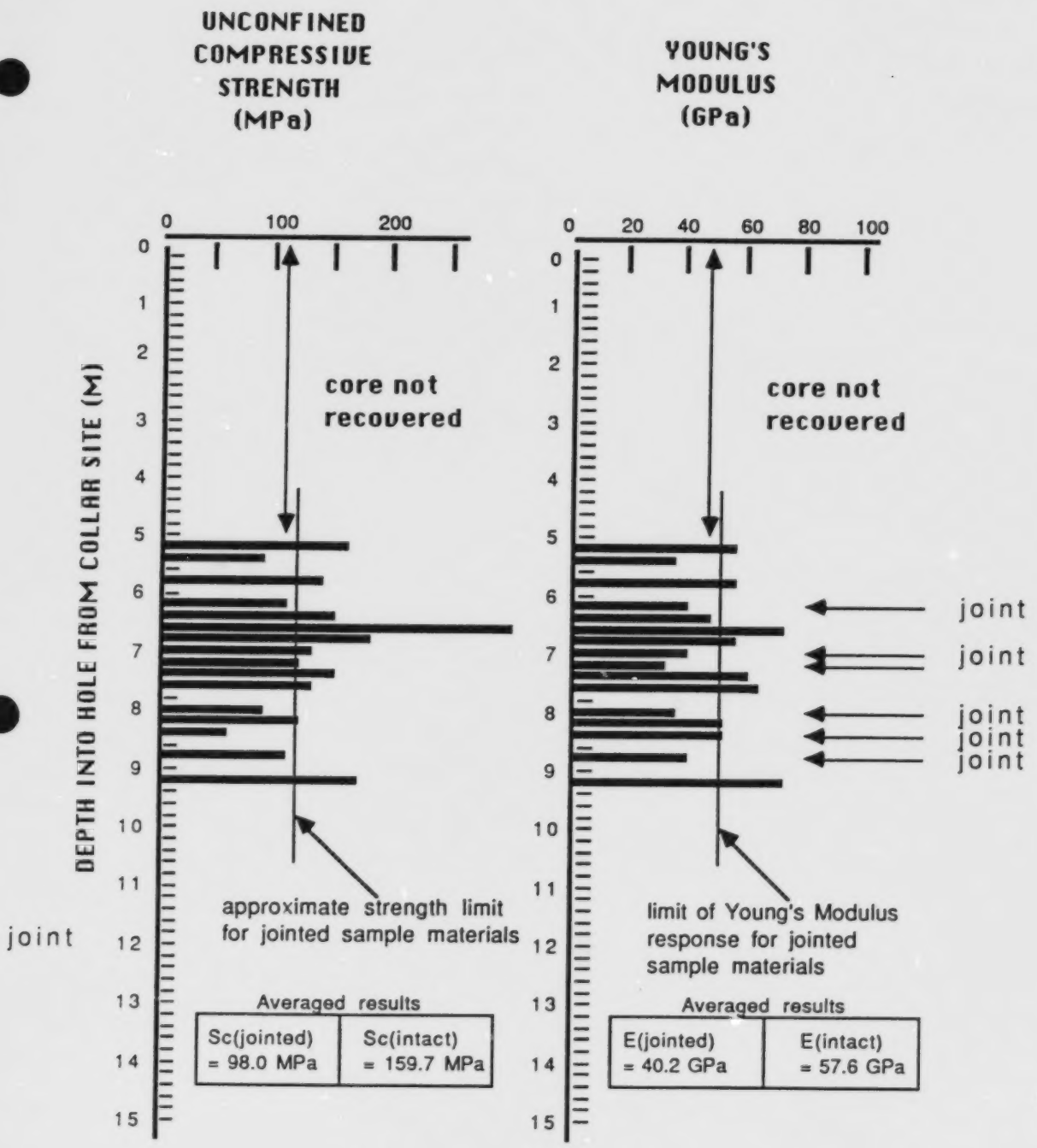

FIGURE 10 - **VARIATION IN UNCONFINED COMPRESSIVE STRENGTH AND YOUNG'S MODULUS BEHAVIOUR VERSUS DEPTH WITHIN STRESS MONITORING BOREHOLES AT Site #2 (26 Garage Area)**

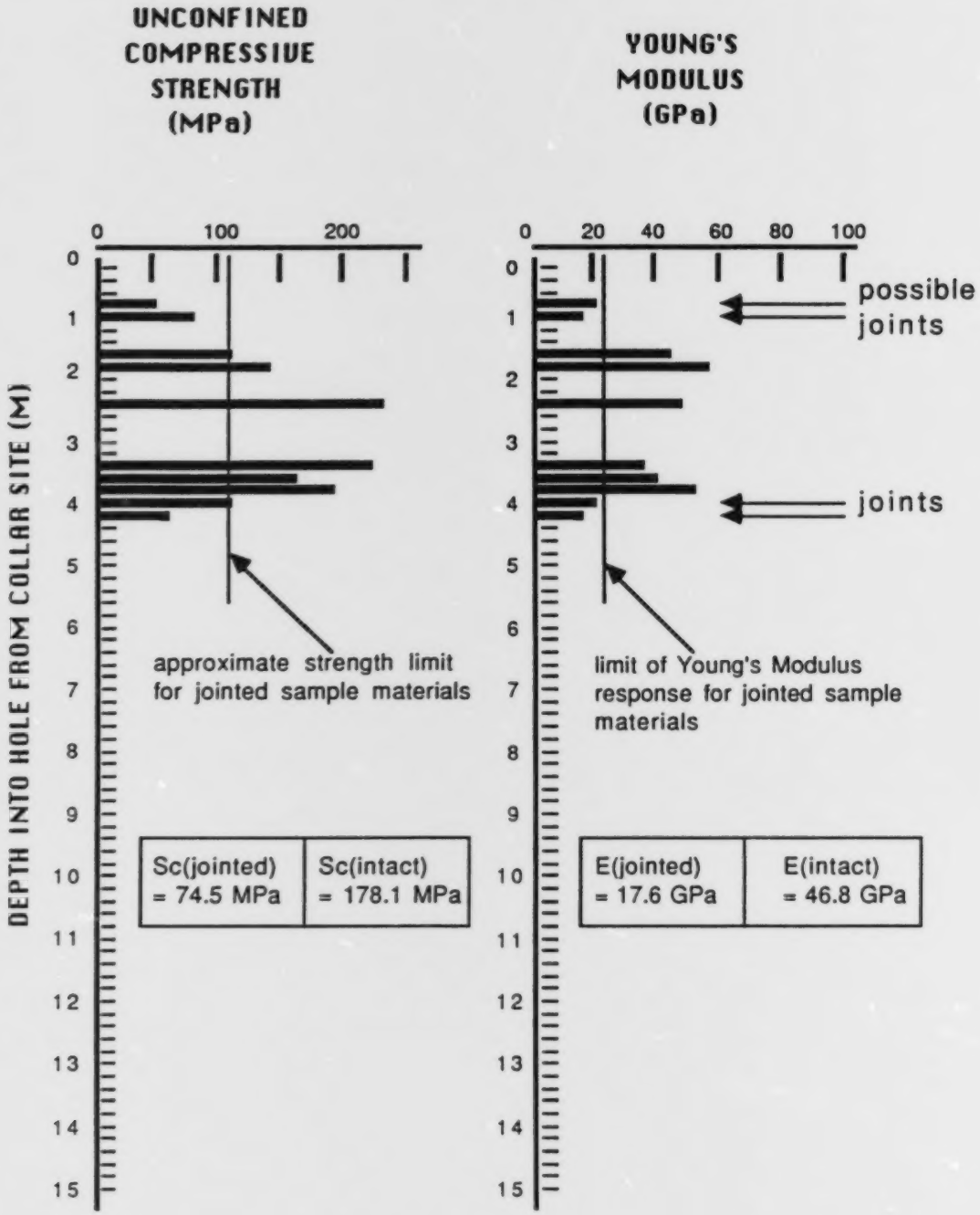

FIGURE 11 - **VARIATION IN UNCONFINED COMPRESSIVE STRENGTH AND YOUNG'S MODULUS BEHAVIOUR VERSUS DEPTH WITHIN STRESS MONITORING BOREHOLES AT Site #3 (26 Garage Area)**

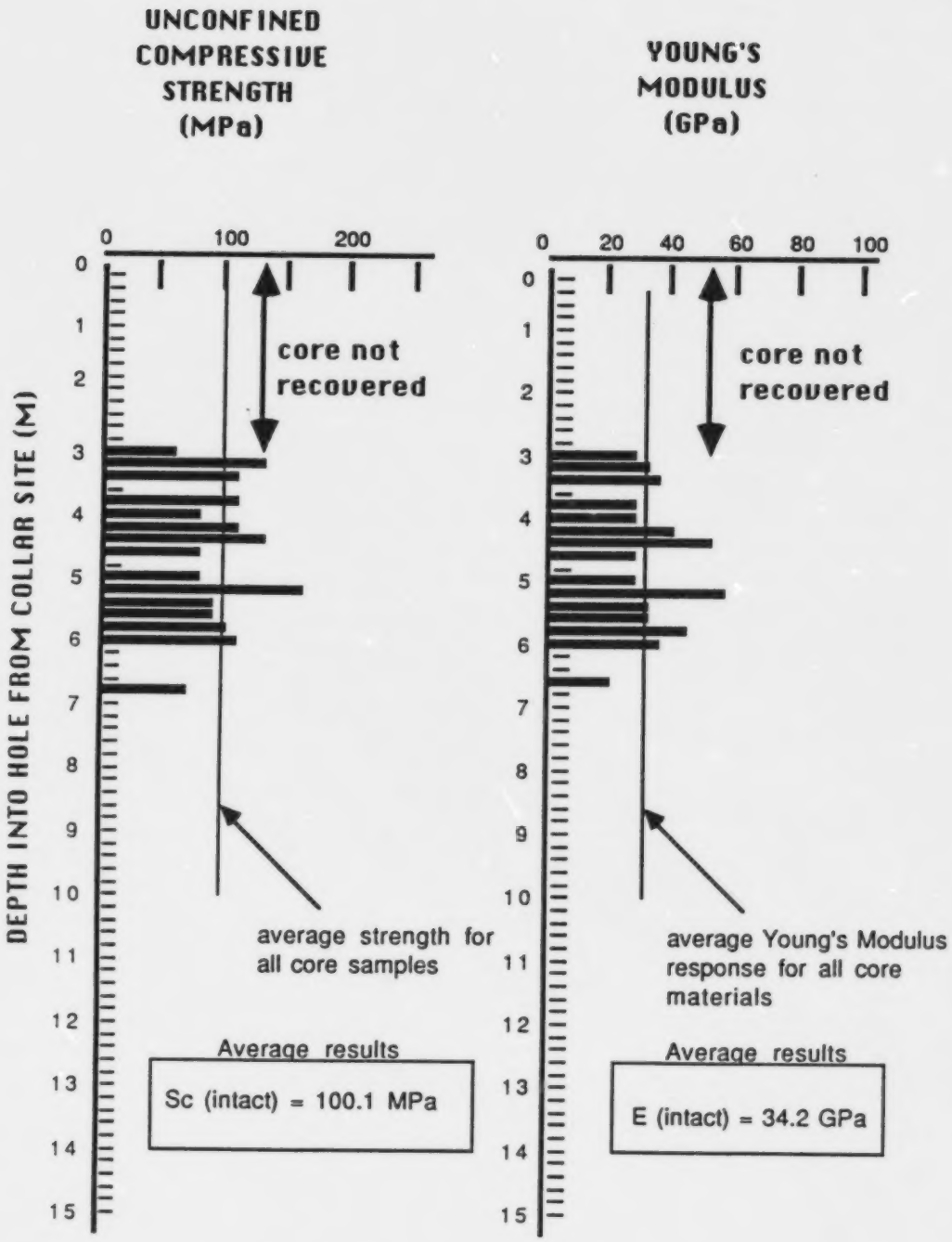

FIGURE 12 - **VARIATION IN UNCONFINED COMPRESSIVE STRENGTH AND YOUNG'S MODULUS BEHAVIOUR VERSUS DEPTH WITHIN STRESS MONITORING BOREHOLES AT Site #4 (26 Garage Area)**

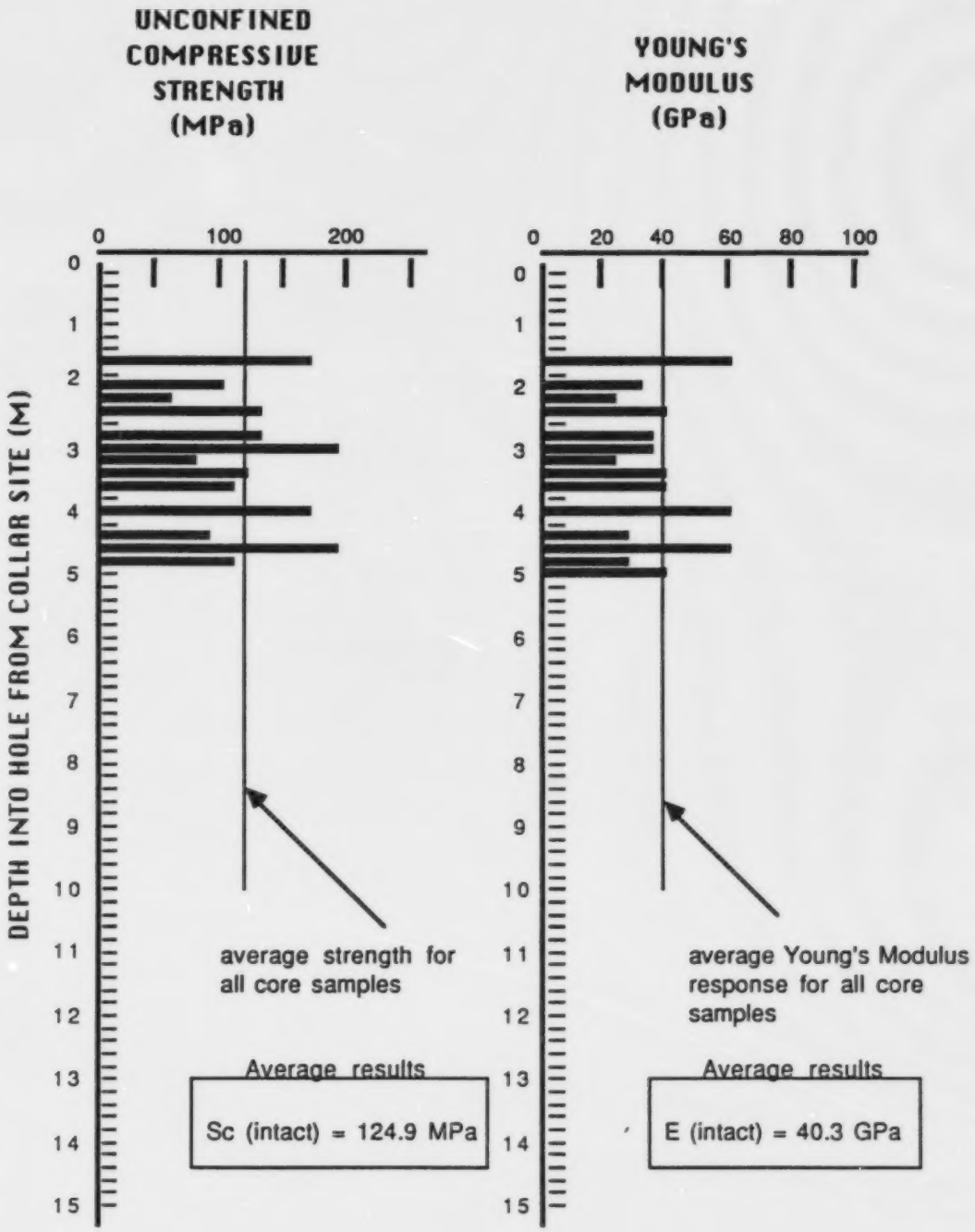

FIGURE 13 - **VARIATION IN UNCONFINED COMPRESSIVE STRENGTH AND YOUNG'S MODULUS BEHAVIOUR VERSUS DEPTH WITHIN STRESS MONITORING BOREHOLES AT Site #5 (26 Garage Area)**

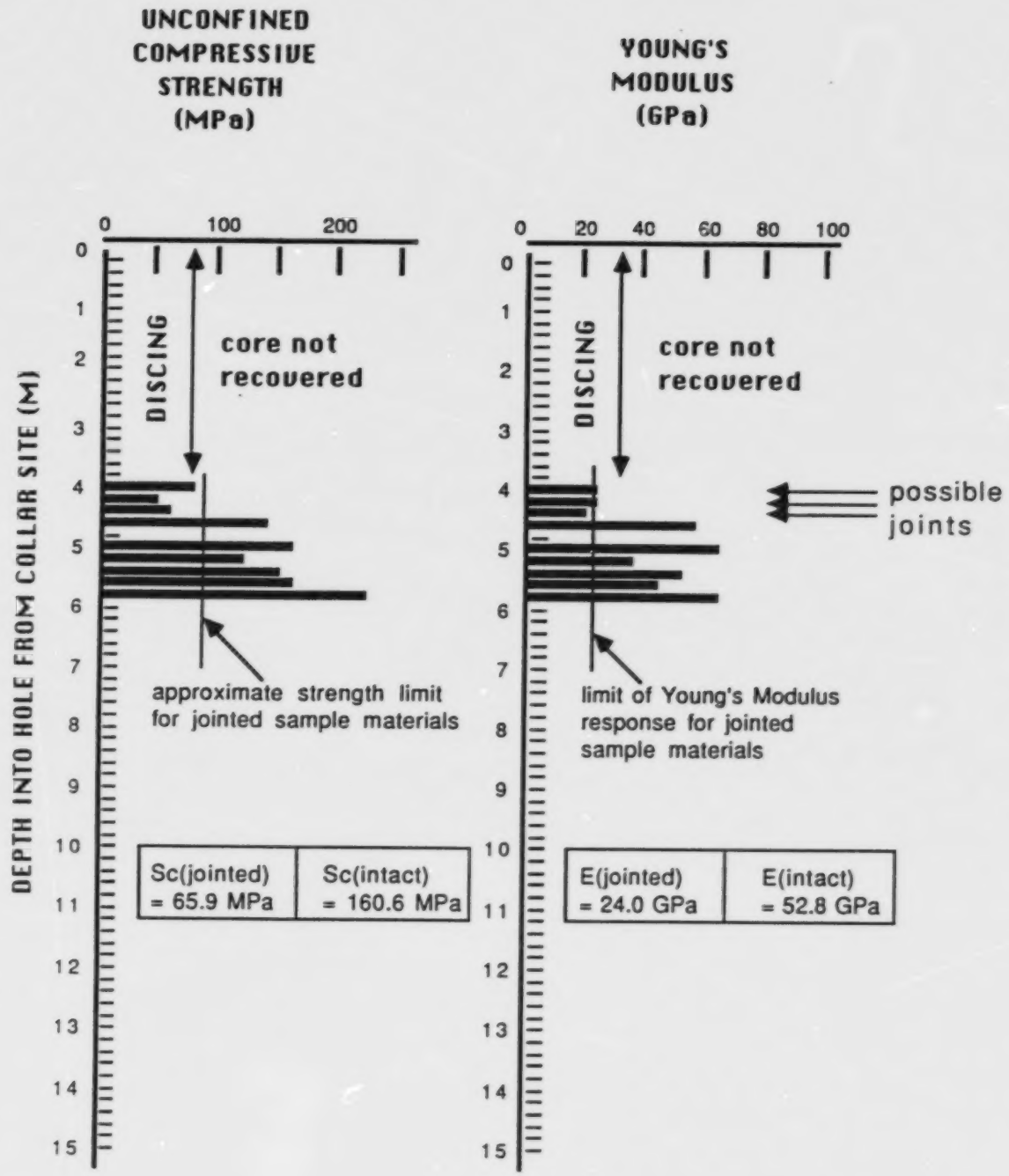

FIGURE 14 - **VARIATION IN UNCONFINED COMPRESSIVE STRENGTH AND YOUNG'S MODULUS BEHAVIOUR VERSUS DEPTH WITHIN STRESS MONITORING BOREHOLES AT Site #6 (35 Panel Area)**

shallow hole depths (less than 4 metre depth), close to the collar and well within the 'fracture zone', where the rock matrix would be subjected to stress-induced fracturing effects. At all Sites, therefore, no stress measurement was conducted at depths less than 4 metres from the collar to improve accuracy of elastic strain response measurements.

Table 7 - Summary of Physical Parameter Results for Site Core Specimens

Test Site	Average Unconfined Strength, (MPa)		Average Young's Modulus, (MPa x 10^3)	
	Intact Core	Jointed Core	Intact Core	Jointed Core
1	211.0	86.7	68.3	33.1
2	159.7	98.0	57.6	40.2
3	178.1	74.5	46.8	17.6
4	100.1	—	34.2	----
5	124.9	—	40.3	----
6	160.6	65.9	52.8	24.0
7	------	—	—	----

3.2.2 - In-Situ Stress (Doorstopper Gage) Evaluation

Doorstopper Gage stress determination tests were conducted at each site immediately following completion of hole drilling and core recovery operations. Such tests, designed to yield biaxial stress components acting within planes oriented perpendicular to the borehole axis only, were utilized rather than more expensive triaxial stress determination methods. Since all test sites were to be established within existing, unconfined pillar structures, subject to plane stress action, no requirement was felt necessary for determination of three-dimensional stress components. The following sections serve to detail stress evaluation work which was performed at each site prior to installation and use of microseismic monitoring networks.

3.2.2.1 - Site #1 Stress Component Determination

Doorstopper stress measurement tests were initially conducted at this site which was located within the Negri Dyke. A total of four tests were attempted, of which three were successfully completed. The second of four tests was observed to undergo gage de-bonding at a location within the borehole where rock jointing was encountered; upon overcore recovery of the gage, core failure at the point of gage bond contact was observed to occur.

Of the three successfully completed tests, test #1 (at a depth of 6.40 metres) was shown (on the basis of unconfined compression failure analysis of core materials recovered) to have been located in close proximity to zone of joint occurrence within the hole. Both the magnitudes of derived principal stresses and the orientation of stress components may therefore have been compromised by the local effect of these joints.

The results of tests #3 and #4 showed good agreement in stress direction, though some variation in magnitude response was also observed. The magnitude variation is directly attributable to differences in measured Young's Modulus parameters derived for the core materials recovered at the two test locations. Core which was recovered at the location of test #3 was shown to be both weaker and to exhibit a considerably lower Young' Modulus response (40% less) with respect to material recovered at the test #4 location. During overcore test procedures, strain responses demonstrated at each site evidenced a high degree of similarity; therefore, had identical deformation modulus response been shown by samples at both sites, similar principal stress magnitudes would have been indicated. Where parametric results attributed to jointed core samples within this hole are deleted from consideration, and all intact sample data is averaged, the unconfined strength (S_c), Young's Modulus (E) and Poisson's ratio (μ) values used to derive stress parameters approximate 211 MPa, 68.3 GPa and 0.15, respectively for Site #1 core materials.

Where averaged, rather than single test parameter data, was utilized to extrapolate stress components for tests #1, #3 and #4 at Site #1, major principal stress values ranging between 10.8 and 19.4 MPa were demonstrated. No variation in directional response from that formerly determined was shown.

On the basis of observations which were made at Site #1 (Negri Dyke) during June, 1987, it was conservatively estimated that the average magnitude of the principal pillar stress approximated 19.4 MPa. Due to the known presence of 'fracture' zones surrounding most access drifts, which was substantiated by stress observations made at this Site, it was considered that more reliable stress measurements would be established from use of deep hole tests, rather than from shallow hole tests. For this reason, and due to the fact that the microseismic transducer was installed at the location of test #4, site stress magnitudes shown by this test were assumed to influence the seismic response at Site #1.

The maximum inferred principal stress for Site #1 was therefore established at 24.0 MPa, acting in an orientation approximately 20^0 clockwise with respect to the

vertical when it was assumed that an observer looks towards the borehole collar (ie.- approximately South and down dip). The results of individual test observations and resultant Site #1 stress summary (both magnitude and orientation data) are illustrated in **Figure 15**.

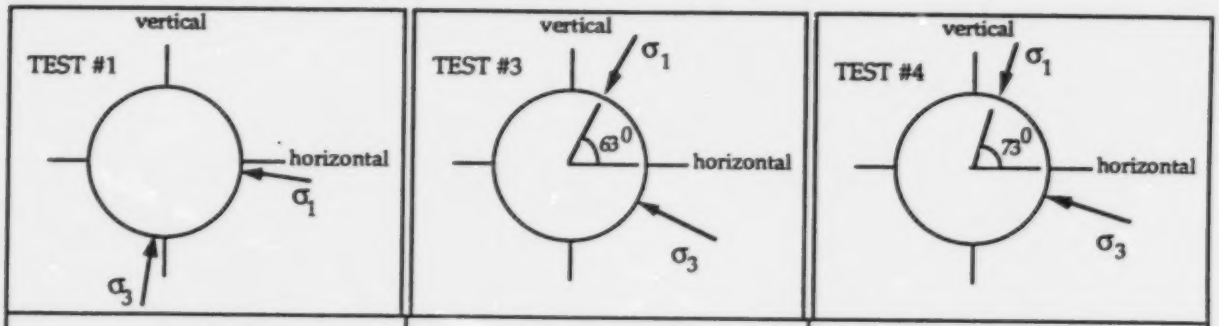

σ_1= 9.34 MPa σ_3= 7.37 MPa	σ_1 = 13.89 MPa σ_3 = 5.13 MPa	σ_1 = 24.05 MPa σ_3 = 16.12 MPa

σ_1 (typical) = 24.05 MPa oriented 68^0 counterclockwise from horizontal
σ_3 (typical) = 16.12 MPa oriented 22^0 clockwise from horizontal

FIGURE 15 - AVERAGE STRESS COMPONENTS FOR SITE #1 DOORSTOPPER TESTS (June, 1987)

3.2.2.2 - Site #2 Stress Component Determination

Additional Doorstopper Gage tests were subsequently performed within a second borehole (Site #2) lying approximately 15 metres east of Site #1. All stress tests, as at the first Site, were carried out within a BX diamond drill hole which was drilled into the Negri Dyke in a direction approximately perpendicular to the orebody strike and at a $+10^0$ dip orientation.

At test locations #1 and #2 (depths of 7.93 and 8.23 metres, respectively) both low level stress magnitudes and poorly correlated orientation data was resolved. For such tests, erratic results were attributed to the local presence of jointed ground, as had been the case for similar test depths at adjacent Site #1. Because the mechanical properties of the rock appeared to vary erratically with depth along each borehole, at least for depths up to 9.0 metres from the collar, no systematic method was devised to minimize the detrimental behaviour of jointed/fractured ground when stress determination tests were being performed.

At the location of tests #3 and #4, good agreement in directional orientation of principal stress components was evidenced. Due to differences between

measured Young's Modulus responses of core specimens taken at these two test locations (possibly influenced by jointing at the #3 test location), it was judged that the stress magnitude response determined for the fourth test location (at which the microseismic transducer was implanted) would be most representative of the in-situ stress condition for Site #2.

The major principal stress component, determined to approximate 11.9 MPa, was lower than the maximum value of stress which was determined to exist at Site #1. Such change may have been the result either of local geological alteration or of local jointing influence. On the basis of rock property comparisons between Sites #1 and #2, it was evident that intact Site #1 core materials exhibited both stronger and more brittle deformation response than did similar core materials retrieved from the Site #2 test locations.

Stress magnitude data for Site #2 was therefore assumed to approximate that which was derived from the fourth Doorstopper test site, though typical orientation data was derived as the average of results for tests #3 and #4 at this Site. The major principal stress component for the Site #2 location (mid-June, 1987) was determined to approximate 11.9 MPa and to trend approximately 40^0 clockwise from the vertical (when it is assumed that the observer view is aligned with the borehole axis and looking towards the borehole collar). The results of individual test observations and resultant Site #2 stress summary (both magnitude and orientation data) are illustrated in **Figure 16**.

TEST #1

σ_1 = 6.37 MPa

σ_3 = 4.46 MPa

(no orientation data)

TEST #2

σ_1 = 5.76 MPa

σ_3 = 5.10 MPa

(no orientation data)

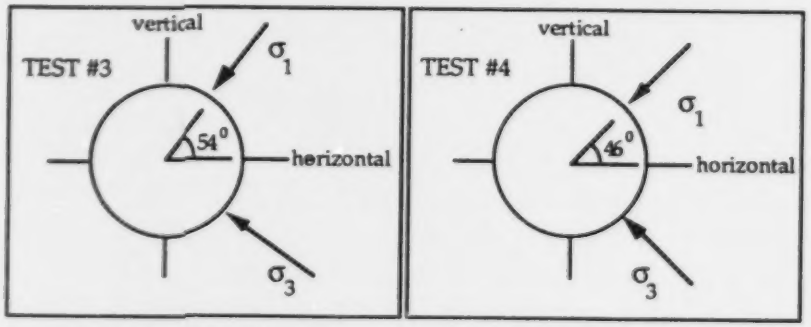

σ_1 = 9.21 MPa

σ_3 = 4.77 MPa

σ_1 = 11.90 MPa

σ_3 = 0.66 MPa

σ_1 (typical) = 11.90 MPa oriented 50^0 counterclockwise from horizontal

σ_3 (typical) = 4.77 MPa oriented 40^0 clockwise from horizontal

FIGURE 16 - AVERAGE STRESS COMPONENTS FOR SITE #2 DOORSTOPPER TESTS (June, 1987)

3.2.2.3 - Site #3 Stress Component Determination

At the request of Denison staff, one additional stress measurement site (Site #3) was drilled within the Negri Dyke for the purpose of comparing local stress conditions with previously-tested Sites (#1 and #2). No microseismic monitoring equipment was installed at this Site following performance of stress evaluation procedures. The borehole orientation was similar to those selected for each of the two previous drilling sites, though maximum penetration depth was approximately half (4.3 metres maximum depth) the previous site drilling depths.

Four stress monitoring tests were conducted, of which three were successfully completed. The fourth, and deepest, test failed within a local zone of jointed rock. From the failure test results listed in Table 3 and shown in Figure 11, no obvious trend of rock strength versus depth variation was shown to be evident for this Site. On average, however, rock samples from the Site #3 borehole showed the lowest Young's Modulus response for all three Sites which were tested within the Negri Dyke. It is thought that, due to the shallow hole depth conditions encountered, the influence of excavation "fracture" zone effects would account for such behaviour. In all future tests, therefore, it is strongly recommended that stress determination tests be conducted within boreholes at depths exceeding 8 - 9 metres from the collar site.

Principal stress components for tests #1, #2 and #3 were derived using site specific rock mechanical property data, and were shown to vary between 7.9 MPa (test #3) and 13.8 MPa (test #1). Where mechanical property data, attributed to jointed samples, was discarded and summary averaged hole data was used for stress magnitude determination, major principal stress components approximating 11.2 MPa (test #1), 9.3 MPa (test #2) and 9.6 MPa (test #3) were derived. On the basis of such measurements, it was conservatively estimated that an average major principal stress component approximating 10.0 MPa existed at this Site during the period of initial monitoring trials (June, 1987). Where site specific rock mechanical data was utilized, maximum stresses approximating 13.8 MPa were assessed. The magnitude range of predicted stress components for the Site #3 location (June, 1987) was shown to be quite similar to values determined for Site #2, though considerably lower than those values determined for Site #1. Because all Site #3 tests were completed in closer proximity to the borehole collar than at previous Sites, it would be expected that the component magnitudes would be lower in comparison with similar results obtained adjacent Sites for deeper test locations.

No predominant trend of principal stress vector orientation was established on the basis of the three tests performed. For this reason, averaged trend data was adopted. The major principal stress component was therefore determined to act at an angle approximately 3^0 clockwise from the vertical (when it is assumed that the observer view is aligned with the borehole axis and looking towards the borehole collar). The results of individual test observations and resultant Site #3 stress summary (both magnitude and orientation data) are illustrated in **Figure 17**.

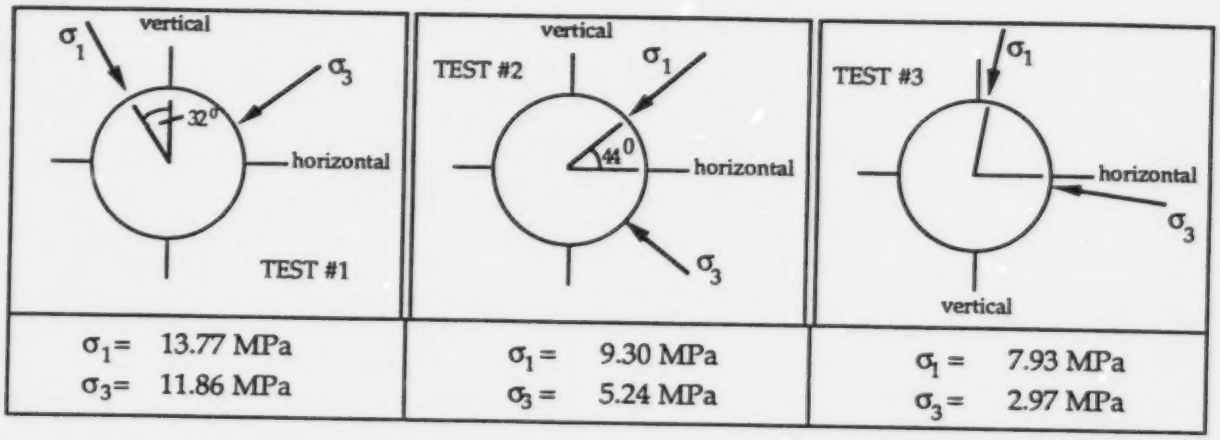

σ_1= 13.77 MPa σ_3= 11.86 MPa	σ_1= 9.30 MPa σ_3= 5.24 MPa	σ_1 = 7.93 MPa σ_3= 2.97 MPa

σ_1 (typical) = 10.33 MPa oriented 87^0 counterclockwise from horizontal
σ_3 (typical) = 6.69 MPa oriented 3^0 clockwise from horizontal

FIGURE 17 - AVERAGE STRESS COMPONENTS FOR SITE #3 DOORSTOPPER TESTS (June, 1987)

3.2.2.4 - Site #4 Stress Component Determination

Site #4 was established within a pillar located at the East boundary of the backfill zone adjacent to the Denison 26 Garage complex, as illustrated in Figure 5. The Site borehole was drilled toward the North, at an up dip angle approximating 8.5^0, for a total distance of 6.71 metres.

Two Doorstopper tests were attempted and were successfully completed at this station. As with other tests, diamond drill core was recovered and subjected to laboratory analysis for determination of rock mechanical properties. In general, pre-existing fracture surfaces were not observed to be present in core samples which were recovered from the drill hole, nor were such surfaces noted to develop within such specimens as the result of unconfined loading, thereby indicating that local jointing effects were minimal. The great majority of recovered samples exhibited uniform strength and deformation response under load, yielding average unconfined strengths (S_c) and Young's Modulus (E) values of 100 MPa and 34.2 GPa respectively. Averaged modulus and Poisson's ratio parametric values, for borehole depths between 5.18 and 6.10 metres, were utilized for determination of stress data.

Doorstopper data evidenced very good magnitude and directional similarity between the two tests which were performed at Site #4. The major principal stress components, determined to be 25.6 and 22.5 MPa respectively, for the two tests, were also shown to act vertically.

Following completion of such tests at Site #4, borehole surveys indicated that the test locations within the hole existed in close proximity to the orebody/footwall

contact plane, as demonstrated in the sketch of **Figure 18.**

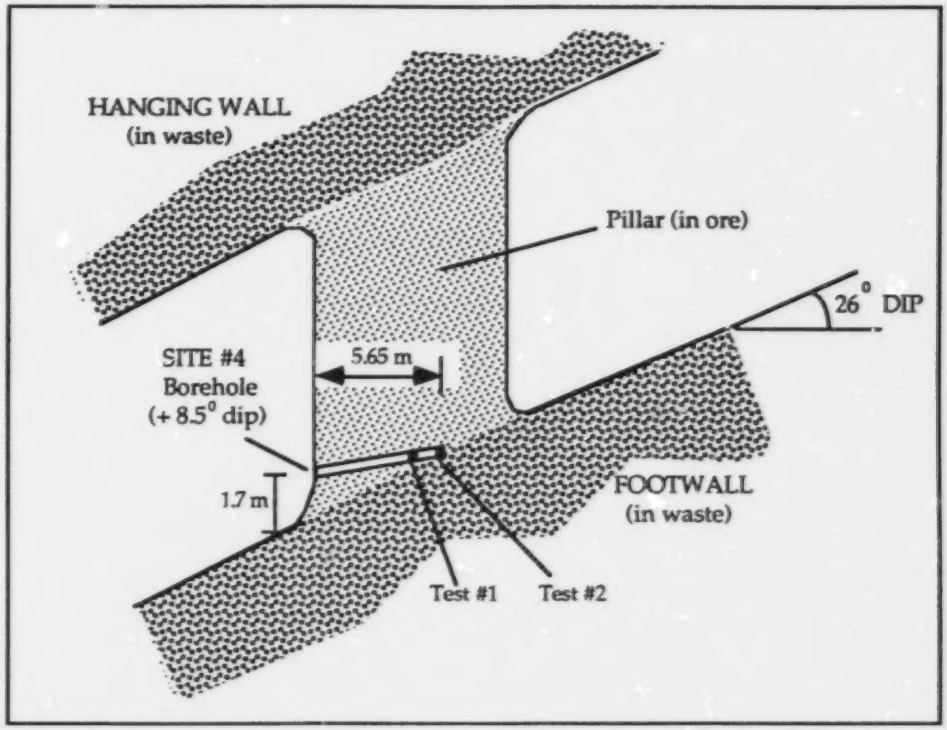

FIGURE 18- Vertical Section Through Site #4 Borehole
(Looking West)

The borehole, drilled up dip at the inclination angle shown and for the depth indicated, was plotted to lie just within the footwall contact. It would be expected, therefore, that the magnitudes of principal stress components actually measured at the Site #4 test locations should be less than those which would exist within the central pillar span, due largely to stress redistribution which would occur over the larger bearing area exposed at the footwall contact zone.

On the basis of the two Doorstopper tests performed at Site #4 during October, 1987, it was determined that a major principal stress component, approximating 24.0 MPa in magnitude and acting in a vertical orientation, existed. Due to drilling orientation problems, however, the indicated level of stress was expected to be lower than the actual pillar stress condition. The results of individual test observations and resultant Site #4 stress summary (both magnitude and orientation data) are illustrated in **Figure 19.**

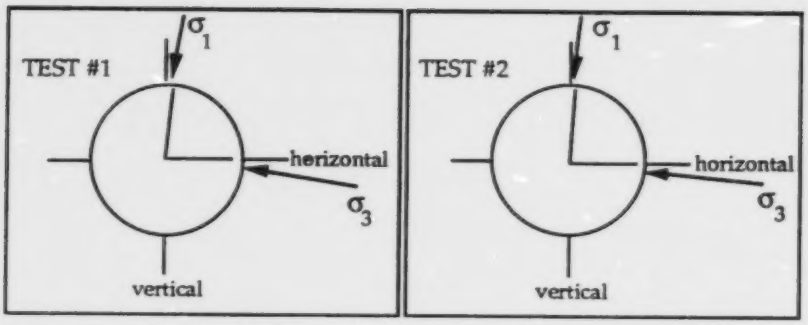

σ_1 = 25.59 MPa σ_1 = 22.50 MPa
σ_3 = 15.19 MPa σ_3 = 9.61 MPa

σ_1 (typical) = 24.05 MPa oriented 87 ^{0} counterclockwise from horizontal
σ_3 (typical) = 12.40 MPa oriented 3 ^{0} clockwise from horizontal

FIGURE 19 - AVERAGE STRESS COMPONENTS FOR SITE #4 DOORSTOPPER TESTS (October, 1987)

3.2.2.5 - Site #5 Stress Component Determination

Drilling at Site #5 was undertake during October, 1987 and within the same pillar structure as had been utilized for Site #4 tests. The borehole was collared on the east face of the pillar and was drilled, at a + 6.5^0 dip, toward the west to an ultimate depth of 4.88 metres. Drilling from the adjacent stope floor permitted the borehole to be centred within the pillar span and at the pillar mid-height elevation, rather than being directed to the footwall contact zone as had the Site #4 borehole. All subsequent Doorstopper Gage tests were established within the central pillar stress envelope and not within the footwall "shadow", as had ben the case for Site #4 tests.

On the basis of characterization tests performed on Site #5 core specimens, generally uniform strength, Young's Modulus and Poisson's ratio parametric data was observed to exist over the length of the drilled hole. The average unconfined compressive strength for the sum of specimens tested approximated 124.9 MPa; similarly, averaged Young's Modulus and Poisson's ratio values approximated 40.3 GPa and 0.12. Both strength and deformation modulus parameters for Site #5 core specimens were found to average approximately 20% higher than those determined for Site #4 specimens. Differences in response between samples retrieved from central pillar locations (Site #5) and footwall contact zones (Site #4) would indicate that rock at each site may have been subjected to variable geological or stress-induced alteration effects.

For stress determination purposes, averaged rock mechanical parametric data

for Site #5 specimens, recovered at depths between 3.96 - 4.88 metres, was utilized. The results of stress evaluation tests showed very good magnitude and directional similarity between the two tests which were completed within the Site #5 borehole. The major principal stress components, at levels of 48.7 and 41.0 MPa, respectively, were determined to act in a direction approximately 36^0 clockwise from the vertical and approximately perpendicular to the orebody dip when it is assumed that the observer view is toward the borehole collar (ie.- looking east towards the Doorstopper gage from the bottom of the hole). The results of individual test observations and resultant Site #5 stress summary (both magnitude and orientation data) are illustrated in **Figure 20**.

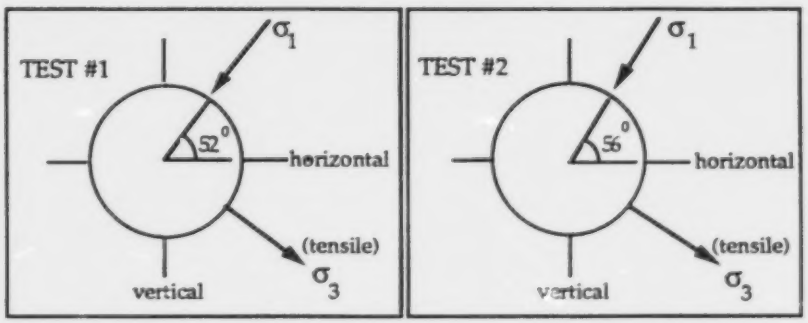

σ_1 = 44.80 MPa $\quad$ σ_1 = 40.99 MPa

σ_3 = -2.93 MPa $\quad$ σ_3 = -7.34 MPa

σ_1 (typical) = 44.85 MPa oriented 54^0 counterclockwise from horizontal

σ_3 (typical) = -5.12 MPa oriented 36^0 clockwise from horizontal

FIGURE 20 - AVERAGE STRESS COMPONENTS FOR SITE #5 DOORSTOPPER TESTS (October, 1987)

3.2.2.6 - Site #6 Stress Component Determination

Drilling at Site #6 was implemented at the up dip end of the 35022 stope during late June and early July, 1987. The borehole was extended to an ultimate depth of 5.79 metres by drilling longitudinally through the pillar centre line at a down dip angle of 31^0, as illustrated in Figure 8.

Two Doorstopper stress tests, of a total of five which were attempted, were successfully completed. The three unsuccessful tests were not carried to completion due to excessive discing failures of the recovered drill core. Over considerable lengths of the test borehole, numerous thin discs were produced immediately upon core drilling within the hole. The presence of such discs is generally associated with

high compressive stress field influence, and was therefore thought to be indicative of high pillar stresses at this Site. At a hole depth of 5.20 metres from the collar, longer core pieces (up to 10 cm in length) were recovered and gage installation was attempted. The results of the two successful stress determination tests indicated very good directional correlation for resolved stress between test locations and demonstrated that the major principal stress component was directed in a generally vertical orientation.

Dissimilar magnitude response was noted to exist between the two test locations within the Site #6 borehole. Upon examination, test #1 overcore material was observed to be heavily fractured. This rock condition would serve to yield low Young's Modulus and strain relief parametric values with subsequent low stress magnitude results. At the location of test #2, longer and more intact overcore pieces were recovered during strain relief operations, and the high level of major principal stress thereby determined (35.9 MPa) would be most likely indicative of the true state of field stress existing at Site #6. Due to the variation between point determinations of strength, Young's Modulus and Poisson's ratio response of core specimens, the average values for all intact specimens (160.6 MPa, 52.8 GPa and 0.15) recovered within this borehole were selected for determination of stress magnitude response. By utilizing average parameter conditions for the entire hole and the test specific strain data from the two test sites, the major principal stress component magnitudes were determined to range between 35.9 and 43.2 MPa.

Directional data was determined as the average of results from both tests #1 and #2 within this borehole; the major principal stress components were therefore determined to trend in an approximately vertical orientation. The results of individual test observations and resultant Site #6 stress summary (both magnitude and orientation data) are illustrated in **Figure 21**.

3.2.3 - Summary of Doorstopper Gage Stress Determination Trials

The majority of the site stress evaluation program was conducted during the interval period between June and October, 1987 when a total of six borehole sites were drilled and instrumented. Four of the Sites (#1, #2, #3 and #6) were investigated during the summer period (June-July, 1987), while Sites #4 and #5 were investigated during September-October, 1987. A summary of completion dates and derived Site stress component data, previously described for each specific Site in Section 3.2.2, is provided in Table 8.

Upon completion of initial stress characterization stages at each of the proposed microseismic monitoring sites, several of the sites were eliminated from consideration for monitoring use. Both Sites #3 and #4 were arbitrarily rejected because stress conditions were demonstrated to be atypical of local mining stress conditions.

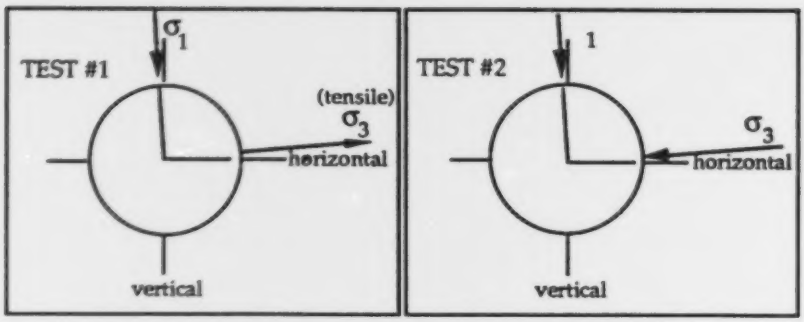

σ_1 = 10.34 MPa σ_3 = -2.63 MPa

σ_1 = 43.20 MPa σ_3 = 17.88 MPa

σ_1 (typical) = 43.20 MPa oriented 3.5 ^{0} counterclockwise from vertical
σ_3 (typical) = 17.88 MPa oriented 3.5 ^{0} counterclockwise from horizontal

FIGURE 21 - AVERAGE STRESS COMPONENTS FOR SITE #6 DOORSTOPPER TESTS (June, 1987)

TABLE 8 - Site Summary of Drilling and Doorstopper Stress Measurement Data

Site #	Drill / Stress Test Interval Date	Principal Stress Magnitudes (σ_1)	(σ_3)
1	June 2 - 5, 1987	24.1 MPa	16.1 MPa
2	June 9 - 15, 1987	11.9 MPa	4.8 MPa
3	June 15 - 19, 1987	10.3 MPa	6.7 MPa
4	October 14 - 16, 1987	24.1 Mpa	12.4 MPa
5	October 20 - 22, 1987	44.9 MPa	-5.12 Mpa (tensile)
6	June 24 - July 7, 1987	(35.9 - 42.3) MPa	17.9 MPa

The borehole length at Site #3 was measured to be shorter than those at the other two adjacent Sites (#1 and #2). This hole was therefore demonstrated to lie within the local zone of fracture (destress zone) which exists in close proximity to the 26 Garage excavation surfaces. Similarly, upon completion of drilling at Site #4, it was determined that the transducer installation zone at the end of this hole fell along the intersection of the site pillar/footwall waste contact zone. For such conditions, and due to low levels of measured stress at this site (approximately 24 MPa versus 44.9 MPa measured at nearby Site #5, in a mid-pillar location) it was thought that atypical stress influence, possibly being induced by a stress reduction

effect of the footwall bearing plane, was being monitored at Site #4. Subsequent acoustic monitoring efforts within the 24962 drift pillar were therefore restricted to data acquisition solely within the Site #5 borehole.

3.2.4 - Additional Stress Evaluation Analysis

In order to facilitate initial stress characterization work, a total of twenty Doorstopper Gage overcore tests were attempted, of which sixteen were successfully completed. Upon subsequent analysis of measured stress parametric data, three principal microseismic monitoring zones, each acted upon by dissimilar stress influence, were identified and selected for long term study. Those zones identified were the Negri Dyke (low stress region, monitored at Sites #1 and #2), 24962 drift pillar (high stress region, monitored at Site #5, within unsupported pillar material) and the 35024 stope pillar (intermediate stress region, monitored at Site #6, within backfill-supported pillar material).

Long term microseismic monitoring trials were implemented at each of the three identified zones immediately following completion of the initial stress characterization phase. At the inception of the Queen's/Denison research program, it had also been planned that periodic stress review would be conducted at each Site to monitor changing stress conditions due to local mining activity. However, because of the very limited funding available with which to permit such stress examination, no additional Doorstopper Gage tests were able to be financed during the remainder of the field study. Therefore, in order to provide some measure of long term Site stress conditions, at minimal expense, limited computer modelling analyses were conducted by Queen's staff in addition to work contracted under the Denison program. This program of modelling was scheduled to begin at an interval period approximately six months following completion of the initial series of in-situ Doorstopper Gage tests (April, 1987). As will be detailed in later sections of this report, little change in activity was monitored to occur over the entire period of in-situ microseismic review at the Site #2 location. Similarly, during the spring of 1988, production planning required implementation of backfilling in regional zones immediately north of the 26 Garage area, including the 24962 access drift pillar within which Site #5 was established. With loss of monitoring access to Site #5, and consequent restriction of microseismic data acquisition, plus lack of apparent change in signal alteration at Site #2, no additional benefits were deemed possible by pursuing further stress analysis review at these Sites.

In view of significantly changing microseismic and stress-related conditions existing at the location of Site #6, however, a detailed stress modelling study of Site #6 was thought to be necessitated which would yield stress data over the long term. All prior Doorstopper measurements were taken at single points within the Site #6 pillar zone, whereas a knowledge of the pillar stresses throughout the entire area would be required to gain a more complete understanding of the processes which controlled microseismic emissions at the monitoring site. For these reasons, modelling techniques were adopted as a means of estimating pillar stresses, at low

cost.

Pillar stresses were modelled [10] using the MINTAB program on the mainframe IBM computer at Queen's University. The program, utilizing software modified from South African displacement-discontinuity programs, models the Denison orebody as a thin, tabular discontinuity lying within an infinite medium. Displacements are calculated by assuming that the rock mass, in its entirety, behaves as an ideal elastic solid. The regional pillar layout near the Site #6 monitoring location is illustrated, in plan, in **Figure 22**. Similarly shown in this Figure is a local area lying immediately adjacent to the Site #6 pillar layout within which detailed stress and displacement analysis was concentrated. The plotted area was sectioned into an array of 80 x 80 square elements, each representing a zone approximating 3.05 metres by 3.05 metres on a side. Both pillars and excavated ore zones which existed within this area were separately coded and indicated on separate plan views (**Figure 23**). Blank spaces signify unmined ore zones (or pillar material), whereas spaces identified by an "E" symbol signify those zones which have been previously excavated (stope voids or drift access ways). In this manner, pillar configurations which were present at the time of modelling or which were anticipated to exist at future time intervals could be set to model effective load bearing areas in plan.

In order to facilitate MINTAB modelling procedures, several assumptions concerning stress and displacement behaviour were made, and include the following:

- the areas external to those zones which are modelled are assumed to be incompressible. Because such areas are, in fact, mined, erroneous results will exist near the model boundaries. To overcome this limitation, a 61 metre wide strip about the area of interest (35022 pillar) was considered sufficient to account for this. The displacements and stresses which were calculated for this zone of influence were therefore assumed to be incorrect, and were not included in result summaries.
- backfill which was emplaced adjacent to the pillar area of interest was assumed to carry no load. Since the rock elastic modulus is quite high with respect to that of backfill, and substantial hanging wall displacements are required to mobilize the passive strength of backfill, this was assumed to be a reasonable assumption.
- the orebody was assumed to dip parallel to the long dimension of the rib pillars; the actual dip direction, however, is approximately 16 degrees to the east.
- the rock mass was assumed to behave both as a homogeneous and isotropic medium; the influence of local faults and the like was not modelled.
-the mining height and orebody dip were assumed to be constant throughout the modelled area.
- the orebody thickness was assumed to be negligible in comparison both with its lateral extent and depth below ground surface.
- no artificial ground support (such as that induced through use of rockbolts) was assumed to exist.
- pillars were assumed to have dimensions which were whole number

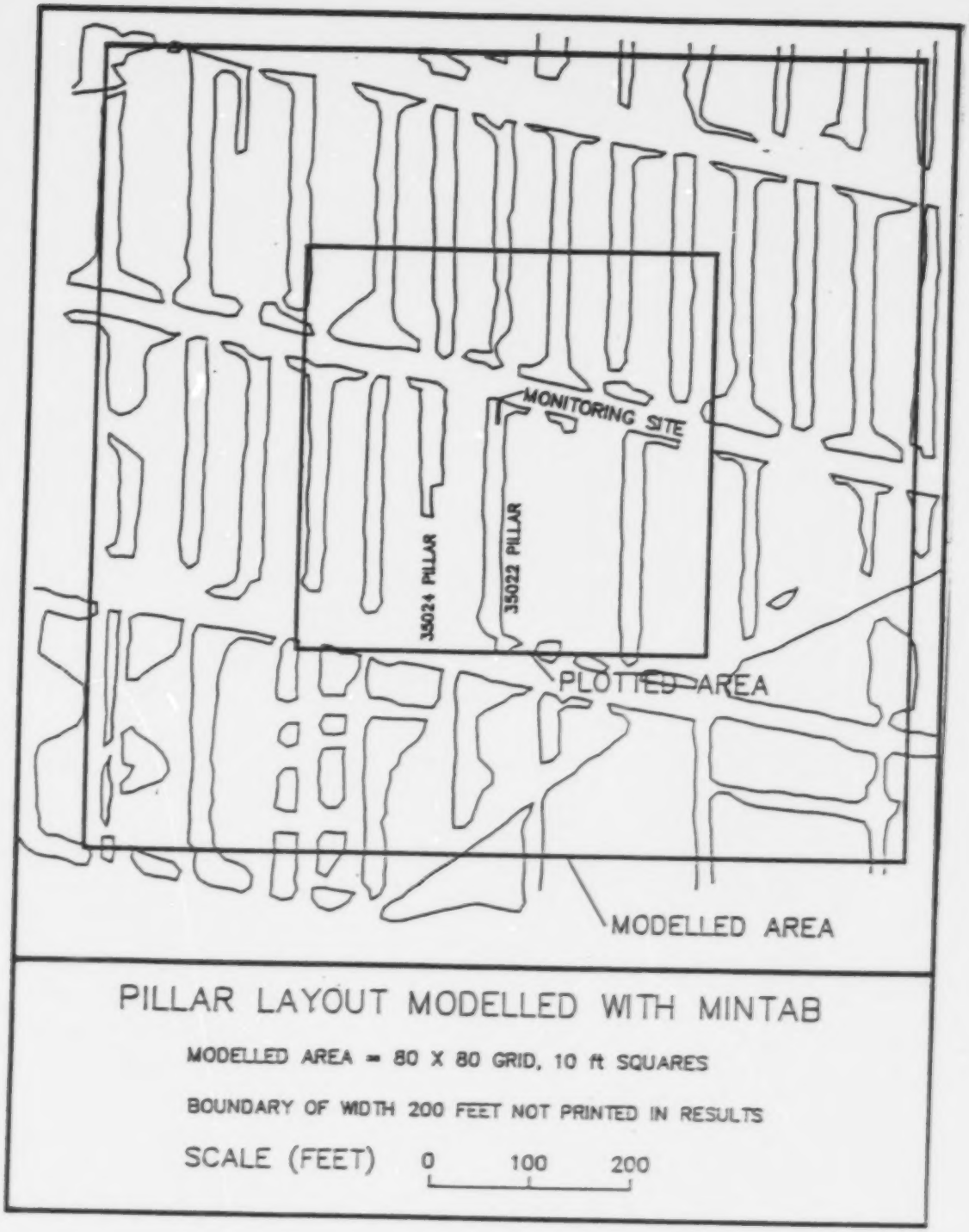
MONITORING SITE
35024 PILLAR
35022 PILLAR
PLOTTED AREA
MODELLED AREA
PILLAR LAYOUT MODELLED WITH MINTAB
MODELLED AREA = 80 X 80 GRID, 10 ft SQUARES
BOUNDARY OF WIDTH 200 FEET NOT PRINTED IN RESULTS
SCALE (FEET) 0 100 200

FIGURE 22 - Plan View of Site #6 Pillar Zone Modelled by MINTAB
(after Madsen [10])

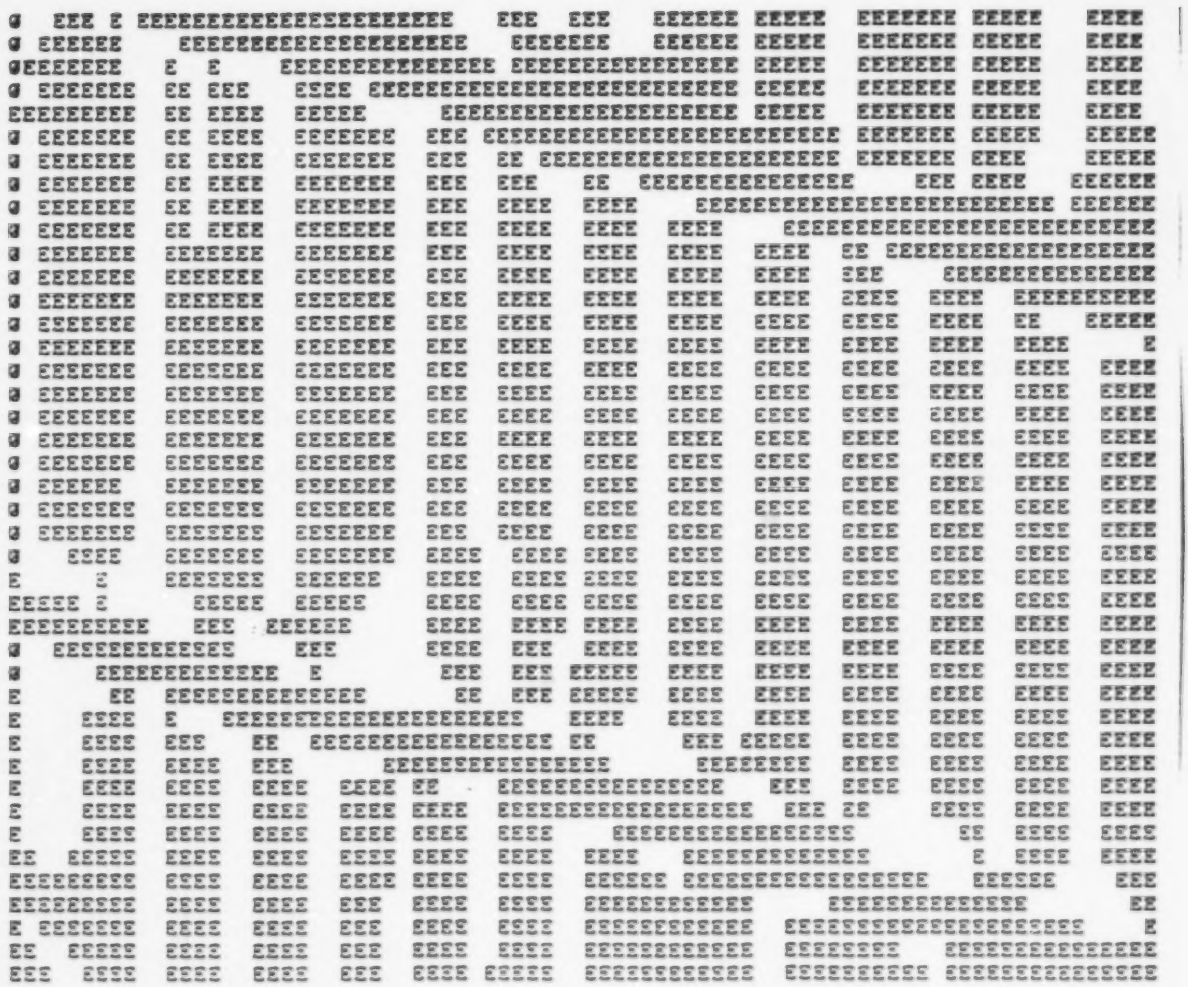

FIGURE 23 - Plan View Showing Close-up of Pillar Modelling Grid
("E" symbols designate mined ore) - (after Madsen [10])

multiples of the basic block width (3.05 metres x 3.05 metres).

- the response of the orebody, hanging wall and footwall rocks was assumed to be ideally elastic, and
- no post-failure stress analysis, occurring as the result of yielding or fracturing behaviour of the pillars, was assumed.

All data concerning the local pillar geometry was estimated from available mine plan information; pre-mining in-situ stress data was inferred from previously published technical information [11]; and rock mechanical property data was obtained as the result of laboratory analysis of recovered core sample materials taken during drilling at Site #6 during the Doorstopper stress evaluation program. A summary of input parametric data which was used to perform MINTAB analysis of Site stress conditions is briefly listed:

Depth to first row of grid elements	=	560 metres
Assumed orebody dip over Site zone	=	23 degrees
Stoping thickness (assumed constant)	=	3.05 metres
Stress coefficient (X direction)	=	0.039 MPa/metre
Stress coefficient (Y direction)	=	0.039 MPa/metre
Stress coefficient (Z direction)	=	0.026 MPa/metre
Convergence criterion for stress solution	=	1%
Maximum number of iterations	=	20
Elastic rock modulus (Young's)	=	55.0×10^3 MPa
Poisson's ratio for rock mass	=	0.15
Normal stiffness for pillars	=	55.0×10^3 MPa
Shear stiffness for pillars	=	23.9×10^3 MPa

In order to check the validity of the selected input parameters and accuracy of computed stress and displacement output data, it is normally required that modelled results be compared versus actual field measurement data. Unfortunately, no in-situ convergence data was available from mining records, and only single site Doorstopper Gage stress information (achieved during borehole installation research) was similarly available from which comparisons could be made. Model results were therefore validated solely in terms of monitored stress conditions which were initially inferred during July, 1987.

Figure 24 illustrates theoretical pillar stresses which were modelled to exist at Site #6 during the time of transducer installation and immediately after completion of Doorstopper Gage stress characterization of this Site. The MINTAB-derived stress condition existing within two grid elements located at the transducer site yielded values approximating 58.6 and 55.7 MPa (stresses for the two grid elements in the second row of the 35022 pillar). The average predicted stress condition (acting normal to the plane of the hanging wall/footwall) for this site approximates 57.2 MPa.

Figure 25 illustrates a theoretical distribution of stresses within a pillar

```
Stress Range within 5 m radius of Transducer: 55.7 - 68.3

Minimum and Maximum Stress (MPa):      0.0     107.7
```

CODE VALUES FOR STRESS:

1 = 0.5 - 10.0 MPa	7 = 60.0 - 70.0 MPa
2 = 10.0 - 20.0 MPa	8 = 70.0 - 80.0 MPa
3 = 20.0 - 30.0 MPa	9 = 80.0 - 90.0 MPa
4 = 30.0 - 40.0 MPa	V = 90.0 - 100.0 MPa
5 = 40.0 - 50.0 MPa	X = 100.0 - 110.0 MPa
6 = 50.0 - 60.0 MPa	Y = 110.0 MPa and more

```
*************************************************
*       55    55    55    55    55    55    *
*       55    55    55    55    55    55    *
*       55    65    66    55    55    55    *
*       55     56    6    55    55    55    *
*      545     55    7    55    55    55    *
*     5445     55    7    55    55    55    *
*    54445     55    7    55    55    55    *
*   544444     55   67    55    55    55    *
*7 65544445    66    6     55    66    55    *
*     555567   76    6     55    66    55    *
*                   876    645    67    65    *
*6                    8   765456   7     66    *
*655667                     766668          66    *
* 55     7   8767                        877    76    *
* 55     7     56                          88    8    *
* 55     7     66     7779                          7*
* 55     7     66     66     V99                     *
* 55     7     66     66      X                      *
* 55    66     66     66                  8788V     *
* 55    66     66     67                  77        *
* 55    66     77     77                  77        *
* 65    66     8      77                  77        *
* 65    66     9      77                  77        *
* 65    66     V      77                  87        *
* 66    66            77                  87        *
* 66    66            77                  88        *
* 66    67            78                  88        *
* 66    77            78                  88        *
* 66     8            88                  88        *
* 77     9            88                  88        *
* 8      9            88                  88        *
* 8      9            88                  88        *
* 9      V            88                  88        *
* X      V            88                  88        *
*       V             87                  87        *
*       X             77                  77        *
*                     77                  77        *
*                     87                  77        *
*                      879                77        *
*                       9    99           78        *
*************************************************
```

FIGURE 24 - MINTAB Modelled Stress Distribution About Site #6 During Initial Stage of Seismic Monitoring (July, 1987) (after Madsen [10])

Contour values are ratio of major principal stress to average pillar stress. Plane strain analysis for uniformly distributed vertical applied stress assuming no horizontal stress.

Reference: Hoek, 1980

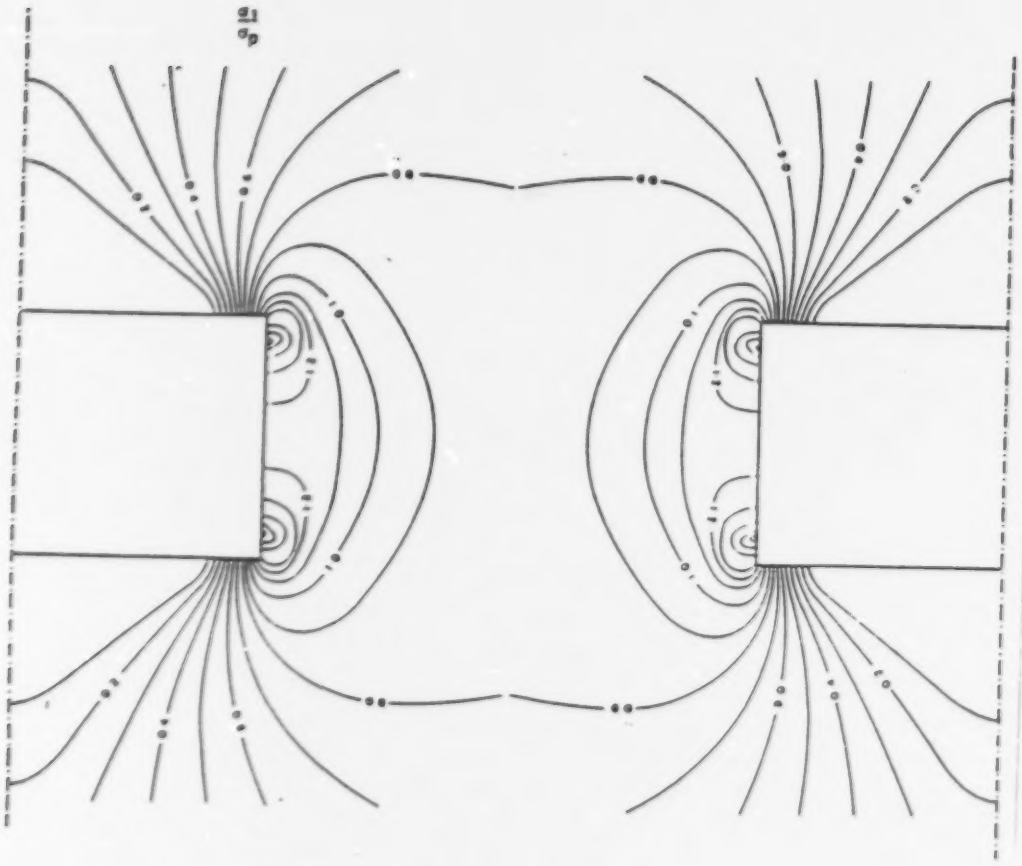

THEORETICAL DOORSTOPPER STRESS = 48.6 MPa

(Based on MINTAB results and diagram above)

MEASURED DOORSTOPPER STRESS = 43.5 MPa

FIGURE 25 - Cross Section of Theoretical Stress Distribution in 35022 Rib Pillar (after Madsen (10))

JULY 1/87 - MINING STEP 1 (TRANSDUCER INSTALLATION)

Grid Size = 80 X 80 elements
Boundary of width 200 ft not printed
Element Size = 10 feet square

Minimum and Maximum Displacement (mm): 0.8 28.0

CODE VALUES FOR STOPE CLOSURES:

0 = -0.5 to 0.5 mm	5 = 20.0 - 25.0 mm
1 = 0.5 - 5.0 mm	6 = 25.0 - 30.0 mm
2 = 5.0 - 10.0 mm	7 = 30.0 - 35.0 mm
3 = 10.0 - 15.0 mm	8 = 35.0 - 40.0 mm
4 = 15.0 - 20.0 mm	9 = 40.0 - 45.0 mm

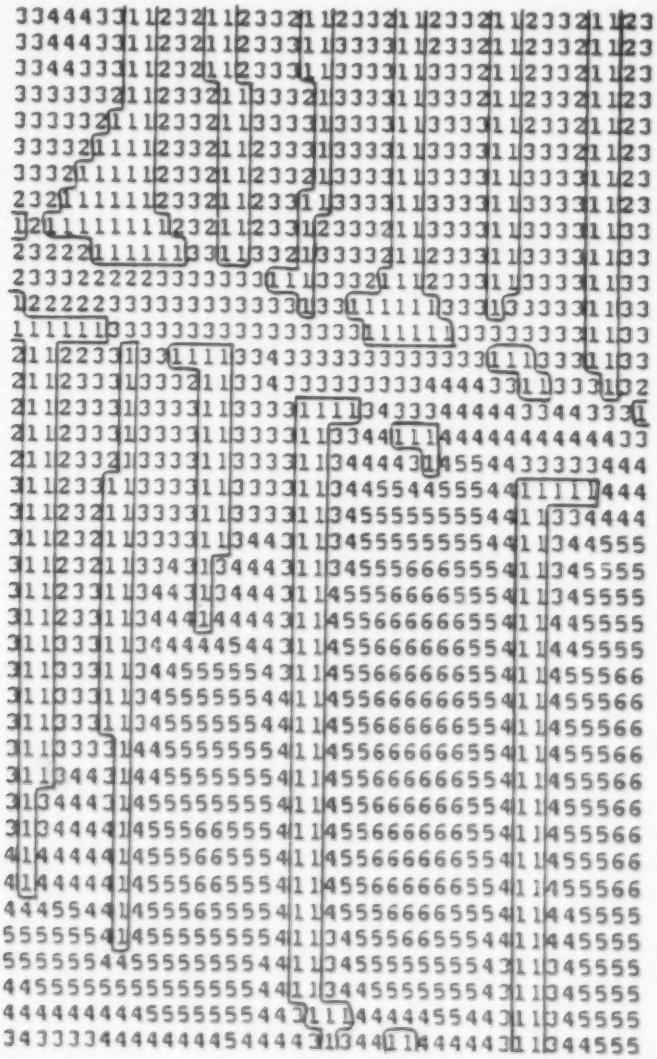

FIGURE 26 - Plan View Showing MINTAB Modelled Vertical Displacements About the Site #6 Monitoring Location during Initial Phase (after Madsen [10])

structure which exhibits a height-to-width ratio of 0.5-to-1, similar to the 35022 rib pillar geometry. In theory, the major pillar stress, acting centrally through the pillar, exhibits a magnitude which is approximately 85% of the average pillar stress condition. On the basis of theoretical stress reduction within central pillar spans, the Doorstopper measured stress for Site #6 would be expected to approximate 48.6 MPa (ie.- 0.85 x 57.2 MPa). In fact, the peak pillar stress which was measured by Doorstopper methods approximated 43.2 Mpa, or a level approximately 12% lower than the modelled stress level. MINTAB predictions, based upon ideal elastic behaviour of the rock, would also contribute to higher than measured results. Given the difficulty in effecting site measurements and considerable variability in measurements between adjacent locations at the same site, the correlation between the measured and modelled stress data is excellent. Similarly, differences between the actual test borehole dip (31^0) and the true orebody dip (23^0) would also place the stress test site at a location closer to the footwall plane. For reasons similar to those detailed in Section 3.2.2.4, the measured Site #6 pillar stress may be lower than the true measure which exists at the central pillar location.

The MINTAB predicted stress parameter therefore agrees quite well with measured Site stress results. The input parameters which were used for stress modelling purposes were thus considered to be reasonable for future modelling purposes and to yield realistic results.

Observation of theoretical stope displacement conditions (shown in **Figure 26**) evidenced stope closure approximating 25 to 30 millimetres in zones where pillars had been recovered and support was removed between the hanging wall and footwall. Given the high modulus of deformation and generally good ground conditions which were noted to exist in this area, closures of this magnitude over total span widths of 30 metres appeared, also, to be quite reasonable. Neither visual nor mechanical observations of local ground movement within the local pillar recovery stopes were made to verify such predictions.

Pillar stresses within the local area adjacent to the 35022 pillar were modelled over six different intervals between July 1 and October 21, 1987. Stress characterization was planned in order to monitor the various stages of 35024 pillar recovery and associated stress transfer to the adjacent 35022 pillar (within which a microseismic transducer was set) following initial microseismic station installation. Each interval corresponded to dates on which high microseismic activity, thought to indicate large increases in local stress, was measured to occur at the Site #6 transducer. On each date, higher than normal rates of microseismic response were shown to correlate with blasting activity which was occurring within the 35024 pillar. The MINTAB modelled stress results, for each of the six stages of mining within the 35024 pillar, are illustrated within Appendix B. At the final stage (October 21, 1987) local, violent rock failure, adjacent to the monitoring site, and extremely high acoustic emission activity were observed to occur coincident with blasting of a final slash round in the 35024 pillar. **Figure 27** illustrates modelled pillar stresses existing at the time of this anomalous activity and the inferred location of the pillar failure source in the right hand, up dip remnant of the 35024

```
Stress Range within 5 m radius of Transducer: 60.6 - 77.7

Minimum and Maximum Stress (MPa):      0.0     109.1
-------------------------------------------------------
                CODE VALUES FOR STRESS:

1 = 0.5 - 10.0 MPa                7 = 60.0 - 70.0 MPa
2 = 10.0 - 20.0 MPa               8 = 70.0 - 80.0 MPa
3 = 20.0 - 30.0 MPa               9 = 80.0 - 90.0 MPa
4 = 30.0 - 40.0 MPa               V = 90.0 - 100.0 MPa
5 = 40.0 - 50.0 MPa               X = 100.0 - 110.0 MPa
6 = 50.0 - 60.0 MPa               Y = 110.0 MPa and more
-------------------------------------------------------
     ****************************************
     *       65   55    55    55    55    55  *
     *       55   55    55    55    55    55  *
     *       55   65    66    55    55    55  *
     *       55    56    6    55    55    55  *
     *      545    55    7    55    55    55  *
     *     5445    55    7    65    55    55  *
     *    54445    55    7    65    55    55  *
     *   644445    66   77    55    56    55  *
     *7 75544446   66    7     55    66    55  *
     *     555567  77    7     55    66    55  *
     *                  877    655    67    66  *
     *6                  8  865556   7     66  *
     *655667                766668         66  *
     * 55    8  99V                      977   76  *
     * 55    8                             88    8  *
     * 55    8        8789                        7*
     * 55    8        77     V99                   *
     * 55    8        77       X                   *
     * 55   77        77                 8788V     *
     * 65   67        77                 77        *
     * 66   67        77                 77        *
     * 66   67        87                 77        *
     * 66   67        88                 87        *
     * 66   67        88                 87        *
     * 66   67        88                 88        *
     * 66   67        88                 88        *
     * 66   77        88                 88        *
     * 66   88        88                 88        *
     * 66    8        88                 88        *
     * 77    9        88                 88        *
     * 8     9        88                 88        *
     * 9     V        88                 88        *
     * 9     V        88                 88        *
     * X     V        88                 88        *
     *       V        88                 88        *
     *       X        87                 77        *
     *                87                 77        *
     *                87                 77        *
     *                 88V               77        *
     *                  9   99           78        *
     ****************************************
```

ROCKBURST

FIGURE 27 - MINTAB Modelled Stress Conditions About Site #6 During Final Stage of Microseismic Monitoring (October 21, 1987) (after Madsen [10])

pillar.

In the first stage of stress modelling (as illustrated in **Figure 24**) it was demonstrated that the 35024 sill element was influenced by an approximate stress of 60 MPa; by October 21, 1987 (sixth modelling stage), this remnant was demonstrated to be influenced by stress in excess of 90 MPa. Similarly, the sequence of stress models indicated that a progressive transfer of stress occurred between the 35024 pillar, which was being mined, and both the permanent rib pillars on either side as well as to the 35024 pillar remnant. The distribution of stress within the 35024 pillar, 35024 pillar remnant and 35022 rib pillar were undoubtedly much more complex than the results of the MINTAB modelling program indicated. The assumption of completely elastic ground response ignores any post-yield failure conditions which could, and most certainly were, present at this site. Denison Mine pillars commonly experience some degree of post-yield failure due to stress concentrations at the excavation boundaries, producing typically "hourglass- shaped pillar cross-sections. During mining of the 35024 pillar, axial cleavage fractures, trending parallel to the rib axis, were observed to exist within the pillar walls. Such features indicated the presence of post-yielding behaviour which would extend inward from the pillar side walls toward the central pillar spans. Strength losses incurred by post-yielding behaviour would induce stress transfer from peripheral pillar zones to the central spans (intact core) of such structures.

The stress distribution within pillars is strongly influenced by the pillar's height-to-width ratio and the excavation shape. Variation in the major principal stress distribution within a rib pillar similar to the 35024 pillar, and which also exhibits a height-to-width ratio of 0.5-to-1, is demonstrated in **Figure 28**. In this illustration it is shown that corner stresses can be as much as 60% higher than the average pillar stress condition. Such concentrations often result in localized shear failures near the pillar boundaries. Progressive axial slabbing often occurs as fractures are formed parallel to the pillar walls, thereby creating a zone of post-yielding in the pillar. As load is progressively transferred, the zone of post-yielding effect would tend to migrate further into the central pillar span. The maximum depth of penetration of the post-yield failure zone will vary depending upon the height-to-width ratio of the pillar. Short, squat pillars will tend to have shallow failure zones (a limited annulus of fracture), whereas more slender pillars will be penetrated to greater depths. Such behaviour has been demonstrated in laboratory post-yield studies (12) for specimens of rock having similar geometric dimensions to those of the Denison rib pillars. In such studies, the penetration depth of axial fractures was approximated at 10% of the pillar width at each boundary. Should similar conditions be met in-situ, it is indicated that 80% of the load bearing area of typical rib pillars would exist in the elastic, pre-yield condition. **Figure 29** demonstrates changes in major principal stress conditions that were modelled to act within the 35024 pillar as it was being progressively extracted. Such stress behaviour was predicted to occur during stages 1, 3 and 6 of interval analysis, for which MINTAB summary data is provided in Appendix B. Stress conditions which are indicated were derived as average values distributed over 3.05 metre square

Contour values are ratio of major principal stress to average pillar stress. Plane strain analysis for uniformly distributed vertical applied stress assuming no horizontal stress.

REFERENCE: HOEK, 1980

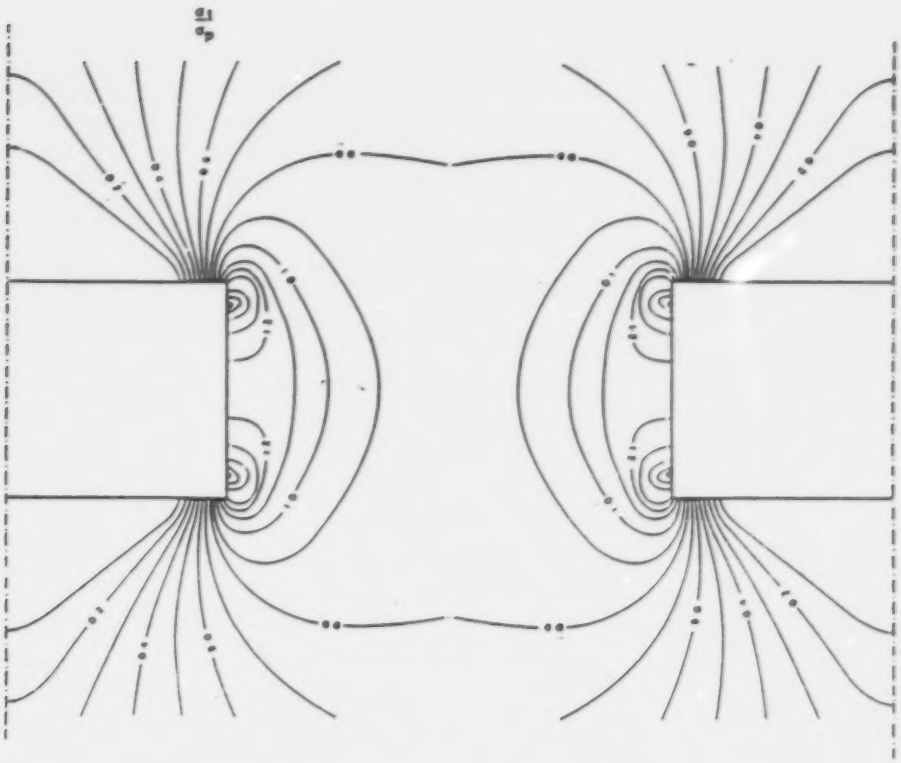

ESTIMATED ZONE OF POST-YIELDING FOR THE 35024 RIB PILLAR

Primary stopes on either side backfilled with cemented tailings

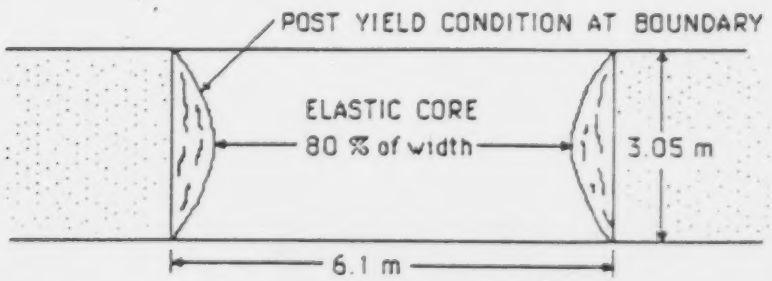

FIGURE 28 - Cross Section of Theoretical Major Principal Stress Distribution in 35024 Rib Pillar (after Madsen [10])

MINTAB PREDICTED STRESSES FOR EACH ELEMENT ON WEST SIDE OF 35024 PILLAR ARE SHOWN WITH 25% INCREASE IN MAGNITUDE OVER COMPUTER PREDICTED VALUES TO ACCOUNT FOR POST-YIELDING AT PILLAR BOUNDARIES. ALL STRESS VALUES SHOWN ARE IN UNITS OF (MPa)

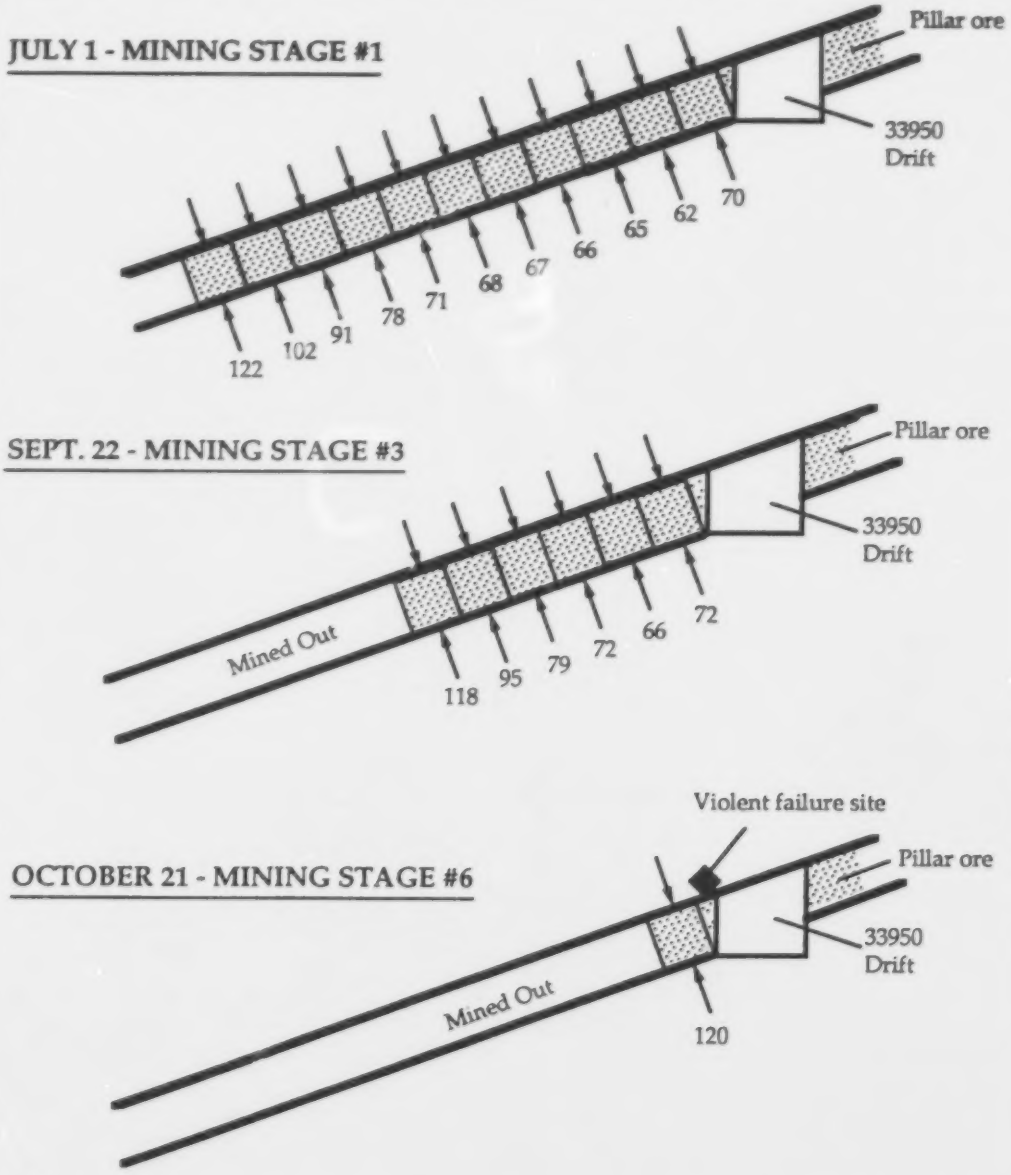

FIGURE 29 - Long Section of 35024 Pillar Showing Predicted Normal Pillar Stress Components at Various Stages of Mining (after Madsen [10])

Grid Size = 80 X 80 elements
Boundary of width 200 ft not printed
Element Size = 10 feet square

Minimum and Maximum Displacement (mm): 0.8 28.4

CODE VALUES FOR STOPE CLOSURES:

0 = -0.5 to 0.5 mm	5 = 20.0 - 25.0 mm
1 = 0.5 - 5.0 mm	6 = 25.0 - 30.0 mm
2 = 5.0 - 10.0 mm	7 = 30.0 - 35.0 mm
3 = 10.0 - 15.0 mm	8 = 35.0 - 40.0 mm
4 = 15.0 - 20.0 mm	9 = 40.0 - 45.0 mm

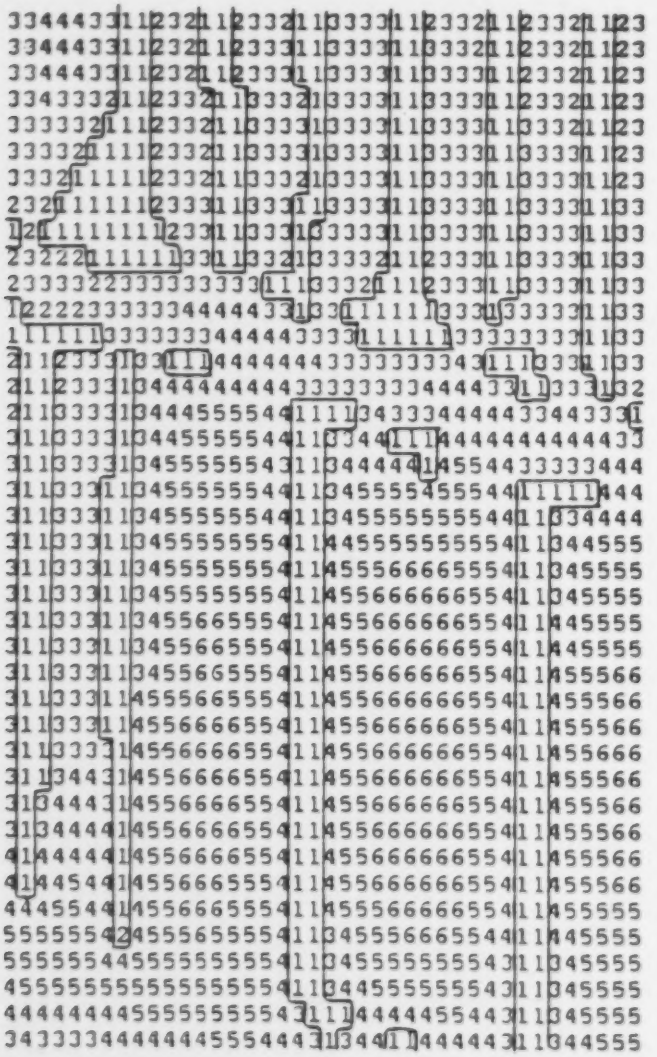

FIGURE 30 - MINTAB Modelled Vertical Displacements About the 35022 Pillar Site During Final Pillar Extraction (October, 1987) (after Madsen [10])

elements of rock, and, though oversimplified, permit a reasonable evaluation of changing stress parameters to be developed. At the latest stage of modelling (October 21, 1987), the remnant pillar element was predicted to mobilize a high stress concentration of approximately 120 MPa which was sufficient to induce rapid, violent failure within the rock mass. The simplified post-yield stress analysis which is illustrated in **Figure 29** provides only a crude measure of inferred pillar stress conditions. In general, however, such an analysis would tend to indicate that MINTAB predicted stress conditions would be overly conservative.

Figure 30 illustrates vertical displacements which occurred at the time of the violent failure of ground. Displacements were greatest at the centre of the adjacent stope spans, and decreased with distance toward the permanent rib pillar formations on either side. As the 35024 pillar was being recovered, stope closures approximating 20 to 30 millimetres were modelled to occur at the centre of the 30 metre excavation span. Displacements predicted to occur along the rib pillar axes totalled less than 5 millimetres, which appeared quite reasonable given the high deformation modulus character and generally good ground conditions typical of the pillar rock.

4.0 - Microseismic Precursor Evaluation Program

During the interval following Site stress characterization at the three test locations, two microcomputer data acquisition units were kept available for monitoring purposes and were utilized to obtain characteristic microseismic information at these sites. Emissions were captured using COMPAQ microcomputers, of ruggedized design, which contained advanced signal digitizing hardware and software. Each unit was used to monitor single Sites, full time, and were shown to be able to continuously monitor seismic activity for periods in excess of one month, unattended, without failure. At the present stage of design, all monitoring units require AC power input to function. No battery system yet exists which will permit observation to be carried out in a truly portable fashion. In certain instances, therefore, and typically during annual maintenance shutdown periods or when severe surface weather conditions rendered power interruptions underground, some permanent losses of data were incurred by the microseismic monitor units.

A summary review of monitoring activities at the three principal Sites will be discussed in the following sections of this report. Typical microseismic waveform data (amplitude response) and transformed frequency characteristics of these waveforms (frequency response), as illustrated in **Figure 3**, were recorded at each of the monitoring sites for the variable conditions of stress existing. The typical data which was obtained indicated that marked differences in acoustic response existed between sites. On this basis, it is clear that differences exist between acoustic information which can be gathered between sites and that such differences occurred consistently with long term observation. Typical features which were extracted from amplitude response data which was recorded include frequency spectrum,

event rate and peak magnitude of signal characteristics. This evidence showed strong indication that the developed monitoring and data extraction techniques may be capable of providing a direct measure of stress conditions within a rock mass based solely upon identification of captured seismic data.

4.1 - Site #1/ Site #2 (Low Stress Zone)

Initial microseismic monitoring activity was initiated at the location of Sites #1 and #2 (airway, North of 26 Garage) during June, 1987. On the basis of previous stress characterization analysis, the major principal site stress was determined to range between 12 - 24 MPa for both installations within the unmined Negri Dyke location. At a working depth of approximately 488 metres below ground surface, the theoretically-predicted pre-mining vertical stress condition should approximate 12.0 MPa. On the basis of both theoretical and observed conditions, this monitoring site was considered to lie within a zone of low stress activity.

Continuous waveform monitoring was attempted at these Sites during a five week interval between mid-July and mid-August. For this period, generally uniform, and low, event rate activity was recorded. A summary of event rate activity at both sites is provided to illustrate typical acoustic response which resulted under low stress conditions.

Site #1	Date	# Waveforms Recorded	Event Rate
	-June 12-15	16	6/day
	-June 18	0	0/day
	-June 19-20	485	*485 (anomalous)
	-Equipment repair and move to Site #2	—	------
	-July 3-7	7	2/day
	-July 7-9	47	23/day
	-July 17	12	12/day
	-July 22	12	12/day
	-Equipment moved to Site #6	—	------
	-July 24-August 10	Mine shutdown	
	-August 10-11	0	0/day
	-August 14	3	3/day
	-August 15-17	6	2/day
	-August 18	3	3/day
	-Computer removed		

Site #2	Date	# Waveforms Recorded	Event Rate
	-June 15-16	65	65/day
	-June 16-17	420	*420 (anomalous)
	-June 26-30	7	2/day
	-July 1-2	380	190/day
	-July 3	1	1/day
	-Equipment moved	---	------
	-July 24-August 10	Mine shutdown	
	-August 11-12	1	1/day

Figure 31 illustrates several amplitude and frequency domain plots of typical acoustic waveform information which was gathered at the Site #1 transducer location during the initial monitoring interval (July, 1987). For the waveforms shown, typical response indicates that the centre frequency of microseisms approximates 90-110 kHz, and that the waveform amplitude ranges between 1 and 4 volts. The majority of signals received exhibited amplitude response less than 1 volt, indicating low energy source signatures.

Figure 32 illustrates similar waveform data which was recorded and derived at the Site #2 transducer location, for the same interval period of sampling. Typical waveforms exhibit low energy amplitude response (less than 1 volt) and centre frequency distributions ranging between 60-125 kHz, with average centre frequencies approximating 100 kHz. In both cases, for Sites which were closely adjacent in the same access airway, very similar, characteristic waveforms and low event rate acoustic response was monitored to occur. Over the initial six months of acoustic monitoring which was performed, very little change in waveform character was measured, indicating that little variation in local stress field activity was also occurring.

In January, 1988, erratic waveform output was shown to be received at both Sites #1 and #2, and a decision was made to replace the transducers within the Site #2 borehole. The original steel bonding plate/transducer assemblies were retrieved from the two boreholes. On the basis of such recovery operations, it was indicated that the transducer-to-rock grout bond was very competent, but that the transducer-to-installation plate bond was deteriorated. Such deterioration was thought to be due possibly to a reaction between the transducer glue and a polyurethane protective plastic coating that had been applied at the time of transducer installation in June of 1987. The coating agent had been originally intended to provide protection for the transducer and installation plate against deleterious effects of high humidity within the monitoring holes. In all future tests, the application of such protective barrier coatings was to be discontinued; in all other Sites, where no similar protection was placed, no evidence of bond deterioration was observed. A second transducer was successfully installed in the Site #2 borehole in March, 1988, and acoustic monitoring was continued. Similar waveform event rates and waveform response

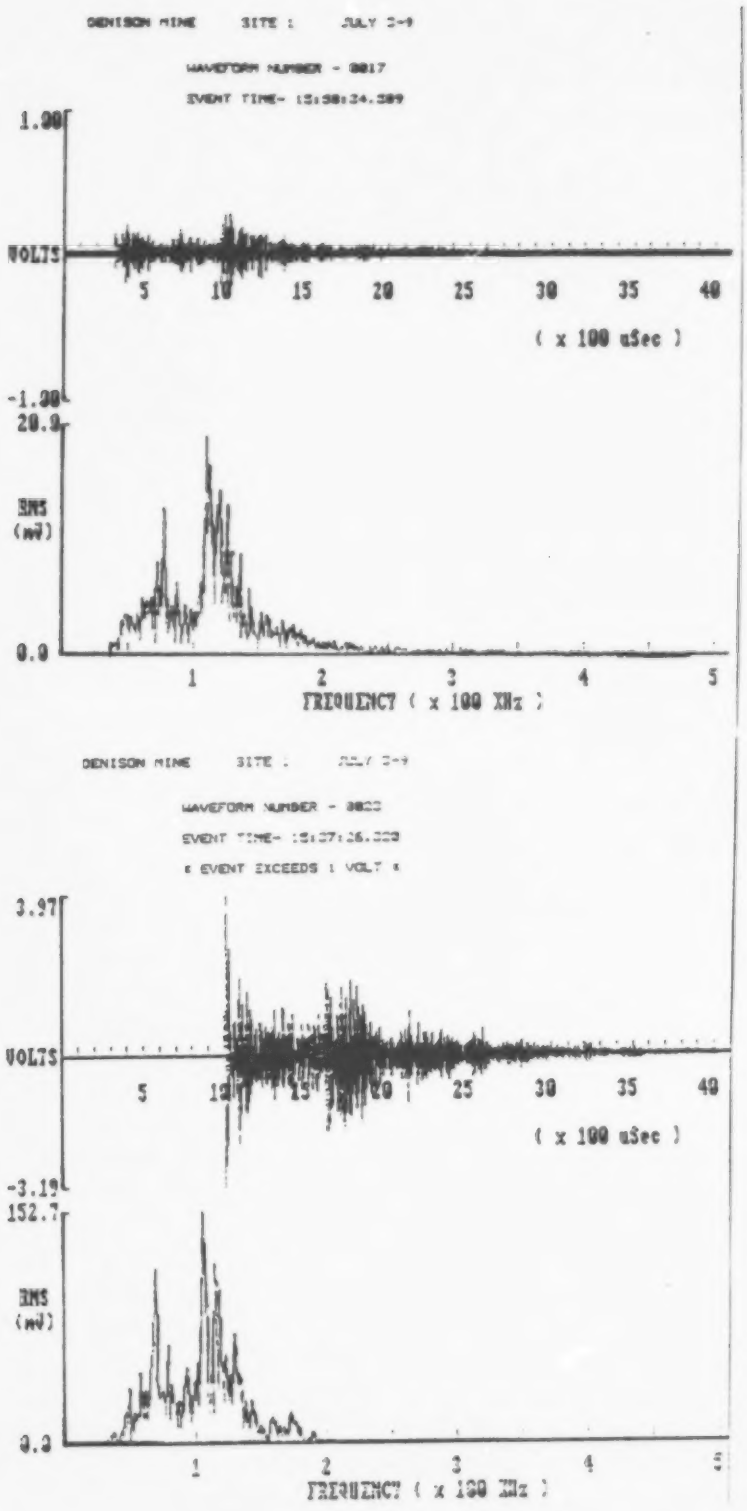

FIGURE 31 - Amplitude and Frequency Domain Plots of Typical Acoustic Waveforms Monitored at Site #1 (June, 1987)

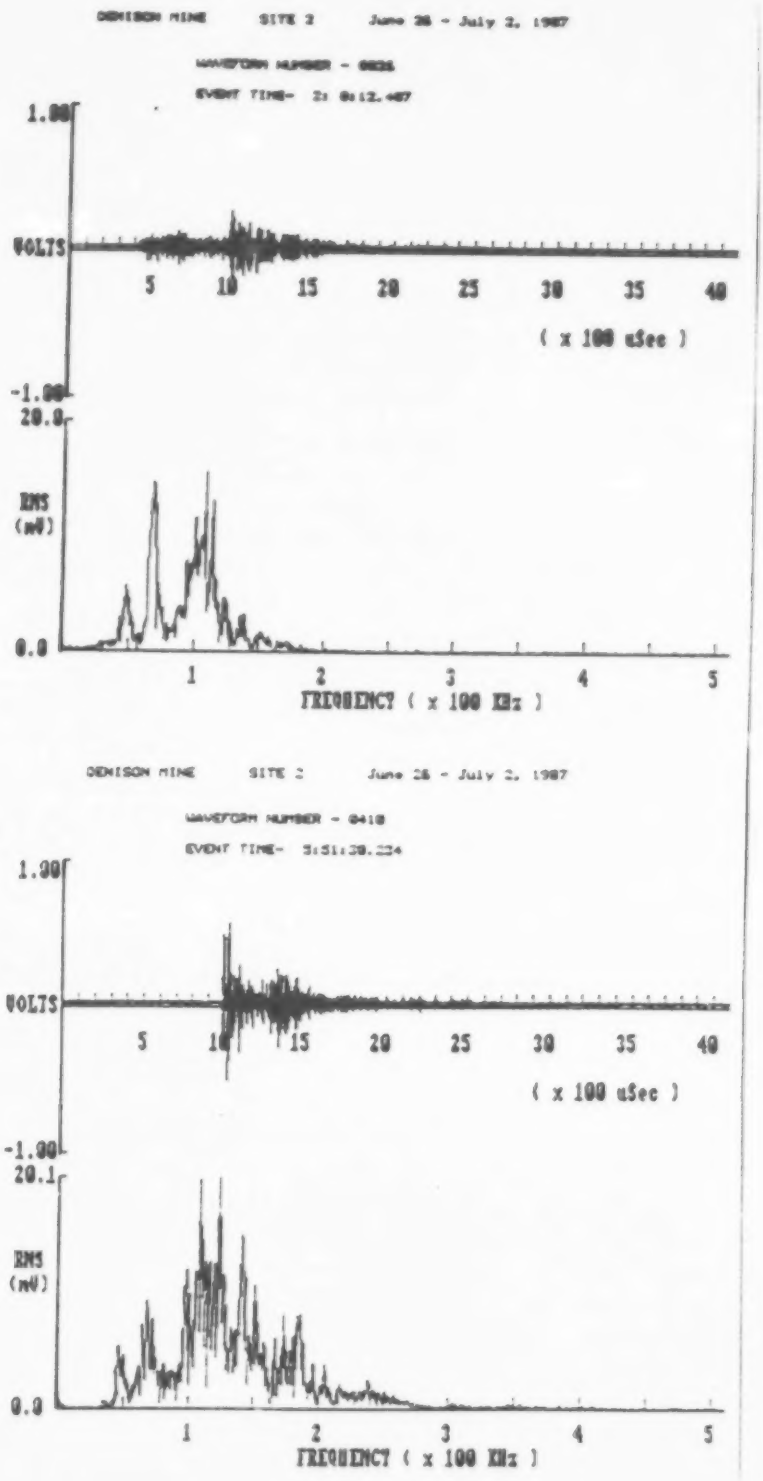

FIGURE 32 - Amplitude and Frequency Domain Plots of Typical Acoustic Waveforms Monitored at Site #2 (June - July, 1987)

to that which is illustrated in **Figure 32** was subsequently recorded.

4.2 - Site #4/ Site #5 (High Stress Zone)

Initial microseismic monitoring activity was initiated at the location of Sites #4 and #5 (24962 drift pillar, Northeast of 26 Garage) during June, 1987. Due to problems associated with properly locating the Site #4 drill hole, only a short term program of acoustic monitoring, lasting between October 22 and November 13, 1987, was initiated at this location. The majority of waveform characterization effort within this pillar location was performed within the Site #5 borehole following termination of efforts at Site #4 on November 13, 1987.

On the basis of previous stress characterization analysis, the major principal site stress was determined to range between 24 MPa (for the Site #4 installation) and 44.9 MPa (within the Site #5 installation). At a working depth of approximately 550 metres below ground surface, the theoretically-predicted pre-mining vertical stress condition would approximate 14.0 MPa. On the basis of observed stress conditions, this monitoring site was considered to lie within a zone of high stress activity.

Continuous waveform monitoring was attempted at these Sites immediately following initial transducer installation in October, 1987. Initially high rates of microseismic event activity were monitored and were thought to be due partially to pre-amplifier triggering problems. Generally higher rates of acoustic activity were monitored to exist at these sites, relative to Sites #1 and #2 (low stress region). Following several months of monitoring, drastic reductions in waveform activity were observed to occur during the early spring of 1988. Intermittent waveform acquisition, through March of 1988, was demonstrated when a series of equipment malfunctions, relating to local mine power failures and transducer decoupling within the borehole, as well as possible pillar destressing conditions, developed. For this period, generally uniform and medium rate activity was recorded. A partial summary of event rate activity at both sites is provided to illustrate typical acoustic response which resulted under the medium-to-high stress conditions which were associated with Sites #4 and #5.

Site #4	Date	# Waveforms Recorded	Event Rate
	-October 22	19	N/A (malfunctions)
	-October 23	17	17/day
	-October 24	6	6/day
	-October 25	1	1/day
	-October 26	7	7/day
	-October 27	3	3/day
	-October 28	1	1/day
	-October 29	6	6/day
	-October 30	4	4/day
	-October 31	3	3/day

-November 3	3	3/day
-November 4	7	7/day
-November 6	1	1/day
-November 7	47	47/day
-November 8	4	4/day
-November 9	19	19/day
-November 10	9	9/day
-November 12	3	3/day
-November 13	13	N/A (malfunctions)

Site #5	Date	# Waveforms Recorded	Event Rate
	-November 13	21	21/day (amp. malfunction)
	-November 14	5	5/day
	-November 15	5	5/day
	-November 16	13	13/day
	-November 17	10	10/day
	-November 18	10	10/day
	-November 19	30	30/day
	-November 25	4	4/day
	-November 26	13	13/day
	-November 27	5	5/day
	-November 29	3	3/day
	-November 30	13	13/day
	-December 1	10	10/day

Figure 33 illustrates several amplitude and frequency domain plots of typical acoustic waveform information which was gathered at the Site #4 transducer location during the initial monitoring interval (October-November, 1987). For the waveforms shown, typical response indicates that the centre frequency of microseisms approximates 130 - 160 kHz, and that the waveform amplitude ranges between 0.5 and 4.0 volts. The majority of signals received exhibited amplitude response in excess of 1 volt, indicating higher energy source signatures than those which were received at the low stress monitoring locations (Sites #1 and #2).

Figure 34 illustrates similar waveform data which was recorded and derived at the Site #5 transducer location, for the interval sampling period between November 13 - December 1, 1987. Very similar centre frequency and amplitude range data to that which was observed for the Site #4 installation was recorded at Site #5, as is shown in **Figures 33 and 34**.

In April, 1988, the Site #5 monitoring station was withdrawn from service due to limitaions in access created by backfilling activity. It was planned by Dension to completely fill the open pillar zones North of the 26 Garage in order to provide additional ground support for this mine region. In order to accomplish this, the 24962 access drift and all entry drifts to the pillar transducer Site were required to be

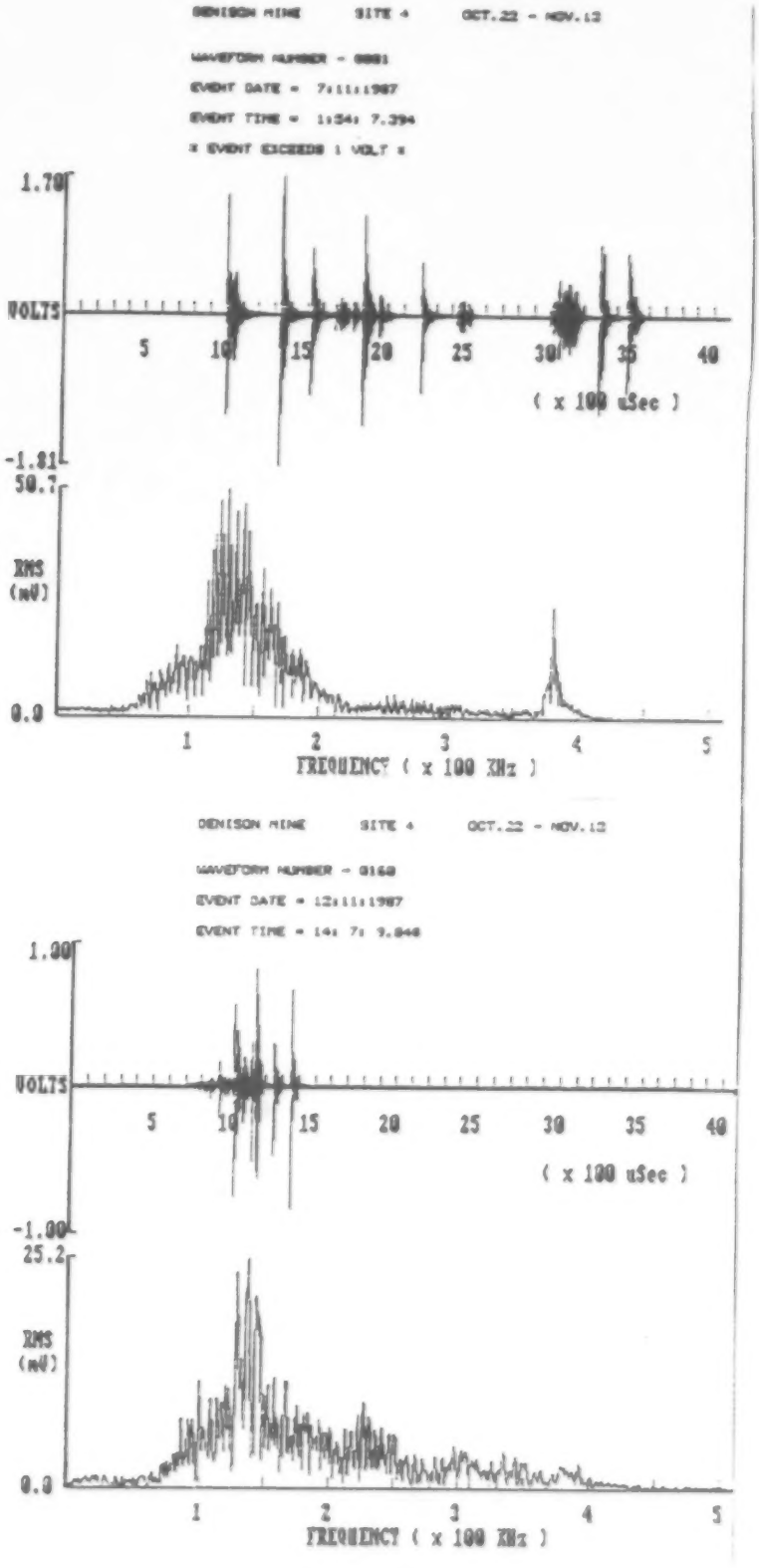

FIGURE 33 - Amplitude and Frequency Domain Plots of Typical Acoustic Waveforms Monitored at Site #4 (October - November, 1987)

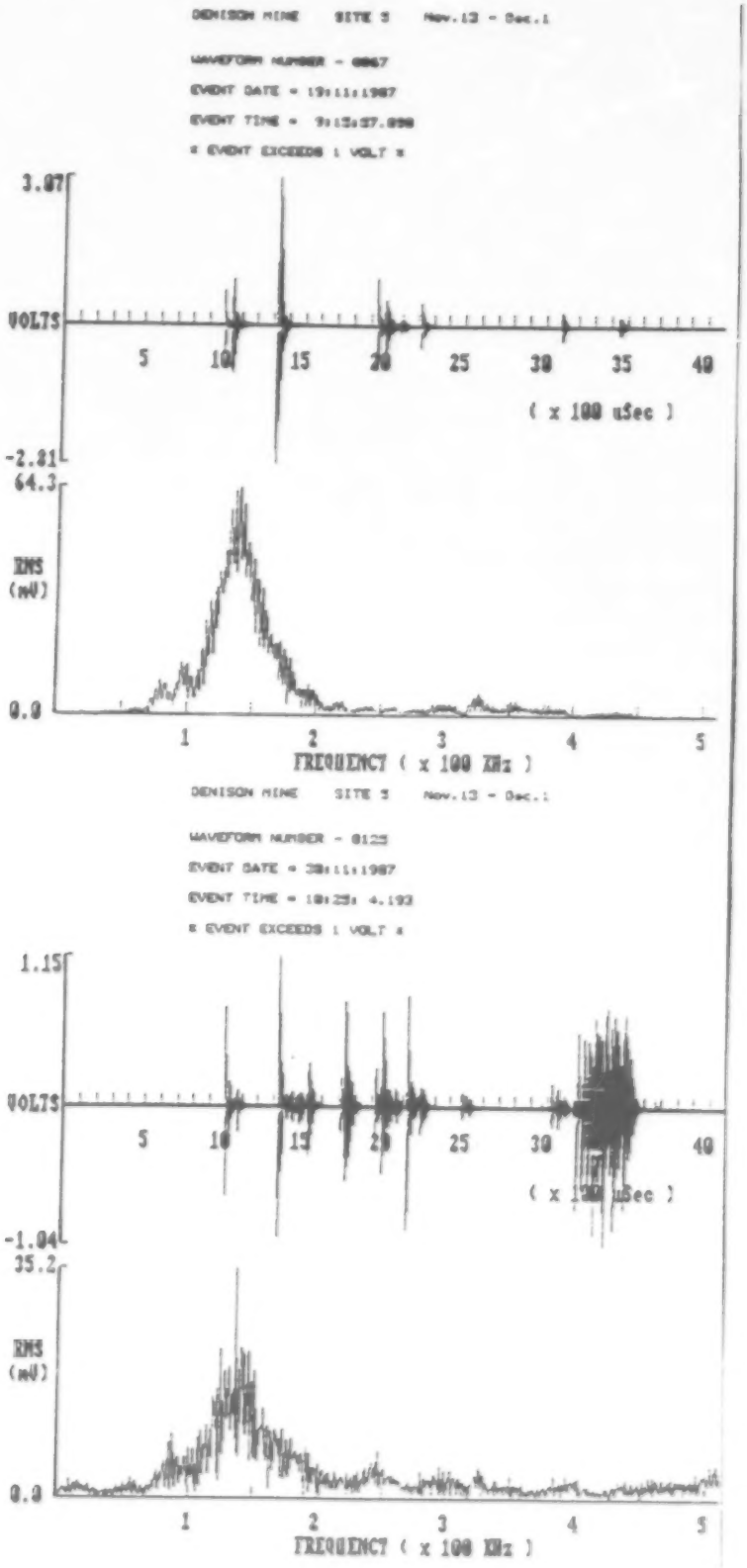

FIGURE 34 - Amplitude and Frequency Domain Plots of Typical Acoustic Waveforms Monitored at Site #5 (October - November, 1987)

completely backfilled and sealed from access. Accordingly, all monitoring and installation hardware associated with the Site #5 station were removed during April, 1988.

4.3 - Site #6 (Medium Stress Zone)

Initial microseismic monitoring activity was initiated at the location of Sites #6 (35022 rib pillar) during July, 1987. A four month program of acoustic monitoring and precursor assessment, lasting between July 29- November 4, 1987, was performed at this location until cessation of acoustic activity coincident with destressing of adjacent rib pillars occurred. The monitoring process at Site #6, as at the other Sites which have been monitored in the long term, was occasionally interrupted by hardware problems and power failures.

This site was selected, following consultation with Denison staff, to be of primary interest during the course of the in-situ acoustic monitoring program due to its location adjacent to rib pillar extraction operations. It was thought that stress changes developing both within the monitored (35022) and mined (35024) pillars, coincident with blasting and ore extraction operations, would induce noticeable changes in acoustic activity and waveform character. Both measured and theoretically-modelled stress conditions existing within this pillar area were shown (Section 3.2.4) to increase substantially with changes in the pillar support geometry.

Considerable microseismic activity was accordingly monitored to develop coincident with blasting activity and theorized changes in stress conditions. Precursor features, characteristic of such waveforms, were derived from a total of 1913 waveforms which were captured during the 99 day monitoring period. Monitoring was occasionally interrupted, the most significant interval being between days 74 and 83 when power shutdowns necessitated by conveyor repairs were in effect. Of particular interest to the project is the fact that, at day 85 of the monitoring cycle at Site #6, waveform activity associated with a rockburst event was recorded when local pillar failure occurred adjacent to the acoustic transducer.

The range of detection of the high frequency microseismic transducers has important implications in terms of precursor analysis. The system was originally designed to monitor local acoustic activity within seismically active or potentially unstable mine areas. Arrival time analysis performed by Madsen [10] and Bullock [13] has indicated that the maximum range of source detection for the existing system varies between 5 - 7 metres. Since failure of nearby pillar material will transfer stress to rock within 5 metres of the transducer site, the monitoring system will record anomalous stress and microseismic activity even though the actual zone of rock failure occurs outside the 5 metre sensing zone. Sensors are therefore capable of monitoring stress buildup and rock failure in a larger "zone of influence" around the monitoring site. Monitoring tests at the Denison Mine have provided some evidence of the extent of this zone of influence. The rockburst event occurred at a distance approximately 20 metres from the transducer location, yet the monitoring network was capable of indicating anomalous microseismic activity

prior to the event. The system has therefore been shown capable of monitoring areas whose extent will be determined by the range of influence of load transfer from nearby pillars.

Event rates at the Site #6 monitoring location were evaluated over a variety of time intervals, of which the 6 hour interval plots were shown to provide the most sensitive event rate fluctuation capability. A graphical summary of 6 hour event rate versus interval period is illustrated in **Figure 35** for the entire period of monitoring at Site #6. The trends in event rate are clear and demonstrate that peaks in event rate activity within the 35022 pillar occurred simultaneous with pillar recovery blasts taking place within the 35024 pillar. Higher peaks generally occurred coincident with the taking of pillar slash rounds, which yielded higher tonnage recovery that normal pilot rounds. As mining was seen to progress up dip towards the transducer location, event rate activity was observed to increase in a general exponential fashion. From July 29th to August 13th, a slow increase in event rate was demonstrated, with average rates over this time interval approximating 2 per day. After August 13th, the event rate was observed to rise and to average over 10 events per day for the month of August. Factors contributing to such increases include increase in the rate of pillar blasting and lessening of the distance between the transducer site and the site of blasting. Since mining progressed up dip, towards the transducer location, propagating acoustic waves would have less distance to travel to the transducer and lower energy emissions could be captured due to lack of attenuation over such distances. On September 30th and October 8th, two anomalous rate conditions were monitored. Daily event rates of 73 and 188 were recorded to occur and to exist on occasions when simultaneous slash and pilot rounds were taken of the pillar. In each case, almost four times the normal rock tonnage was displaced during blasting. An attempt was also made to correlate increases in event rate with inferred changes in pillar stress which were modelled to occur about the transducer location. The change in stress condition, as modelled by MINTAB and approximated for post-yield conditions which would realize a higher pillar core stress, was related versus event rate activity, and is illustrated in **Figure 36**. Event rate activity was demonstrated to vary exponentially with cumulative pillar stress change; similarly, event rate activity was shown to vary linearly with respect to the cube of cumulative stress change. The equation which relates these two parameters, solely for Site #6 observations and the limited number of acoustic emissions recorded, is represented as:

$$\text{(Peak event rate per 6 hour time interval)} = 0.17\ (DSIG)^3$$

where: DSIG = cumulative change in pillar stress, (MPa)

An exception to this trend occurred between the 29th and 56th days of monitoring, during which no mining activity took place due to mine shutdown conditions. Event rates per day dropped below 10. With lack of mining activity, it is feasible that stress redistribution or transfer of pillar loads away from the

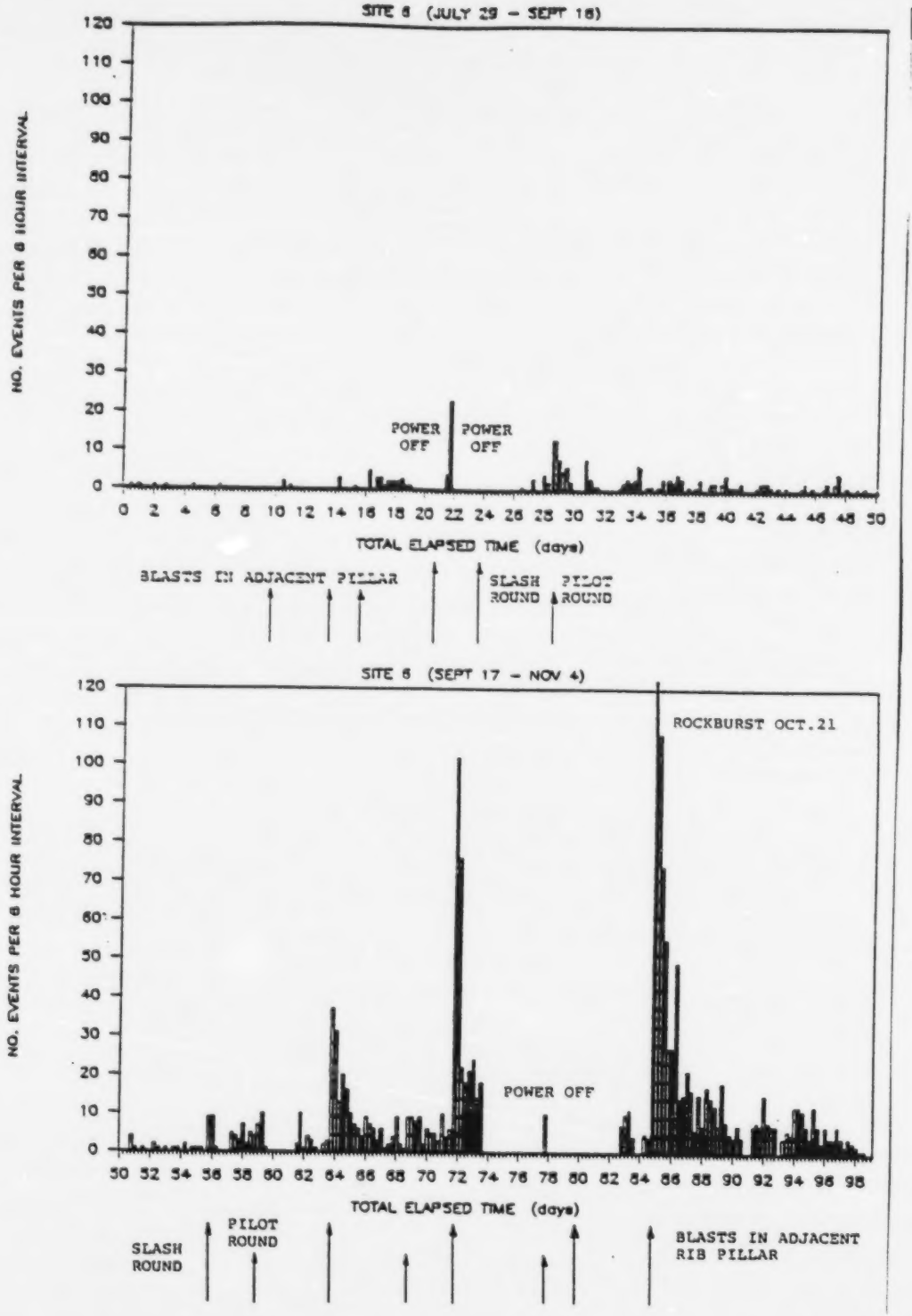

FIGURE 35 - Event Rate Activity versus Interval Time for Site #6 Monitoring Site (July 29 - November 4, 1987)

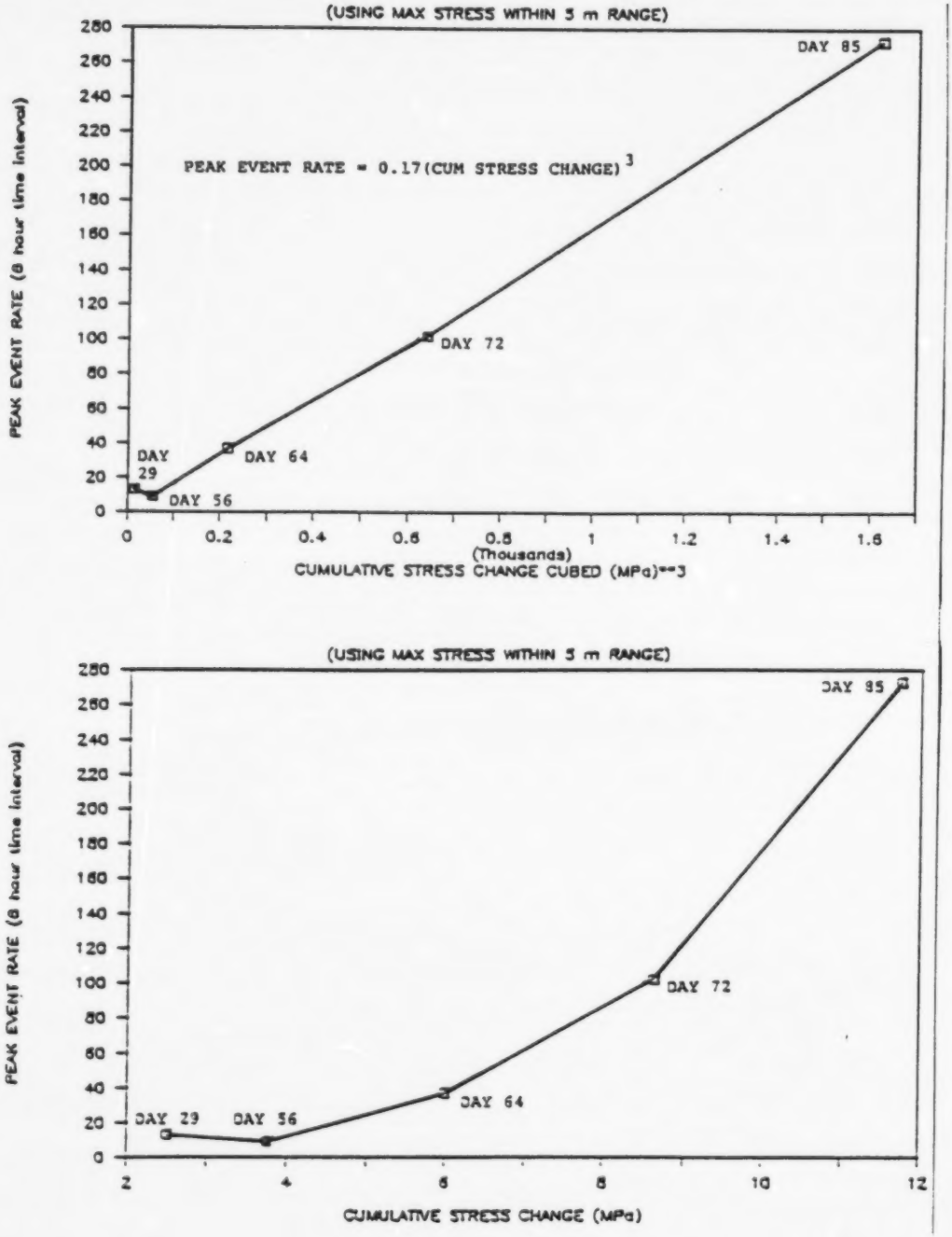

FIGURE 36 - Peak Event Rate Activity (Site #6) versus Cumulative Stress Change and (Cumulative Stress Change)3 Effects (July 29 - November 4, 1987)

monitoring site could have occurred. Immediately following resumption of mining substantial increases in activity rate were developed. During shutdown or periods of strike-induced inactivity at Site #6, the background activity rate of microseismic emissions approximated 7 events per 24 hour period. In general, however, the monitored peak event rate was shown to be a sensitive and consistent indicator of increasing stress at this Site. The rate of blasting also affected the daily event rate condition which was monitored. On August 7, a single blast induced an event rate rise to 4 events per day, lasting 2 days, following which the event rate term fell to zero. Between August 11 and 13, when two blasts were taken, the event rate rose to 12 events per day, and lasted for 7 days. After the first blast, stress would have been redistributed to the surrounding rock mass. In the second case, where additional blast energy was input to the rock in a short interval and possibly before the initial stress increment could be shed, the cumulative effect of increasing stress would result in higher event rate behaviour as well as an increased time frame over which the stress would be redistributed.

The most dramatic event rate activity occurred during the month of October, 1987. Significant event rate increases, from averages of 20 per day during the month of September, to averages approximating 300 per day in October, were recorded. Pillar blasts were taken on the fifth, eighth and fourteenth of this month, whereupon immediate event rate activity increases of over 200% compared to the background activity rates existing prior to the blasts were recorded. Event rate background noise and duration increased after each of these blasts, indicating that the ground near the monitoring site was becoming increasingly stressed.

On October 21, a slash round was blasted just prior to a rockburst event which was detected by the Denison MP-250 System to take place at 4:23 a.m. The result of this event was that approximately 50 tonnes of finely-broken muck was displaced from the back adjacent to a fault zone travelling through the Northeast corner of the 35024 pillar. Following the event, microseismic event rates were monitored to decrease over the next week to background levels approximating 10 per day.

Event rate monitoring may therefore provide a valid precursor to rockbursting phenomena. In this single recorded rockburst event, significant increases in rates preceded the actual rockburst failure. Such increases, along with increased event rate duration (length of time during which event rate activity is higher than background activity) may provide valuable precursor indications. Owing to a considerable lack of data concerning additional rockburst events during the term of in-situ measurement, no specific correlation between these parameters has been able to be developed.

Figure 37 illustrates a cumulative event rate plot versus time for the entire period of monitoring which took place at the Site #6 station. Generally linear behaviour is illustrated for the months of July, August and September, when low stress and event rate activity were measured to exist. In October, four major increments were demonstrated. On September 30, following simultaneous slash and pilot round blasting, an increase in event rate from 8 to 73 acoustic waveform arrivals per day was recorded. On October 7, for similar blasting conditions, the

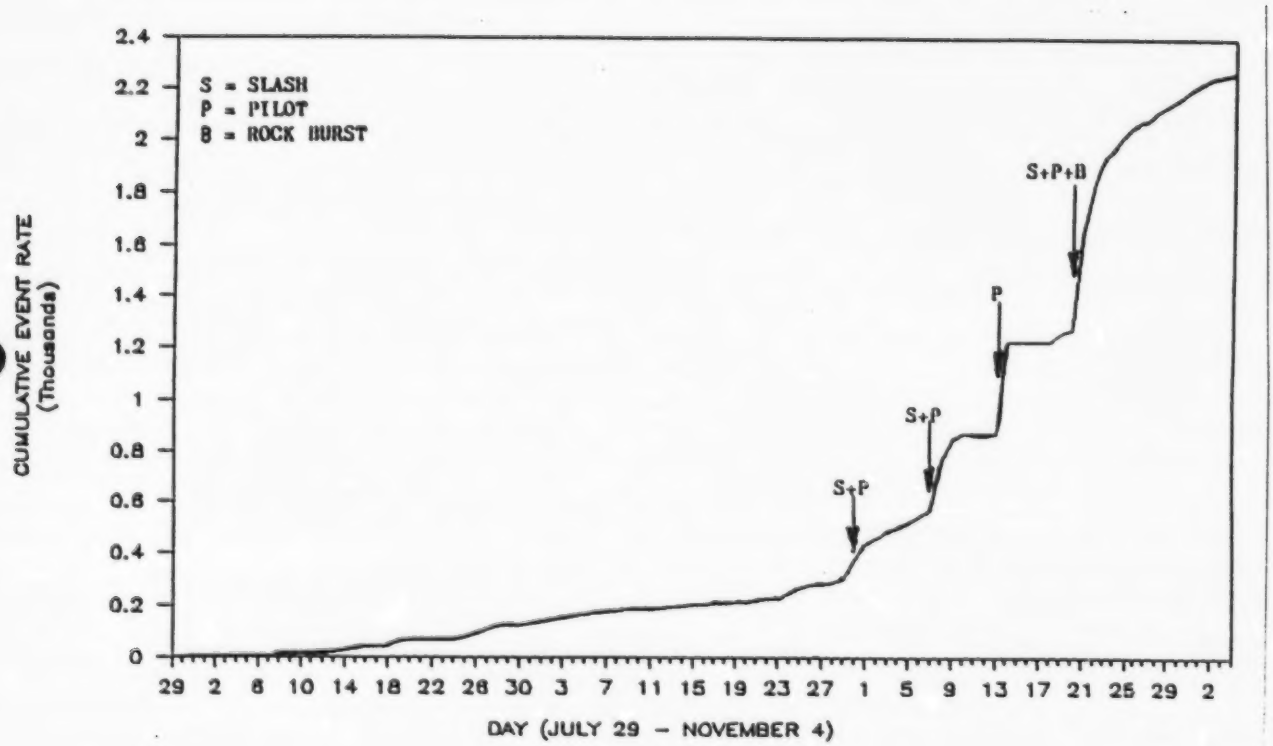

FIGURE 37 - Cumulative Event Rate versus Day for Site #6 Monitoring Site (July 29 - November 4, 1987)

event rates altered from 23 to 188 per day. On October 14, following a slash round and before a power failure condition cancelled monitoring operations, a rate increase to 355 events per day was observed. On October 21, rate activity changed from 15 to 384 per day.

The rate of event rate decay is also known to be inversely related to the magnitude of stress relative to the sample strength. A similar feature was evident in observed event rate data. As the stress level was shown to increase at Site #6 due to mining in the adjacent pillar, the rate of event decay after each new peak dropped. For example, the time required for the event rate to decrease to less than ten per 6 hour interval varied from 36 hours after the blast at dat 63 to 66 hours after the rockburst event (day 99). This feature would provide a quantitative indicator that the microseismic event rate takes longer to return to previous levels as the pillar stress approaches the rock strength, thus providing a measure of failure susceptibility of the rock.

The peak magnitude of microseismic emissions received can also be used to classify the relative intensity of events. In order to permit one of the principal study goals, attempts were made to correlate peak magnitude of emissions versus pillar stress at the various Site locations. The peak magnitude represents the maximum voltage value received from each microseismic waveform event which was produced by vibration of the piezoelectric transducer. For all Sites, the trigger voltage level at which recording was initiated was set at 0.098 volts; no calibration is or was available to relate transducer voltage output to conventional magnitude measurement of peak displacement. In Sections 4.1 and 4.2, displays of typical waveform signals received at Sites (1/2) and (4/5) were presented. A similar display of amplitude and frequency domain plots for typical microseismic waveform input, as measured at Site #6 during intervals leading up to and including the violent failure event, is presented in **Figure 38**. This Figure illustrates a typical event which occurred one minute before the rockburst as well as the burst event as it was measured at Site #6. The distribution of peak magnitude values for all waveforms received at the Site #6 installation are illustrated in **Figure 39**. In this Figure, both daily average peak magnitude data as well as a frequency histogram of total magnitude response is indicated. The sum of waveform data over the entire four month monitoring interval was shown to be lognormally distributed, to have an average magnitude of 0.72 volts and to present a maximum amplitude display of 8.57 volts (at the time of rockburst occurrence).

Anomalous peak magnitude response, shown in **Figure 39**, was indicated to occur on several occasions, though no significant correlation between amplitude and event rate parameters was able to be established. This would indicate either that peak magnitude effects act independent of other precursor effects induced by rock stress or that magnitude anomalies respond to conditions other than stress-related changes. The present inability to determine why anomalies occur at various times is not as important as the requirement to use such anomalous behaviour to provide indication of impending stress change which may ultimately lead to rockbursting. In order to provide such capabilities, other rockburst events would have to be captured

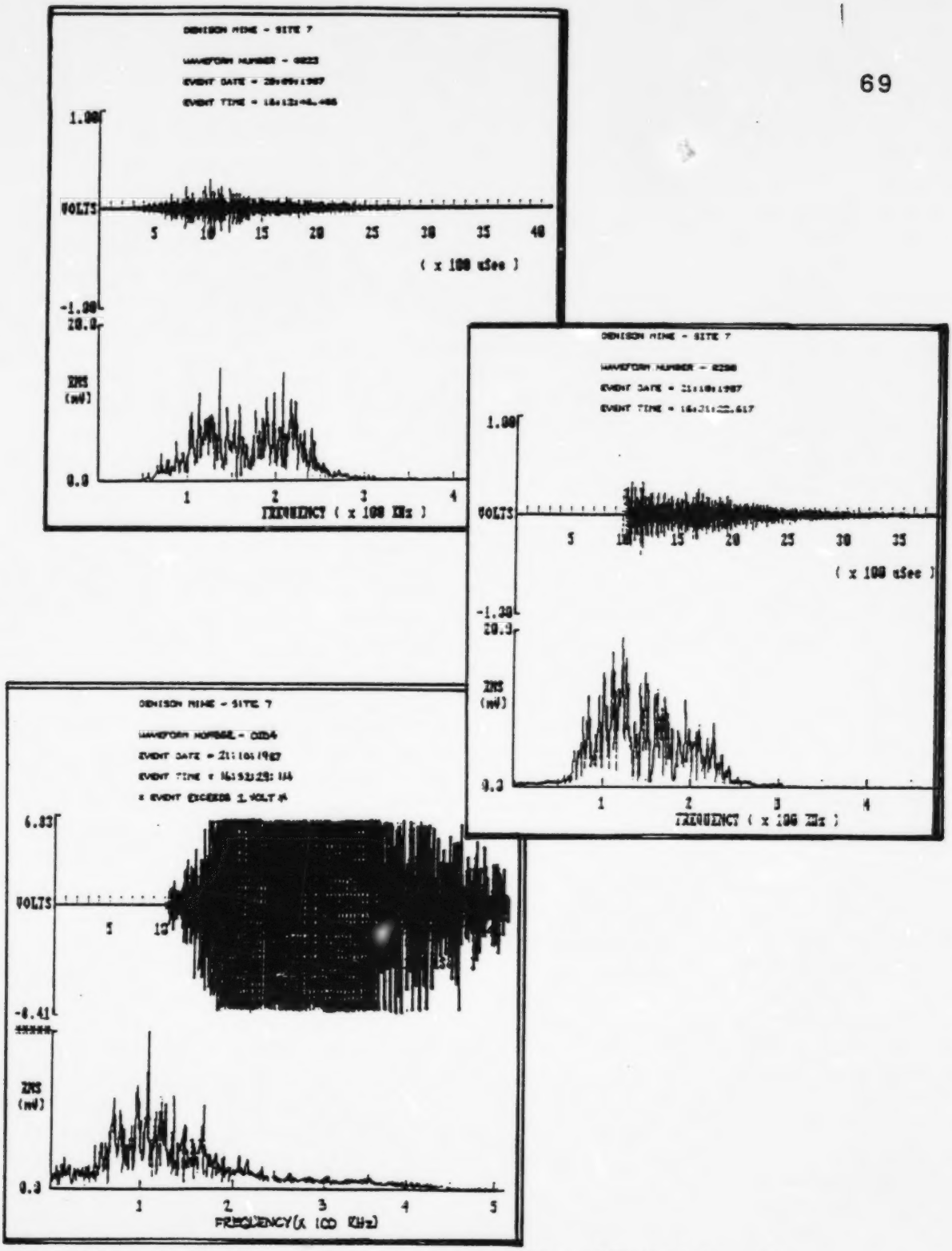

FIGURE 38 - Amplitude and Frequency Domain Plots of Typical Acoustic Waveforms Monitored at Site #6 (July - November, 1987)

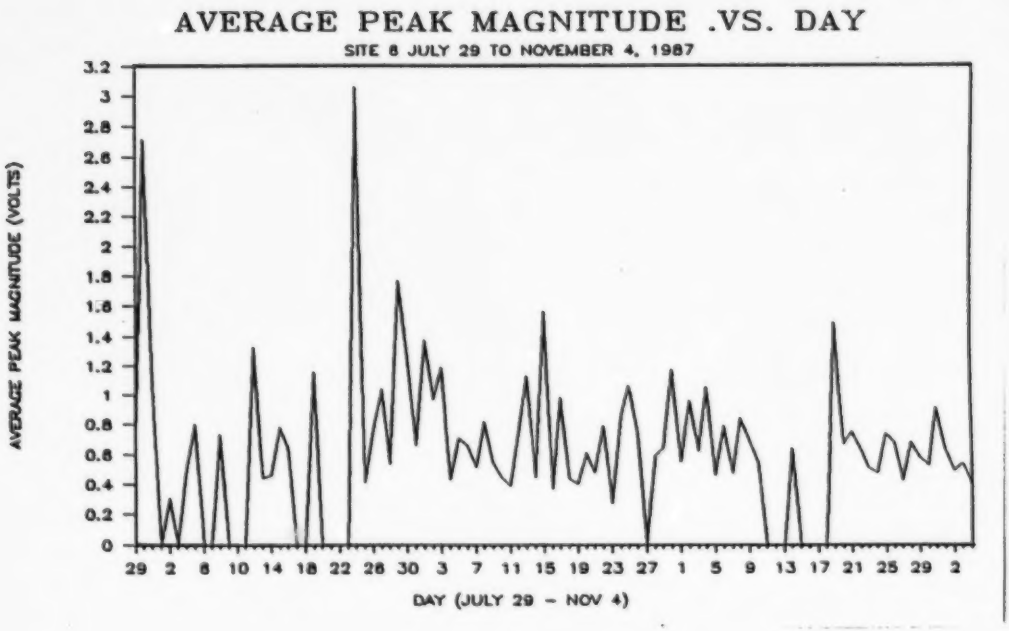

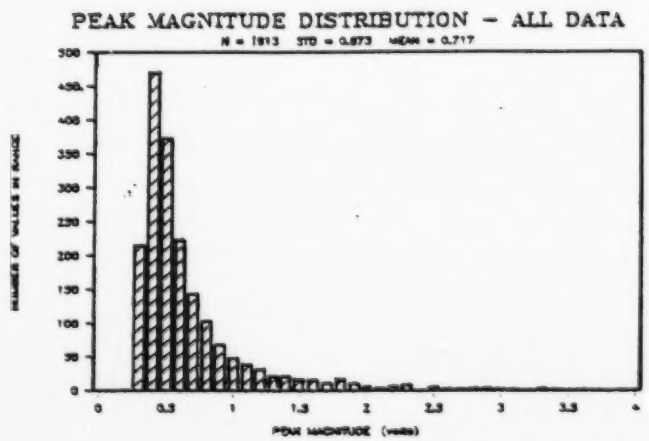

FIGURE 39 - Peak Magnitude versus Time Summary and Frequency Distribution of Total Magnitude Data for Site #6 Monitoring Location

before any valid conclusions could be made concerning the effects of peak magnitudes generated by rapid, high energy stress changes.

A summary of cumulative peak magnitude information versus interval time between the start of monitoring to just after the rockburst event, as illustrated in **Figure 40**, demonstrates a well defined trend. The trend was also shown to continue past the time at which rockbursting occurred, indicating that event peak magnitude data may be independent of the energy which is emitted by microseismic event sources. The energy output associated with rockbursting will certainly be anomalous and large, yet, for the one case which was observed, no anomalous peak magnitude microseismic response was recorded. In order to provide positive conclusions concerning the validity of peak magnitude data as a rockburst precursor signal, more data from similar event conditions will have to be obtained.

An additional parameter which was examined as a possible precursor for high stress or rockburst prediction capability was the "b" value condition. On the basis of seismological review [14], it has been found that the magnitude of both seismic and microseismic events fits the general equation:

$$\text{Log}(N) = a - b(M)$$

where: N = number of events occurring with a magnitude of (M) or greater
M = magnitude of seismic event

The "b" value can be defined to be the slope of the curve which is generated when the log of cumulative events in the time domain is plotted versus the log of peak magnitude averaged over the same time domain. Work which has been conducted [10], [13], [14] has indicated that larger "b" values generally correspond to lower peak magnitude events and are indicative of rock failure which occurs as the result of sliding along existing fracture plane surfaces. Lower "b" values generally correspond to higher peak magnitude events and are indicative of events produced through formation of new fracture surfaces in the rock mass.

Typical "b" value analysis plots are illustrated in **Figure 41** to demonstrate the sum of all waveform data received at Site #6 as well as both results occurring prior to and after the rockburst event on October 21. The "b" value conditions both prior to and after the rockburst event correspond to microseismic emissions obtained from two different stress regimes and were analyzed in order to assess variation in "b" value output versus site stress. The following values were used to classify the site stress conditions:

Low stress condition - (69.6 - 91.4) MPa within 5 metres of transducer for time interval between (July 29 - October 8,1987)

High stress condition - (75.8 - 97.1) MPa within 5 metres of transducer for time interval between (October 21 - November 3, 1987)

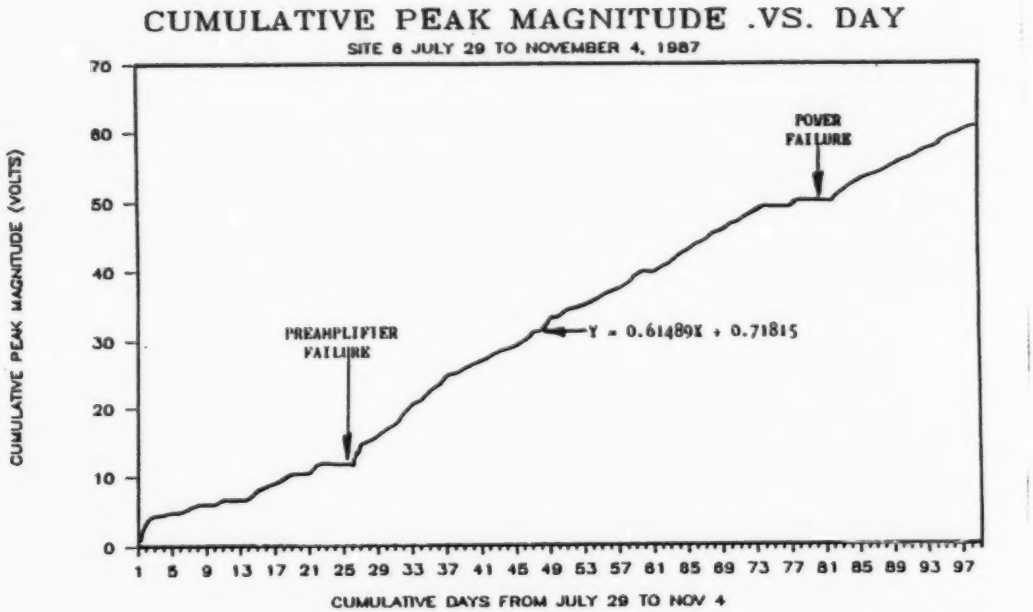
CUMULATIVE PEAK MAGNITUDE .VS. DAY
SITE 6 JULY 29 TO NOVEMBER 4, 1987
CUMULATIVE PEAK MAGNITUDE (VOLTS)
70
60
50
40
30
20
10
0
POWER FAILURE
PREAMPLIFIER FAILURE
Y = 0.61489X + 0.71815
1 5 9 13 17 21 25 29 33 37 41 45 49 53 57 61 65 69 73 77 81 85 89 93 97
CUMULATIVE DAYS FROM JULY 29 TO NOV 4

FIGURE 40 - Cumulative Peak Magnitude versus Interval Time for Microseismic Waveforms at Site #6 (July 29 - November 3, 1987)

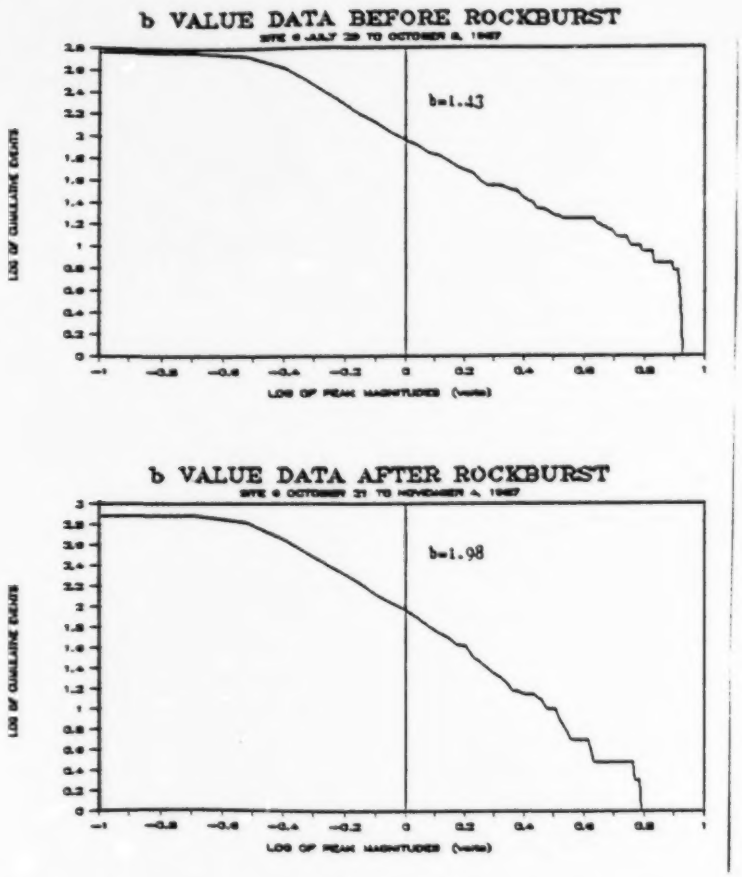

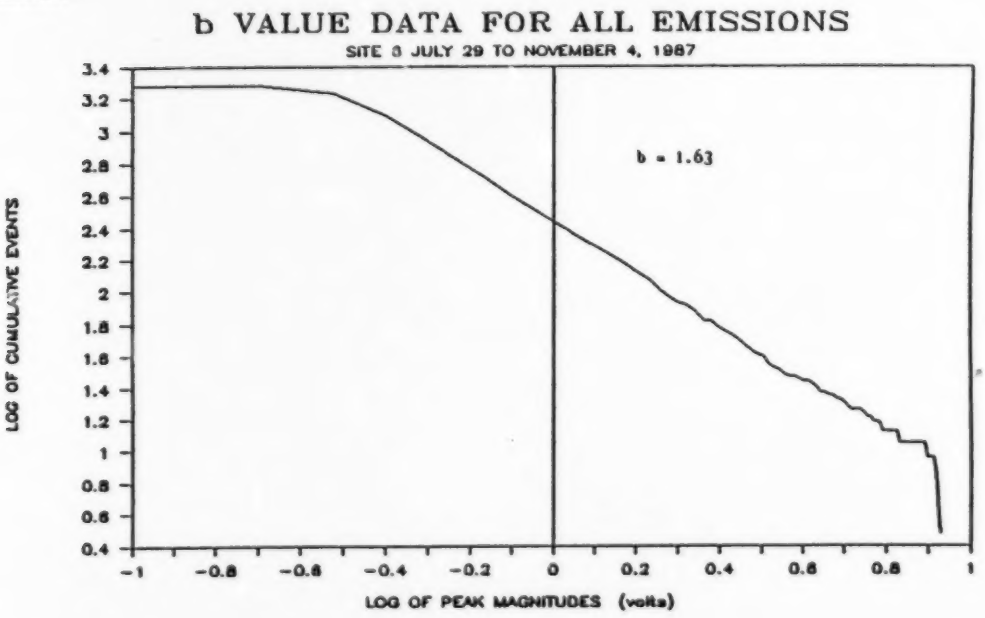

FIGURE 41 - "b" Value Analysis for Site #6 Waveform Data

The ranges of stress which were inferred were predicted on the basis of MINTAB-modelled data as well as post-yield stress increases occurring within the central rib pillar spans of the 35022 pillar structure.

On the basis of plotted data, the "b" value for the sum of microseismic data which was monitored at Site #6 (1913 events) was determined to approximate 1.63; for the pre-burst interval (low stress conditions), the similar "b" value was approximated to be 1.43; for the post-burst interval (high stress interval), the "b"value approximated 1.98. Such data indicates that the peak magnitude of events occurring after the rockburst were generally lower than for similar events existing prior to the burst, and that frictional sliding along existing fracture surfaces was the dominant source mechanism of microseismic events. Since a "b" value analysis can provide assistance in indicating the mechanism of rock deformation, it may also be useful as a precursor indication to rockbursting.

A general waveform trend towards lower "b" values would indicate the formation of new fracture surfaces within the rock mass acted upon by active ground stress, thus indicating possible rock instability. Higher "b" values would indicate that sliding failure along pre-existing fracture planes may be taking place, and that rockburst susceptibility is low. Such conditions were observed after the rockburst, where pillar stress release and fracture formation were theorized to have occurred. Because no major differences in pillar stress conditions at the monitoring site were indicated to exist both prior to and after the burst event, it would appear that "b" value parameters may be more suitable as indicators of rock deformation mechanisms than as rockburst indicators.

Analysis of the frequency content of microseismic emissions was also studied in detail as a means of developing precursor indication of ground stress and rockburst conditions. In studies previously conducted at the Denison Mine and within the Queen's Laboratories, it had been demonstrated that the frequency content of microseismic emissions exhibits some measure of dependence with the rock stress state. In intact rock, it has been theorized that stress-induced fracturing yields high frequency acoustic output resulting from formation of new microfractures or cracks. As rock stresses approach a failure condition, larger microfractures will be produced which tend to generate lower frequency events coincident with propagation of larger cracks and sliding deformation along these crack surfaces. At near failure conditions, both the large size and great density of cracks which are produced within the rock mass would tend to filter out the high frequency components of microseismic emissions which are typically being monitored by the system equipment. With the present state of monitoring at Denison, insufficient and limited evidence from three monitoring Sites has been obtained with which to make judgement concerning trends in frequency shift as a precursor signal to rockbursting.

The centre frequency of a microseismic emission is that frequency which divides the area beneath a waveform frequency spectrum into two equal halves. Variation in centre frequency data was used to infer trends in frequency shift versus stress level existing. The equipment adopted for the Denison study was capable of

monitoring frequency input up to 500 kHz, though frequency data above 350 kHz was known to be distorted by the low pass filtering system that was adopted to screen data. On the basis of in-situ observations, it was also shown that little variation in waveform data at levels above 300 kHz occurred for all stress conditions known to exist. For this reason, input waveform data at frequencies existing above approximately 280 kHz was excluded to minimize the complexity of and computational time involved in analysis. **Figure 42** provides a summary plot of daily averaged centre frequency information versus time over the entire sampling interval for Site #6. The normal distribution of all centre frequency values is illustrated in **Figure 43**. Similarly, the centre frequency information is plotted by normal distribution for two separate intervals (**Figures 44**) corresponding to periods when the pillar structure was considered to be acted upon by low stress (July 29 - October 8) and high stress conditions (October 21 - November 3). The sum of all data yields a mean centre frequency of 160.3 kHz with a standard deviation of 19.8 kHz. That portion of the data which corresponds to the low stress range yields a mean centre frequency of 164.3 kHz (standard deviation - 19.1 kHz) while the high stress data summary yields a mean centre frequency of 158.8 kHz (standard deviation - 21.0 kHz). The calculated stress difference which was determined to result in a centre frequency shift of approximately 5.5 kHz in waveform signal input corresponded to a 5.7 MPa stress increase within the pillar local to the transducer installation.

On this basis, Denison measurements indicated that the frequency content of acoustic signals may decrease as the local rock stress condition increases. During the low stress period, longer sampling intervals were necessary to produce reasonable sample populations sizes. During the high stress period, alternately, shorter sampling intervals were found to produce an equivalent number of acoustic events due to increases in the event rate activity. To reduce the effects of long term averaging, centre frequency distribution data was also analyzed for shorter periods corresponding to intervals immediately following pillar blasts, when sudden stress shifts (increases) normally produced high event rate activity. Six short interval summaries of centre frequency data versus stress condition are illustrated in **Figures 45, 46 and 47**. The designated pillar stress was derived as the maximum derived stress existing within 5 metres of the transducer location. The trend in centre frequency versus stress for these short interval summaries is illustrated in **Figure 48**. With the exception of the initial data point (anomalous due to the small sample population (6 samples) from which it was derived) a small decrease in centre frequency was demonstrated to occur with increasing stress. In all cases, the data trend lies within the standard deviation of the mean centre frequency. Accordingly, no significant or conclusive trend was indicated to exist which would demonstrate that consistent shifts in frequency output of waveforms correlate with stress.

Signal energy can be calculated for transducers using energy integration algorithms, though such values were not utilized as part of the Queen's approach due to deficiencies in the transducer manufacturer's calibration procedures. A measure of signal energy, called energy sum, was, however, calculated in the frequency domain by summing up the RMS voltage magnitude values. Though not

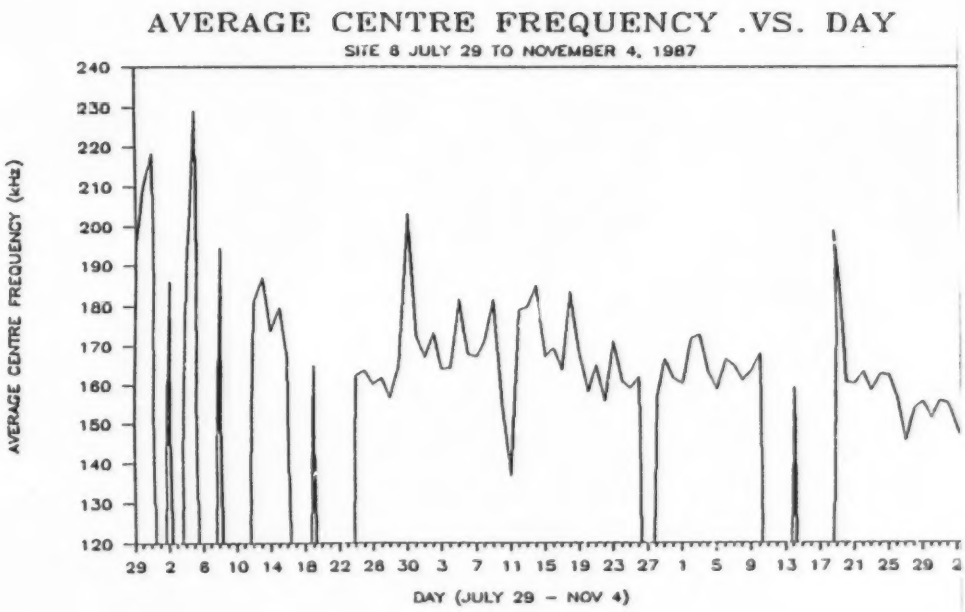

FIGURE 42 - Average Centre Frequency versus Day (Site #6) (13)

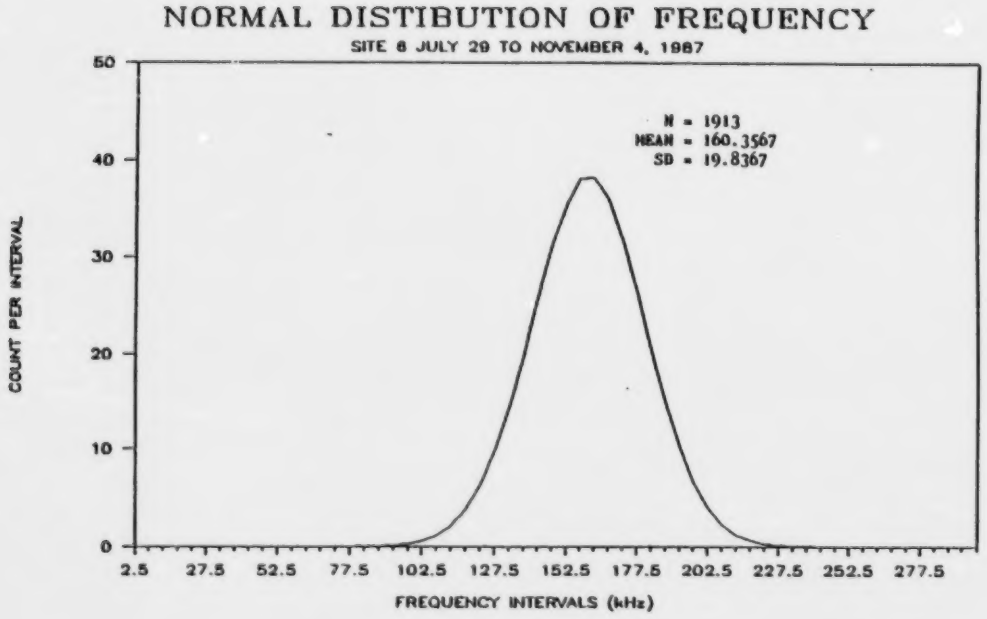

FIGURE 43 - Normal Distribution Plot of Centre Frequencies for Site #6 (13)

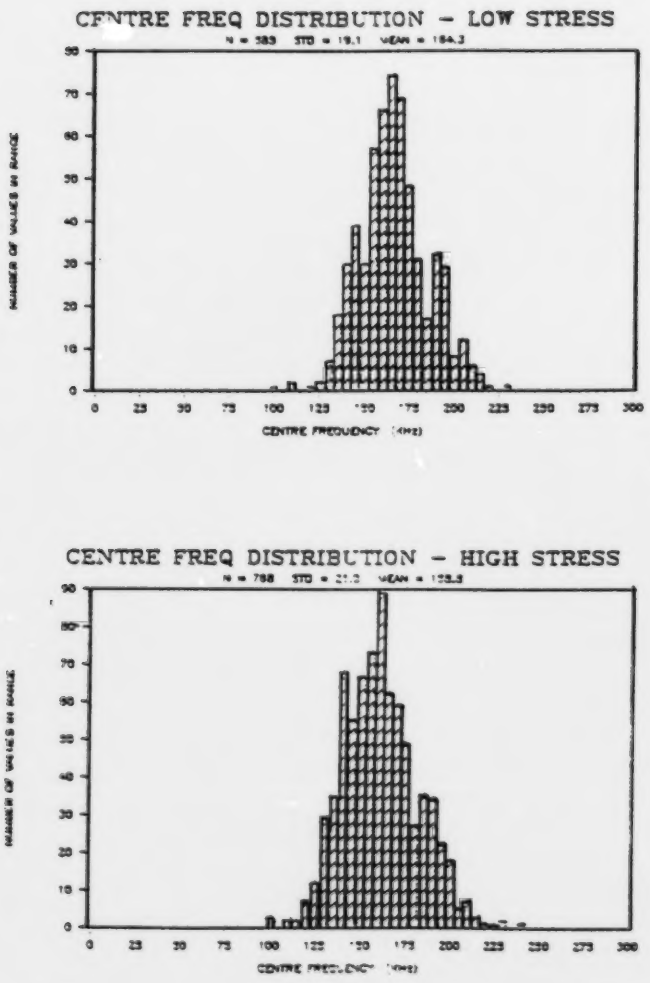

FIGURE 44 - Centre Frequency Distribution For Low and High Stress Interval Monitoring Periods at Site #6 (10)

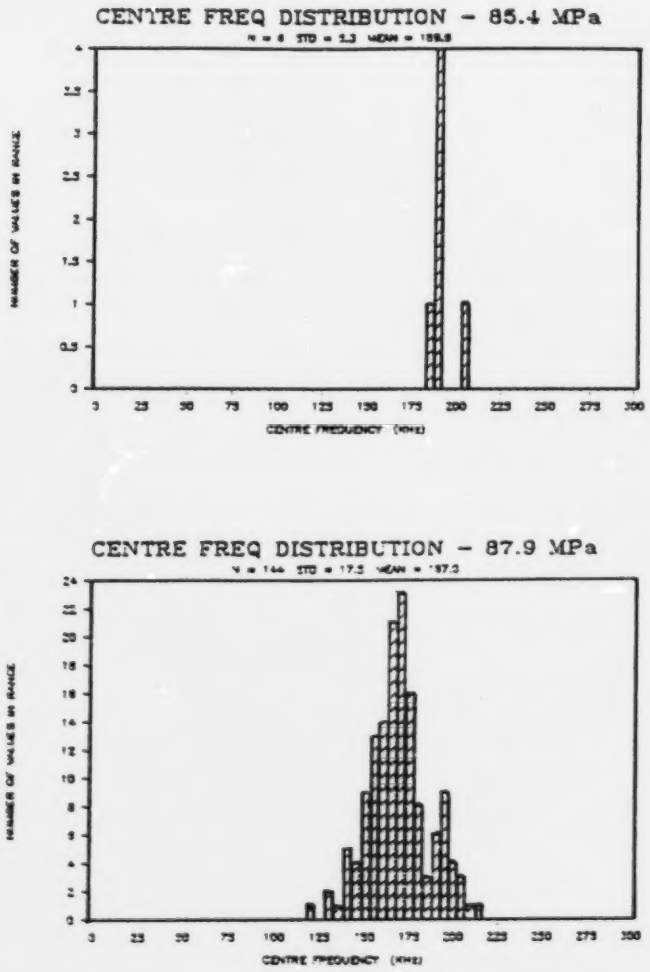

FIGURE 45 - Centre Frequency Distribution for Low Stress Ranges at Site #6 (10)

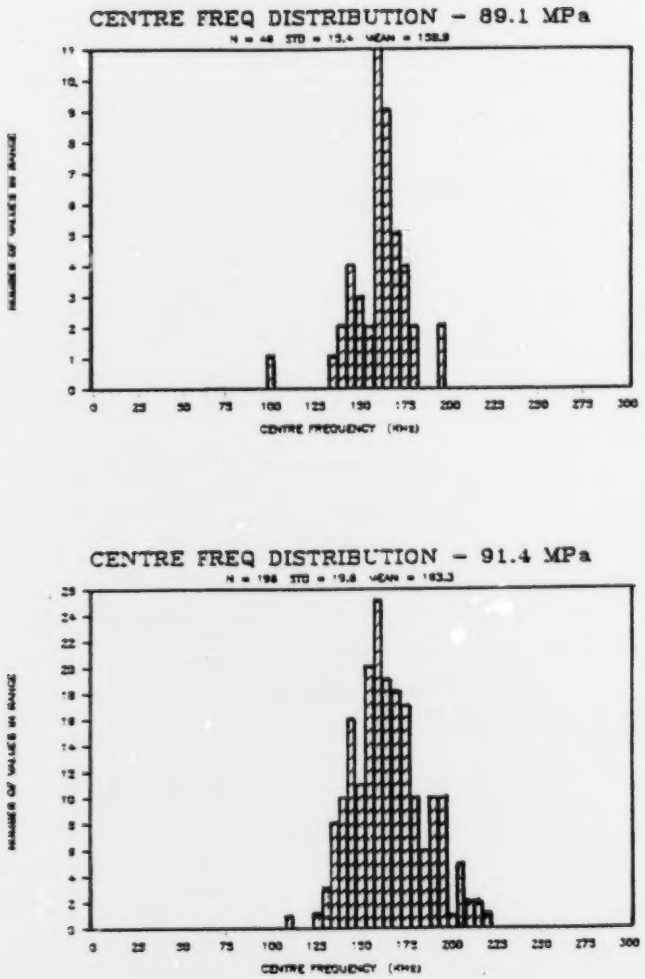

FIGURE 46 - Centre Frequency Distribution for Medium Stress Ranges at Site #6 (10)

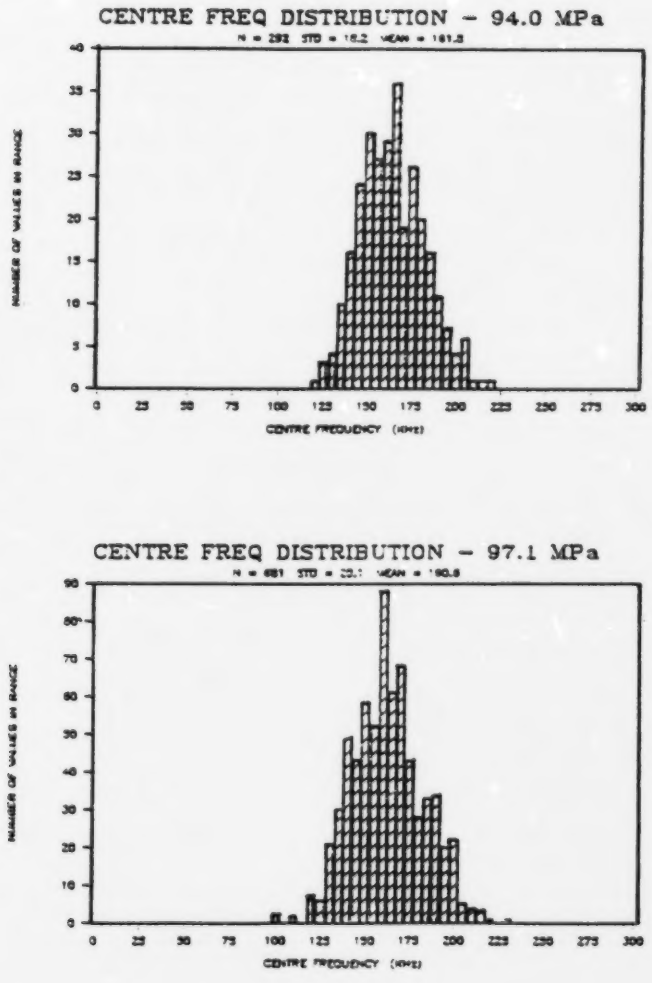

FIGURE 47 - Centre Frequency Distribution for High Stress Ranges at Site #6 (10)

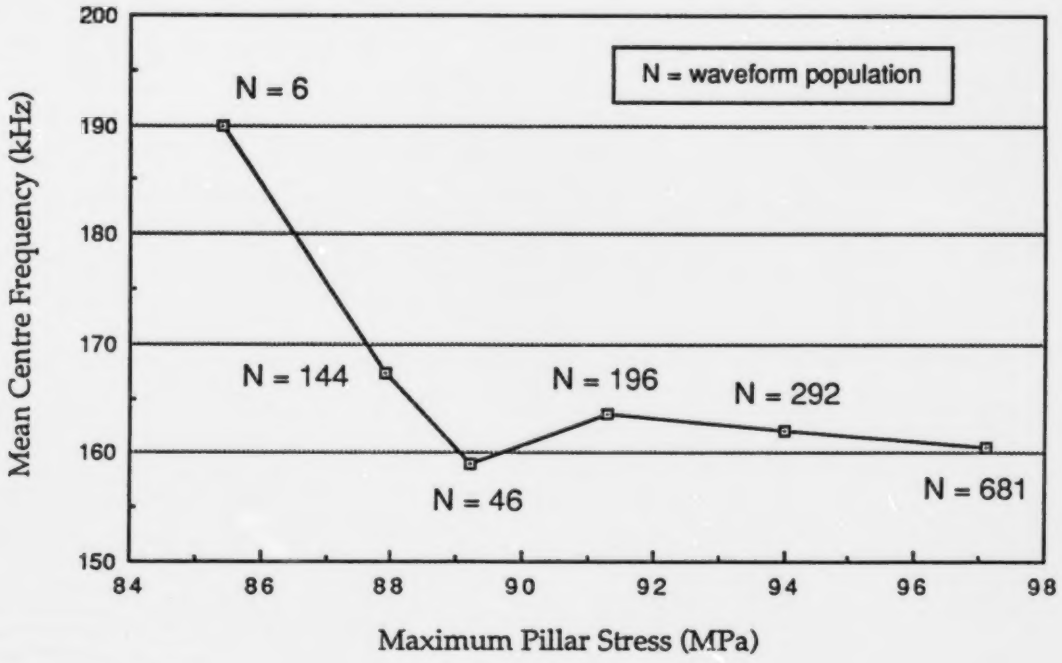

FIGURE 48 - Mean Centre Frequency versus Modelled Pillar Stress Condition for Site #6 (10)

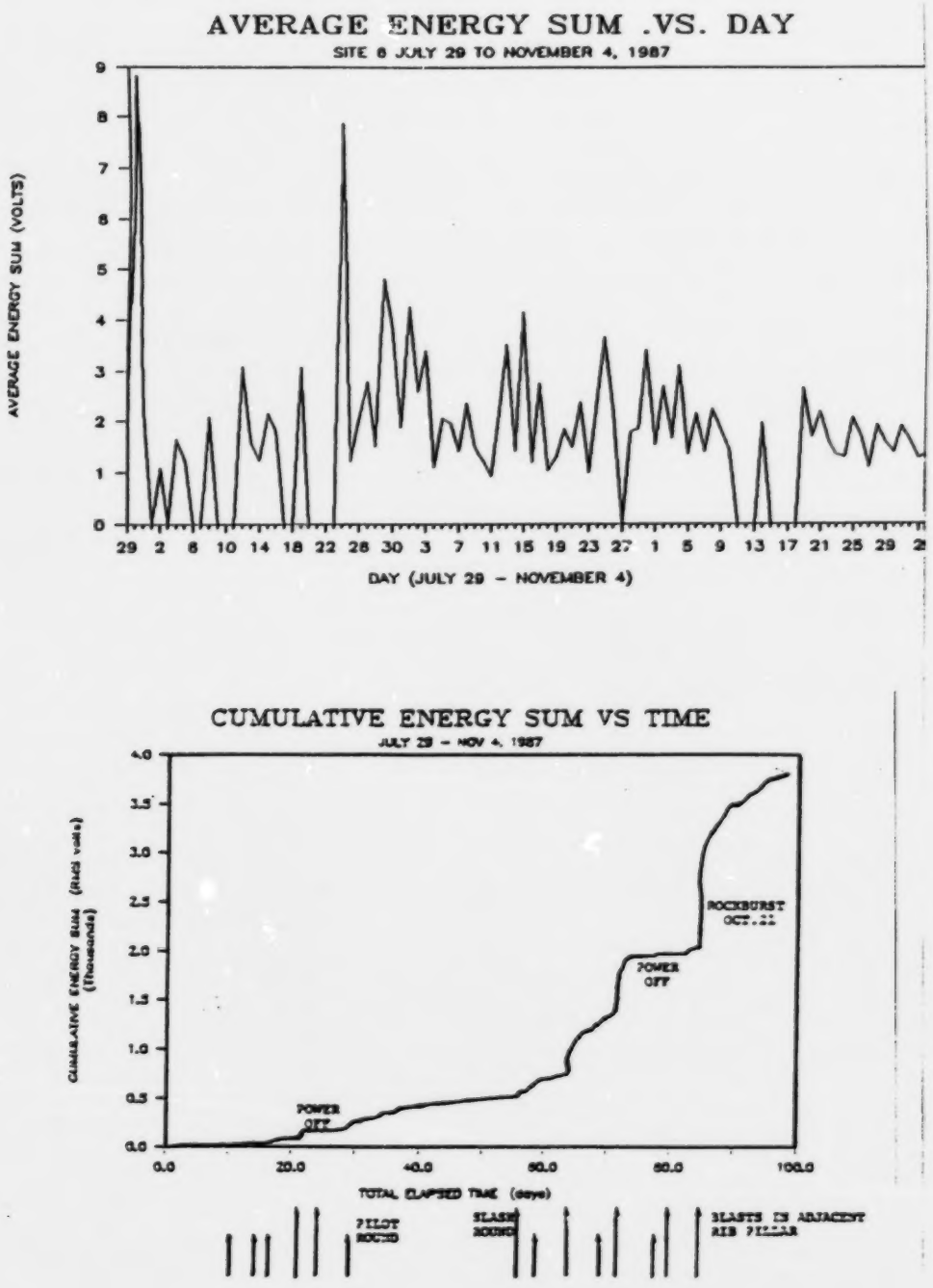
AVERAGE ENERGY SUM .VS. DAY
SITE 6 JULY 29 TO NOVEMBER 4, 1987
AVERAGE ENERGY SUM (VOLTS)
0 1 2 3 4 5 6 7 8 9
29 2 6 10 14 18 22 26 30 3 7 11 15 19 23 27 1 5 9 13 17 21 25 29
DAY (JULY 29 - NOVEMBER 4)
CUMULATIVE ENERGY SUM VS TIME
JULY 29 - NOV 4, 1987
CUMULATIVE ENERGY SUM (Root volts) (Thousands)
0.0 0.5 1.0 1.5 2.0 2.5 3.0 3.5 4.0
0.0 20.0 40.0 60.0 80.0 100.0
TOTAL ELAPSED TIME (days)
POWER OFF
POWER OFF
ROCKBURST OCT. 21
PILOT ROUND
SLASH ROUND
SLASHES IN ADJACENT RIB PILLAR

FIGURE 49 - Average and Cumulative Energy Sum versus Time for Site #6 Monitoring Site (10), (13)

a true measure of energy contained in each microseismic emission, the sum values were utilized as features in pattern recognition analysis to provide evaluation of precursor behaviour of acoustic signals. Past research [15] has shown that the rate of energy release can be closely related to seismicity and the incidence of damage within mines. If such findings can be similarly applied to the Denison observations, then higher energy release rates observed through microseismic emission analysis should provide indication of greater rockburst potential. **Figure 49** illustrates both average energy sum and cumulative energy sum data versus time for all microseismic data which was observed at Site #6. The energy sum was shown to closely follow average peak magnitude data trends, indicating that these two features are dependent upon similar emission parameters. The cumulative sum plot evidences a strong correlation with pillar recovery operations, where large sum changes occur coincident with pillar slash and pilot extractions. The greatest increase in energy occurred coincident with the rockburst event, which obviously induced a significant release of seismic energy into the monitored rock mass.

The rate of energy release indicated by microseismic emission capture was demonstrated by taking the slope of the cumulative energy sum versus time graph. From observation, three phases of time dependent rate effects were demonstrated to occur following pillar blasts, these being:

-Phase 1 - instantaneous stress shock coincident with stress transfer to the monitored rock mass

-Phase 2 - short term stress readjustment occurs as pillar stresses approach equilibrium, and

-Phase 3 - long term energy release occurring in a static stress field

The phases of energy release indicate the process of stress redistribution between the pillar which was being mined and the pillar which was being monitored. During the first phase, occurring effectively instantaneously during the blast, the greatest energy quantity is released corresponding to the largest amount of rock deformation taking place within the mined pillar. Phase approximates a stress readjustment period as the rock mass gradually returns to a condition of stress equilibrium (dynamic to static conditions). In this phase, the energy release rate gradually decreases as the amount of rock deformation decreases. Phase 3 effects model stable release rates of energy, typical of long term, static stress conditions in the rock.

As the pillar stress was seen to gradually increase with each subsequent blast, the rock mass was shown to require longer time intervals to reach a Phase 3 condition (stress equilibrium) following each blast; from **Figure 49**, this interval period was seen to alter from approximately 2 days, after the blast taken on day 64 of monitoring, to 4 days, following the rockburst event.

Similarly, during Phase 2 behaviour, slopes of the energy release rate plots were shown to increase for each subsequent slash blast taken prior to the rockburst. Such behaviour may prove to be a valid indicator of characteristic stress conditions relative to known rock strength. As a check on this information, and based on empirical pillar strength estimates for the Elliot Lake region [16], Phase 2 slope data

was plotted versus the (pillar stress/pillar strength) ratio, and is shown in **Figure 50.**

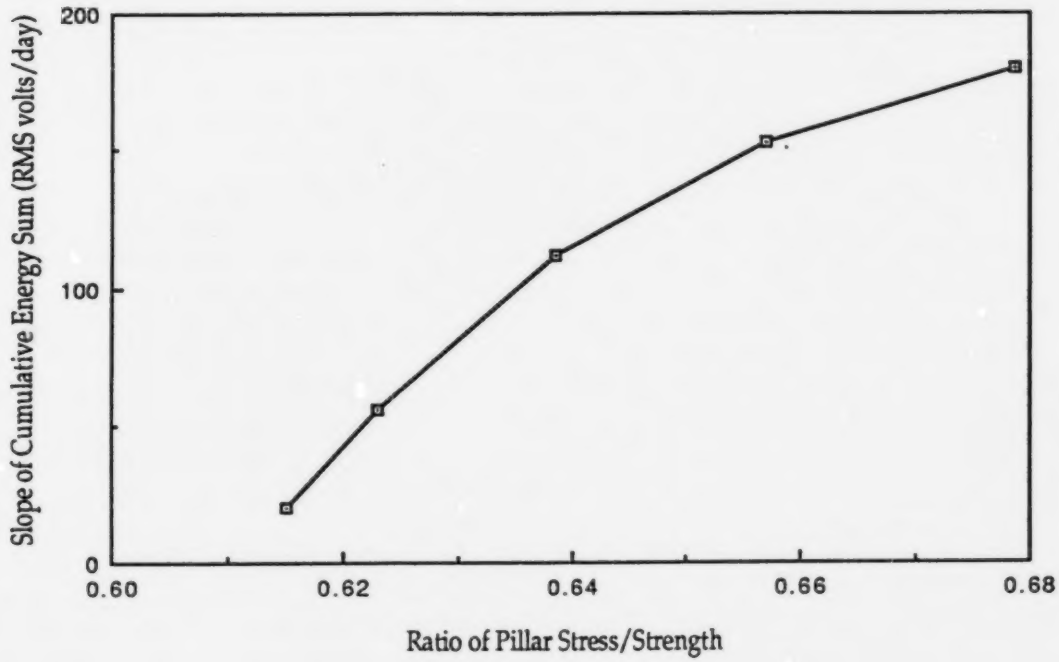

FIGURE 50 - Slope of Phase 2 Energy Release Rate Curve versus Ratio of (Pillar Stress/Pillar Strength) [13]

Although some trendwise behaviour does appear to be demonstrated, the relationship is not linear and is shown to be less sensitive to pillar stress prediction as the ultimate failure strength of the rock is approached. Based on such data, the measured slope values of energy release rate curves would not be well suited for use in rockburst precursor analysis.

5.0 Pattern Recognition Assessment

Much information has been previously been published [1], [2], [3], [4], [10], [13] concerning pattern recognition as a tool to be used in predicting stress conditions within rock based solely on evaluation of characteristic waveform features. Where accurate prediction of in-situ stress parameters may be effected, it has been proposed that rockburst potential may also be predicted.

The orthogonal pattern recognition technique was selected for use by the Queen's group [13] based both upon the accuracy and speed of analysis of waveform features. The technique was used to classify groups of waveforms from differing stress regimes, monitored in-situ over the period of field research. When incorporated into the QSTESS program, and as each incoming waveform is received, the recognition system is designed to instantly classify each waveform with regard to the stress regime from which it originated.

Pattern recognition analysis of data which as acquired at the Denison Mine was limited, in large part, to those waveforms which were collected at the Site #6 monitoring station, largely because of the small and limited number of waveforms which were received at all other Sites. Data which was applied to recognition review was arbitrarily grouped into five data sets, by data of acquisition, and two classes (Class 1 - low stress; Class 2 - high stress) as detailed in the following:

Data Set Number	Centre Interval Date	Number of Waveforms	MINTAB Stress (MPa)	Stress Difference versus Class average shown
1 (Class 1)	July 1	52	62.0	-1.7 MPa
2 (Class 1)	August 26	247	63.7	0.0 MPa
3 (Class 1)	September 22	610	64.5	+0.8 MPa
4 (Class 2)	October 8	681	68.4	-0.8 MPa
5 (Class 2)	October 21	381	69.2	0.0 MPa

In training the recognition program, waveforms from data sets #2 and #5 were utilized to set average stress magnitude conditions for each of Classes 1 and 2. Data sets 1, 2 and 3 were chosen as Class 1 waveforms since the rock stress conditions from which each originated were less than the stress average for Class 1 and Class 2 (66.5 MPa). Data sets 4 and 5 were chosen as Class 2 waveforms since the rock stress conditions characteristic of each were greater than the average of Class 1 and Class 2 (66.5 MPa).

Data sets were tested to determine whether they would be placed by the recognition program into the correct stress Class. In order to test, a base data set of

100 known waveforms from known stress regimes was selected. For Class 1 data, waveforms acquired during the end of August (August 28), for which average ground stresses approximating 63.7 MPa existed, were utilized. For Class 2 data, waveforms acquired between the date of rockbursting and just after (October 21 - 23), for which average ground stresses approximating 69.2 MPa existed, were utilized. Class 1 data was therefore characteristic of pre-burst stress conditions, while Class 2 data was characteristic of burst and post-burst conditions. The base data set upon which classification was to be generated contained two classes of information, each derived from rock exhibiting a 5.5 MPa stress difference and for which an average interclass stress condition of 66.5 MPa existed.

All waveform data sets were thereafter classified, and the results are illustrated in Table 9.

TABLE 9 - Pattern Recognition Analysis Results for Site #6 Data [13]

Data Set Number	Origin Stress (MPa)	Class	Percent Correctly Classified	Average Stress Difference (MPa)	Standard Deviation (MPa)
1	62.0	1	38 %	- 1.88	2.50
2	63.7	1	69 %	- 1.11	2.84
3	64.5	1	51 %	- 0.91	2.78
4	68.4	2	73 %	2.28	2.05
5	69.2	2	82 %	0.86	1.25

From the classification data, it was shown that Class 2 waveforms were correctly classified 77.5 % of the time, but that Class 1 waveforms classification accuracy averaged only 52.7 % (slightly better than random classification). In part, poor accuracy was due to the low number of waveforms acquired for set #1 data and to the small stress differences which were noted to exist between different data sets as well as between the two Class systems. Such small differences would create overlap between Classes. A classification accuracy of 51% would indicate that waveforms were being placed into Classes 1 and 2 in a random manner, showing that the system, as presently configured and with the limited data in hand, cannot accurately distinguish between classes with less than a 2 MPa difference in stress.

An important factor to consider when analyzing results is the standard deviation parameter. The pattern recognition program classifies incoming waveforms and assigns ideal values of (-1) if belonging to Class 1 and ideal values of (+1) if belonging to Class 2. Depending upon the goodness of fit, values may range from well below (-1) to well above (+1). In all Class 1 cases shown in Table 9, the

standard deviation range for each set of data was wider than for each set of Class 2 data.

For a variety of reasons, and predominantly because much larger data populations of waveform information are necessary to provide more accurate classification capability, the present classification analysis has been shown to be ineffective for its intended purpose of identifying local rock stress within the Denison Mine with great accuracy. For the limited numbers of Sites which were investigated as part of this study, it has been shown that variable waveform rates of acquisition exist, from very low (at low stress sites) to high (at high stress sites). Even though the total period of in-situ investigation was in excess of 18 months, an insufficient population of data was thought to be obtained with which effective comparison of data between Sites could be carried out. In work which had been performed previous to this research effort [2], also at the Denison Mine, acoustic emission classification analysis was able to correctly distinguish between waveforms arising from sites having stress differences of approximately 10 MPa with 75% accuracy. On the basis of emission monitoring at three distinct sites, the following results were obtained:

Site	Site Stress (Measured Vertical Stress Component, MPa)	Percent Waveforms Correctly Classified
A	40.9	72.2
B	50.0	91.1
C	60.0	63.0
	Average -	74.5

The high rate of classification success for mid-stress range waveform samples was thought to be due to masking effects between the sample populations, as is the case for this latest Denison study. As a test, Site B data was eliminated (middle stress class) and a two case classification analysis was performed. In this evaluation, successful waveform versus stress component prediction was made at a level of 90.7%. Such improvement occurred both because fewer classes of data needed to be examined and because the stress difference, at 20 MPa, would be sufficient to develop significant precursor variation in acoustic waveforms.

At Site #6, in the existing study, much smaller stress differences (less than 2 MPa increments) for each of the five sets of waveform data were modelled to exist. Because of such limited stress differences, the classification procedure would be realistically expected to generate much lower rates of success in waveform classification, as was indeed shown. The sum of waveform information obtained from Site #6 was then separated into two, distinct sets of data, these being the low stress set (July 29 - October 8; average magnitude 63.7 MPa) and the high stress set (October 21 - November 3; average magnitude 69.2 MPa). One hundred random waveforms were selected from each time interval set, corresponding to specific

stress conditions, and were used to train the pattern recognition system. When these same waveforms from each of the two time populations were again inputted and classified by the trained system, success rates approximating 88.5% were realized.

6.0 Conclusions and Recommendations

The Queen's microseismic system, in its present form, has shown to operate very effectively in terms of physical reliability under harsh environmental conditions. As well, based upon measured in-situ waveform results, the system pattern recognition feature has been demonstrated capable of detecting stress variation in the rock mass, during mining cycles, solely on the basis of waveform observation and characterization. Although such observations cannot presently be performed simultaneous with waveform acquisition, such stress trends are noticeable.

Valid precursor information contained in high frequency seismic waveform data appears to be highly dependent upon event rate parameters, as was evidenced prior to the rockburst event which took place adjacent to Site #6 on October 21, 1987. A daily plot of waveform occurrence clearly showed significant increases in event rate to precede the rockburst. Similarly, as local pillar stresses were modelled to increase, high event rate durations above measurable background levels also provided indication that event rate may be useful as a precursor indicator to stress change.

Neither peak magnitude nor cumulative peak magnitude parametric data for acoustic emissions appeared to correlate well with change in pillar stress condition. Changes in "b" value parameters prior to and after the high stress rockburst event did indicate some significant stress correlation effect to exist. Since the "b" value is inferred from peak magnitude information, this feature should not necessarily be deleted from pattern recognition evaluation at this time, and may prove viable in future studies.

Centre frequency information also shows some level of correlation versus stress condition existing within rock, though not greatly significant.

Energy sum and waveform duration variables are related to the energy released by acoustic emission processes. That is, the greater the energy released from an event, the greater the energy sum will be, irrespective of the nature of the emission (either creation of new microfractures or sliding along pre-existing microfractures). Waveform duration was indicated to be a valid precursor to stress change since shifts in energy release created changes in waveform duration. Where energy was liberated due to sliding processes, long duration waveforms were generated; upon creation of new microfractures, shorter duration waveforms were shown to result.

No general conclusion as to the applicability of the high frequency acoustic emission monitoring system for rockburst prediction can presently be made. In limited cases, for several class intervals of wide stress difference, this system can be

shown to effectively distinguish between changing stress conditions. More data, acquired over the long term, will definitely be required in order to maximize the ability of such systems to accurately characterize ground stresses over regional mine environments. Pattern recognition was carried out using a limited data base acquired from a small number of site environments. Limited physical access to several monitoring locations (Sites 4 and 5), slow rates of waveform acquisition resulting from transducer location within low stress rock environments and occasional equipment breakdowns all served to yield small data populations.

Pattern recognition analysis on a total of approximately 2000 collected waveforms from Site #6 showed that, for a two stress class identification test, waveforms could be effectively classified over 88% of the time. This accuracy was obtained, however, where the training and testing waveforms were identical. Under similar test, where training and tested waveforms were independent of each other and a larger number of sets of data were analyzed, lower accuracies of prediction resulted. In general, by being able to distinguish between pre-burst and post-burst waveform data at the 88% accuracy level, the microseismic system has demonstrated some, though limited, capability to function as an instrument for stress discrimination (at stress level changes as low as 5.5 MPa).

In the multi-class stress identification test, Class 2 data was successfully identified 77.5% of the time, versus much lower rates for Class 1 data. Such results indicate that the present system exhibits greater prediction accuracy for waveforms deriving from higher stress regions, typically where greater chance for rockburst failure can develop. In early prototype system tests [1], accuracy rates of 74.5% were achieved for waveform discrimination from laboratory stress sources having 10 MPa stress differences; using present recognition capabilities and measured Denison field data, the recognition accuracy was improved to 88% for source stress differences approximating 5.5 MPa.

Although the rockburst detection system which is being developed by the Queen's University Mining Engineering Department has shown considerable improvement over the course of the Denison Mine study, a number of improvements are still required. Of primary interest would be streamlining the data acquisition and analysis process. Present software is packaged individually to permit operator access, observation and manipulation of information while waveform data acquisition occurs. When operating, certain data processing functions are disabled; similarly, classification operations are only enabled once raw data has been operator filed. Future applications would group together all software operations and process data concurrently, thereby eliminating human intervention and reducing processing time required.

Another system improvement would require that more compact hardware be acquired. It is generally not necessary to view acquired waveform data if all system functions operate effectively. In such cases, computer video output could be deleted from system hardware requirements. Also, having a small computer system without the necessity to also have screen display of data would make the system more applicable to a portable power supply use. Where power can be self contained,

significant reductions in down time problems, presently associated with mine power failures, and the need to provide local power sources prior to setup could be obviated.

On the basis of observations made during the course of in-situ study, several significant features could either be deleted or added to the present operating system to help optimize the feature extraction process. Frequency data at levels above 250 kHz is currently analyzed, though no changes in any high frequency output in this range, for any of the Sites observed and different stress regimes known, was shown to exist. It is therefore recommended that processing of waveform data at lower frequency ranges be concentrated upon. Where lower frequency monitoring is implemented, the number of channels of waveform capture, and therefore the effective use of each computer, can be increased. Similarly, features which have been shown to be more susceptible to stress changes should also help to increase the reliability of the pattern recognition system if other features, shown not to be as significant, can be deleted from consideration.

In many Ontario mines, as is the case at the Denison Mine, MP-250 locator-type seismic networks are being utilized. It is recommended that attempts be made to combine the Queen's system with locator-type networks in order to make use of the considerable quantities of low frequency seismic data which are currently being inputted to such systems, but not being used. An additional benefit to practical operation of the existing system would be derivation of methods to successfully bond transducers to exposed rock surfaces rather than having to drill deep installation holes. Present borehole installation is required for avoidance of fractured rock zones about excavations and associated attenuation problems which result during waveform capture. Were transducers capable of being attached directly to rock faces, time and cost of installation could be very significantly reduced.

LIST OF REFERENCES

1) Archibald, J. F., Calder, P. N., Moroz, B. J., Semadeni, T. A. J., Korenberg, M. and Yeo, T. K.; "**Development of Techniques for Rapid In-Situ Stress Analysis and Rockburst Prediction**"; Canadian Mining Journal, Volume 107, No. 4, April, 1986.

2) Archibald, J. F., Calder, P. N., Korenberg, M., Moroz, B. J., Semadeni, T. A. J., Yeo, T. K. and McIlroy, P.; "**Application of Microseismic Monitoring to Stress and Rockburst Prediction**"; Canadian Institute of Mining and Metallurgy Annual General Meeting, Montreal, Quebec, May, 1986.

3) Moroz, B. J.; "**Examination of the Frequency of Acoustic Emissions as a Method of Predicting Violent Failure and Stress Conditions in Rock**"; M. Sc. Thesis, Department of Mining Engineering, Queen's University, January, 1987.

4) Semadeni, T. A. J.; "**High Frequency Microseismic Monitoring Applied to the Determination of Stress Levels in Hard Rock Mines**"; M. Sc. Thesis, Department of Mining Engineering, Queen's University, January, 1988.

5) Hardy, H. R. and Leighton, F. W.; "**Discussions to the Proceedings of the Second Conference on Acoustic Emission/Microseismic Activity in Geologic Structures and Materials**"; Pennsylvania State University, November, 1978; Trans Tech Publications (1980).

6) Archibald, J. F., Calder,P. N., Moroz, B. J., Semadeni, T. A. J. and Yeo, T. K.; "**Applications of Microseismic Monitoring to Stress and Rockburst Precursor Assessment**"; Mining Science and Technology, Elsevier Press (Netherlands), Volume 7, March, 1988.

7) Korenberg, M.; "**Pattern Recognition Via Non-Linear System Identification**"; Midwest Symposium on Circuits and Systems, IEEE, 1985.

8) Korenberg, M.; "**Statistical Identification of Volterra Kernels of High Order Systems**"; International Symposium on Circuits and Systems, IEEE, 1984.

9) Yeo, T.K.; "**Development of Microseismic Monitoring Software**"; Proceedings of the Fred Leighton Memorial Workshop on Mining Induced Seismicity, Montreal, Quebec, August, 1987.

10) Madsen, D. A.; "**A Case Study of High Frequency Microseismic Monitoring Prior to a Rockburst**", M. Sc. Thesis, Department of Mining Engineering, Queen's University, April, 1988.

11) Hedley, D. G. F. and Grant, F.; "**Stope-and-Pillar Design for the Elliot Lake Uranium Mines**"; Canadian Institute of Mining and Metallurgy Bulletin, July, 1972.

12) Archibald, J. F.; "**Investigations of the Post-Pillar Support Mechanism**"; Ph. D. Thesis, Department of Mining Engineering, Queen's University, December, 1976.

13) Bullock, K.; "**A Study of High Frequency Microseismic Emissions from an Underground Hard Rock Mine**"; M. Sc.Thesis, Department of Mining Engineering, Queen's University, December, 1988.

14) Semadeni, T. A. J.; "**High Frequency Microseismic Monitoring Applied to the Determination of Stress Levels in Hard Rock Mines**"; M. Sc. Thesis, Department of Mining Engineering, Queen's University, January, 1988.

15) Hodgson, K. and Joughin, N. C.; "**The Relationship Between Energy Release Rate, Damage and Seismicity in Deep Mines**"; Proceedings of the 8th Symposium on Rock Mechanics - Failure and Breakage of Rocks, C. Fairhurst (editor), University of Minnesota, 1967 (pp. 194 - 203).

16) Hedley, D. G. F. and Grant, F.; "**Stope-and-Pillar Design for the Elliot Lake Uranium Mines**"; Canadian Institute of Mining and Metallurgy Bulletin, Volume #65, No. 723, July, 1972.

APPENDIX A

Summary of In-Situ Microseismic Monitoring Instrumentation Used

Table A-1 - Components of Queen's High Frequency Monitoring System (Moroz [3])

COMPONENT	DESCRIPTION
Vibration Transducers	-Physical Acoustics Corporation (PAC) Model μ30 acoustic emission sensors (piezoelectric type - lead azide titanate) -Resonant frequency threshold @ 300 kHz ± 20 kHz
Pre-Amplifiers	-Physical Acoustics Corporation (PAC) Model 1221 -Nominal amplification @ 40 dB -Dynamic range up to 90 dB -Output range @ 20 V peak-to-peak into 50 ohms -Impedance matched to PAC Model μ30 transducers
Power Supply and Decoupling Network	-Manufactured in-house (Queen's Mining Dept.) -15 V.D.C. power supply to pre-amplifier -Decoupling network required to prevent D.C. power input to pre-amplifier from entering output line
Post Amplifier	-Physical Acoustics Corporation (PAC) Model AE1A -Frequency response linear between 20 kHz - 2 MHz -Amplification adjustable between (3 - 41) dB -Input range between 1 mV - 2 V rms -Output range maximum at 10 V peak-to-peak into 50 ohms -Impedance matched to Model 1221 pre-amplifier
Microcomputer	-Zenith Model 151/158 equipped with 640 K RAM and 10 or 20 MByte Winchester disk/math coprocessor -COMPAQ Model 286, similarly equipped
Digitizing Card	-RC Electronics Model ISC-16 card -Sixteen channel input with single channel A/D conversion -Input range adjustable between 2.5 - 10 V peak -Horizontal and vertical range expansion (16 x) -Maximum sampling rate @ 1 MHz, adjustable -12 bit resolution, and sample length adjustable from 1 K point to maximum computer capacity

APPENDIX B

Summary of MINTAB Modelled Pillar Stress Conditions Existing About the Site #6 Microseismic Installation (35022 Pillar) During Six Stages of Monitoring (July 1 - October 21, 1987)

```
Stress Range within 5 m radius of Transducer: 55.7 - 68.3

Minimum and Maximum Stress (MPa):      0.0     107.7
-------------------------------------------------------

                CODE VALUES FOR STRESS:

1 = 0.5 - 10.0 MPa                7 = 60.0 - 70.0 MPa
2 = 10.0 - 20.0 MPa               8 = 70.0 - 80.0 MPa
3 = 20.0 - 30.0 MPa               9 = 80.0 - 90.0 MPa
4 = 30.0 - 40.0 MPa               V = 90.0 - 100.0 MPa
5 = 40.0 - 50.0 MPa               X = 100.0 - 110.0 MPa
6 = 50.0 - 60.0 MPa               Y = 110.0 MPa and more
-------------------------------------------------------
     ****************************************
     *       55   55    55    55    55    55  *
     *       55   55    55    55    55    55  *
     *       55   65    66    55    55    55  *
     *       55    56    6    55    55    55  *
     *      545    55    7    55    55    55  *
     *     5445    55    7    55    55    55  *
     *    54445    55    7    55    55    55  *
     *   544444    55   67    55    55    55  *
     *7 65544445   66   6     55    66    55  *
     *     555567  76   6     55    66    55  *
     *                876    645    67    65  *
     *6                 8  765456   7     66  *
     *655667                766668        66  *
     * 55    7  8767                    877   76  *
     * 55    7    56                      88   8  *
     * 55    7    66    7779                     7*
     * 55    7    66    66    V99                 *
     * 55    7    66    66      X                 *
     * 55   66    66    66              8788V     *
     * 55   66    66    67              77        *
     * 55   66    77    77              77        *
     * 65   66    8     77              77        *
     * 65   66    9     77              77        *
     * 65   66    V     77              87        *
     * 66   66          77              87        *
     * 66   66          77              88        *
     * 66   67          78              88        *
     * 66   77          78              88        *
     * 66    8          88              88        *
     * 77    9          88              88        *
     * 8     9          88              88        *
     * 8     9          88              88        *
     * 9     V          88              88        *
     * X     V          88              88        *
     *       V          87              87        *
     *       X          77              77        *
     *                  77              77        *
     *                  87              77        *
     *                   879            77        *
     *                     9    99       78        *
     ****************************************
```

FIGURE B-1 - MINTAB Modelled Stresses (Stage 1 - July 1, 1987)

Stress Range within 5 m radius of Transducer: 57.1 - 70.3

Minimum and Maximum Stress (MPa): 0.0 108.5

CODE VALUES FOR STRESS:

1 = 0.5 - 10.0 MPa	7 = 60.0 - 70.0 MPa
2 = 10.0 - 20.0 MPa	8 = 70.0 - 80.0 MPa
3 = 20.0 - 30.0 MPa	9 = 80.0 - 90.0 MPa
4 = 30.0 - 40.0 MPa	V = 90.0 - 100.0 MPa
5 = 40.0 - 50.0 MPa	X = 100.0 - 110.0 MPa
6 = 50.0 - 60.0 MPa	Y = 110.0 MPa and more

```
**********************************************
*       55   55    55    55    55    55   *
*       55   55    55    55    55    55   *
*       55   65    66    55    55    55   *
*       55    56    6    55    55    55   *
*      545    55    7    55    55    55   *
*     5445    55    7    55    55    55   *
*    54445    55    7    55    55    55   *
*   644444    55   67    55    55    55   *
*7 65544445   66   6     55    66    55   *
*     555567  77   6     55    66    55   *
*                876    645   67    65   *
*6                 8   765456  7     66   *
*655667                766668        66   *
* 55    8  8767                    877  76   *
* 55    7    66                      88   8   *
* 55    7    66    8779                     7*
* 55    7    66    76    V99                 *
* 55    7    77    76      X                 *
* 55   66    8     77              8788V     *
* 55   66    V     77              77        *
* 65   66          77              77        *
* 65   66          77              77        *
* 66   66          77              87        *
* 66   67          77              87        *
* 66   67          77              87        *
* 66   67          88              88        *
* 66   67          88              88        *
* 66   77          88              88        *
* 66    8          88              88        *
* 77    9          88              88        *
* 8     9          88              88        *
* 9     9          88              88        *
* 9     V          88              88        *
* X     V          88              88        *
*       V          87              88        *
*       X          77              77        *
*                  87              77        *
*                  87              77        *
*                   87V            77        *
*                    9   99        78        *
**********************************************
```

FIGURE B-2 - MINTAB Modelled Stresses (Stage 2 - August 26, 1987)

Stress Range within 5 m radius of Transducer: 57.6 - 71.3

Minimum and Maximum Stress (MPa): 0.0 108.6

CODE VALUES FOR STRESS:

1 = 0.5 - 10.0 MPa	7 = 60.0 - 70.0 MPa
2 = 10.0 - 20.0 MPa	8 = 70.0 - 80.0 MPa
3 = 20.0 - 30.0 MPa	9 = 80.0 - 90.0 MPa
4 = 30.0 - 40.0 MPa	V = 90.0 - 100.0 MPa
5 = 40.0 - 50.0 MPa	X = 100.0 - 110.0 MPa
6 = 50.0 - 60.0 MPa	Y = 110.0 MPa and more

```
**************************************************
*       55    55     55    55     55     55     *
*       55    55     55    55     55     55     *
*       55    65     66    55     55     55     *
*       55     56     6    55     55     55     *
*      545     55     7    55     55     55     *
*     5445     55     7    55     55     55     *
*    54445     55     7    55     55     55     *
*   644444     55    77    55     55     55     *
*7 65544445    66     6     55     66     55     *
*     555567   77     6     55     66     55     *
*                   876     645     67     65     *
*6                    8   765456    7      66     *
*655667                     766668             66     *
* 55     8   8767                          877    76     *
* 55     7     66                             88     8     *
* 55     7     67     8779                                 7*
* 55     7     78     76      V99                          *
* 55     7     8      77        X                          *
* 55    66     V      77                  8788V           *
* 55    66            77                  77              *
* 65    66            77                  77              *
* 65    66            77                  77              *
* 66    67            77                  87              *
* 66    67            77                  87              *
* 66    67            78                  87              *
* 66    67            88                  88              *
* 66    77            88                  88              *
* 66    77            88                  88              *
* 66     8            88                  88              *
* 77     9            88                  88              *
* 8      9            88                  88              *
* 9      9            88                  88              *
* 9      V            88                  88              *
* X      V            88                  88              *
*       V             87                  88              *
*       X             77                  77              *
*                     87                  77              *
*                     87                  77              *
*                      87V                77              *
*                       9    99           78              *
**************************************************
```

FIGURE B-3 - MINTAB Modelled Stresses (Stage 3 - September 22, 1987)

```
Stress Range within 5 m radius of Transducer: 58.5 - 73.1

Minimum and Maximum Stress (MPa):      0.0     108.8
```



```
                CODE VALUES FOR STRESS:

1 = 0.5 - 10.0 MPa                  7 = 60.0 - 70.0 MPa
2 = 10.0 - 20.0 MPa                 8 = 70.0 - 80.0 MPa
3 = 20.0 - 30.0 MPa                 9 = 80.0 - 90.0 MPa
4 = 30.0 - 40.0 MPa                 V = 90.0 - 100.0 MPa
5 = 40.0 - 50.0 MPa                 X = 100.0 - 110.0 MPa
6 = 50.0 - 60.0 MPa                 Y = 110.0 MPa and more
```

```
     ********************************************
     *        55    55     55     55     55     55  *
     *        55    55     55     55     55     55  *
     *        55    65     66     55     55     55  *
     *        55     56     6     55     55     55  *
     *       545     55     7     55     55     55  *
     *      5445     55     7     55     55     55  *
     *     54445     55     7     55     55     55  *
     *    644444     55    77     55     56     55  *
     *7  65544445    66    6      55     66     55  *
     *      555567   77    6      55     66     55  *
     *                    876     655     67     66  *
     *6                     8   865456    7      66  *
     *655667                      766668          66  *
     * 55     8   8778                       877    76  *
     * 55     7     67                          88     8  *
     * 55     7     8      8789                          7*
     * 55     7     9      76     V99                     *
     * 55     7     V      77       X                     *
     * 55    77            77                 8788V      *
     * 55    66            77                 77         *
     * 65    66            77                 77         *
     * 66    67            77                 77         *
     * 66    67            77                 87         *
     * 66    67            88                 87         *
     * 66    67            88                 88         *
     * 66    67            88                 88         *
     * 66    77            88                 88         *
     * 66    78            88                 88         *
     * 66     8            88                 88         *
     * 77     9            88                 88         *
     * 8      9            88                 88         *
     * 9      9            88                 88         *
     * 9      V            88                 88         *
     * X      V            88                 88         *
     *        V            88                 88         *
     *        X            77                 77         *
     *                     87                 77         *
     *                     87                 77         *
     *                      87V               77         *
     *                       9    99          78         *
     ********************************************
```

FIGURE B-4 - MINTAB Modelled Stresses (Stage 4 - September 30, 1987)

Stress Range within 5 m radius of Transducer: 59.6 - 75.2

Minimum and Maximum Stress (MPa): 0.0 109.0

CODE VALUES FOR STRESS:

1 = 0.5 - 10.0 MPa	7 = 60.0 - 70.0 MPa
2 = 10.0 - 20.0 MPa	8 = 70.0 - 80.0 MPa
3 = 20.0 - 30.0 MPa	9 = 80.0 - 90.0 MPa
4 = 30.0 - 40.0 MPa	V = 90.0 - 100.0 MPa
5 = 40.0 - 50.0 MPa	X = 100.0 - 110.0 MPa
6 = 50.0 - 60.0 MPa	Y = 110.0 MPa and more

```
**********************************************
*       55   55     55     55     55     55   *
*       55   55     55     55     55     55   *
*       55   65     66     55     55     55   *
*       55    56     6     55     55     55   *
*      545    55     7     55     55     55   *
*     5445    55     7     55     55     55   *
*    54445    55     7     55     55     55   *
*   644444    55    77     55     56     55   *
*7 65544445   66     7     55     66     55   *
*     555567  77     7     55     66     55   *
*                  877    655     67     66   *
*6                   8   865456   7      66   *
*655667                    766668            66   *
* 55     8  8879                        977    76   *
* 55     7    8                           88    8   *
* 55     7    V      8789                          7*
* 55     8           76     V99                    *
* 55     7           77       X                    *
* 55    77           77                 8788V      *
* 55    67           77                 77         *
* 65    67           77                 77         *
* 66    67           77                 77         *
* 66    67           88                 87         *
* 66    67           88                 87         *
* 66    67           88                 88         *
* 66    67           88                 88         *
* 66    77           88                 88         *
* 66    78           88                 88         *
* 66     8           88                 88         *
* 77     9           88                 88         *
* 8      9           88                 88         *
* 9      9           88                 88         *
* 9      V           88                 88         *
* X      V           88                 88         *
*       V            88                 88         *
*       X            77                 77         *
*                    87                 77         *
*                    87                 77         *
*                     88V               77         *
*                      9    99          78         *
**********************************************
```

FIGURE B-5 - MINTAB Modelled Stresses (Stage 5 - October 8, 1987)

```
Stress Range within 5 m radius of Transducer: 60.6 - 77.7

Minimum and Maximum Stress (MPa):      0.0    109.1
-------------------------------------------------------
                CODE VALUES FOR STRESS:

1 = 0.5 - 10.0 MPa                7 = 60.0 - 70.0 MPa
2 = 10.0 - 20.0 MPa               8 = 70.0 - 80.0 MPa
3 = 20.0 - 30.0 MPa               9 = 80.0 - 90.0 MPa
4 = 30.0 - 40.0 MPa               V = 90.0 - 100.0 MPa
5 = 40.0 - 50.0 MPa               X = 100.0 - 110.0 MPa
6 = 50.0 - 60.0 MPa               Y = 110.0 MPa and more
-------------------------------------------------------
     ****************************************
     *       65   55    55    55    55    55  *
     *       55   55    55    55    55    55  *
     *       55   65    66    55    55    55  *
     *       55    56    6    55    55    55  *
     *      545    55    7    55    55    55  *
     *     5445    55    7    65    55    55  *
     *    54445    55    7    65    55    55  *
     *   644445    66   77    55    56    55  *
     *7 75544446   66    7     55    66    55  *
     *     555567  77    7     55    66    55  *
     *                 877     555    67    66  *
     *6                  8   866556    7     66  *
     *655667                    766668          66  *
     * 55    8  99V                        977   76  *
     * 55    8                               88    8  *
     * 55    8          8789                        7*
     * 55    8          77     V99                   *
     * 55    8          77       X                   *
     * 55   77          77                 8788V     *
     * 65   67          77                 77        *
     * 66   67          77                 77        *
     * 66   67          87                 77        *
     * 66   67          88                 87        *
     * 66   67          88                 87        *
     * 66   67          88                 88        *
     * 66   77          88                 88        *
     * 66   88          88                 88        *
     * 66    8          88                 88        *
     * 77    9          88                 88        *
     * 8     9          88                 88        *
     * 9     V          88                 88        *
     * 9     V          88                 88        *
     * X     V          88                 88        *
     *       V          88                 88        *
     *       X          87                 77        *
     *                  87                 77        *
     *                  87                 77        *
     *                    88V              77        *
     *                     9   99          78        *
     ****************************************
```

FIGURE B-6 - MINTAB Modelled Stresses (Stage 6 - October 21, 1987)

APPENDIX 4

APPENDIX 4-1

Picture No.	Description
1	Pillar 26305 looking west before filling 1987. Severe spalling and possible shearing (ride) action of bedding planes.
2	Pillar down-dip side 26304 west and looking east. Minor to moderate spalling with same hourglassing and possible shearing action. Pillar height about 8 m.
3	Pillar 26304 down-dip side looking west in west end of panel. Moderate to severe spalling.
4	26305 looking west at initial stage of filling. In the background the competent Negri dyke shown - June 1987.
5	26304 looking west showing 2 "mousetrap" drainage tiles suspended from stope back. Mousetraps extended down through fill fence in 26305 west.
6	Post pillar 26302-303 looking east. Showing mousetrap in foreground. Pillar shows moderate to severe spalling with some apparent off-setting of bedding planes.
7	Post pillar 26304. Showing severe spalling, hourglassing and axial splitting or fracturing from Hangingwall to Footwall.
8	26302 looking west showing fill tight against H/W. Inclined H/W (15^0-25^0) was favourable to tight hydraulic fill placement.
9	Local back failure in wider section (about 15m) in 26305. Failure was controlled by low angled intersecting faults and was probably triggered by a seismic event. September 1987
10	Pillar 26304/26303 looking east. Severe spalling and crushing. Backfill level at about 1/3 of pillar height. January 1988
11	26305 looking west. Pillar on left (Negri Dyke) about 1/2 buried in fill. January 1988
12	26302 at top of test panel looking west, note tight fill against hangingwall and spalled pillar on up-dip side - December 1988.

APPENDIX 4-2

Picture No.	Description
13	Convergence meter in fill in 26035 looking south at Negri dyke. Convergence meter about 0,5 m from pillar wall and anchored at about 1,5m depth in back. Fill is about 1,5 from the back. December 1987
14	Pillar in 22 panel (22203), 2 panels up-dip from 26 panel. Note prominent fracture inclined at about 45^0 to horizontal. Movement has recently occurred along the discontinuity. Pillars in the immediate area have experienced moderate to severe spalling. Mid 1988
15	Pillar in 22 panel (22202) up-dip from fill test panel looking west and down-dip side of the post pillar. Moderate to severe spalling, pillar fractured throughout. Note possible differential movement of oxidized beds indicating possible shearing or ride component mid 1988.
16	Rib pillar between 18090/18091 stopes north of 18951 roadway looking north. Pillar has experienced axial slitting or fracturing from hangingwall to footwall. Pillar is up-dip about 275 m from 26 panel, and on northern limit of area of pillar deterioration. Early 1989
17	Up-dip side at floor level roadway pillar 18951 up-dip from test panel about 275-300 m. Apparent pillar rotation resulting is about 150 mm of lateral shearing. Probable cause is footwall moving up-dip relative to hangingwall.
18	18951 roadway. Apparent floor heave about 100 mm. March 1988
19	Exposed fault surface with slickensided surface and gouge infilling at location of ground failure in the east end of 22951 roadway just north of test panel.

2

1

3

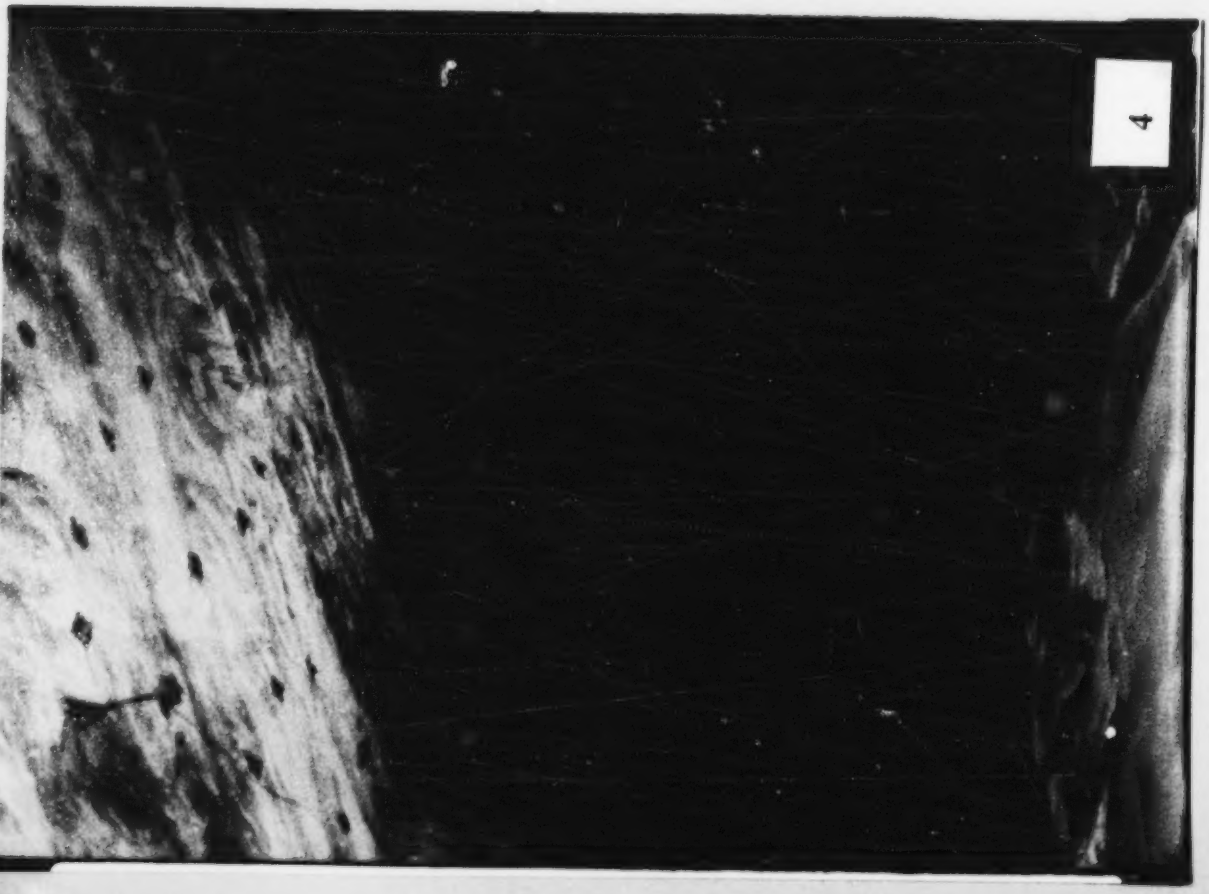
4

5

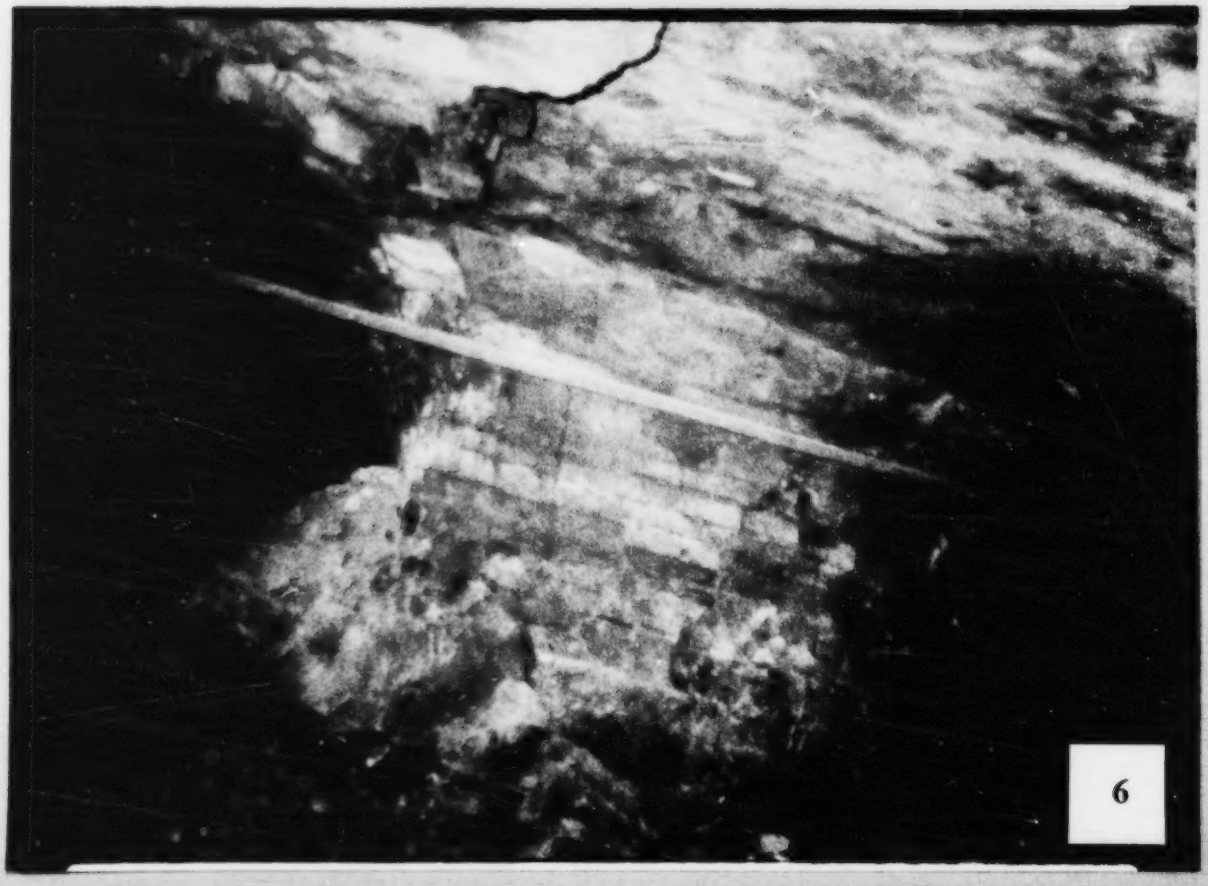
6

7

8

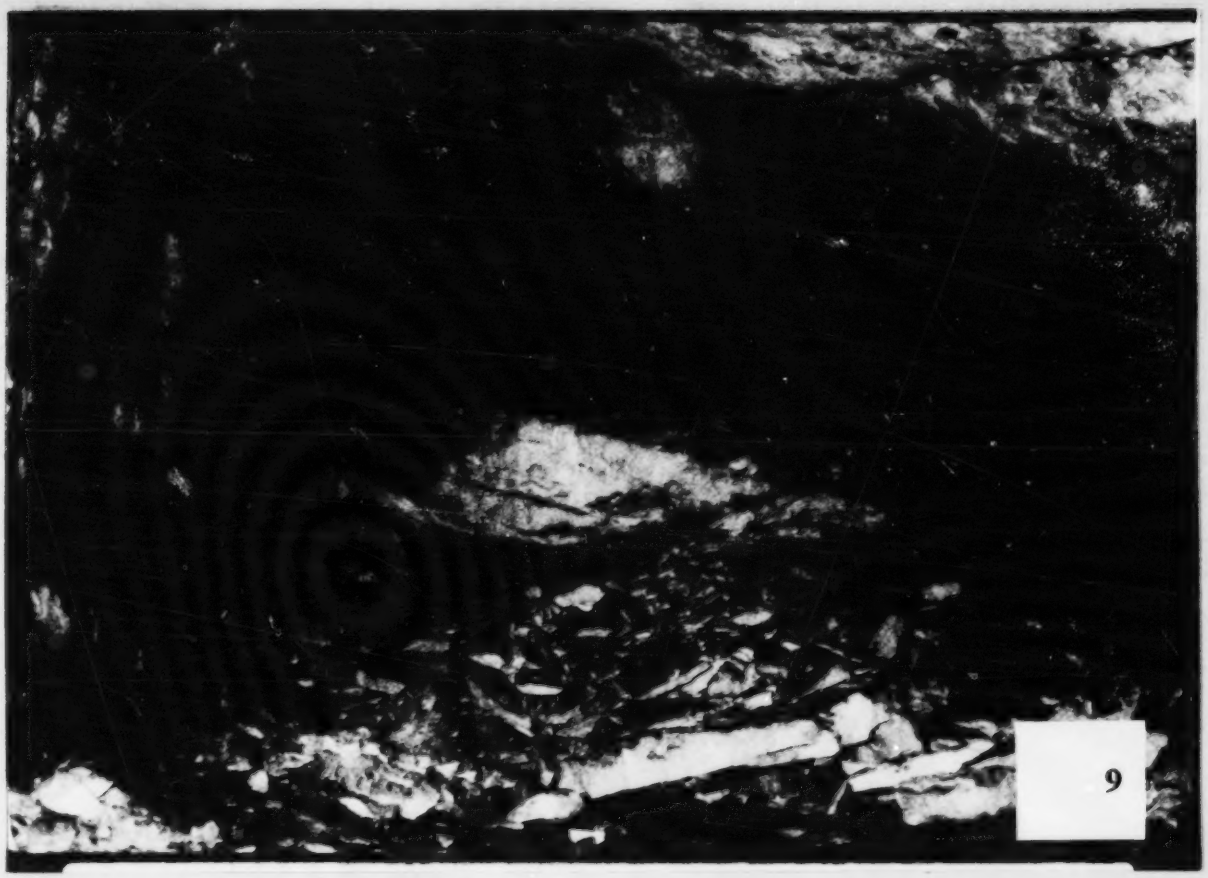
9

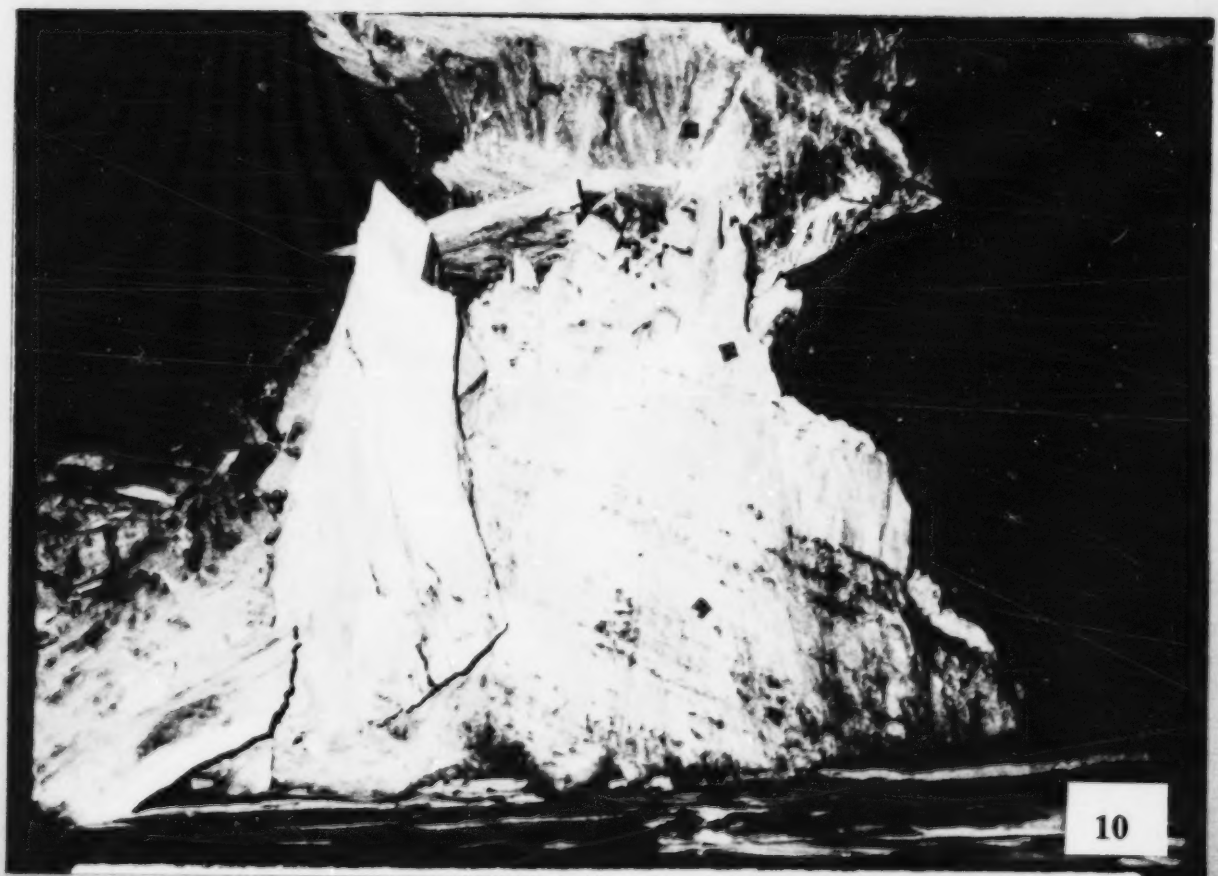
10

11

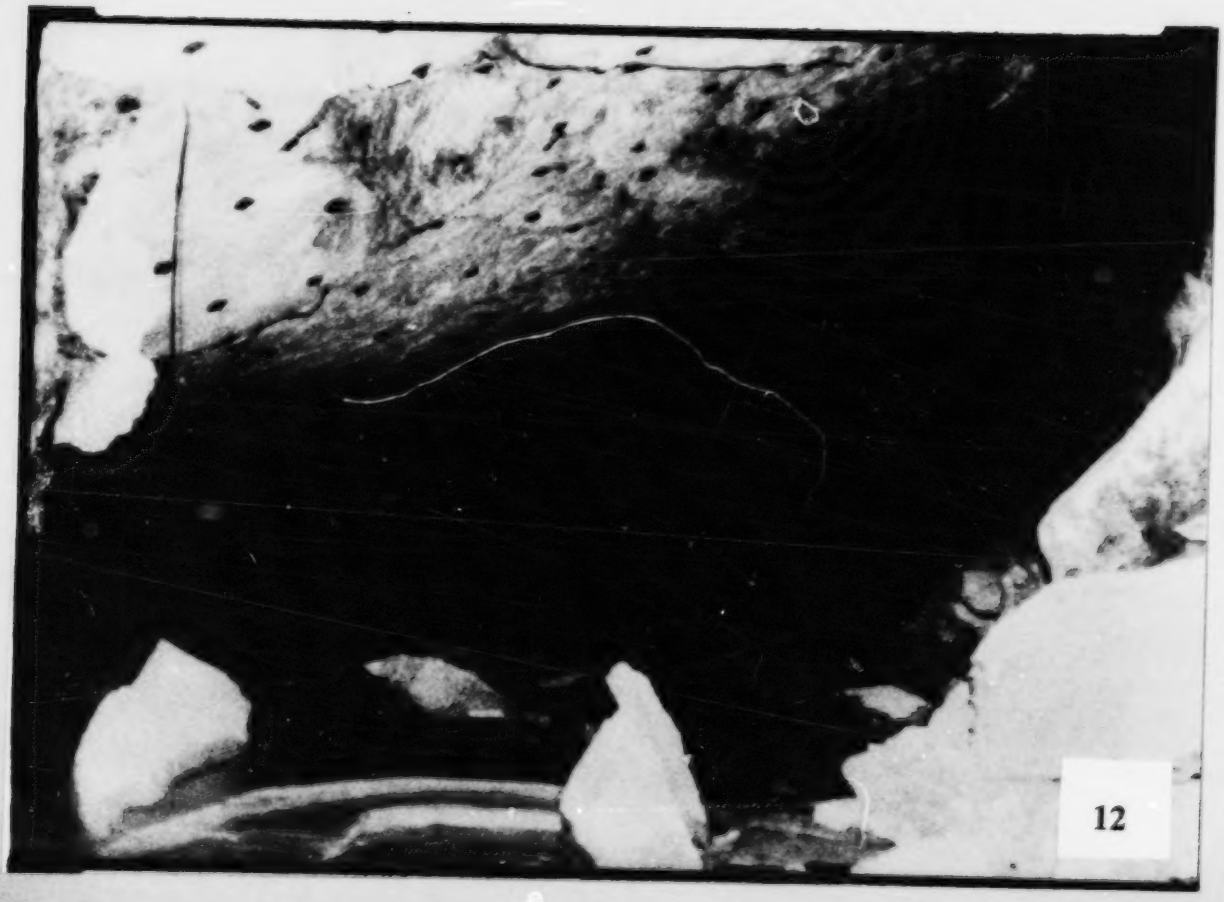
12

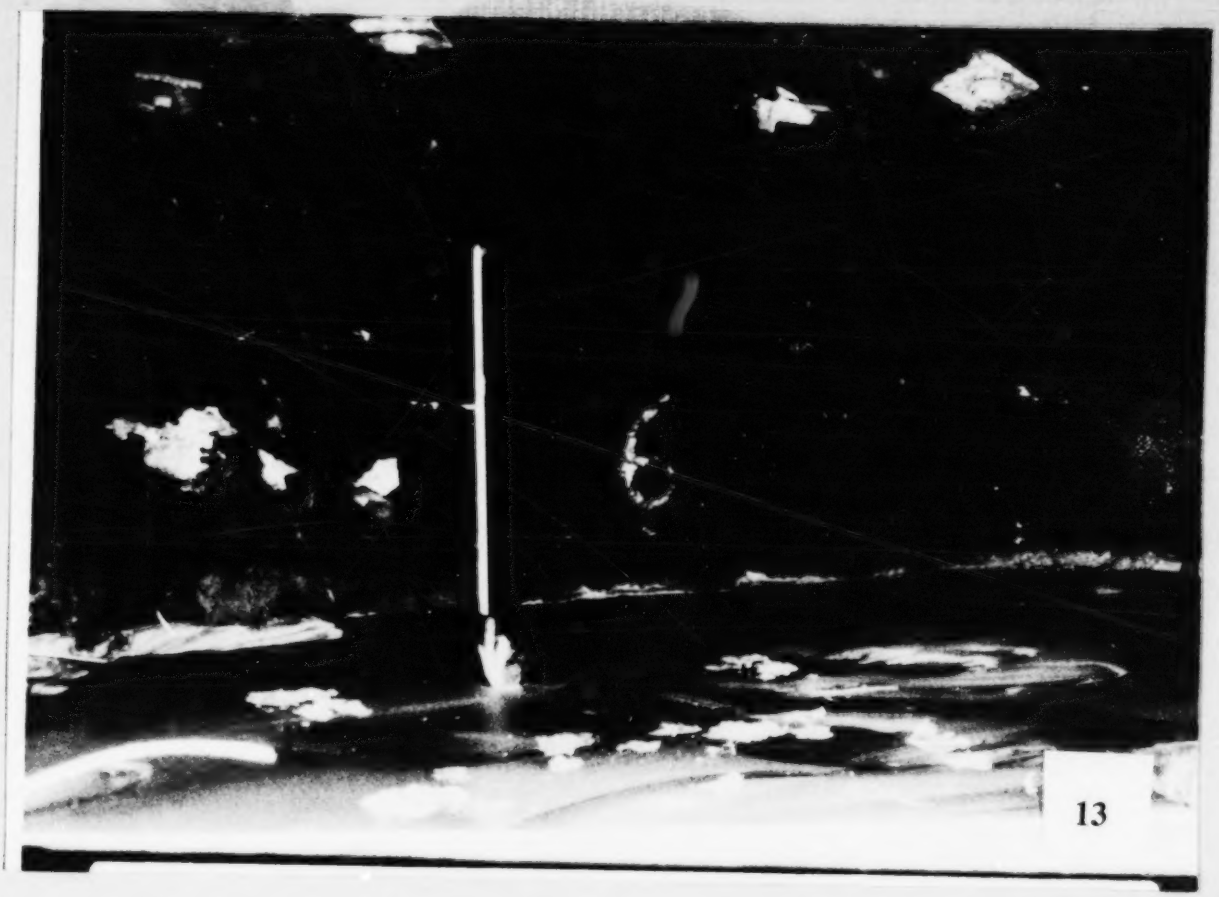

13

14

15

16

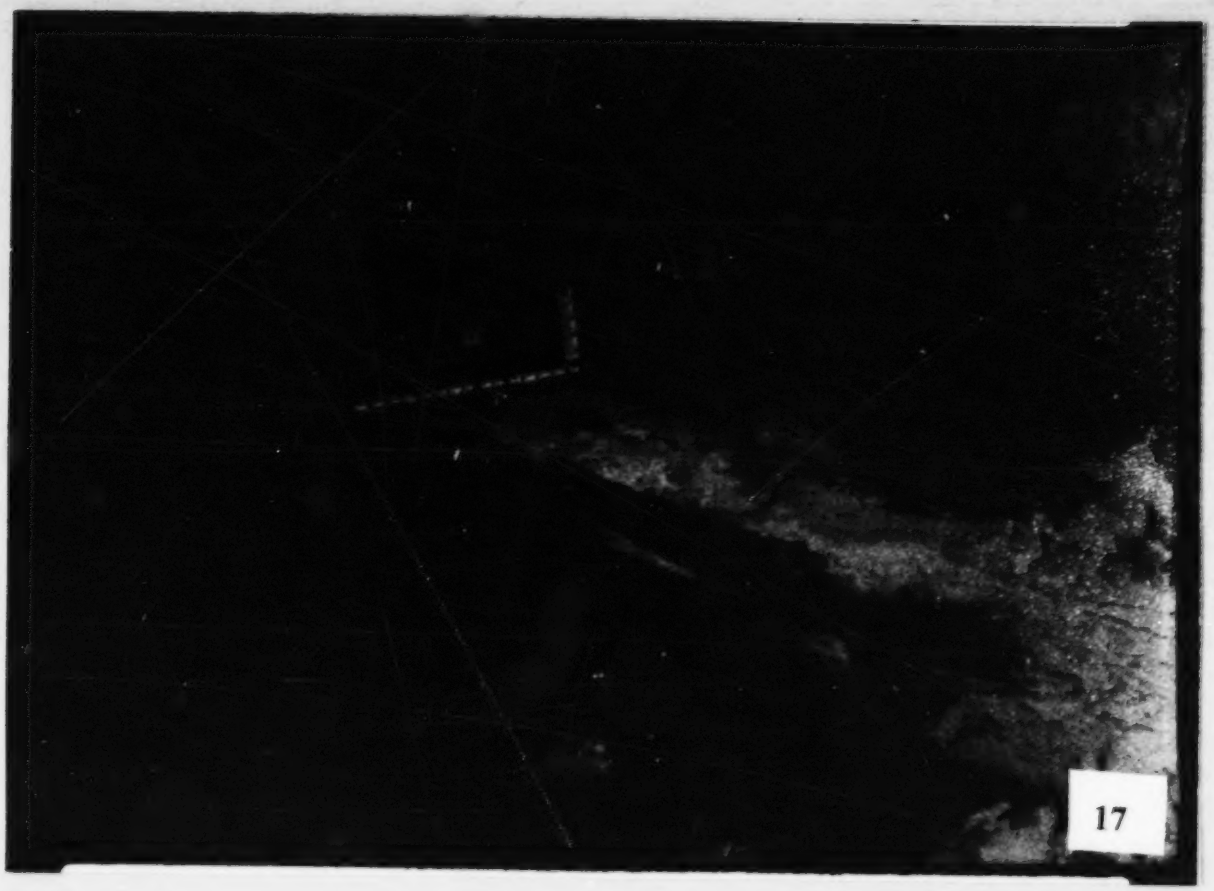
17

18

19

MAPS
NOT
FILMED

CARTES
OMISES